

NASA Contractor Report 4617

ORIGINAL CONTAINS  
COLOR ILLUSTRATIONS

# Results of the Examination of LDEF Polyurethane Thermal Control Coatings

ORIGINAL CONTAINS  
COLOR ILLUSTRATIONS

---

*Johnny L. Golden*  
*Boeing Defense & Space Group • Seattle, Washington*

National Aeronautics and Space Administration  
Langley Research Center • Hampton, Virginia 23681-0001

Prepared for Langley Research Center  
under Contracts NAS1-18224 and NAS1-19247

---

July 1994



## FOREWORD

This report describes the results from the testing and analysis of polyurethane thermal control coatings flown on the Long Duration Exposure Facility (LDEF). This work was carried out by Boeing as part of two contracts, NAS1-18224, Task 12 (October 1989 through May 1991), and NAS1-19247, Tasks 1 and 8 (initiated May 1991). Sponsorship for these two programs was provided by the National Aeronautics and Space Administration, Langley Research Center, Hampton, Virginia.

Mr. Lou Teichman, NASA LaRC, was the NASA Task Technical Monitor. Mr. Teichman was replaced by Ms. Joan Funk, NASA LaRC, following his retirement. Mr. Bland Stein, NASA LaRC, was the Materials Special Investigation Group Chairman, and was replaced by Ms. Joan Funk and Dr. Ann Whitaker, NASA MSFC, following Mr. Stein's retirement. The Materials & Processes Technology organization of the Boeing Defense & Space Group was responsible for providing the support to both contracts. The following Boeing personnel provided critical support throughout the program.

Bill Fedor	Program Manager
Sylvester Hill	Task Manager
Dr. Gary Pippin	Technical Leader
Dr. Johnny Golden	Testing and Analysis

The following Boeing personnel provided critical support during the program.

Dr. Wally Plagemann	Testing and Analysis
Russ Crutcher	Contamination Analysis
Pete George	Testing and Analysis

The successful completion of this work would not have been possible without the contributions of the LDEF Project Office staff and the LDEF Ground Operations team.

PRECEDING PAGE BLANK NOT FILMED



## TABLE OF CONTENTS

	<u>Page</u>
FOREWORD	iii
LIST OF TABLES	vi
LIST OF FIGURES	vii
ACRONYM LIST	xix
1.0 INTRODUCTION	1
2.0 LDEF MISSION PROFILE	1
3.0 HARDWARE DESCRIPTIONS AND LOCATIONS	2
4.0 RESULTS AND DISCUSSION	3
4.1 Optical Microscopy	3
4.2 Contamination Analysis	4
4.3 Cross-Sectioning	5
4.4 Surface Analysis	6
4.5 Optical Properties Measurements	7
4.6 Other Measurements and Analysis	10
5.0 CONCLUSIONS	11
6.0 REFERENCES	12
7.0 FIGURES	13
APPENDICES:	
A. Chemglaze A276 Optical Property and Environmental Exposure Data	84
B. Infrared Reflectance Measurements for Chemglaze A276	88
C. Color Photographs from Section 7.0 Figures	124

## LIST OF TABLES

	<u>Page</u>
Table 1. Optical Properties For A971 Yellow Polyurethane Coating.	10
APPENDIX A. Chemglaze A276 Optical Property and Environmental Exposure Data	84

## LIST OF FIGURES

	<u>Page</u>
Figure 1. LDEF retrieved as viewed from the Shuttle Columbia on January 12, 1990. NASA Langley Research Center Photo No. 90-10472. See p.124 for color figure.	13
Figure 2. LDEF Atomic Oxygen (AO) Fluence Map (ref. 1)	14
Figure 3. LDEF Ultraviolet (UV) Exposure Map (ref. 2)	14
Figure 4. On-orbit view of paint disks on LDEF tray clamps in the atomic oxygen fluence transition region, tray E6. NASA Johnson Space Center Photo No. S32-82-040. Disks on upper longeron (see arrow) were in high AO fluence and are white, disks on lower longeron were in low AO fluence and are brown. See p.125 for color figure.	15
Figure 5. Cross-sectional representation of the components in a LDEF tray clamp paint disk. A276 and Z306 are Chemglaze polyurethane thermal control coatings. This depiction is not to scale.	16
Figure 6. On-orbit view of paint disks on the space end of LDEF. NASA Johnson Space Center Photo No. S32-75-036. U. S. flag is above tray H12. See p.126 for color figure.	17
Figure 7. Tray clamp position numbering system for LDEF side trays.	18
Figure 8. Tray clamp position numbering systems for LDEF Earth and space end trays.	19
Figure 9. LDEF bay and row position map with experiment numbers.	20
Figure 10. LDEF Experiment M0003 - painted composite panel, postflight. The coatings are (clockwise from upper left) Chemglaze A276, Chemglaze Z306, BMS 10-60 White Polyurethane, and unpainted T300 graphite / 934 epoxy composite.	21
Figure 11. Chemglaze A971 yellow paint on components of the leading (above) and trailing edge scuff plates. See p.127 for color figure.	22
Figure 12. Chemglaze Z306 black polyurethane paint on tray clamp position A6-2, viewed at 16X magnification. Contaminant fiber imbedded in the paint film. See p.128 for color figure.	23

## LIST OF FIGURES (Continued)

	<u>Page</u>
Figure 13. Chemglaze A276 white polyurethane paint on tray clamp A6-2, viewed at 16X magnification. A contaminant fiber is imbedded in the coating and solvent marks are visible. See p. 128 for color figure.	23
Figure 14. Chemglaze Z306 black polyurethane paint on tray clamp B7-2, viewed at 16X magnification. Visible are a fastener hole and particles of yellow paint, intact on most of the surface but smeared under the washer during assembly. See p.129 for color figure.	24
Figure 15. Chemglaze A276 white polyurethane paint on tray clamp B4-7, viewed at 16X magnification. Solvent mark discoloration. See p. 129 for color figure.	24
Figure 16. Chemglaze A276 white polyurethane paint on tray clamp B7-2, viewed at 16X magnification. Example of cracking with atomic oxygen erosion. See p.130 for color figure.	25
Figure 17. Chemglaze A276 white polyurethane paint on tray clamp C8-5, viewed at 16X magnification. Edge cracking and fragility of the surface are shown. See p. 130 for color figure.	25
Figure 18. Chemglaze A276 white polyurethane paint on tray clamp C8-5, viewed at 16X magnification, showing parallel surface cracks. See p. 131 for color figure.	26
Figure 19. Chemglaze A276 white polyurethane paint on tray clamp B7-2, viewed at 16X magnification. Occlusions in paint were exposed with AO erosion. See p.132 for color figure.	27
Figure 20. Chemglaze A276 white polyurethane paint on tray clamp B7-2, viewed at 16X magnification, showing additional AO erosion exposed paint contaminants. See p. 132 for color figure.	27
Figure 21. Chemglaze A276 white polyurethane paint on tray clamp C8-5, viewed at 16X magnification, showing the fragile nature of the eroded surface layer. See p.133 for color figure.	28
Figure 22. Chemglaze A276 white polyurethane paint on tray clamp C8-5, viewed at 16X magnification, showing a small debris impact and handling damage. See p. 133 for color figure.	28

## LIST OF FIGURES (Continued)

	<u>Page</u>
Figure 23. Chemglaze Z306 black polyurethane paint on tray clamp C8-5, viewed at 16X magnification, near a fastener location. Erosion through to the red primer occurred in a band just inside of the paint edge (see arrow). See p. 134 for color figure.	29
Figure 24. Chemglaze A276 white polyurethane paint on tray clamp A6-2, viewed at 100X magnification under bright field illumination.	30
Figure 25. Chemglaze A276 white polyurethane paint on tray clamp B4-7, viewed at 100X magnification under bright field illumination.	30
Figure 26. Chemglaze A276 white polyurethane paint on tray clamp B7-2, viewed at 100X magnification under bright field illumination.	31
Figure 27. Chemglaze A276 white polyurethane paint on tray clamp C8-5, viewed at 100X magnification under bright field illumination.	31
Figure 28. Chemglaze A276 white polyurethane paint on tray clamp A6-2, viewed at 1000X magnification under dark field illumination.	32
Figure 29. Chemglaze A276 white polyurethane paint on tray clamp B4-7, viewed at 1000X magnification under dark field illumination.	32
Figure 30. Chemglaze A276 white polyurethane paint on tray clamp B7-2, viewed at 1000X magnification under dark field illumination.	33
Figure 31. Chemglaze A276 white polyurethane paint on tray clamp C8-5, viewed at 1000X magnification under dark field illumination.	33
Figure 32. Chemglaze Z306 black polyurethane paint on Experiment M0003 composite panel, viewed at 200X magnification. The focus is on a silicate inclusion but atomic oxygen erosion to the red primer layer is visible. See p.135 for color figure.	34
Figure 33. Chemglaze Z306 black polyurethane paint on Experiment M0003 composite panel, viewed at 200X magnification. The focus is on another silicate inclusion but atomic oxygen erosion to the red primer layer is visible. See p.136 for color figure.	35
Figure 34. Chemglaze Z306 black polyurethane paint on Experiment M0003 composite panel, viewed at 200X magnification, showing a dispersed silicate layer. See p. 136 for color figure.	35

## LIST OF FIGURES (Continued)

	<u>Page</u>
Figure 35. Chemglaze A971 yellow polyurethane paint from the leading edge (row 9) scuff plate, shown at 200X magnification. At center is loose clump of pigment, dark freckles are areas of darkened organic resin. See p. 137 for color figure.	36
Figure 36. Chemglaze A971 yellow polyurethane paint from the leading edge (row 9) scuff plate, shown at 200X magnification. The focus is on the track (see arrow) of a organic fiber which was a contaminant in the paint and subsequently eroded by AO where it emerged through the surface. See p. 138 for color figure.	37
Figure 37. Chemglaze A276 white polyurethane paint <u>control</u> specimen total reflectance spectra, 300 to 2500 nm range (integrated to determine solar absorptance).	38
Figure 38. Chemglaze A276 white polyurethane paint <u>control</u> specimen diffuse reflectance spectra, 300 to 2500 nm range.	39
Figure 39. Chemglaze A276 white polyurethane paint E2-8 specimen (trailing edge) total reflectance spectra, 300 to 2500 nm range (integrated to determine solar absorptance).	40
Figure 40. Chemglaze A276 white polyurethane paint E2-8 specimen (trailing edge) diffuse reflectance spectra, 300 to 2500 nm range.	41
Figure 41. Chemglaze A276 white polyurethane paint C8-5 specimen (leading edge) total reflectance spectra, 300 to 2500 nm range (integrated to determine solar absorptance).	42
Figure 42. Chemglaze A276 white polyurethane paint C8-5 specimen (leading edge) diffuse reflectance spectra, 300 to 2500 nm range.	43
Figure 43. Chemglaze A276 white polyurethane paint, control specimen infrared spectra.	44
Figure 44. Chemglaze A276 white polyurethane paint , B9-7 specimen (leading edge) infrared spectra.	45
Figure 45. Chemglaze A276 white polyurethane paint , A3-7 specimen (trailing edge) infrared spectra.	46
Figure 46. Cross-section of Chemglaze A276 white paint on tray clamp C8-5 (500X magnification), showing lifting of loose pigment into the encapsulant. See p.139 for color figure.	47

## LIST OF FIGURES (Continued)

	<u>Page</u>
Figure 47. Cross-section of Chemglaze A276 white paint on tray clamp C8-5 (500X magnification), showing a typical crack passing down to aluminum substrate. See p. 139 for color figure.	47
Figure 48. Cross-section of Chemglaze Z306 black polyurethane paint on tray clamp A6-2 at 500X magnification, protected from environmental exposure.	48
Figure 49. Cross-section of Chemglaze Z306 black polyurethane paint on tray clamp A6-2 at 500X magnification, full environmental exposure.	48
Figure 50. Cross-section of Chemglaze Z306 black polyurethane paint on tray clamp B4-7 at 500X magnification, protected from environmental exposure.	49
Figure 51. Cross-section of Chemglaze Z306 black polyurethane paint on tray clamp B4-7 at 500X magnification, full environmental exposure.	49
Figure 52. Cross-section of Chemglaze Z306 black polyurethane paint on tray clamp B7-2 at 500X magnification, protected from environmental exposure.	50
Figure 53. Cross-section of Chemglaze Z306 black polyurethane paint on tray clamp B7-2 at 500X magnification, full environmental exposure.	50
Figure 54. Cross-section of Chemglaze Z306 black polyurethane paint on tray clamp C8-5 at 500X magnification, protected from environmental exposure.	51
Figure 55. Cross-section of Chemglaze Z306 black polyurethane paint on tray clamp C8-5 at 500X magnification, full environmental exposure.	51
Figure 56. Cross-section of Chemglaze A276 white polyurethane paint on tray clamp B4-7 at 2500X magnification. Titania particles are visible to the very surface of the paint. The discolored layer is very thin, ~ 0.2 $\mu\text{m}$ . See p. 140 for color figure.	52
Figure 57. SEM of Chemglaze A276 white paint on tray clamp E10-6, 1000X magnification.	53
Figure 58. SEM of Chemglaze A276 white paint on tray clamp E10-6, 5000X magnification.	53

## LIST OF FIGURES (Continued)

	<u>Page</u>
Figure 59. SEM of Chemglaze A276 white paint on tray clamp E10-6, 10,000X magnification.	54
Figure 60. SEM of Chemglaze A276 white paint on tray clamp E10-6, 25,000X magnification.	54
Figure 61. Electron microprobe chemical analysis of Chemglaze A276 white paint taken from tray clamp E10-6, during the scan for figure 58.	55
Figure 62. Electron microprobe chemical analysis of Chemglaze A276 white paint taken from tray clamp E10-6 during the scan for figure 60, focusing on the darker flake material.	56
Figure 63. SEM of Chemglaze A276 white paint on tray clamp E10-6, showing two unusual and adjacent surface features at 150X magnification.	57
Figure 64. Electron microprobe chemical analysis of the spiral particle in figure 63.	58
Figure 65. Electron microprobe chemical analysis of the dark clump adjacent to the spiral particle in figure 63.	59
Figure 66. SEM of Chemglaze A276 white paint on tray clamp E10-6, focusing on a micrometeoroid or debris impact in the surface (250X magnification).	60
Figure 67. Electron microprobe chemical analysis of the crater bottom in figure 66.	61
Figure 68. Electron microprobe chemical analysis of Chemglaze Z306 black paint on tray clamp E10-6.	62
Figure 69. ESCA data for Chemglaze A276 white paint control specimen.	63
Figure 70. ESCA data for Chemglaze A276 white paint on E2-3 specimen.	64
Figure 71. ESCA data for Chemglaze A276 white paint on C3-2 specimen.	65
Figure 72. ESCA data for Chemglaze A276 white paint on B7-7 specimen.	66
Figure 73. ESCA data for Chemglaze A276 white paint on E9-3 specimen.	67
Figure 74. ESCA data for Chemglaze Z306 black paint on control specimen.	68

## LIST OF FIGURES (Continued)

	<u>Page</u>
Figure 75. ESCA data for Chemglaze Z306 black paint on E2-3 specimen.	69
Figure 76. ESCA data for Chemglaze Z306 black paint on C3-2 specimen.	70
Figure 77. ESCA data for Chemglaze Z306 black paint on B7-7 specimen.	71
Figure 78. ESCA data for Chemglaze Z306 black paint on E9-3 specimen.	72
Figure 79. Solar absorptance / thermal emittance ratio for Chemglaze A276 white polyurethane paint on LDEF Earth and space end tray clamps.	73
Figure 80. Map of LDEF side tray clamps with thermal control paint disks available to the MSIG.	74
Figure 81. Solar absorptance for Chemglaze A276 white paint versus row position.	75
Figure 82. Thermal emittance for Chemglaze A276 white paint versus row position.	75
Figure 83. Solar absorptance for Chemglaze A276 white paint versus atomic oxygen incidence angle.	76
Figure 84. Thermal emittance for Chemglaze A276 white paint versus atomic oxygen incidence angle.	76
Figure 85. Solar absorptance for Chemglaze A276 white polyurethane paint versus atomic oxygen fluence.	77
Figure 86. Solar absorptance for Chemglaze A276 white polyurethane paint versus ultraviolet radiation exposure.	77
Figure 87. Laser profilometry scan of Chemglaze A276 white polyurethane paint, moving from a protected area to an AO exposed surface, from which all loose paint pigment had been removed. Specimen was taken from the bare-to-A276 paint interface on the Experiment M0003 composite panel (see figure 10).	78
Figure 88. Laser profilometry scan of Chemglaze A276 white polyurethane paint, moving from a protected area to an AO exposed surface, from which all loose paint pigment had been removed. Specimen was taken from the Z306-to-A276 paint interface on the Experiment M0003 composite panel (see figure 10).	79

## LIST OF FIGURES (Continued)

	<u>Page</u>
Figure 89. Laser profilometry scan of Chemglaze A276 white polyurethane paint, moving from a protected area to an AO exposed surface, from which all loose paint pigment had been removed. Specimen was taken from the A276 paint corner of the Experiment M0003 composite panel (see figure 10).	80
Figure 90. Laser profilometry scan of Chemglaze A276 white polyurethane paint, moving from a protected area to an AO exposed surface, from which all loose paint pigment had been removed. Specimen was taken from the A276 paint corner of the Experiment M0003 composite panel (see figure 10). Scan taken 90° from figure 89 scan.	81
Figure 91. Laser profilometry scan of Chemglaze A276 white polyurethane paint, moving from a protected area to an AO exposed surface, from which all loose paint pigment had been removed. Specimen was taken from the A276 paint corner of the Experiment M0003 composite panel (see figure 10). Scan taken 90° from figure 90 scan.	82
Figure 92. Laser profilometry scan of Chemglaze A276 white polyurethane paint, moving from a protected area to an AO exposed surface, from which all loose paint pigment had been removed. Specimen was taken from the A276 paint corner of the Experiment M0003 composite panel (see figure 10). Scan taken 90° from Figure 91 scan.	83
<b>APPENDIX B.</b>	
Figure B1. Chemglaze A276 Control Specimen - Total Hemispherical Infrared Reflectance	88
Figure B2. Chemglaze A276 Control Specimen - Diffuse Infrared Reflectance	89
Figure B3. Chemglaze A276 Control Specimen - Specular Infrared Reflectance	90
Figure B4. Chemglaze A276 B1-4 Specimen - Total Hemispherical Infrared Reflectance	91
Figure B5. Chemglaze A276 B1-4 Specimen - Diffuse Infrared Reflectance	92
Figure B6. Chemglaze A276 B1-4 Specimen - Specular Infrared Reflectance	93
Figure B7. Chemglaze A276 E2-3 Specimen - Total Hemispherical Infrared Reflectance	94

## LIST OF FIGURES (Continued)

	<u>Page</u>
Figure B8. Chemglaze A276 E2-3 Specimen - Diffuse Infrared Reflectance	95
Figure B9. Chemglaze A276 E2-3 Specimen - Specular Infrared Reflectance	96
Figure B10. Chemglaze A276 E2-8 Specimen - Total Hemispherical Infrared Reflectance	97
Figure B11. Chemglaze A276 E2-8 Specimen - Diffuse Infrared Reflectance	98
Figure B12. Chemglaze A276 E2-8 Specimen - Specular Infrared Reflectance	99
Figure B13. Chemglaze A276 C3-2 Specimen - Total Hemispherical Infrared Reflectance	100
Figure B14. Chemglaze A276 C3-2 Specimen - Diffuse Infrared Reflectance	101
Figure B15. Chemglaze A276 C3-2 Specimen - Specular Infrared Reflectance	102
Figure B16. Chemglaze A276 E3-8 Specimen - Total Hemispherical Infrared Reflectance	103
Figure B17. Chemglaze A276 E3-8 Specimen - Diffuse Infrared Reflectance	104
Figure B18. Chemglaze A276 E3-8 Specimen - Specular Infrared Reflectance	105
Figure B19. Chemglaze A276 B4-7 Specimen - Total Hemispherical Infrared Reflectance	106
Figure B20. Chemglaze A276 B4-7 Specimen - Diffuse Infrared Reflectance	107
Figure B21. Chemglaze A276 B4-7 Specimen - Specular Infrared Reflectance	108
Figure B22. Chemglaze A276 A6-2 Specimen - Total Hemispherical Infrared Reflectance	109
Figure B23. Chemglaze A276 A6-2 Specimen - Diffuse Infrared Reflectance	110
Figure B24. Chemglaze A276 A6-2 Specimen - Specular Infrared Reflectance	111
Figure B25. Chemglaze A276 B7-2 Specimen - Total Hemispherical Infrared Reflectance	112
Figure B26. Chemglaze A276 B7-2 Specimen - Diffuse Infrared Reflectance	113

## LIST OF FIGURES (Continued)

	<u>Page</u>
Figure B27. Chemglaze A276 B7-2 Specimen - Specular Infrared Reflectance	114
Figure B28. Chemglaze A276 B7-7 Specimen - Total Hemispherical Infrared Reflectance	115
Figure B29. Chemglaze A276 B7-7 Specimen - Diffuse Infrared Reflectance	116
Figure B30. Chemglaze A276 B7-7 Specimen - Specular Infrared Reflectance	117
Figure B31. Chemglaze A276 C8-5 Specimen - Total Hemispherical Infrared Reflectance	118
Figure B32. Chemglaze A276 C8-5 Specimen - Diffuse Infrared Reflectance	119
Figure B33. Chemglaze A276 C8-5 Specimen - Specular Infrared Reflectance	120
Figure B34. Chemglaze A276 G6-2 Specimen - Total Hemispherical Infrared Reflectance	121
Figure B35. Chemglaze A276 G6-2 Specimen - Diffuse Infrared Reflectance	122
Figure B36. Chemglaze A276 G6-2 Specimen - Specular Infrared Reflectance	123
<b>APPENDIX C.</b>	
Figure C1. LDEF retrieved as viewed from the Shuttle Columbia on January 12, 1990. NASA Langley Research Center Photo No. 90-10472. Color version of figure 1, page 13.	124
Figure C4. On-Orbit view of paint disks on LDEF tray clamps in the atomic oxygen fluence transition area, tray E6. NASA Johnson Space Center Photo No. S32-82-040. Disks on upper longeron were in high AO fluence and are white, disks on lower longeron were in low AO fluence and are brown. Color version of figure 4, page 15.	125
Figure C6. On-Orbit view of paint disks on the space end of LDEF. NASA Johnson Space Center Photo No. S32-75-036. U. S. flag is above tray H12. Color version of figure 6, page 17.	126
Figure C11. Chemglaze A971 yellow paint on components of the leading (above) and trailing edge scuff plates. Color version of figure 11, page 22.	127
Figure C12. Chemglaze Z306 black polyurethane paint on tray clamp position A6-2, viewed at 16X magnification. Contaminant fiber imbedded in the paint film. Color version of figure 12, page 23.	128

## LIST OF FIGURES (Continued)

	<u>Page</u>
Figure C13. Chemglaze A276 white polyurethane paint on tray clamp A6-2, viewed at 16X magnification. A contaminant fiber is imbedded in the coating and solvent marks are visible. Color version of figure 13, page 23.	128
Figure C14. Chemglaze Z306 black polyurethane paint on tray clamp B7-2, viewed at 16X magnification. Visible are a fastener hole and particles of yellow paint, intact on most of the surface but smeared under the washer during assembly. Color version of figure 14, page 24.	129
Figure C15. Chemglaze A276 white polyurethane paint on tray clamp B4-7, viewed at 16X magnification. Solvent mark discoloration. Color version of figure 15, page 24.	129
Figure C16. Chemglaze A276 white polyurethane paint on tray clamp B7-2, viewed at 16X magnification. Example of cracking with atomic oxygen erosion. Color version of figure 16, page 25.	130
Figure C17. Chemglaze A276 white polyurethane paint on tray clamp C8-5, viewed at 16X magnification. Edge cracking and fragility of the surface are shown. Color version of figure 17, page 25.	130
Figure C18. Chemglaze A276 white polyurethane paint on tray clamp C8-5, viewed at 16X magnification, showing parallel surface cracks. Color version of figure 18, page 26.	131
Figure C19. Chemglaze A276 white polyurethane paint on tray clamp B7-2, viewed at 16X magnification. Occlusions in paint were exposed with AO erosion. Color version of figure 19, page 27.	132
Figure C20. Chemglaze A276 white polyurethane paint on tray clamp B7-2, viewed at 16X magnification, showing more AO erosion exposed paint contaminants. Color version of figure 20, page 27.	132
Figure C21. Chemglaze A276 white polyurethane paint on tray clamp C8-5, viewed at 16X magnification, showing the fragile nature of the eroded surface layer. Color version of figure 21, page 28.	133
Figure C22. Chemglaze A276 white polyurethane paint on tray clamp C8-5, viewed at 16X magnification, showing a small debris impact and handling damage. Color version of figure 22, page 28.	133

## LIST OF FIGURES (Continued)

	<u>Page</u>
Figure C23. Chemglaze Z306 black polyurethane paint on tray clamp C8-5, viewed at 16X magnification, near a fastener location. Erosion through to the red primer occurred in a band just inside of the paint edge. Color version of figure 23, page 29.	134
Figure C32. Chemglaze Z306 black polyurethane paint on Experiment M0003 composite panel, viewed at 200X magnification. The focus is on a silicate inclusion but atomic oxygen erosion to the red primer layer is visible. Color version of figure 32, page 34.	135
Figure C33. Chemglaze Z306 black polyurethane paint on Experiment M0003 composite panel, viewed at 200X magnification. The focus is on another silicate inclusion but atomic oxygen erosion to the red primer layer is visible. Color version of figure 33, page 35.	136
Figure C34. Chemglaze Z306 black polyurethane paint on Experiment M0003 composite panel, viewed at 200X magnification, showing a dispersed silicate layer. Color version of figure 34, page 35.	136
Figure C35. Chemglaze A971 yellow polyurethane paint from the leading edge (row 9) scuff plate, shown at 200X magnification. At center is loose clump of pigment, dark freckles are areas of darkened organic resin. Color version of figure 35, page 36.	137
Figure C36. Chemglaze A971 yellow polyurethane paint from the leading edge (row 9) scuff plate, shown at 200X magnification. The focus is on the track of a organic fiber which was a contaminant in the paint and subsequently eroded by AO where it emerged through the surface. Color version of figure 36, page 37.	138
Figure C46. Cross-section of Chemglaze A276 white paint on tray clamp C8-5 (500X magnification), showing lifting of loose pigment into the encapsulant. Color version of figure 46, page 47.	139
Figure C47. Cross-section of Chemglaze A276 white paint on tray clamp C8-5 (500X magnification), showing a typical crack passing down to aluminum substrate. Color version of figure 47, page 47.	139
Figure C56. Cross-section of Chemglaze A276 white polyurethane paint on tray clamp B4-7 at 2500X magnification. Titania particles are visible to the very surface of the paint. The discolored layer is very thin, ~ 0.2 $\mu\text{m}$ . Color version of figure 56, page 52.	140

## ACRONYM LIST

AO	Atomic Oxygen
ASTM	American Society for Testing and Materials
ESCA	Electron Spectroscopy for Chemical Analysis
ESH	Equivalent Sun Hours
FEP	Fluorinated Ethylene Propylene
IR	Infrared
KSC	Kennedy Space Center
LDEF	Long Duration Exposure Facility
LEO	Low Earth Orbit
MSIG	Materials Special Investigation Group
NASA	National Aeronautics and Space Administration
SAEF-2	Spacecraft Assembly and Encapsulation Facility - 2
SEM	Scanning Electron Microscopy
UV	Ultraviolet



## 1.0 INTRODUCTION

This report summarizes the examination and testing of thermal control materials, specifically polyurethane paints, flown for approximately sixty-nine months in low Earth orbit (LEO) on exterior locations of the Long Duration Exposure Facility (LDEF). The purpose of the LDEF was to provide a platform for experiments requiring long-term exposure to a known LEO space environment. The thermal control coatings analyzed and reported here by the Materials Special Investigation Group (MSIG) came from various experiments and LDEF structural components, such as tray clamps and trunnion scuff plates. The materials in this report were subjected to the full range of environmental conditions generated by the LDEF mission.

## 2.0 LDEF MISSION PROFILE

The LDEF is a large (about 9 meters in length, 4.3 meters in diameter), reusable, unmanned spacecraft built to accommodate technology, science, and applications experiments which require long-term exposure to the space environment. LDEF is designed to be transported into space in the payload bay of a Space Shuttle, free-fly in LEO for an extended time period, and then be retrieved by a Space Shuttle during a later flight. The LDEF is passively stabilized when in orbit, and each surface maintains a constant orientation with respect to the direction of motion.

The LDEF was deployed by the Space Shuttle Challenger into a 482 km nearly circular orbit with a 28.4 degree inclination on April 7, 1984. The planned 10-month to 1-year mission carried 57 experiments. Due to schedule changes and the loss of Challenger, the duration of the LDEF flight extended well beyond the original planned exposure period.

The LDEF was retrieved by the Space Shuttle Columbia on January 12, 1990 after spending 69 months in orbit. During the 69 months, LDEF completed 32,422 orbits of Earth and had decreased in altitude to 340 km when it was recovered. Extensive photography was conducted from the Shuttle crew cabin, as demonstrated by figure 1, and then LDEF was placed in the Shuttle payload bay for return to Earth. The LDEF remained in the payload bay of the Shuttle for the landing at Edwards Air Force Base and during the ferry flight to Kennedy Space Center (KSC). At KSC, the LDEF was removed from Space Shuttle Columbia and transported to the Spacecraft Assembly and Encapsulation Building (SAEF-2) where the LDEF and its experiments were examined visually and photographed, radiation measurements were conducted, and the experiments removed from the structure tray-by-tray. Each tray was photographed individually after removal. System level tests were carried out for particular experiments and support hardware, and external surfaces were examined for evidence of impacts, contamination, and other exposure induced changes.

The atomic oxygen and ultraviolet radiation environmental conditions to which thermal control surfaces were exposed are summarized in figures 2 and 3, as a function of location on LDEF surfaces (ref. 1 and 2). The thermal environment experienced by these materials can be inferred from temperature measurements recorded during the first year of the LDEF mission (ref. 3). LDEF used a passive thermal design, relying on

thermal control coatings and internal heat paths for temperature control and equalization. A moderate thermal environment was achieved, as modeled, with measured temperatures ranging from a low of 39°F to a high of 134°F. Consequently, a thermal contribution was not considered in this analysis of LDEF thermal control materials.

### 3.0 HARDWARE DESCRIPTIONS AND LOCATIONS

Boeing Defense & Space Group analyzed several thermal control coatings as the contractor to NASA Langley Research Center in support of the Long Duration Exposure Facility MSIG, and as investigators on LDEF subexperiment M0003-8. The materials to be discussed in this report are polyurethane paints, specifically the Chemglaze A276, A971, and Z306 coatings from Lord Corporation, Coatings Division.

White-on-black disks of polyurethane thermal control paints were applied to over two hundred of the experiment tray clamps on LDEF. The purpose of these disks was to act as highly visible reference points in video and photographs of LDEF (see figure 4) as part of a spacecraft stabilization experiment after deployment (ref. 4). These paint disks now exhibit varying degrees of discoloration and deterioration as a result of space environmental exposure. Since the specific thermal control paints used are standard materials for spacecraft use, the extent and nature of the changes in these materials needed to be determined for future design. In addition, these disks also provided a unique opportunity to characterize two common materials for all surface locations available on LDEF.

The thermal control coating disks are described as 4 cm diameter disks of Chemglaze Z306 black polyurethane thermal control paint applied to 38% of the anodized 6061-T6 aluminum alloy tray clamps. A 3 cm diameter aluminum foil disk, which had been coated with Chemglaze A276 white polyurethane thermal control paint, was adhesively bonded in the center of each black disk. Chemglaze 9924 primer was used prior to the application of Z306 on the tray clamps, and prior to the application of A276 to the adhesive backed aluminum foil. A cross-sectional depiction of a thermal control coating disk is shown in figure 5.

The appearance of the thermal control coating paint disks at retrieval varied as a function of position on LDEF. The white paint disks on leading edge rows were mottled but still white, with black paint occasionally eroded down to the red primer. The disks on trailing edge rows showed that the white paint had discolored to a brown color, and that the black paint appeared unaffected. The transition region, showing the area where the white paint disks changed from white to brown, is pictured in figure 4. Disks on Earth and space ends had varying degrees of discoloration, with some disks showing a partial discoloration of the white coating, as shown in figure 6. After extended exposure to the terrestrial atmosphere since the LDEF recovery, the discolored white coating specimens have not measurably recovered any of their original reflectivity. Although it is not quantifiable, the appearance of white paint disks in on-orbit photographs is not different from how they currently appear 45 months after LDEF retrieval.

Identification for the paint disk specimens is; Bay (letter) Row (number) to identify the tray held by the clamp and a number corresponding to the clamp position on that tray.

Clamp position numbering for all side trays is illustrated in figure 7. The clamp position number for Earth and space end trays are shown in figure 8, defined by the removal sequence performed during LDEF deintegration. Bay and row positions are defined in figure 9, including LDEF experiment identification numbers. Positions of paint disk specimens, with corresponding atomic oxygen (AO) and ultraviolet (UV) radiation exposure conditions (ref. 1 and 2) are located in Appendix A. The row numbers used in Appendix A indicate a half row number for specimens located on longerons.

The Z306 black and A276 white polyurethane coatings were also applied to a graphite epoxy composite panel flown on experiment M0003-8. This experiment was located on tray D9, with the coatings subsequently exposed to  $8.7 \times 10^{21}$  oxygen atoms /  $\text{cm}^2$  and to 11,200 equivalent sun hours (ESH) of UV radiation (ref. 1 and 2). A photograph of the painted composite panel, taken during LDEF deintegration, is shown in figure 10. Impacts on the panel are visible on the A276 white paint in the upper left quadrant. The Z306 black paint is located in the upper right quadrant. Another white polyurethane paint flown only on this particular experiment, Boeing Material Specification 10-60, is located in the lower right quadrant. The lower left quadrant is unpainted composite.

The A971 yellow polyurethane coating specimens were parts from trunnion scuff plate assemblies, located between trays C3 and D3 and between trays C9 and D9 on the LDEF center ring frame. The trunnion scuff plates are part of the interface between LDEF and the Space Shuttle payload bay. The A971 coating specimens are shown in figure 11. The lower specimen was exposed to  $1.3 \times 10^{17}$  oxygen atoms/ $\text{cm}^2$  and 11,100 ESH of UV radiation. The upper specimen, lighter in color, was exposed to  $9.0 \times 10^{21}$  oxygen atoms/ $\text{cm}^2$  and 11,200 ESH of UV radiation (ref. 1 and 2).

## 4.0 RESULTS AND DISCUSSION

### 4.1 Optical Microscopy

Low magnification (16X) microscopy was used to observe contaminants and the general integrity of tray clamp paint disk specimens. Contamination from numerous sources was observed on all specimens. Fibers and shop debris were seen imbedded in uneroded paint coatings (see figures 12 and 13). Yellow particles were observed on and around the black paint on one specimen, apparently the result of paint overspray from when the tray clamp disks were originally painted (see figure 14). The yellow particles, from an unidentified paint, were determined to be preflight contamination because of the smearing of these particles under fastener hardware applied at the time of spacecraft integration, also visible in figure 14. Uneroded white paint disks exhibited solvent marks, where it appears that a solvent wiping operation wicked contaminants into the coating surfaces, resulting in a mottled discoloration pattern after environmental exposure (see figures 13 and 15).

Cracking was observed in the white paint disks located in high AO fluence areas but not in those located in low AO fluence areas. Cracking was sometimes localized to the edge region of these disks (see figures 16 and 17), but was also observed as a pattern of parallel cracks on large areas of the bulk white coating (see figure 18). Occlusions in the

white paint were also made visible through the process of AO erosion (see figures 19 and 20). AO erosion left a very fragile surface layer on the white A276 paint that was occasionally damaged by incidental handling during deintegration and storage (see figures 17, 21, and 22). AO erosion of the black Z306 paint is also apparent, based on visibility of the red primer layer (see figure 23).

High magnification (100X to 1000X) optical microscopy was used to observe the white paint disk surfaces with both bright field and dark field illumination. Bright field illumination indicated that trailing edge white paint surfaces were still resin rich (see figures 24 and 25), whereas leading edge white paint surfaces were now pigment rich (see figures 26 and 27). Dark field illumination revealed that the pigment particles in discolored white paint disks were still very reflective (see figures 28 and 29), indicating that the pigment particles themselves had not discolored due to space environmental exposure. Dark field illumination micrographs for leading edge white paint are shown in figures 30 and 31 for comparison.

High magnification (200X) optical microscopy was used to examine the Z306 black paint surface on the experiment M0003 composite panel. AO erosion had removed a significant portion of the black thermal control coating, revealing the underlying red primer. Figures 32 - 34 focus principally on inhomogeneities left behind on the eroded Z306 surface, but each also includes a representative indication of the state of the Z306 after exposure to atomic oxygen. Also visible was what appeared to be a silicate residue (highly visible in figure 34), left behind after AO erosion had oxidized the bulk of the Z306 paint layer. Silicates are used as part of the pigment package in Z306. Optical microscopy measurements indicated that the cracks in this AO eroded Z306 specimen extended approximately 20 $\mu$ m down into the coating material from the present surface.

The surface of A971 yellow paint on the scuff plate located on the leading edge of LDEF (row 9) is shown in figures 35 and 36. As with the white paint surfaces located in the leading edge environment, AO had largely removed the organic resin from the paint surface. Figure 35 shows a clump of pigment protruding from the paint surface. Also visible are small pockets of UV-radiation damaged paint resin not completely removed by reaction with atomic oxygen. Figure 36 focuses on the imprint left behind by a fiber that had been imbedded in the paint surface during application. The fiber was apparently composed entirely of organic material since it was completely eroded by AO where accessible to the surface.

## 4.2 Contamination Analysis

Contamination analysis was conducted to determine if the A276 white coating discoloration was due, principally or in part, to the deposition of a contaminant. Initial analyses were conducted nondestructively. Twelve white paint specimens from various locations around LDEF were measured for total and diffuse infrared reflectance using a BioRad Digilab FTS-6 Fourier Transform Infrared Spectrophotometer (the resulting spectra are located in Appendix B). Specular reflectance spectra for each material were calculated by difference. No significantly different absorptances from specimen to specimen, indicative of surface contaminants, were observed by this method.

Several specimens were analyzed spectroscopically from the visible through near infrared (IR) wavelengths, as is used to evaluate solar absorptance characteristics. Measurements were made using a Perkin-Elmer Lambda 9 Ultraviolet/Visible-Near Infrared Spectrophotometer. Representative total and diffuse reflectance spectra are included here for illustrating the results of these measurements: control specimen in figures 37 and 38; a trailing edge specimen in figures 39 and 40; and a leading edge specimen in figures 41 and 42. All of the specimens are principally diffuse in their reflective character. The total reflectance spectra for leading and trailing edge specimens were nearly identical in the near IR region (see figures 39 and 41), but trailing edge specimens were much less reflective in the visible region of the spectra (400 to 700 nm), as expected by their obvious discoloration. There was no evidence of absorptions due to organic contaminants on trailing edge specimens as compared to control specimens.

Secondary analyses were conducted destructively. The discoloration of trailing edge white paints could not be removed with solvent wiping, using either methyl ethyl ketone or petroleum ether. Since the surface could not be removed for analysis with solvents, scrapings from control, leading edge, and trailing edge specimens were delicately taken with the aid of a microscope, in an attempt to remove the extreme surface layer (approximately 1 micron thick) for transmission IR spectroscopy. Examples of the resulting spectra are shown in figures 43 - 45. These spectra were made using a Perkin Elmer Model 1710 Fourier Transform Infrared Spectrophotometer with a Spectra-Tech Model 0043-033 IR microscope. The control spectrum in figure 43 indicates characteristic absorptions for the polyurethane resin (wavenumbers 2920, 2850, 1750, 1450 and 1280) and for the silicate binder (wavenumber 1010) in the paint pigment. The spectrum in figure 44 indicates that there was no detectable resin left on the surface of the leading edge white paint specimen, with the only absorption band attributable to the silicate binder. The spectrum in figure 45 for the trailing edge specimen, when compared directly with figure 43, indicates that the darkened paint surface is only slightly modified paint resin. If any organic contaminant contributes to the darkened surface of trailing edge white paint, it is not detectable or discernible by this technique.

### 4.3 Cross-Sectioning

Cross-sections were made of four disk specimens from different environments on the LDEF surface, after all nondestructive measurements for those specimens had been completed. Cross-sectioning done in an attempt to measure the depth of atomic oxygen induced resin recession on the leading edge white paint specimen was not successful. The surface of the eroded white paint specimens is essentially pigment particles, held in place by weak attractive forces due to the small size of the particles. When trying to mount the cross sections prior to polishing, those loosely attached pigment particles 'washed' off of the surface as seen in figure 46, making resin erosion measurements impossible.

Cracks observed by optical microscopy in the surfaces of leading edge white paint specimens (see figure 18) were observed in cross-section, as shown in figure 47. All cracks observed went completely through the coating system to substrate.

Cross sections were also used in an attempt to measure the extent of erosion on leading edge black paint. The results are questionable due to observed variability in the black paint coating thickness. Measurements of black paint thickness on trailing edge specimens, which should not be eroded by atomic oxygen, indicated as high as a 50% variation in paint thickness, as is seen in figures 48 - 51. In general, the black paint was observed to be thinner toward the outer (subsequently exposed) edge, probably as a consequence of the painting operation. The result of this variation is that the comparison of coating thicknesses in protected (under the white paint disk) and exposed areas to determine extent of coating erosion has a high degree of uncertainty. Cross-sections for leading edge Z306 specimens are shown in figures 52 - 55 for comparison.

Cross-sectioning was also used to characterize the darkened surface of trailing edge white paint on specimen B4-7. As pictured in figure 56, the darkened, or discolored layer in the white paint was found to be extremely thin, comparable to the size of the titania pigment particles or approximately 0.2  $\mu\text{m}$  in thickness. There also appeared to be titania pigment particles located in the discolored portion, indicating that the discoloration was due to radiation darkening of the very surface layer of the paint resin.

#### 4.4 Surface Analysis

A number of surface spectroscopy techniques were used to characterize the subject surfaces. Scanning electron microscopy (SEM) images of a leading edge A276 white paint disk are shown in figure 57 - 60. The 1000X and 5000X magnifications (figures 57 and 58) show the rough, porous character of the eroded surface. The 10,000X and 25,000X magnification images (figures 59 and 60) illustrate the near total absence of resin on paint surfaces subjected to high AO fluences. Electron microprobe chemical analyses of these surfaces are shown in figures 61 and 62. The submicron sized spherical particles are titania pigment. The larger plate-like particles have been identified as a magnesium silicate (see figure 62), most likely talc, a common binder or flattener in white paint pigment packages.

Additional SEM images were taken of irregular features on the A276 white paint surface. Figure 63 shows two such irregular surface features. Microprobe analysis of the spiral fiber indicated it to be an aluminum turning contaminating the paint (see figure 64). Analysis of the "flake" adjacent to the aluminum turning (see figure 65) is essentially identical to that of the bulk eroded paint surface (see figure 61). The "flake" was apparently a clump of pigment in the paint which was not completely dispersed during mixing prior to the paint application. Another interesting feature is that of a micrometeoroid/debris impact, shown in figure 66. Electron microprobe analysis of the bottom of the impact crater (see figure 67) indicated primarily aluminum (the paint disk substrate), titanium (from titania particles transferred from the eroded paint surface), and iron and manganese.

SEM images of the Z306 black paint surface from paint disks were of poor quality because of surface charging, despite multiple applications of vapor-deposited conductive metal. However, surface chemical analysis was obtainable by electron microprobe, as shown in figure 68. The presence of silicon was strongly indicated, caused by the silica used in the paint pigment package. The presence of chromium, iron, and zinc was

expected because the coating on this specimen had been eroded down to the primer layer in some areas, exposing the zinc chromate and iron oxide pigments in the primer. Potassium was also observed, apparently a contaminant in the primer pigments, and aluminum where coating cracks extended to the substrate.

Electron spectroscopy for chemical analysis (ESCA) was used to identify the chemical composition of the very surface (10Å depth) of A276 white and Z306 black coatings on paint disks. The ESCA measurements for A276 white are shown in figures 69 - 73, for Z306 black are shown in figures 74 - 78. In general, the presence of fluorine was detected on all specimen surfaces, with the exception of the control specimen and the leading edge black paint surface. That the fluorine was not observed on the control specimen indicated that the fluorine was deposited as a result of environmental exposure. The leading edge black paint specimen was in a continual state of erosion during exposure, especially in the latter stage of the LDEF mission, and the surface was being cleaned of any deposited materials. The source of fluorine would most likely have been from the decomposition and erosion of nearby FEP thermal control blankets, with deposition of fluorine on the subject paint surfaces not occurring through a typical line-of-sight mechanism.

Increased surface concentrations of silicon, as compared to the control specimen surfaces, were also observed using ESCA. The increased levels of silicon observed on leading edge A276 white and Z306 black thermal control paints would be expected. Both the black and white paints contain a significant amount of silicates as part of their pigment systems, which was left behind after AO erosion of the paint resin fraction. However, the increased levels of silicon on trailing edge specimens were indicative of contaminant deposition.

#### 4.5 Optical Properties Measurements

Solar absorptance and thermal emittance measurements were made for 120 of the A276 white paint disks on LDEF. Optical property measurements for the Z306 black paint areas on the disks were not obtained due to their dimension and shape. Solar absorptance measurements were made in accordance with ASTM E424-71 (or ASTM E903-82), thermal emittance in accordance with ASTM E408-71. These measurements were made without removing the disks from the tray clamps.

Measurements made for white paint disks from the Earth and space ends of LDEF are shown in figure 79. Emittance measurements indicated no significant differences between disks on the Earth or space ends. The absorptance readings were generally greater for the peripheral areas at either end. Further discussion of the Earth and space end absorptance measurements will be made later with the correlations to environmental exposure.

The disks from the side trays which were available for MSIG analysis of absorptance and emittance are shown in figure 80. A portion of these disks were selected for analysis, as shown in figure 80, representing all available incidence angles and selecting additional specimens to test measurement variability along the length of the spacecraft.

Optical property measurements for LDEF tray clamps are located in Appendix A, including estimates of AO fluence and UV radiation exposure.

Absorptance measurements as a function of row position are shown in figure 81. Multiple specimens measured along a particular row indicated limited variability in absorptance. This variability was random, not indicating any trends in absorptance along the length of the spacecraft. The data do not quite form a symmetric distribution due to the offset in LDEF yaw (ref. 5). Control specimen absorptance was comparable to that from specimens on rows 9 and 10.

Emittance measurements as a function of row position are shown in figure 82. Control specimen emittance was comparable to measurements made for specimens on trailing edge surfaces, rows 1 through 6.

The absorptance and emittance measurements were plotted versus angle of AO incidence in figures 83 and 84. The incidence angles were based on an assumed eight degree offset in yaw angle (ref. 5). Figure 83 shows that the erosion effect of atomic oxygen yielded low absorptance levels for the A276 paint for incidence angles up to 80 degrees, with an apparent atomic oxygen effect discernible to an incidence angle of 100 degrees. It is actually fortunate for the present analysis that LDEF had a yaw offset. Due to the extremely steep solar absorptance change in the AO fluence transition region, the yaw offset provided two separate incidence angle environments in the transition area. Statistical analysis conducted on the emittance measurements graphed in figure 84 indicated a marginal but significant increase in emittance for leading edge white paint specimens (incidence angle less than 70°,  $\epsilon = 0.89 \pm 0.01$ ) as compared to the control ( $\epsilon = 0.87$ ) and to trailing edge specimens (incidence angle greater than 100°,  $\epsilon = 0.86 \pm 0.01$ ). The increase in emittance is consistent with the roughening of leading edge surfaces observed by microscopy, caused by atomic oxygen erosion of the paint resin.

In an attempt to characterize the environmentally induced changes observed for A276 paint, figure 85 represents solar absorptance measurements as a function of atomic oxygen fluence. The atomic oxygen fluence levels used in figure 85 are predictions based on the LDEF AO fluence model developed by Boeing (ref. 1). Atomic oxygen fluence is represented logarithmically. Absorptance data from Earth and space end disks are not included in figure 85, due to the scatter in those data which will be discussed later. From figure 85, a fluence level of  $10^{21}$  oxygen atoms per  $\text{cm}^2$  was necessary to cause sufficient resin erosion in the A276 white thermal control paint to maintain coating optical performance, removing the darkened resin which degraded the coating's absorptance.

However, it must be recognized that coupled with the atomic oxygen effect was the effect of UV radiation. Figure 86 shows the absorptance of all A276 white paint disks measured, including Earth and space end disks, as a function of predicted solar fluence in equivalent sun hours (ref. 2). Also included in figure 86 are data from LDEF Experiment S0069 for comparison (ref. 6).

The scatter in solar absorptance data obtained for the Earth and space ends paint disks mentioned previously is shown in figure 86. Both Earth and space end disks were

predicted to receive approximately the same fluences of atomic oxygen, with a one degree vehicle pitch offset, ignoring any over-riding effects of local environments. However, it was apparent that there were some local environmental differences which resulted in the observed absorptance data scatter. A trend of increased solar absorptance with increasing UV exposure was apparent with the Earth and space end disk data. But the ends of the LDEF spacecraft were in the transition region with regards to atomic oxygen, where slight differences in surface orientation and position could markedly affect atomic oxygen fluence. When compared to absorptance data from the disks on LDEF side trays, data from the space end disks indicated incidence angles ranging from 85 to 105 degrees.

Figure 86 suggests a solar absorptance increase for A276 that accompanied increasing UV exposure in the absence of atomic oxygen. Part of the evidence for this trend is from the data provided by experiment S0069, where in-situ absorptance measurements were made and recorded as a function of mission time. Experiment S0069 measured an increase in the absorptance of A276 occurring in the early, low atomic oxygen flux portion of the LDEF mission. Taken as a whole, the data in figure 86 suggest that all of the A276 paint disks were darkening according to this trend in the initial years of the LDEF mission. This was when LDEF was still in a relatively high orbit. But as the orbital altitude began to decay, the atomic oxygen flux began to increase rapidly. The AO flux model has predicted that about 54% of the atomic oxygen fluence on LDEF occurred in the last six months of the mission (ref. 1). It was during this latter phase of the LDEF mission that atomic oxygen erosion removed UV damaged paint resin where the total fluence was sufficient, and brought A276 absorptance readings back to nominal levels on leading edge specimens. It does not appear that the trailing edge specimens have yet reached an end-of-life condition versus UV exposure, although the apparent rate of absorptance degradation with UV exposure has decreased significantly for the highest level UV exposed specimens. It does, however, appear that the leading edge specimens have reached an end-of-life condition versus AO exposure.

The optical properties of the Z306 black thermal control coating were measured from the coated composite specimen on experiment M0003. The solar absorptance was measured to be 0.93, which was only a 0.02 unit reduction from the initial absorptance of 0.95 for the coating. This was somewhat of a surprising result considering the amount of red primer pigment readily visible on the surface. The thermal emittance was measured as 0.94, which was an increase of 0.04 apparently due to the roughening and diffuse character of the eroded surface.

Optical properties have been analyzed for the A971 yellow coating on LDEF scuff plates, shown in Table 1. Solar absorptance for the trailing edge specimen was 0.12 higher than what was measured on a vendor supplied sample. It is significant that the absorptance of the trailing edge A971 coating was comparable to that measured for A276 white polyurethane paint exposed to the same environmental conditions. The absorptance of the leading edge A971 specimen was slightly degraded compared to the control. Apparently not quite all of the UV damaged polyurethane resin had been removed from the scuff plate surface (see also figure 35). The thermal emittance for the trailing edge specimen was 0.87, essentially what was expected for a gloss polyurethane paint without atomic oxygen exposure and consistent with observations for comparably

exposed A276 white polyurethane paint. However, comparison to the "control" was poor, indicating a difference in coating thicknesses for the two specimens. The leading edge thermal emittance was slightly higher than that measured for the trailing edge specimen, again comparable to what was observed for the A276 white paint disks based on increased surface roughness due to AO erosion.

Table 1. Optical Properties For A971 Yellow Polyurethane Coating.

Specimen	Solar Absorptance	Thermal Emittance
Vendor Applied in 1992 ("Control")	0.46	0.83
Leading Edge Scuff Plate Segment, Part No. LDE816105-1C182	0.50	0.89
Trailing Edge Scuff Plate Segment, Part No. LDE816105-1C33	0.58	0.87

#### 4.6 Other Measurements and Analysis

Additional measurements were made in an attempt to clarify the extent of AO attack on the thermal control coatings, where attempts such as cross-sectioning had failed. One such measurement involved the A276 paint on the composite panel from experiment M0003. The composite panel had areas totally protected from atomic oxygen attack, where washers had been used for attachment of the panel to support structure. The measurement involved determining how deeply atomic oxygen was able to penetrate into the layer of remaining pigment particles by measuring how deep the exposed paint was damaged from a physical integrity perspective. Specimens were cut from around the protected attachment areas, and the loose pigment on AO eroded surfaces was totally removed by repeated rag wiping until no more pigment loss was observed. Surface profiles from the specimens were then measured using laser profilometry. Height profiles from these measurements are shown in figures 87 - 92. Figure 87 exhibits an anomalous region at the protected to exposed interface, apparently the result of a cut formed by the sharp edge of the washer when it spun on the surface during fastener removal. Maximum coating loss measurements ranged from 0.00025 inch in figure 92 to 0.00050 inch in figure 90. Average AO erosion damage depth was determined to be 0.00038 inch or 9.6  $\mu\text{m}$ .

The extent of black thermal control paint AO erosion was estimated by cross-sectioning (see section 4.3) to be about 10  $\mu\text{m}$  (0.0004 inch), but the extent of Z306 erosion can be analyzed qualitatively from another perspective. Many of paint disks from the leading edge area had the exposed black paint completely eroded away, leaving only the characteristic red of the underlying primer pigment. The primary surface on tray E9 had also been painted with Z306, and portions of this surface were eroded down to the primer as a result of atomic oxygen exposure. The Z306 applied to the composite panel on experiment M0003 was also largely removed as a result of AO erosion. If one considers the minimum and typical thickness at which Z306 is generally applied, it can lead to at least a range of erosion that occurred for this material. The minimum thickness of paint measured on paint disk cross-sections was 10  $\mu\text{m}$ . Polyurethane paints are more typically applied to a minimum thickness of 25  $\mu\text{m}$ . These thicknesses provide a range

of Z306 black paint erosion that occurred on LDEF leading edge surfaces. This erosion range would indicate that the Z306 coating was more resistant to atomic oxygen erosion than the unpainted graphite fiber reinforced epoxy composite, which exhibited complete erosion to an average depth of 86  $\mu\text{m}$  (ref. 7). However, the AO erosion "resistance" of Z306 as compared to the composite can be attributed to the silicate content in the paint, which when left behind on surfaces eroded by AO slowed further erosion. Silicate residues on eroded Z306 were verified in surface analyses (see section 4.4)

Erosion measurements were also made for the A971 yellow coating. The assumption was made that the two parts were painted to the same coating thicknesses, since they were painted commensurately. The trailing edge specimen from row 3 had an average total coating thickness of 58  $\mu\text{m}$  (0.0023 inch) based on 18 measurements. After thoroughly rag wiping the leading edge specimen from row 9, the average total coating thickness was 48  $\mu\text{m}$  (0.0019 inch), indicated an AO erosion damage depth of 10  $\mu\text{m}$  (0.0004 inch). This measurement is in close agreement with the measurements made for the A276 white paint erosion depth using laser profilometry from protected to AO damaged areas.

## 5.0 CONCLUSIONS

The first goal of the thermal control coating disks analysis was to determine if the discoloration observed for A276 white paint was due to pigment discoloration, resin degradation, contaminant deposition, or a combination of these effects. Surface microscopy has shown that pigment discoloration did not occur. Cross-sectioning microscopy also indicated that the A276 surface discoloration was limited to the upper 0.1-0.2  $\mu\text{m}$  of the paint surface and did not involve the paint pigment. Surface spectroscopy has shown that there are contaminants detectable on stable surfaces. Fluorine and increased levels of silicon were detected on all flight specimens, with the exception of no fluorine on Z306 black paint on leading edge disks which were in a continual state of atomic oxygen erosion. However, the amount of these contaminants was quite low, much too low to cause the measured increases in solar absorptance for A276 white paint. IR spectra of surface scrapings from discolored A276 paint, as compared to control paint, indicated that the discoloration was principally in the paint resin itself, induced by the thousands of hours of UV exposure attained with LDEF.

The second goal of the analysis was to quantify changes in design properties which resulted from space environmental exposure. Surfaces exposed to atomic oxygen up to an incidence angle of 100 degrees showed evidence of surface erosion. A276 paint surfaces at and near the leading edge had very little visible organic resin remaining, and this AO erosion apparently led to cracking and crazing. The depth of erosion damage which occurred for A276 specimens was determined to be approximately 10  $\mu\text{m}$  (0.0004 inch). Measurements made with leading edge and trailing edge specimens of A971 yellow paint corroborated the A276 results. This erosion damage depth is interpreted as the limit to which AO damage can occur into a paint with inert pigments. Measurements of AO erosion for Z306 black paint based on cross-sections have been questionable, due to the observed variability in coating thickness. Typical Z306 coating thickness coupled with observation of near complete coating loss because of AO erosion has lead to an

estimate of 25  $\mu\text{m}$  of coating loss during the LDEF mission. Silicate residues from the Z306 pigment system, left behind during AO erosion, provided some protection to the coating, making an estimate of Z306 atomic oxygen erosion rate of questionable value.

Optical property measurements for A276 white paint have been matched to modeled predictions of atomic oxygen fluence and UV exposure. These comparisons have suggested a trend of increasing absorptance for A276 white paint with UV exposure. This trend helps to corroborate the spectroscopic evidence that the darkened A276 paint was caused by UV induced degradation of the paint resin system. Solar absorptance measurements also indicated that sufficient atomic oxygen fluences were received at incidence angles up to 100 degrees to infer paint resin erosion. AO erosion significantly degraded the mechanical integrity of the paint coatings, but at incidence angles up to 80 degrees on the LDEF mission (with corresponding fluences of  $10^{21}$  oxygen atoms per  $\text{cm}^2$ ), this erosion was sufficient to bring UV damaged white paint back to near-original absorptance levels.

## 6.0 REFERENCES

1. R. J. Bourassa and H. G. Pippin; Model of Spacecraft Atomic Oxygen and Solar Exposure Microenvironments: LDEF Materials Results for Spacecraft Applications Conference, October 1992.
2. R. J. Bourassa and J. R. Gillis; Solar Exposure of LDEF Experiment Trays. NASA Contractor Report No. 189554, February 1992.
3. W. M. Berrios, Use of the LDEF's Thermal Measurement System for the Verification of Thermal Models, LDEF 69 Months in Space; First LDEF Post-Retrieval Conference, NASA CP-3134, Part I, p.69 (1991).
4. W. H. Kinard, ed.; LDEF Spaceflight Environmental Effects Newsletter, Vol. II, No. 5, p. 2 (1991).
5. P. N. Peters, P. L. Whitehouse, and J. C. Gregory; Refinements on the Pinhole Camera Measurements of the LDEF Attitude. Second LDEF Post-Retrieval Symposium, NASA CP-3194 Part I, p. 3, 1993.
6. D. R. Wilkes and L. L. Hummer; Thermal Control Surfaces Experiment Initial Flight Data Analysis Final Report. Prepared under NASA Contract No. NAS8-36289-SC03. AZ Technology Report No. 90-1-100-2, June 1991.
7. P. E. George, H. W. Dursch, and S. G. Hill; Space Environmental Effects on LDEF Composites: A Leading Edge Coated Graphite Epoxy Panel. Second LDEF Post-Retrieval Symposium, NASA CP-3194 Part III, p.923, 1993.

## 7.0 FIGURES

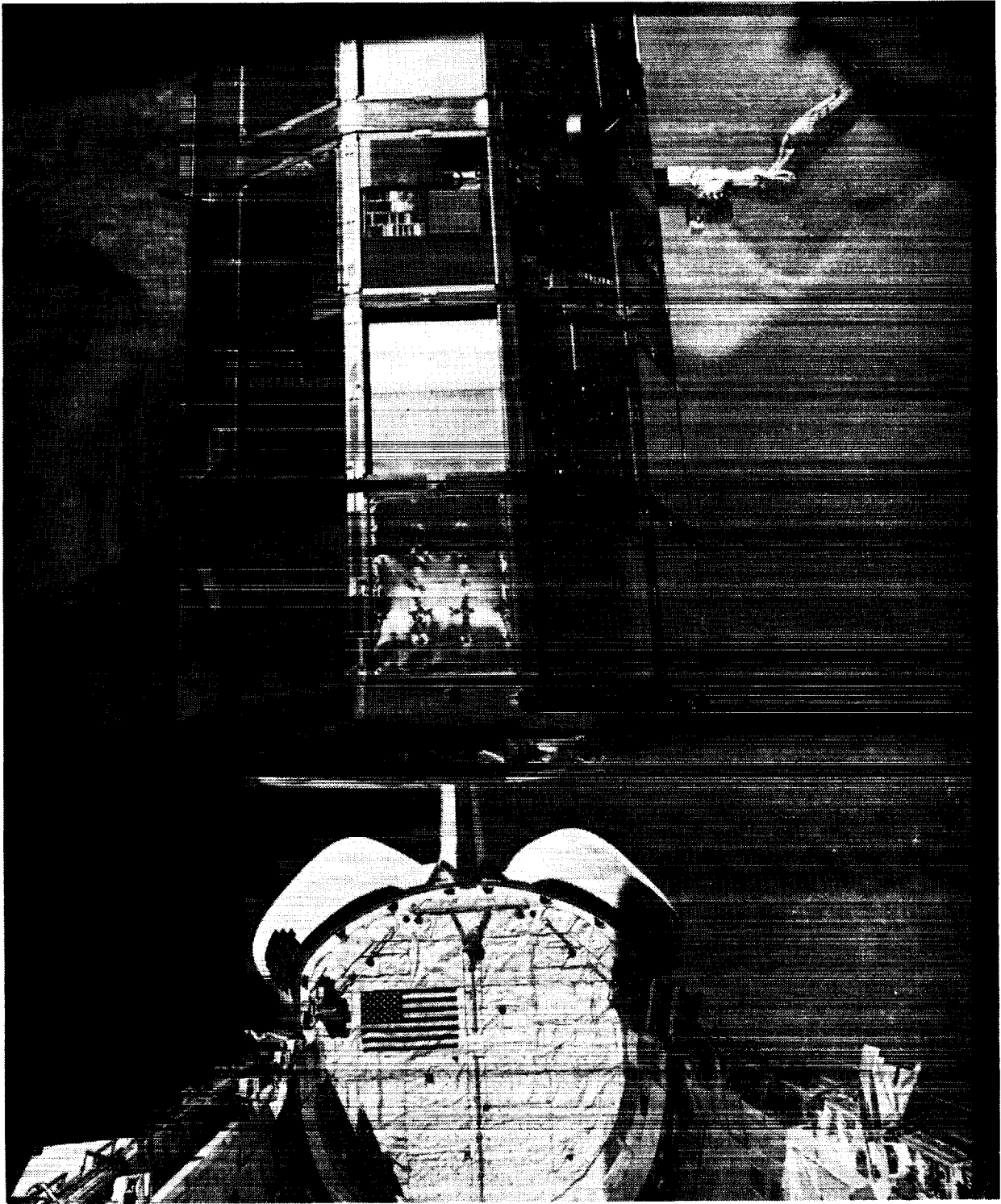


Figure 1. LDEF retrieved as viewed from the Shuttle Columbia on January 12, 1990. NASA Langley Research Center Photo No. 90-10472. See Appendix C for color figure.

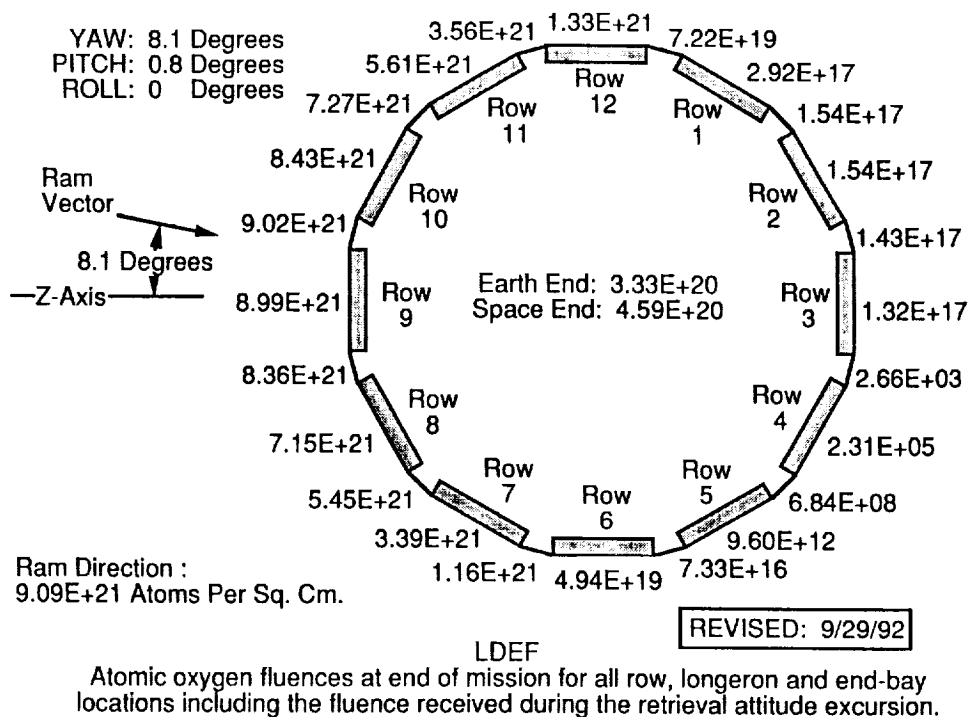


Figure 2. LDEF Atomic Oxygen (AO) Fluence Map (ref. 1)

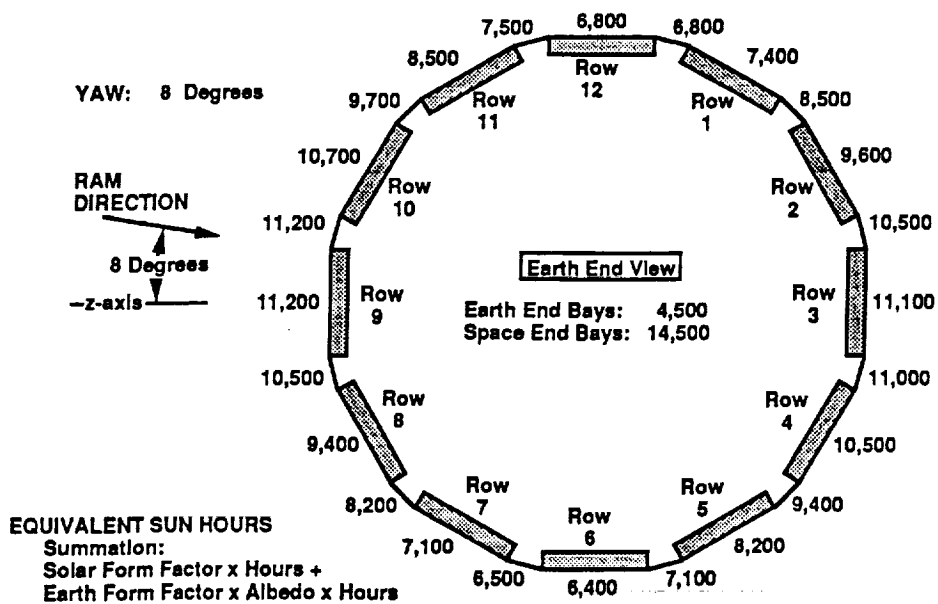


Figure 3. LDEF Ultraviolet (UV) Exposure Map (ref. 2)

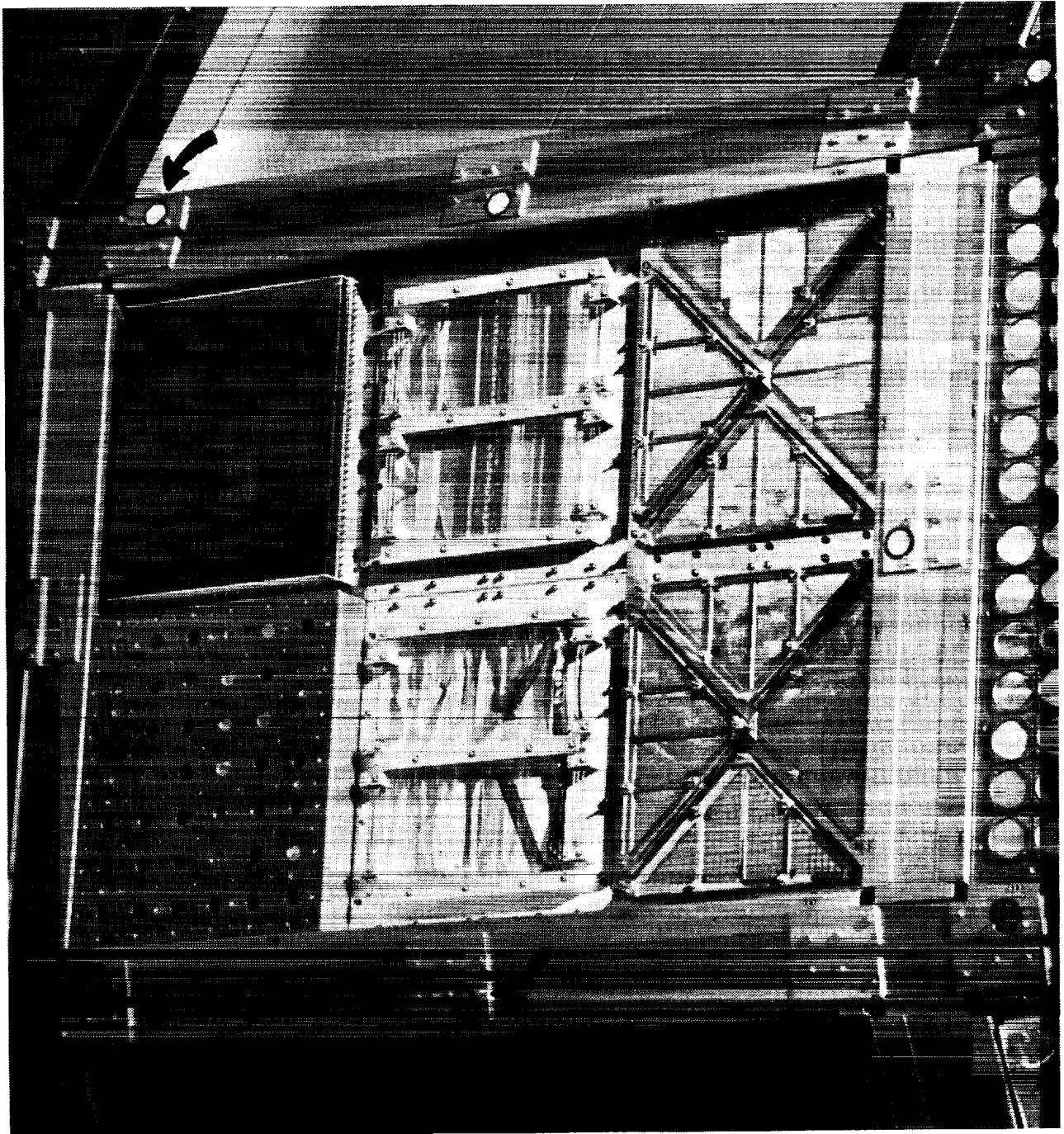


Figure 4. On-orbit view of paint disks on LDEF tray clamps in the atomic oxygen fluence transition region, tray E6. NASA Johnson Space Center Photo No. S32-82-040. Disks on upper longeron (see arrow) were in high AO fluence and are white, disks on lower longeron were in low AO fluence and are brown. See Appendix C for color figure.

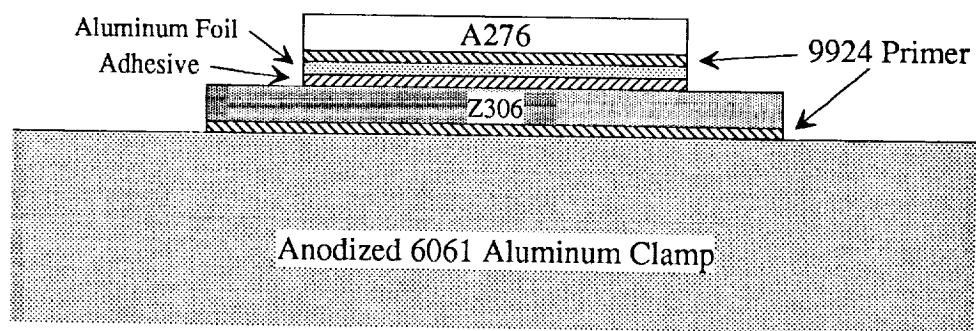


Figure 5. Cross-sectional representation of the components in a LDEF tray clamp paint disk. A276 and Z306 are Chemglaze polyurethane thermal control coatings. This depiction is not to scale.

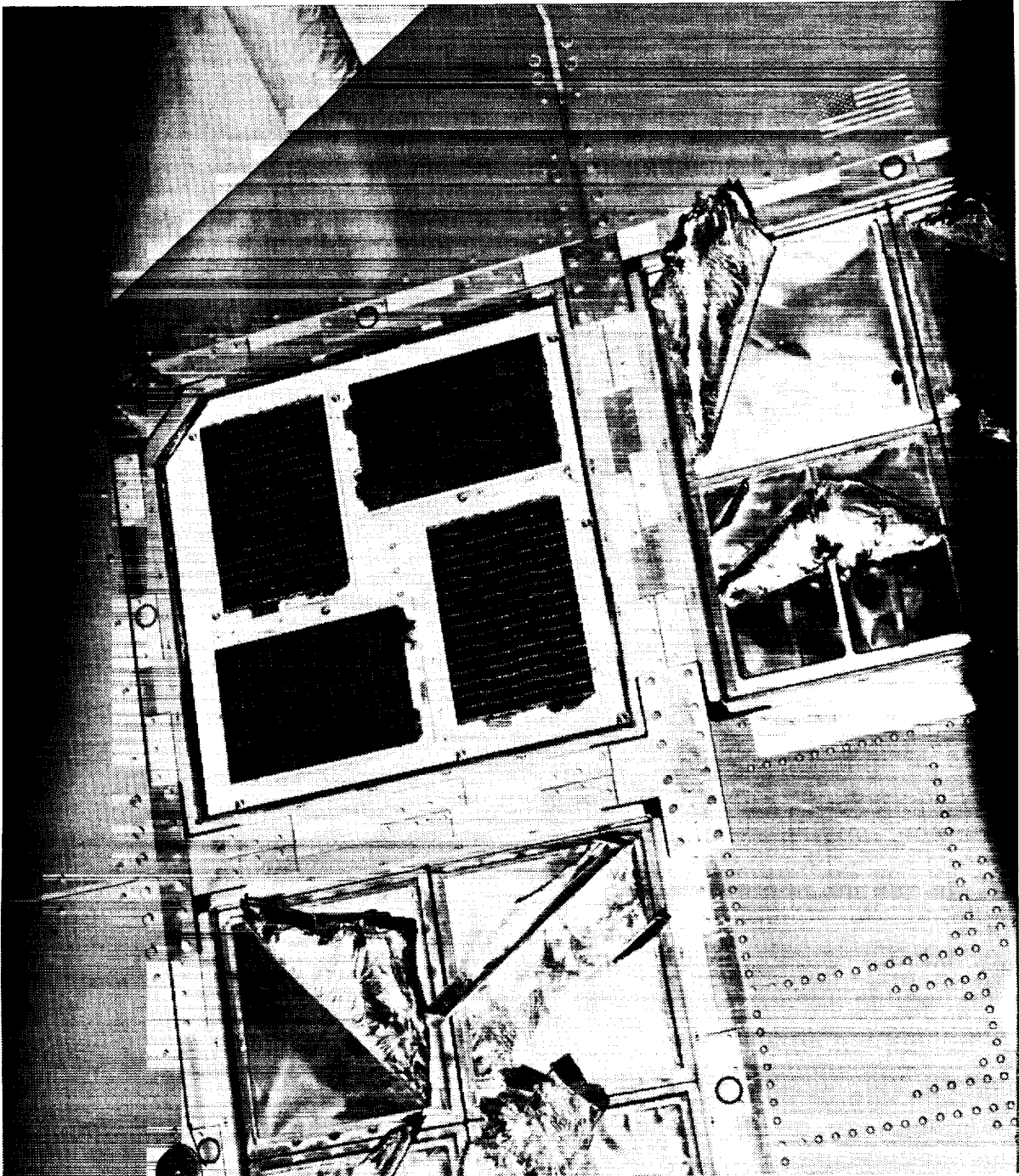


Figure 6. On-orbit view of paint disks on the space end of LDEF. NASA Johnson Space Center Photo No. S32-75-036. U. S. flag is above tray H12. See Appendix C for color figure.

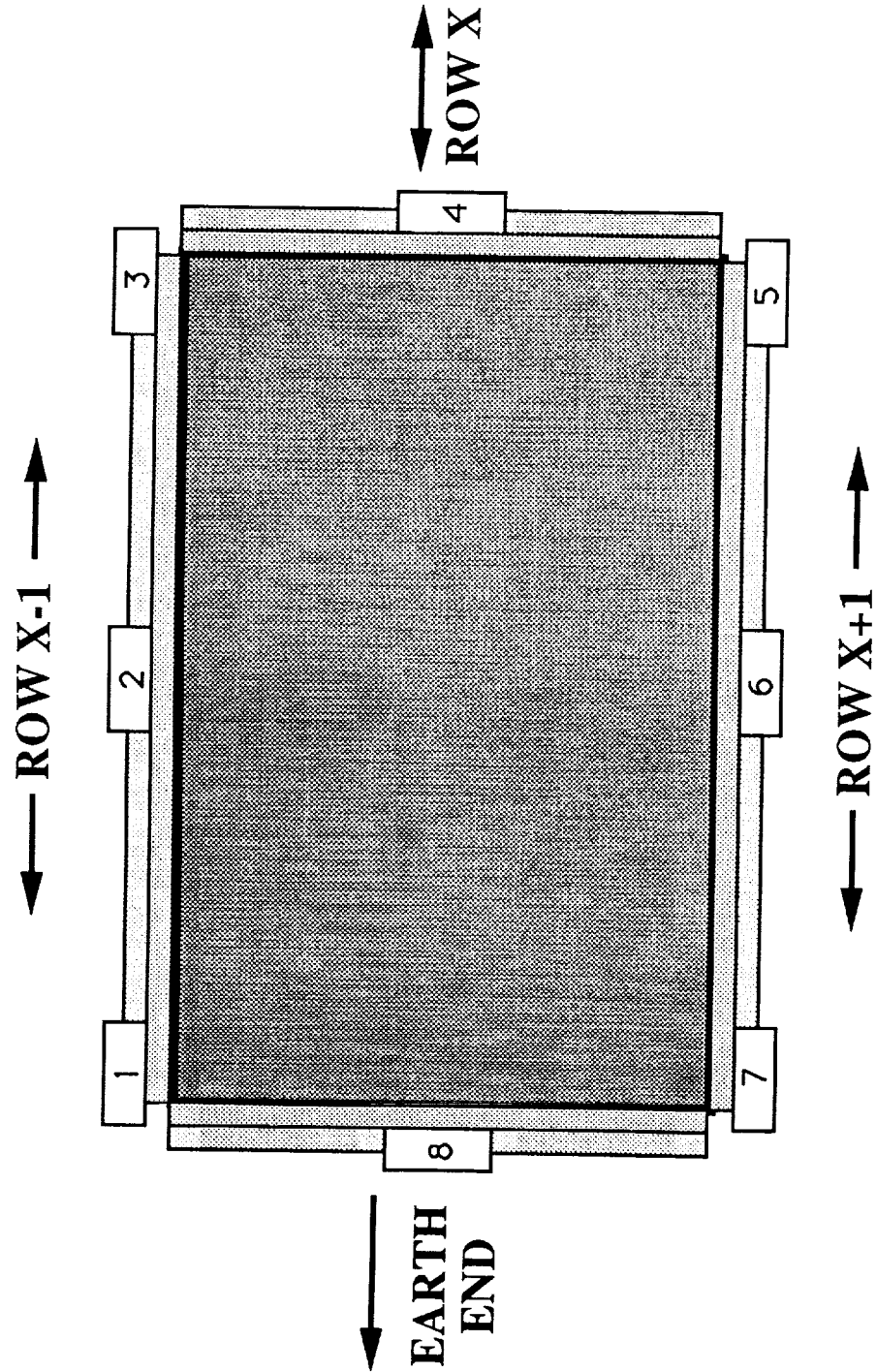


Figure 7. Tray clamp position numbering system for LDEF side trays.



BAY ROW	A	B	C		D	E	F
1	A0175	S0001	GRAPPLE		A0178	S0001	S0001
2	A0178	S0001	A0015, A0187, M0006		A0189, A0172 S0001	A0178	P0004, P0006
3	A0187	A0138	A0023, A0034, A0114, A0201	TRAILING EDGE	M0003, M0002	A0187, S1002	S0001
4	A0178	A0054	S0001		M0003	S0001	A0178
5	S0001	A0178	A0178		A0178	S0050, A0044, A0135	S0001
6	S0001	S0001	A0178	P0005 P0003	A0201, S0001	A0023, S1006 S1003, M0002	A0038
7	A0175	A0178	S0001		A0178	S0001	S0001
8	A0171	S0001, A0056, A0147	A0178		M0003	A0187	M0004
9	S0069	S0010, A0134	A0023, A0034 A0114, A0201	LEADING EDGE	M0003, M0002	S0014	A0076
10	A0178	S1005	GRAPPLE		A0054	A0178	S0001
11	A0187	S0001	A0178		A0178	S0001	S0001
12	S0001	A0201	S0109		A0023, A0019, A0180	A0038	S1001

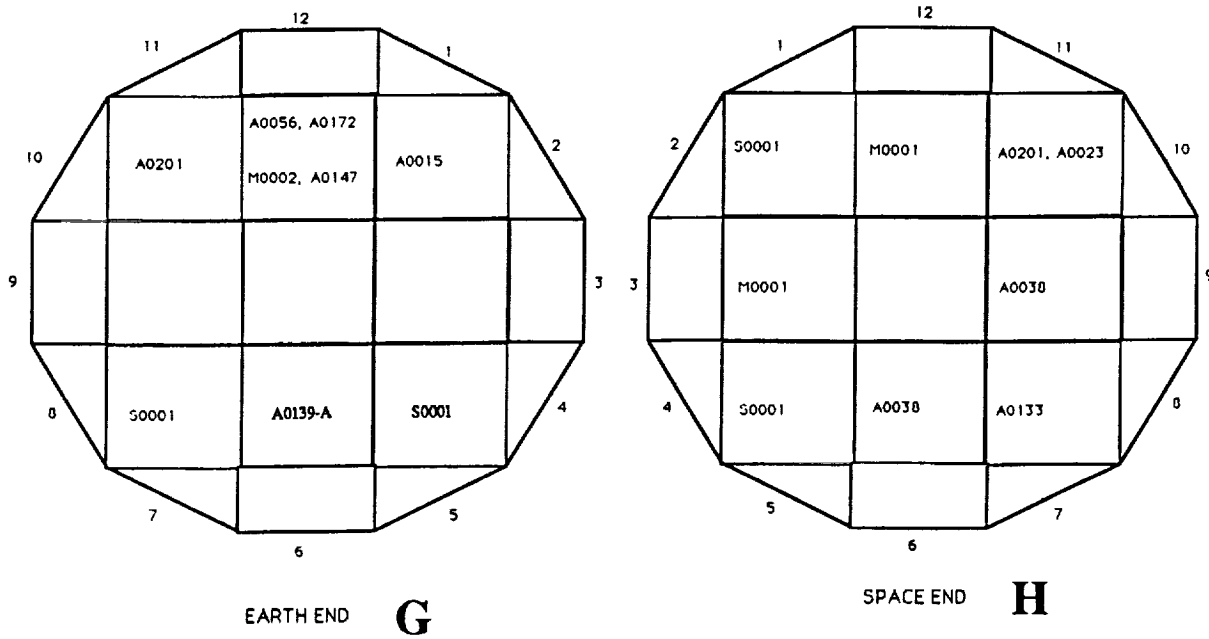


Figure 9. LDEF bay and row position map with experiment numbers.

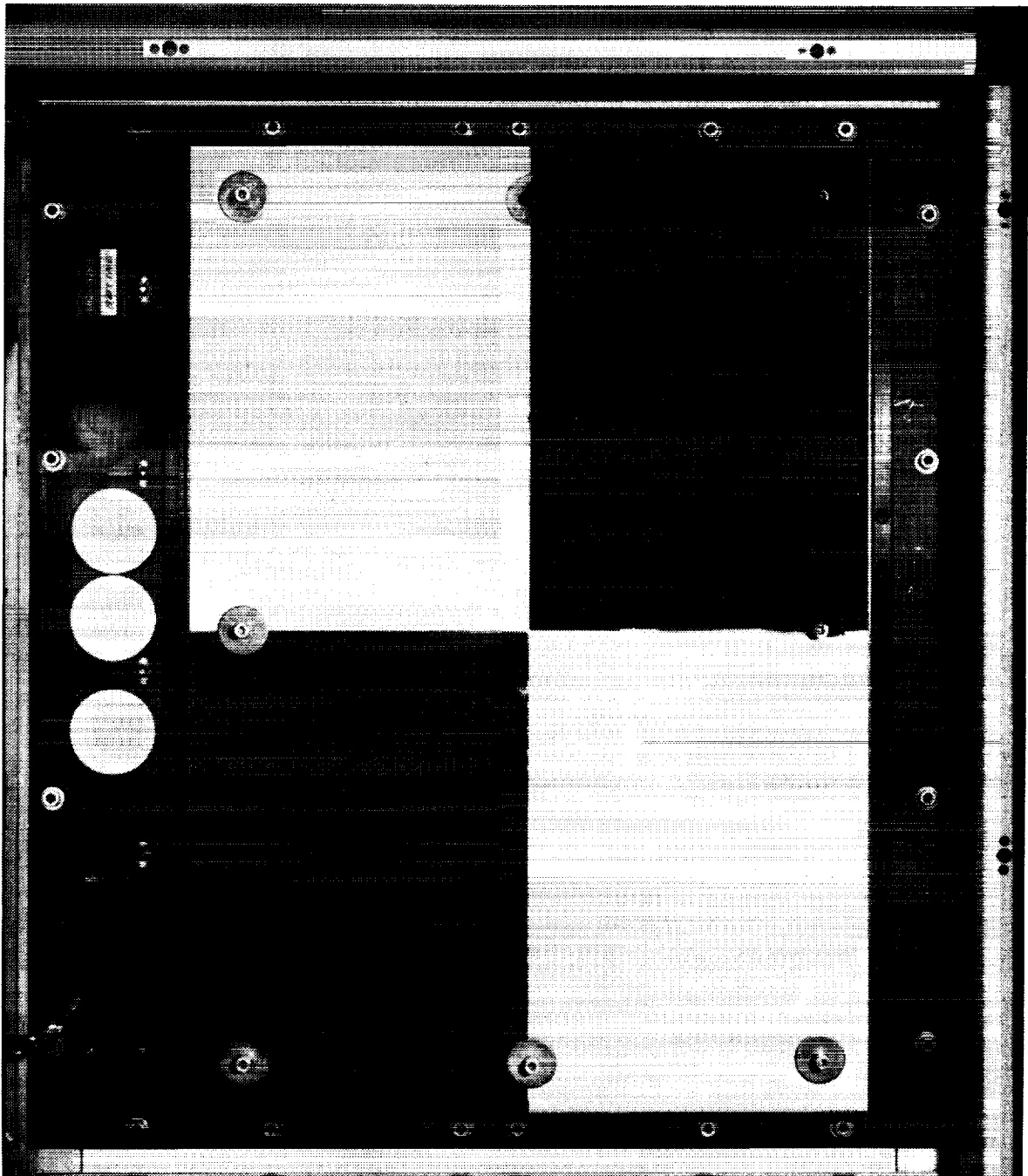


Figure 10. LDEF Experiment M0003 - painted composite panel, postflight. The coatings are (clockwise from upper left) Chemglaze A276, Chemglaze Z306, BMS 10-60 White Polyurethane, and unpainted T-300 graphite / 934 epoxy composite.

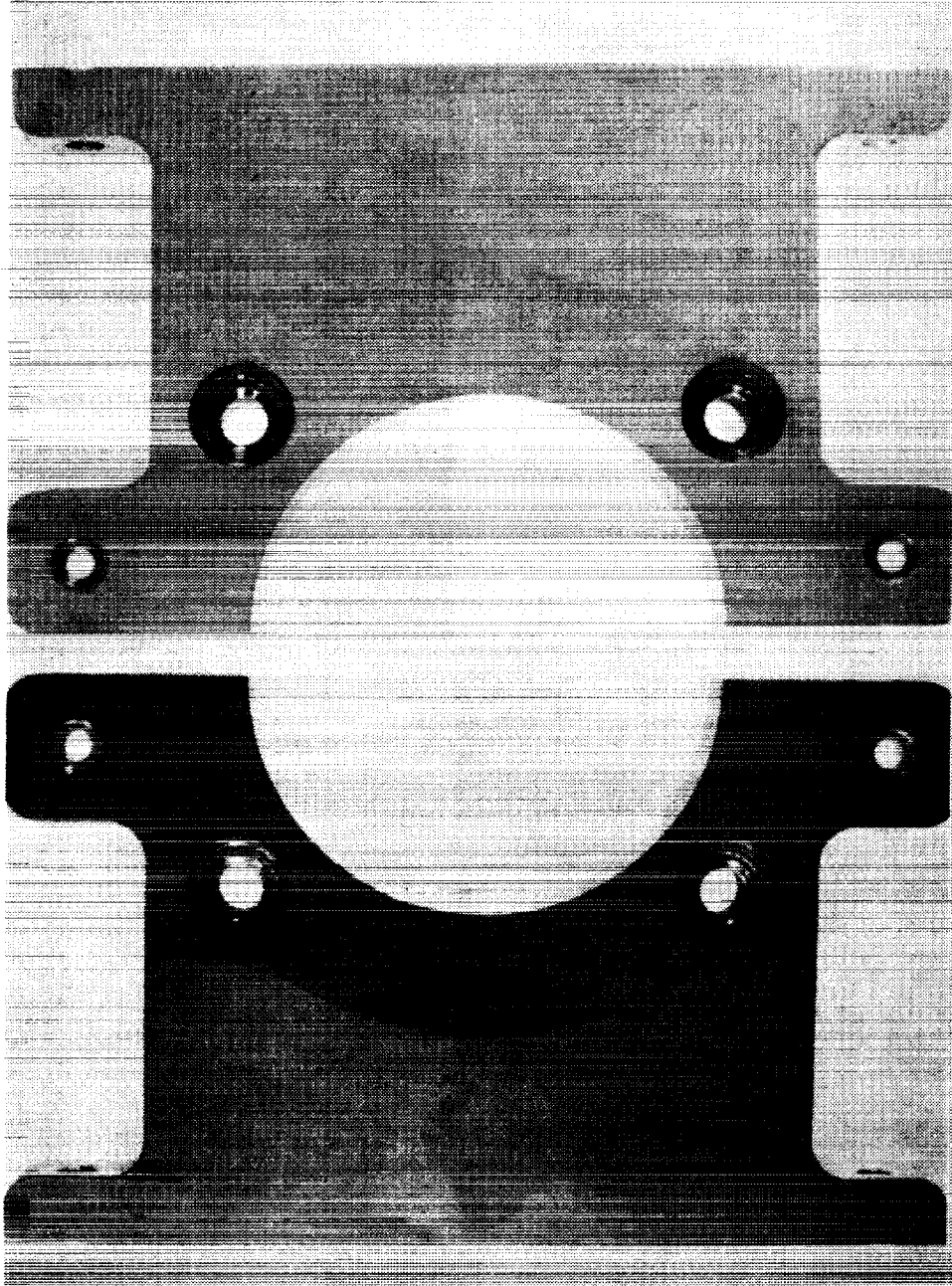


Figure 11. Chemglaze A971 yellow paint on components of the leading (above) and trailing edge scuff plates. See Appendix C for color figure.

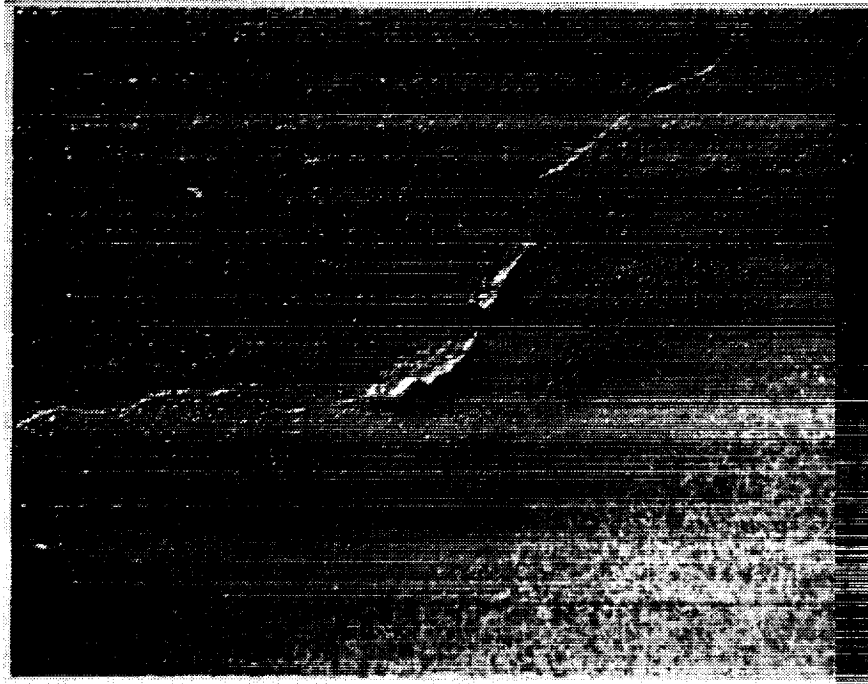


Figure 12. Chemglaze Z306 black polyurethane paint on tray clamp position A6-2, viewed at 16X magnification. Contaminant fiber imbedded in the paint film.

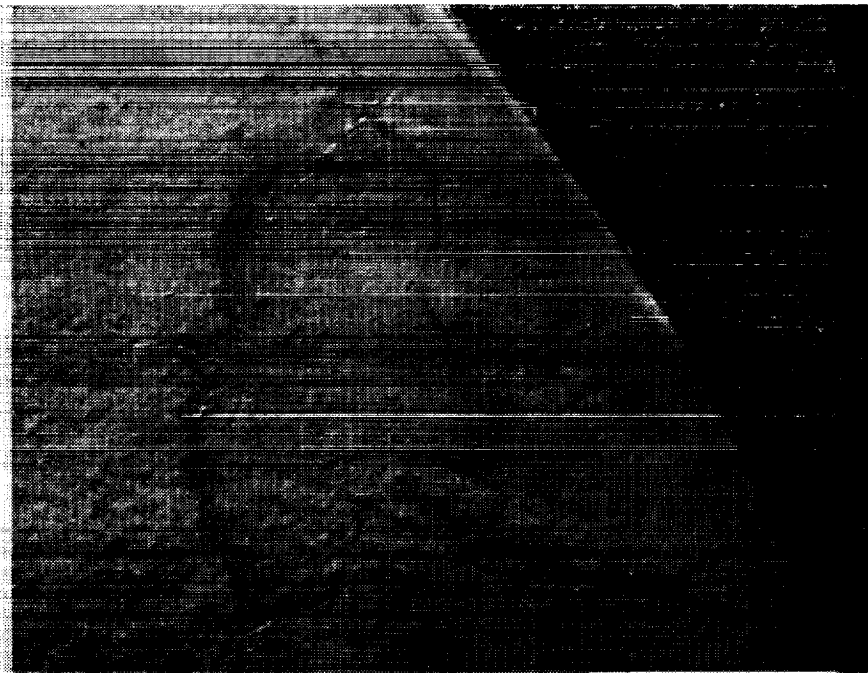


Figure 13. Chemglaze A276 white polyurethane paint on tray clamp A6-2, viewed at 16X magnification. A contaminant fiber is imbedded in the coating and solvent marks are visible. See Appendix C for color figure.



Figure 14. Chemglaze Z306 black polyurethane paint on tray clamp B7-2, viewed at 16X magnification. Visible are a fastener hole and particles of yellow paint, intact on most of the surface but smeared under the washer during assembly.



Figure 15. Chemglaze A276 white polyurethane paint on tray clamp B4-7, viewed at 16X magnification. Solvent mark discoloration. See Appendix C for color figure.

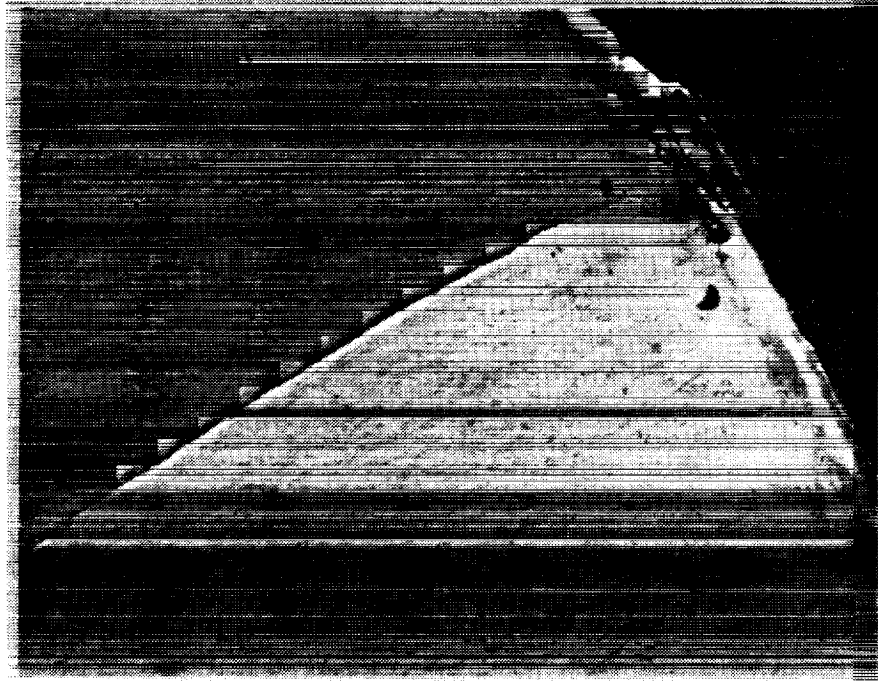


Figure 16. Chemglaze A276 white polyurethane paint on tray clamp B7-2, viewed at 16X magnification. Example of cracking with atomic oxygen erosion.



Figure 17. Chemglaze A276 white polyurethane paint on tray clamp C8-5, viewed at 16X magnification. Edge cracking and fragility of the surface are shown. See Appendix C for color figure.

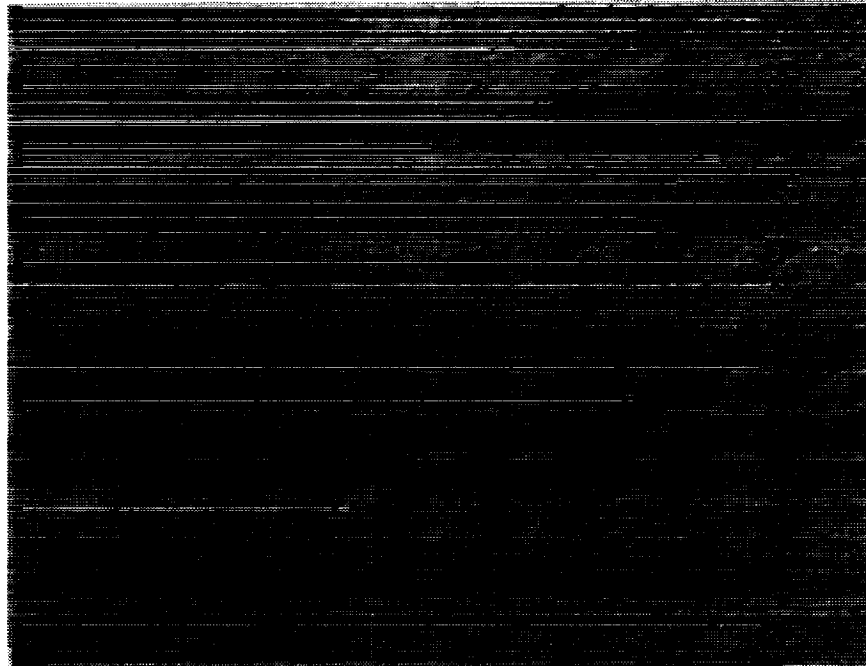


Figure 18. Chemglaze A276 white polyurethane paint on tray clamp C8-5, viewed at 16X magnification, showing parallel surface cracks. See Appendix C for color figure.

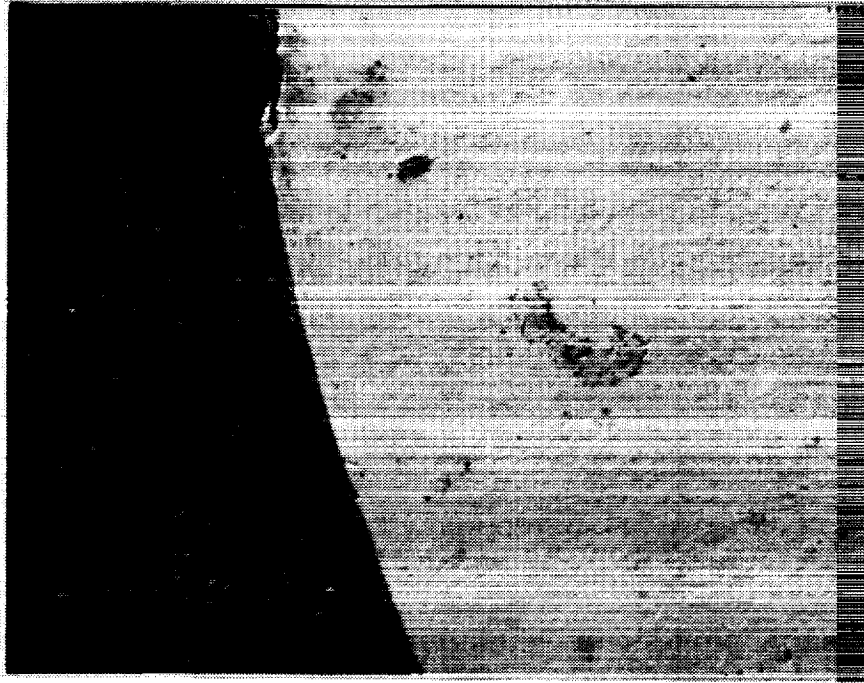


Figure 19. Chemglaze A276 white polyurethane paint on tray clamp B7-2, viewed at 16X magnification. Occlusions in paint were exposed with AO erosion.

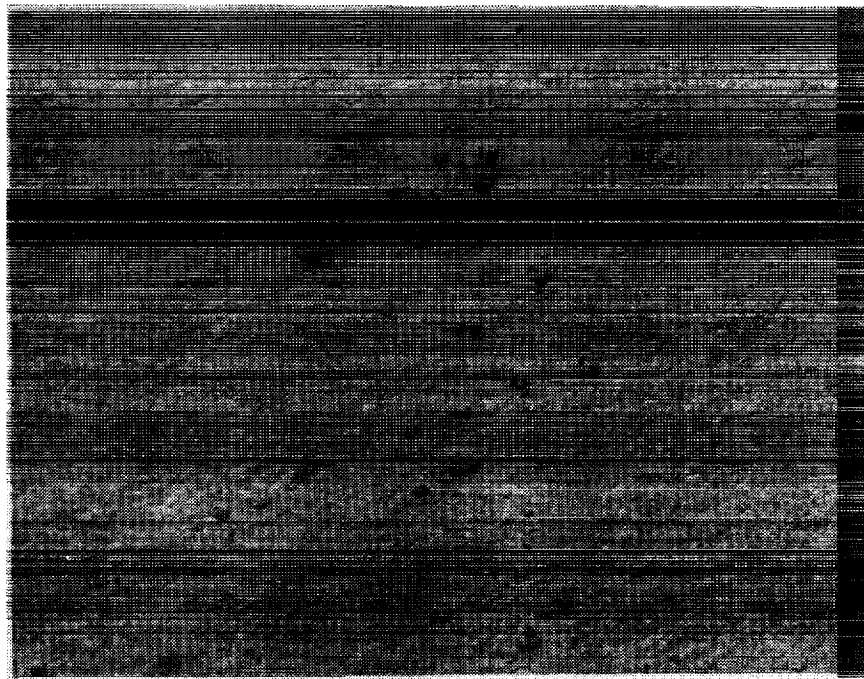


Figure 20. Chemglaze A276 white polyurethane paint on tray clamp B7-2, viewed at 16X magnification, showing additional AO erosion exposed paint contaminants. See Appendix C for color figure.

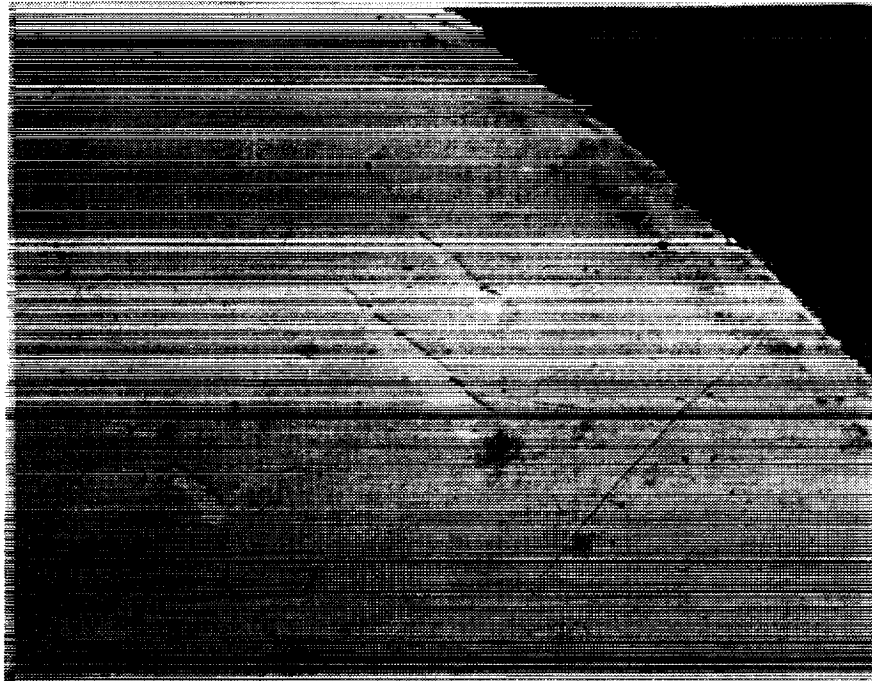


Figure 21. Chemglaze A276 white polyurethane paint on tray clamp C8-5, viewed at 16X magnification, showing the fragile nature of the eroded surface layer.

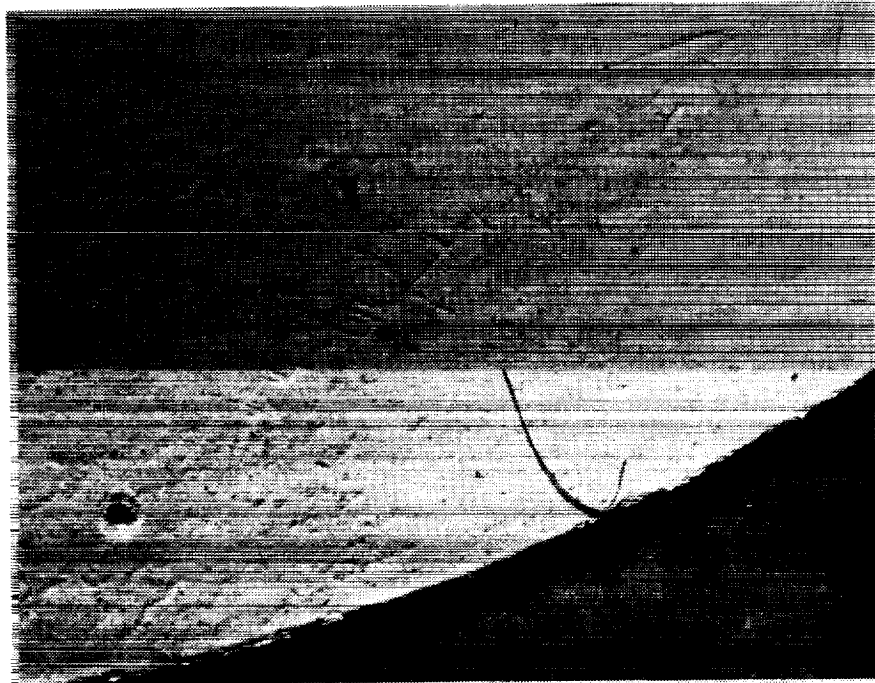


Figure 22. Chemglaze A276 white polyurethane paint on tray clamp C8-5, viewed at 16X magnification, showing a small debris impact and handling damage. See Appendix C for color figure.

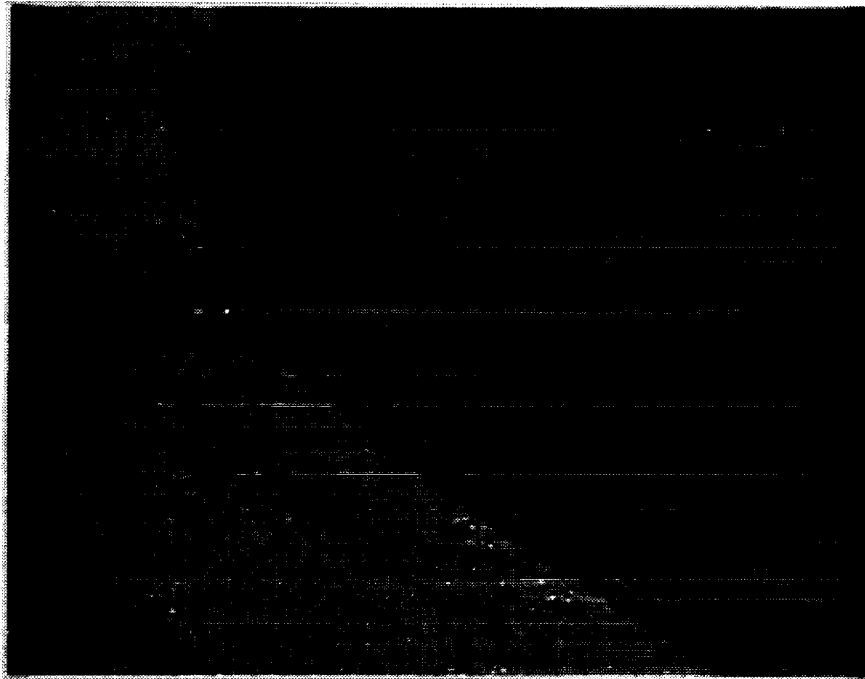


Figure 23. Chemglaze Z306 black polyurethane paint on tray clamp C8-5, viewed at 16X magnification, near a fastener location. Erosion through to the red primer occurred in a band just inside of the paint edge (see arrow). See Appendix C for color figure.

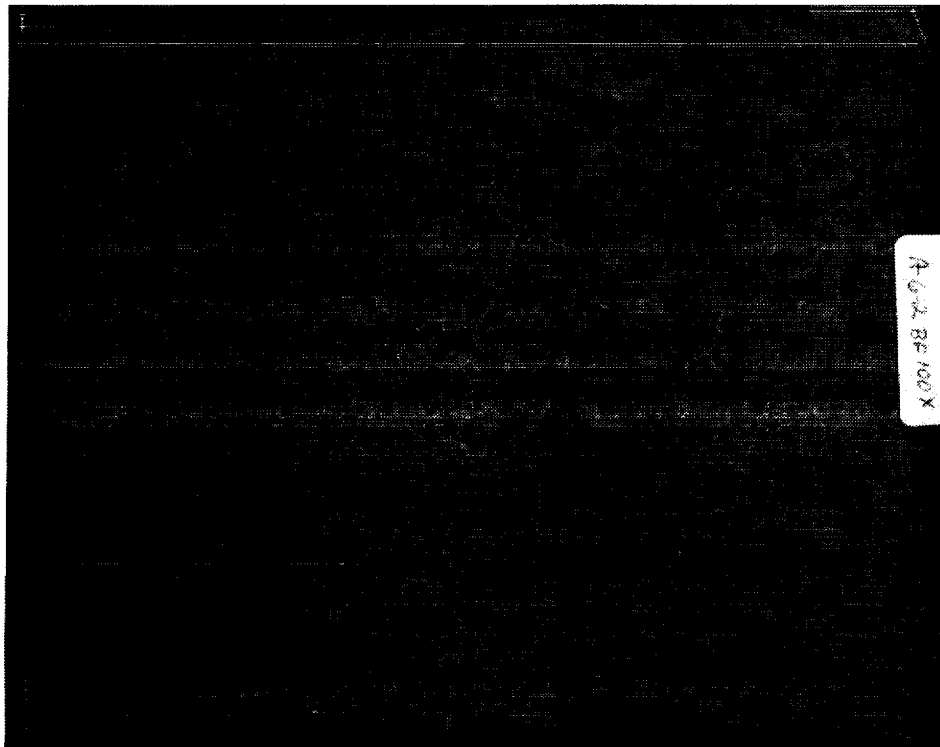


Figure 24. Chemglaze A276 white polyurethane paint on tray clamp A6-2, viewed at 100X magnification under bright field illumination.

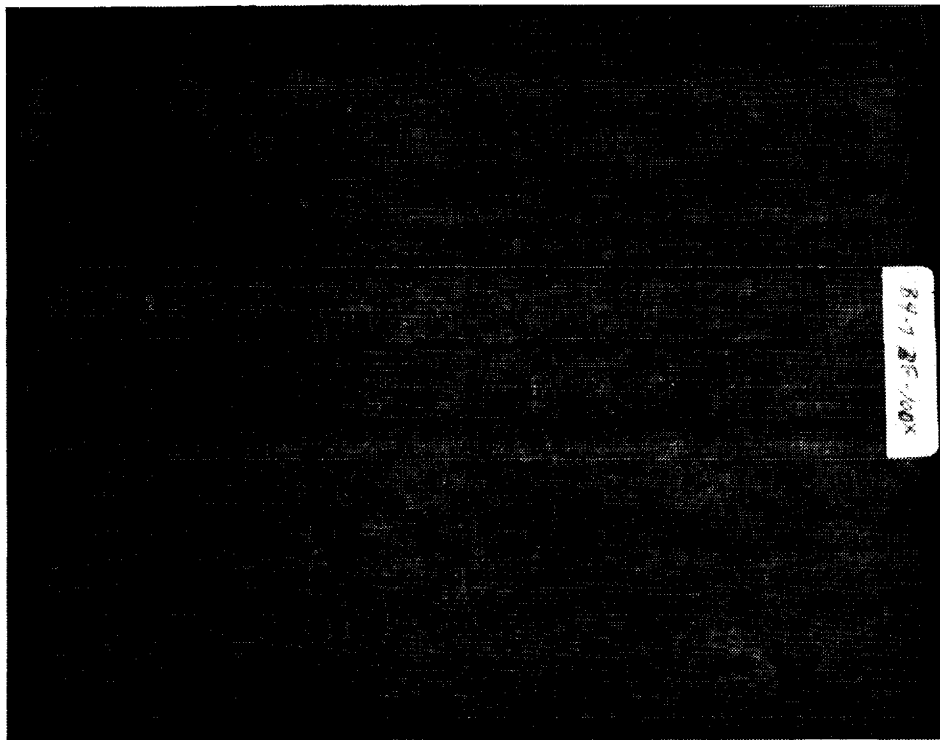


Figure 25. Chemglaze A276 white polyurethane paint on tray clamp B4-7, viewed at 100X magnification under bright field illumination.

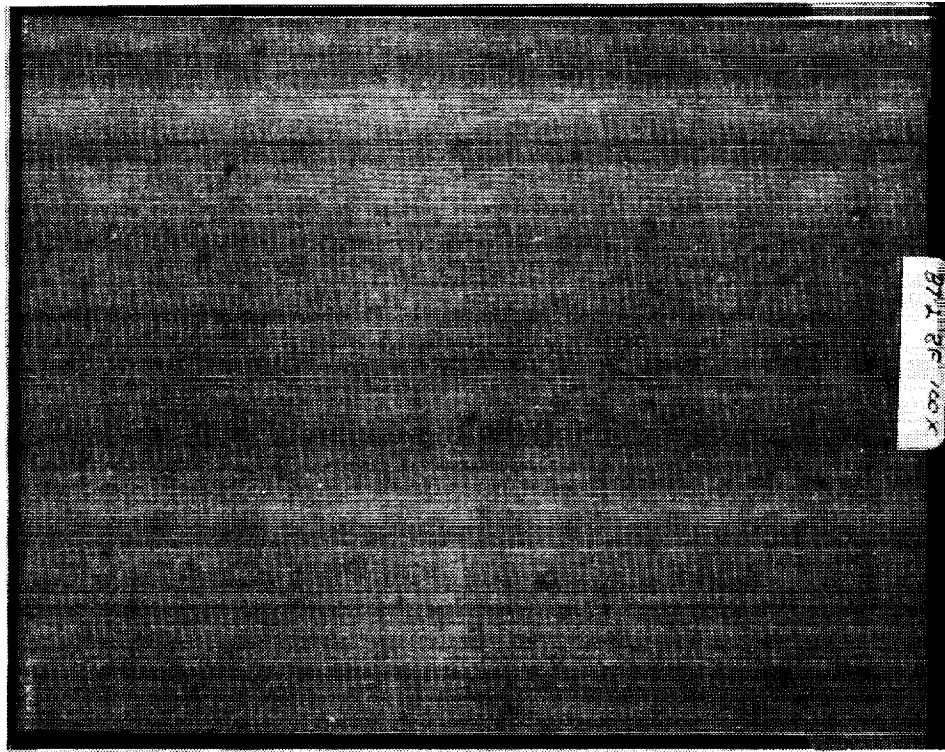


Figure 26. Chemglaze A276 white polyurethane paint on tray clamp B7-2, viewed at 100X magnification under bright field illumination.

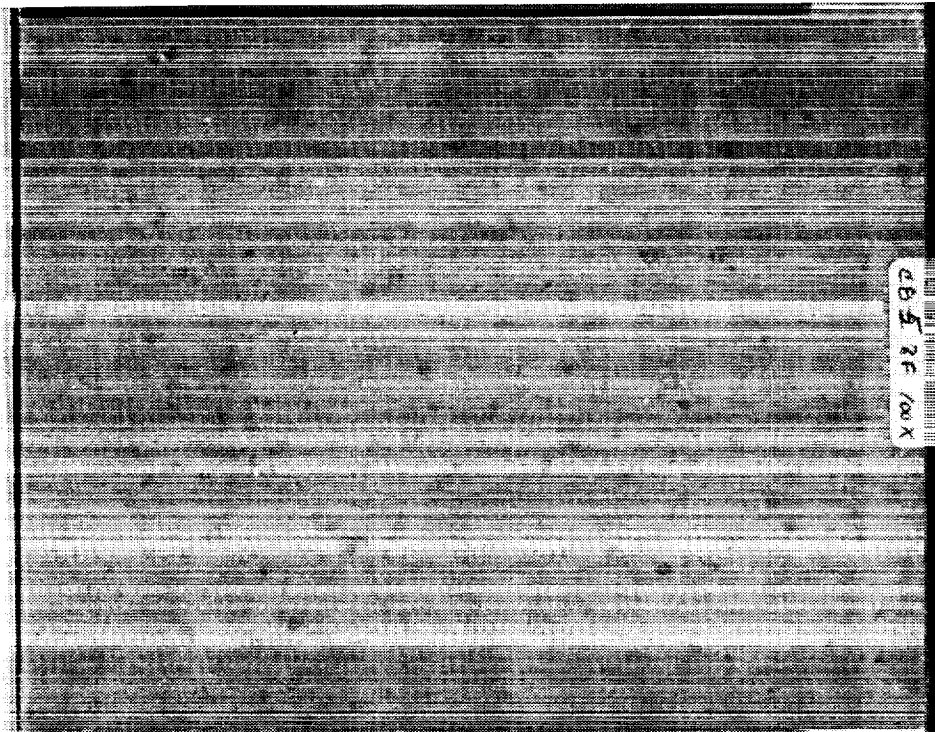


Figure 27. Chemglaze A276 white polyurethane paint on tray clamp C8-5, viewed at 100X magnification under bright field illumination.

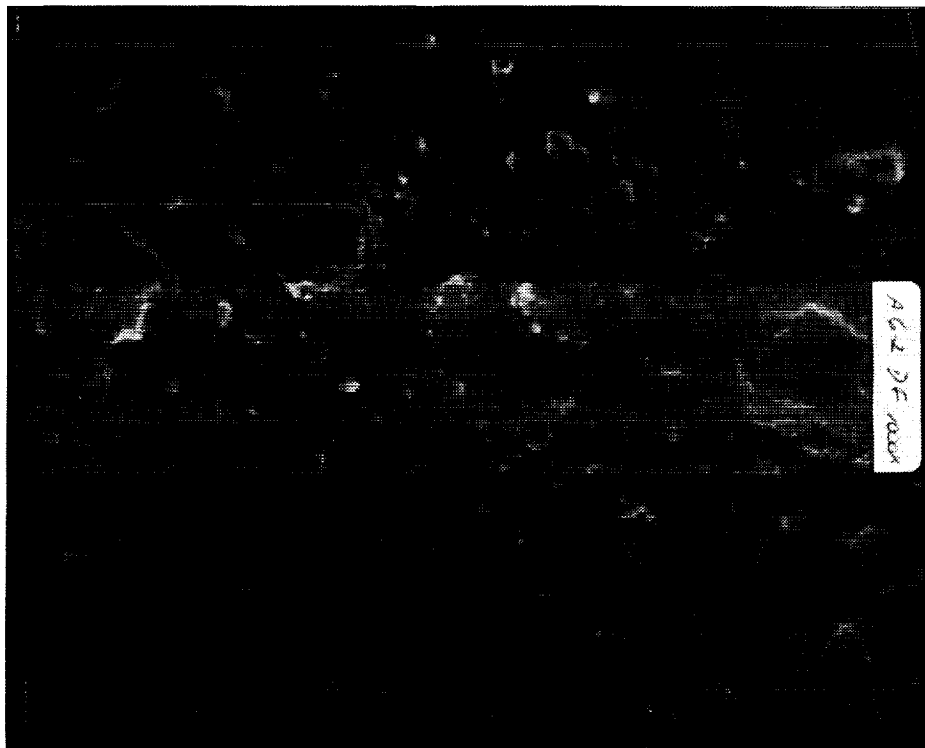


Figure 28. Chemglaze A276 white polyurethane paint on tray clamp A6-2, viewed at 1000X magnification under dark field illumination.

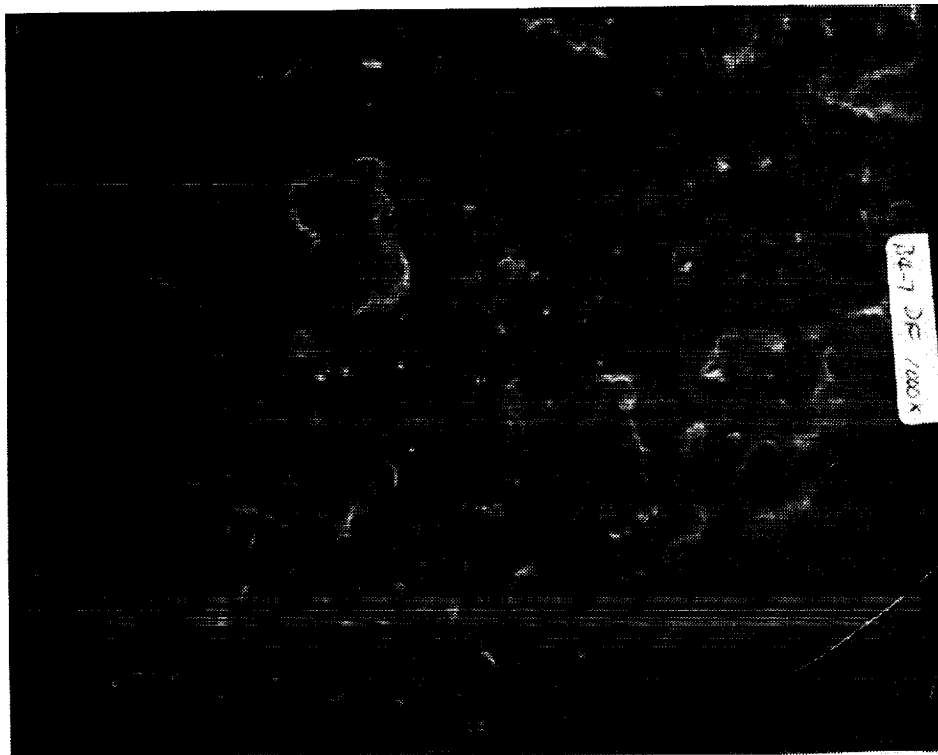


Figure 29. Chemglaze A276 white polyurethane paint on tray clamp B4-7, viewed at 1000X magnification under dark field illumination.

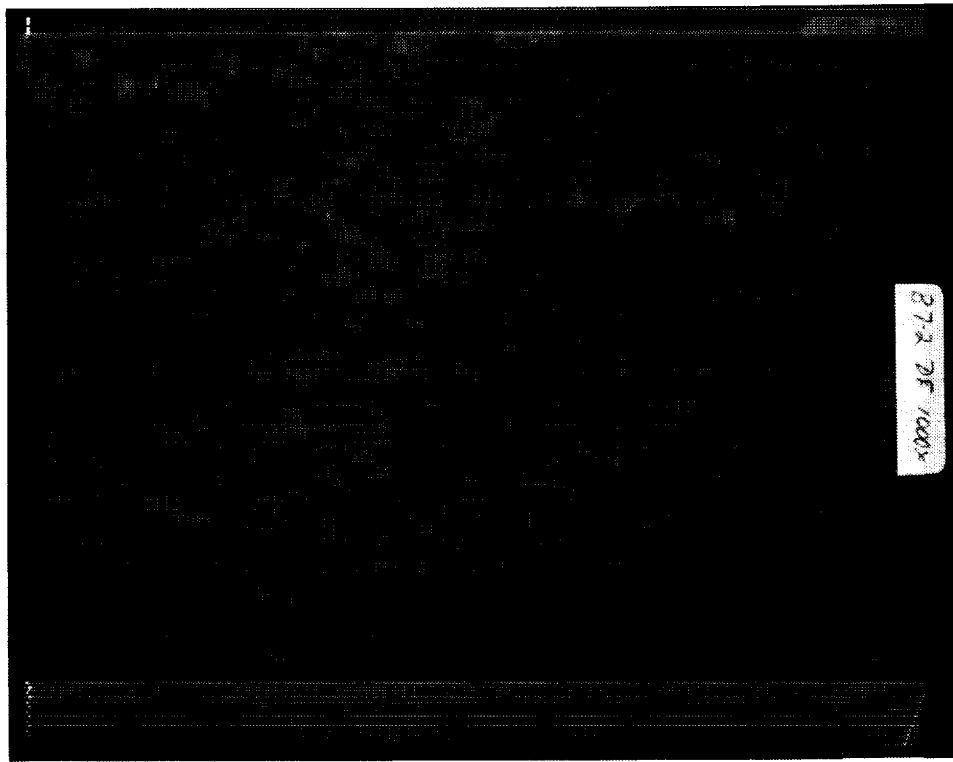


Figure 30. Chemglaze A276 white polyurethane paint on tray clamp B7-2, viewed at 1000X magnification under dark field illumination.

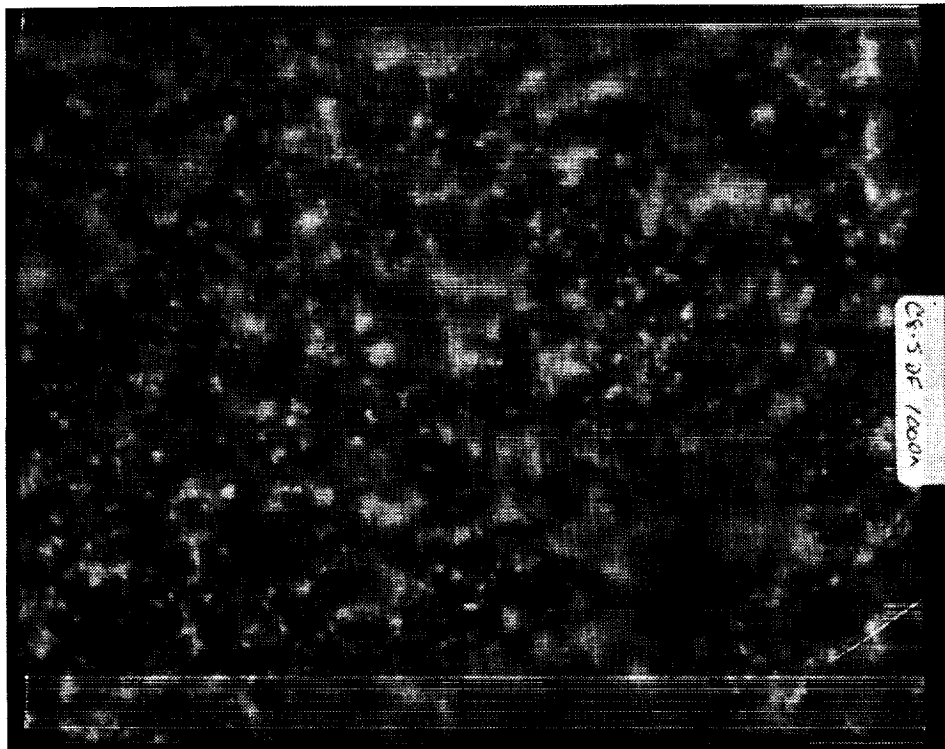


Figure 31. Chemglaze A276 white polyurethane paint on tray clamp C8-5, viewed at 1000X magnification under dark field illumination.

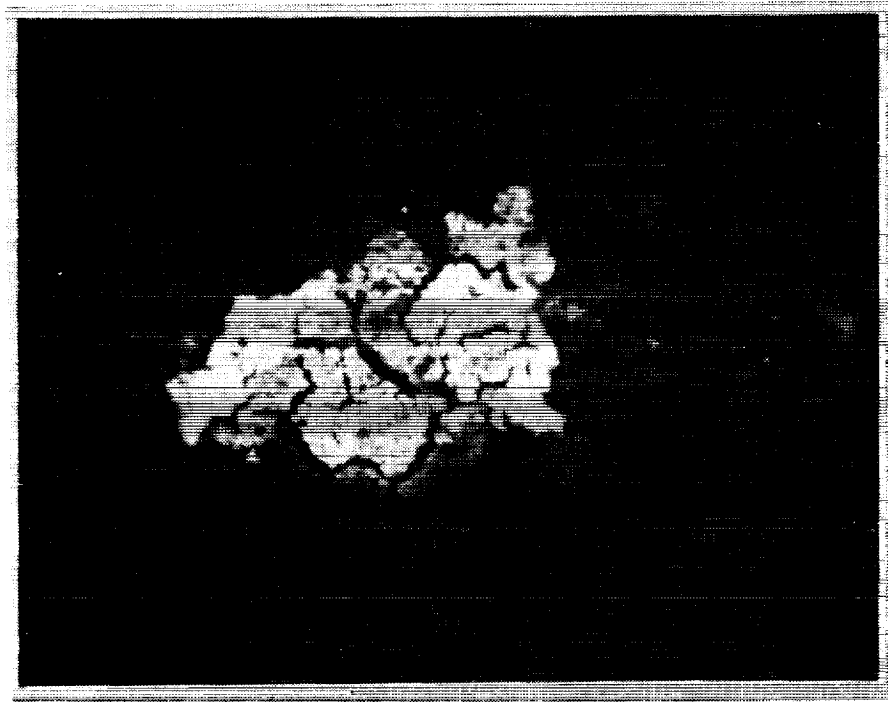


Figure 32. Chemglaze Z306 black polyurethane paint on Experiment M0003 composite panel, viewed at 200X magnification. The focus is on a silicate inclusion but atomic oxygen erosion to the red primer layer is visible. See Appendix C for color figure.



Figure 33. Chemglaze Z306 black polyurethane paint on Experiment M0003 composite panel, viewed at 200X magnification. The focus is on another silicate inclusion but atomic oxygen erosion to the red primer layer is visible.

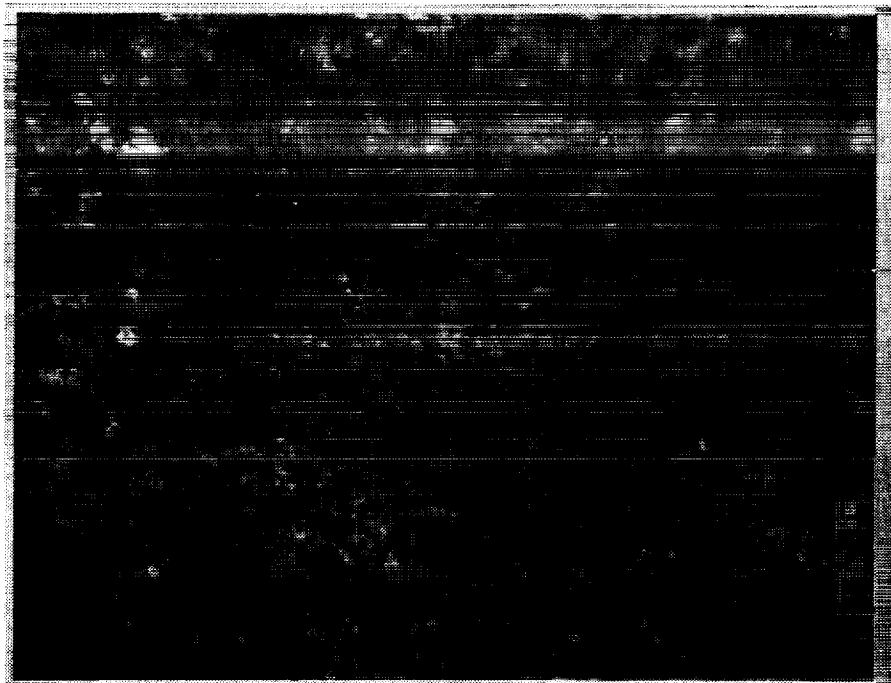


Figure 34. Chemglaze Z306 black polyurethane paint on Experiment M0003 composite panel, viewed at 200X magnification, showing a dispersed silicate layer. See Appendix C for color figure.

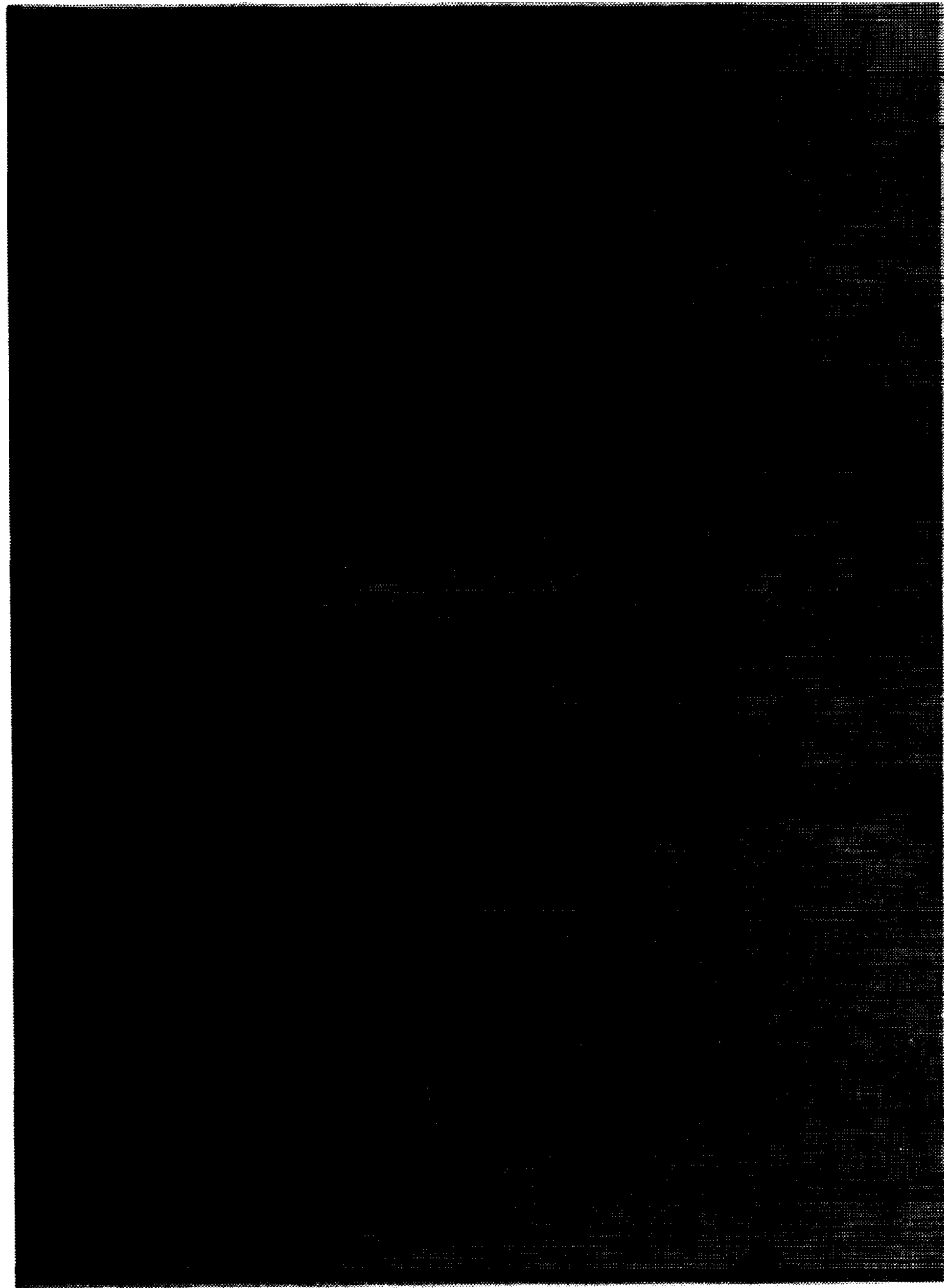


Figure 35. Chemglaze A971 yellow polyurethane paint from the leading edge (row 9) scuff plate, shown at 200X magnification. At center is loose clump of pigment, dark freckles are areas of darkened organic resin. See Appendix C for color figure.

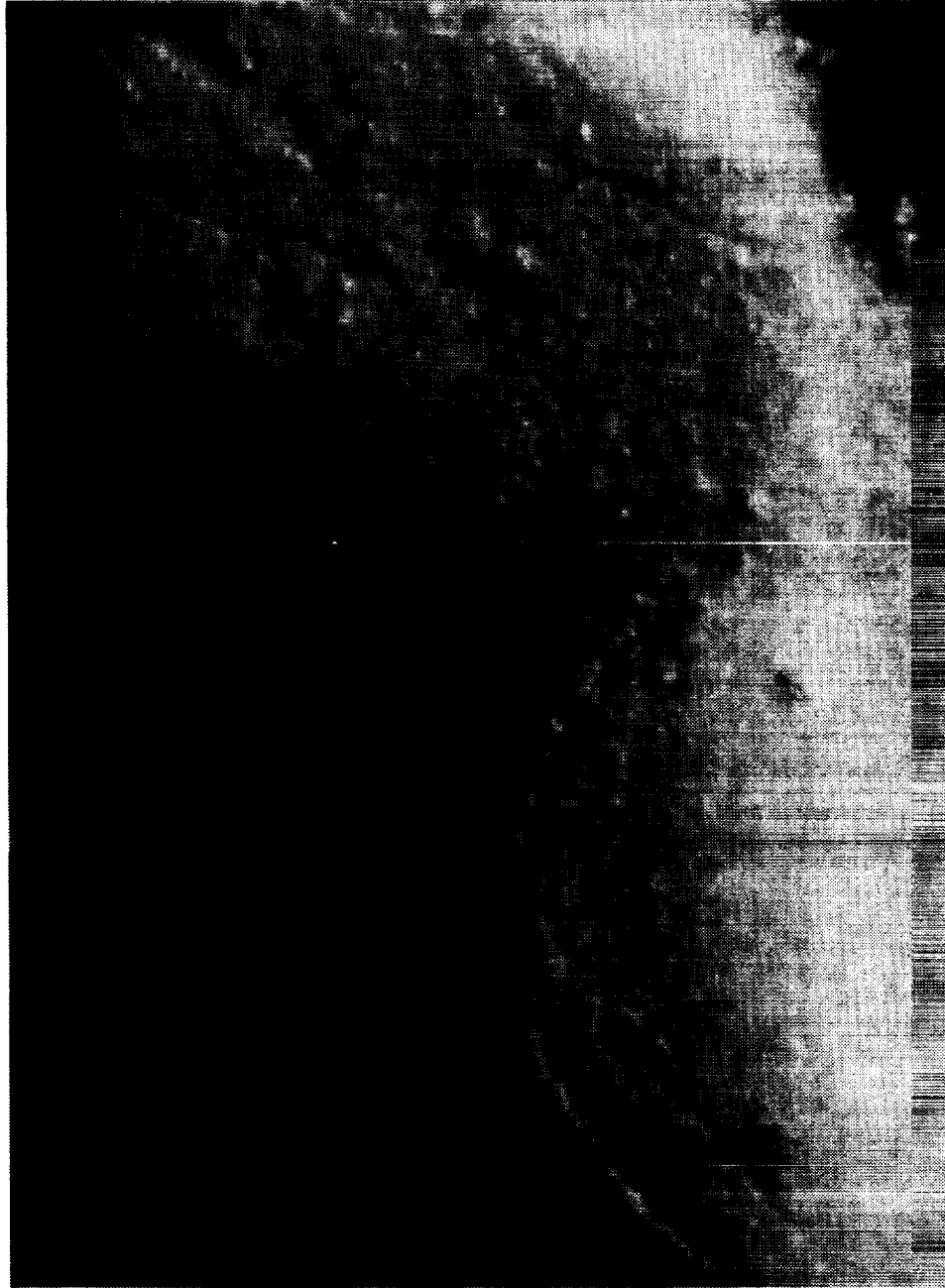


Figure 36. Chemglaze A971 yellow polyurethane paint from the leading edge (row 9) scuff plate, shown at 200X magnification. The focus is on the track (see arrow) of a organic fiber which was a contaminant in the paint and subsequently eroded by AO where it emerged through the surface. See Appendix C for color figure.

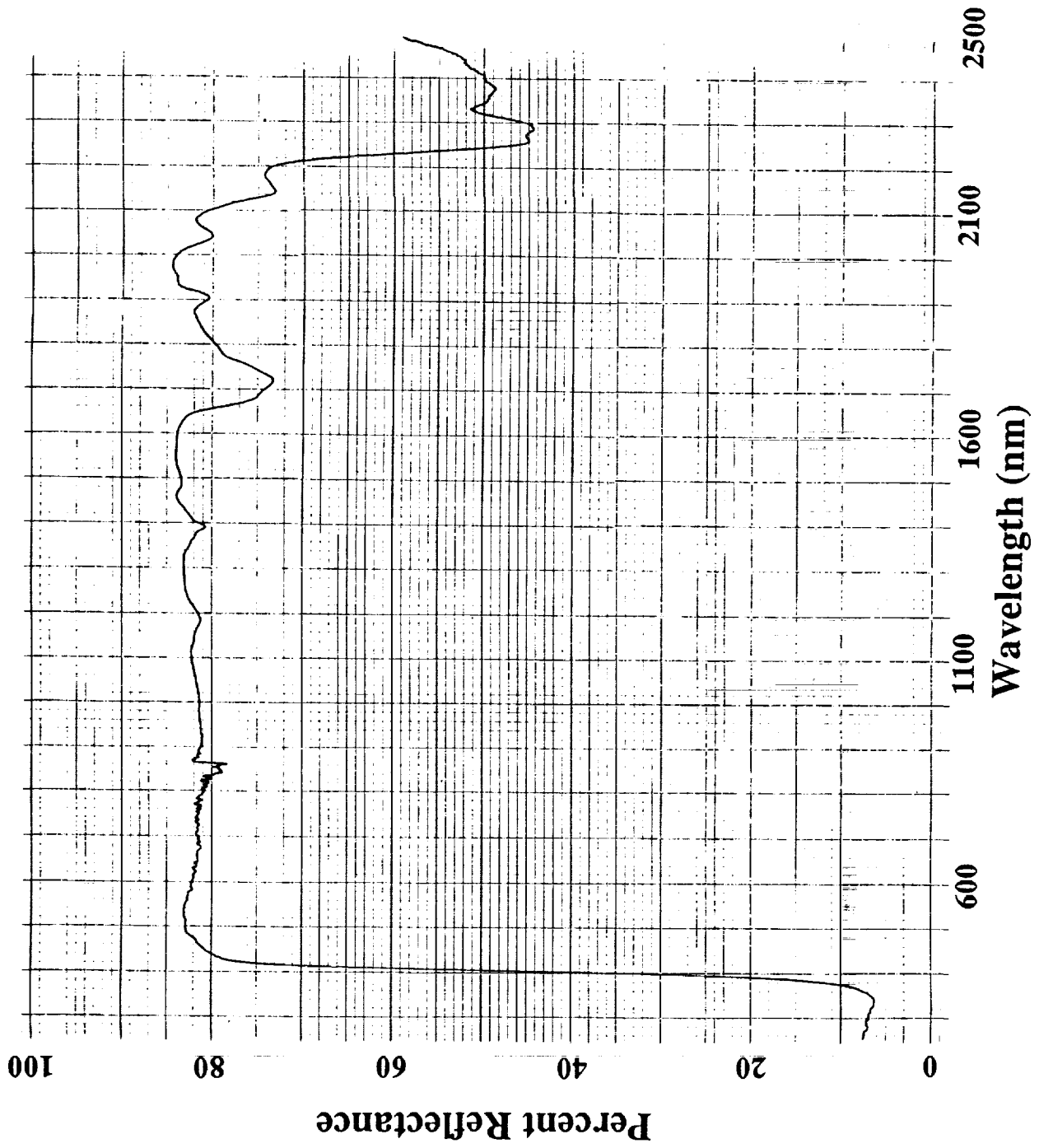


Figure 37. Chemglaze A276 white polyurethane paint control specimen total reflectance spectra, 300 to 2500 nm range (integrated to determine solar absorptance).

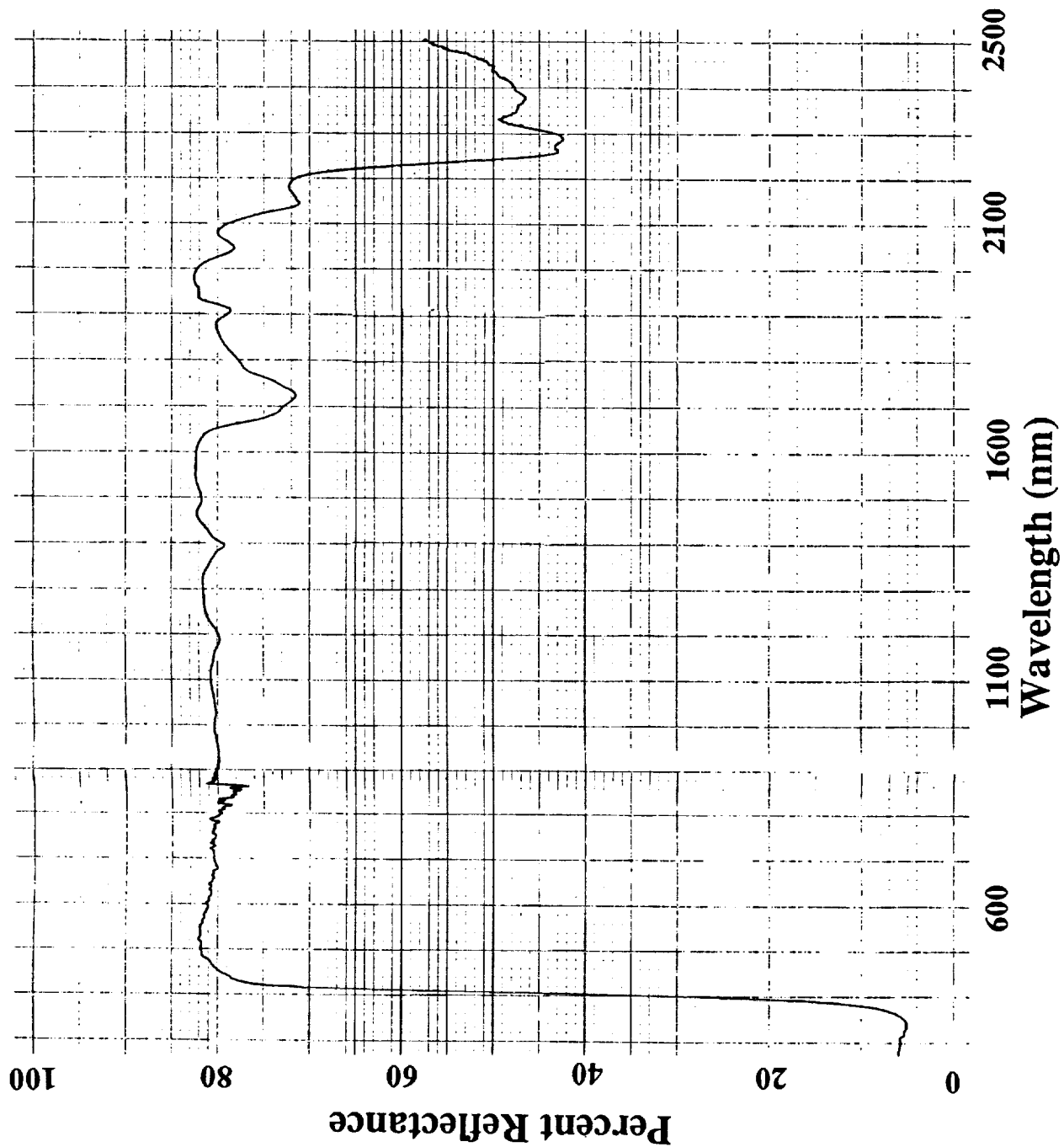


Figure 38. Chemglaze A276 white polyurethane paint control specimen diffuse reflectance spectra, 300 to 2500 nm range.

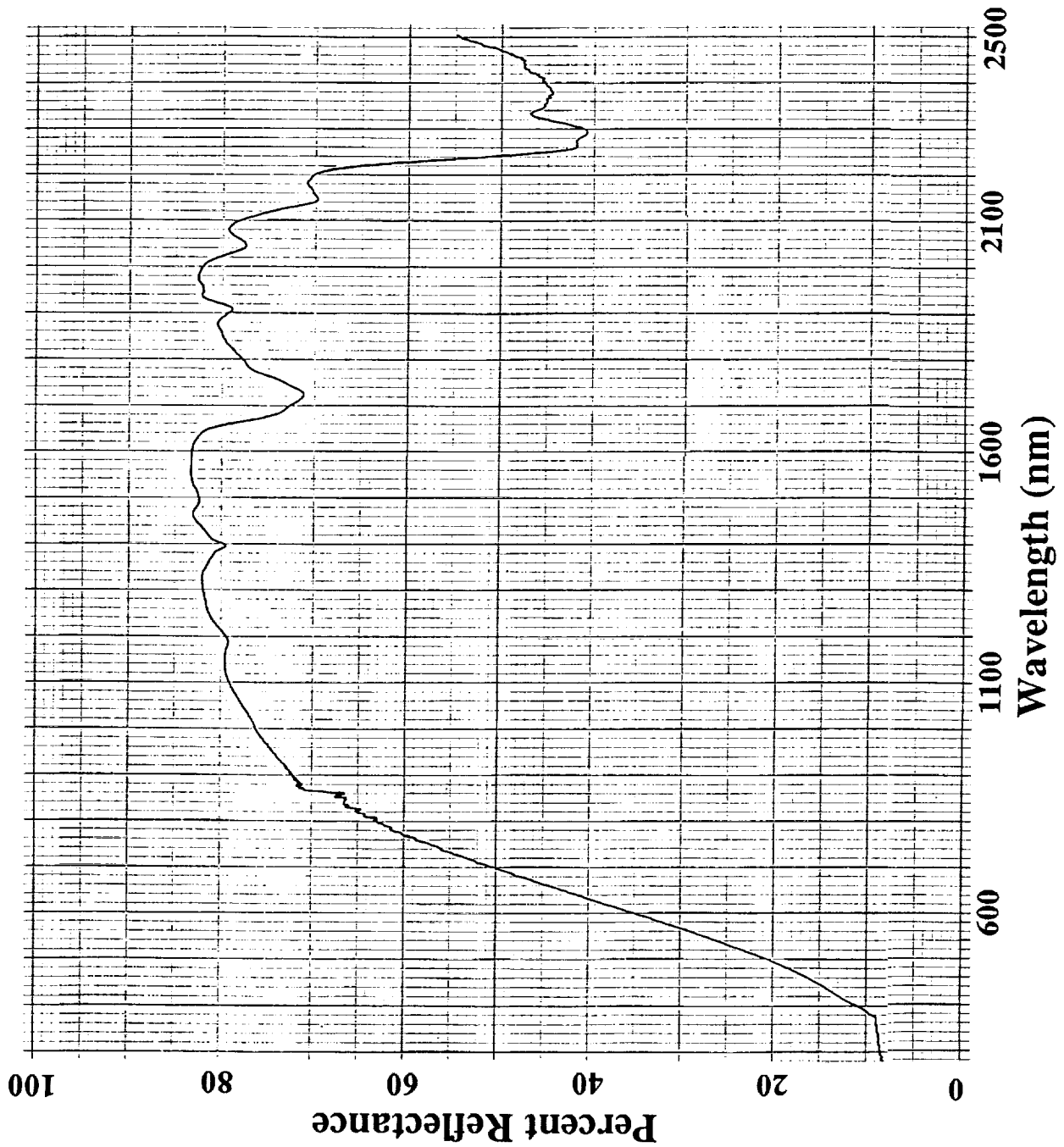


Figure 39. Chemglaze A276 white polyurethane paint E2-8 specimen (trailing edge) total reflectance spectra, 300 to 2500 nm range (integrated to determine solar absorptance).

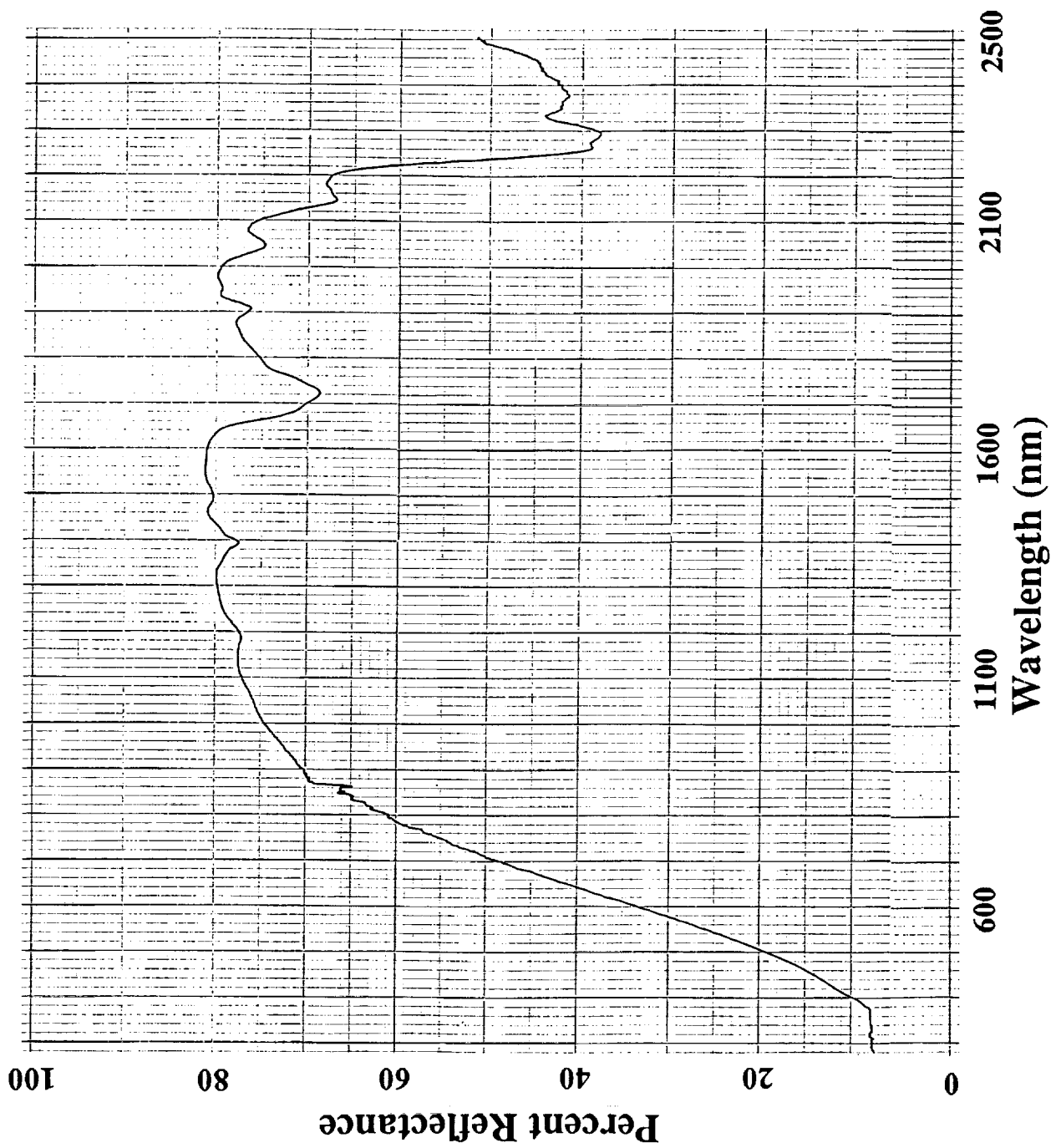


Figure 40. Chemglaze A276 white polyurethane paint E2-8 specimen (trailing edge) diffuse reflectance spectra, 300 to 2500 nm range.

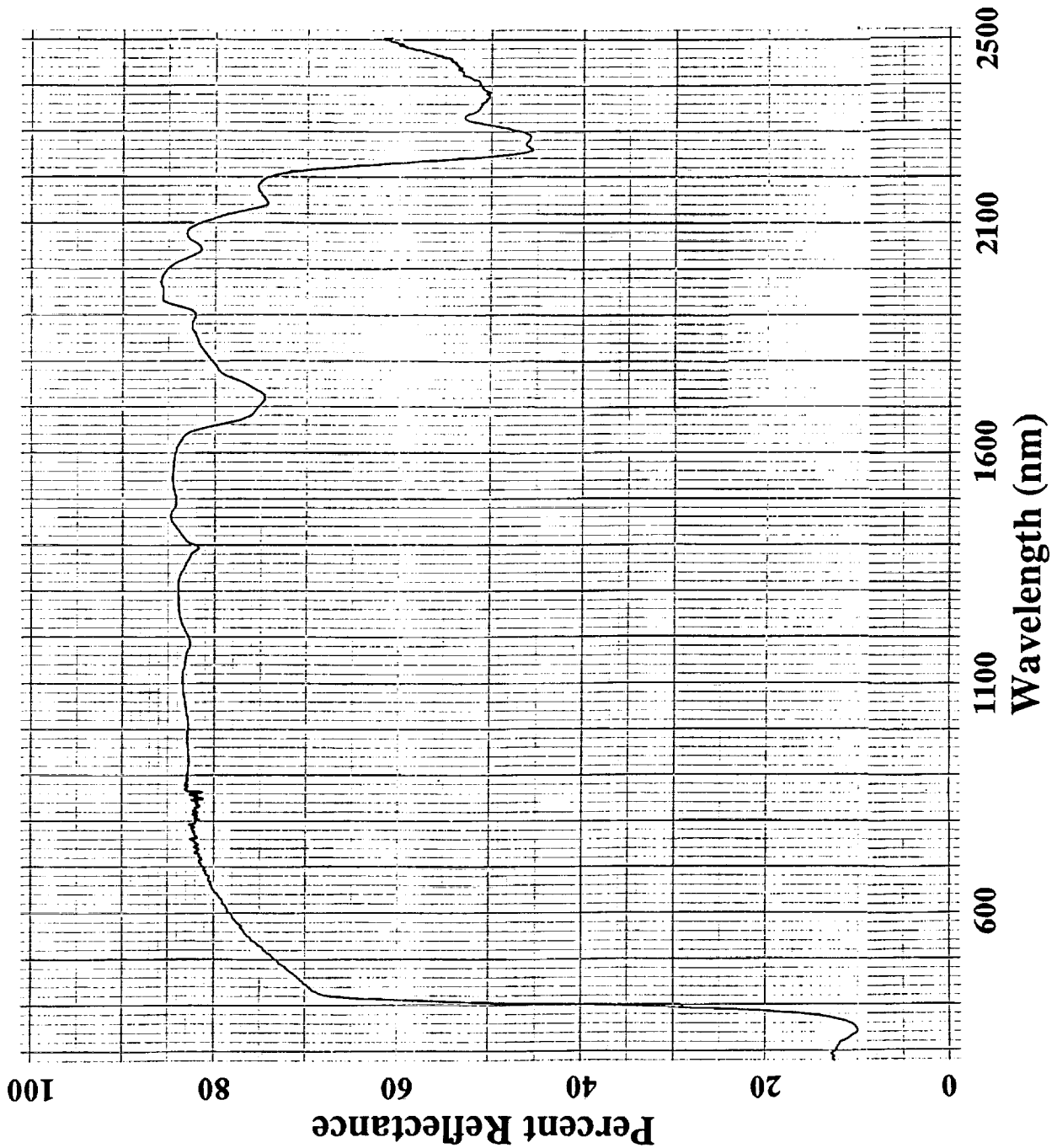


Figure 41. Chemglaze A276 white polyurethane paint C8-5 specimen (leading edge) total reflectance spectra, 300 to 2500 nm range (integrated to determine solar absorptance).

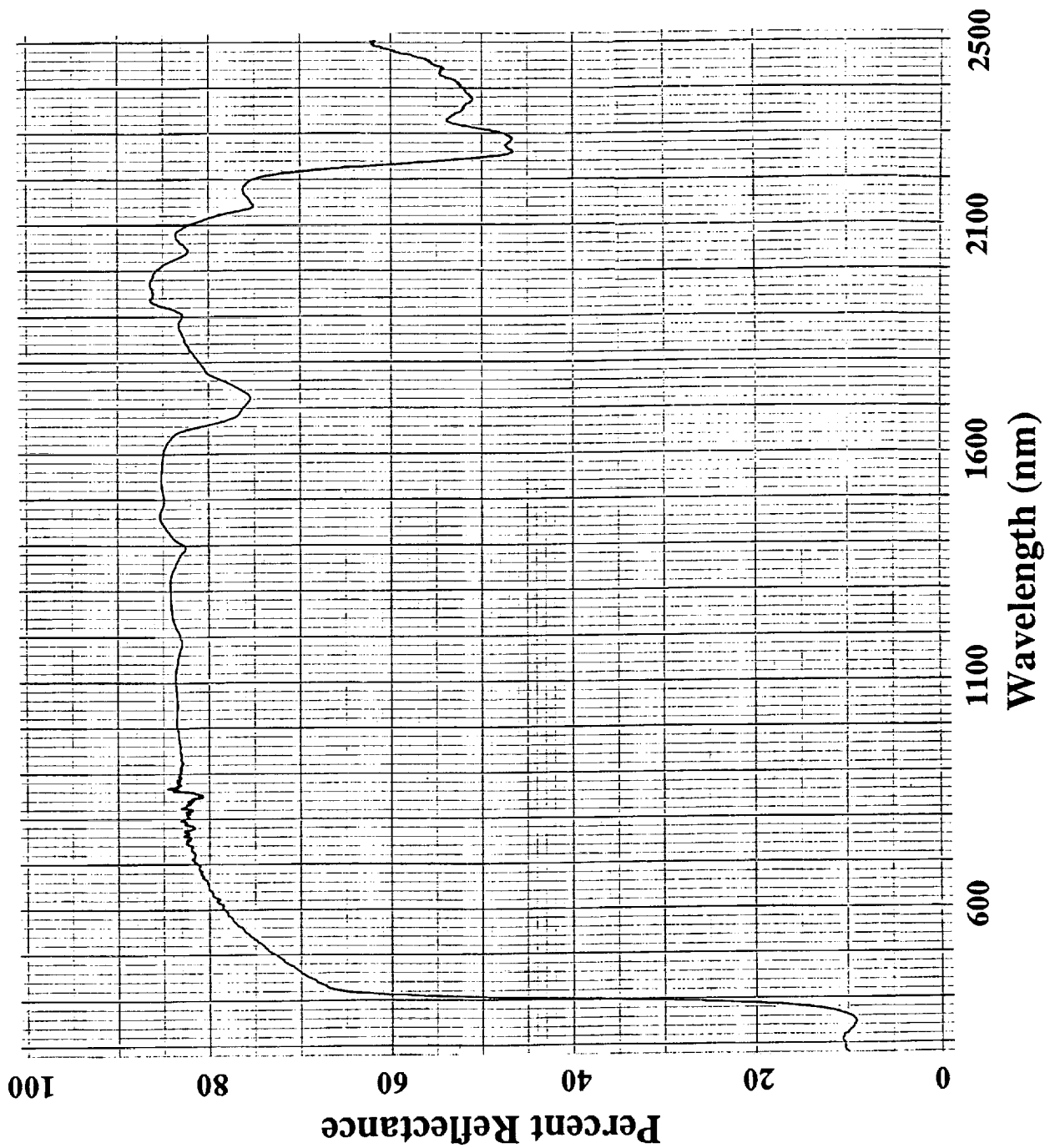


Figure 42. Chemglaze A276 white polyurethane paint C8-5 specimen (leading edge) diffuse reflectance spectra, 300 to 2500 nm range.

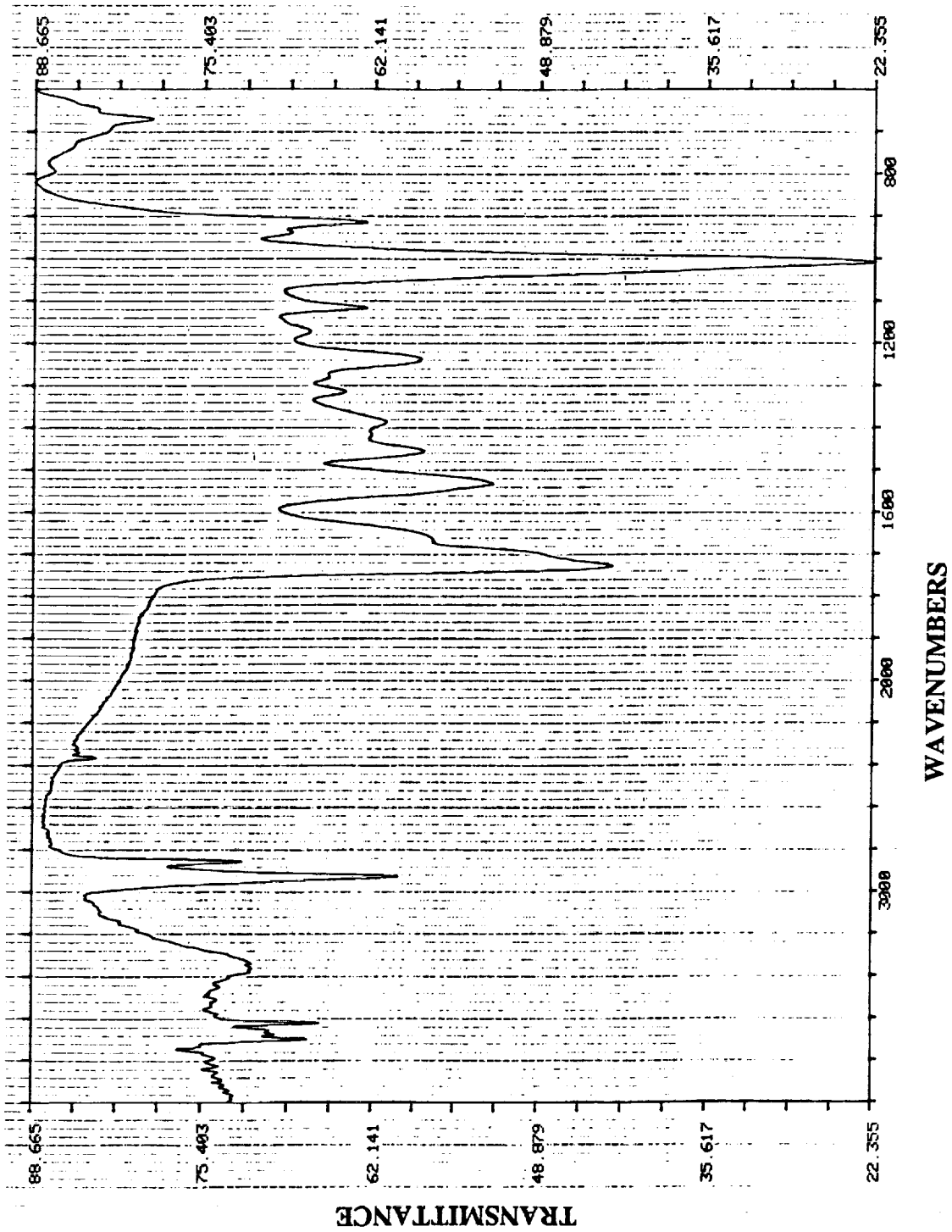


Figure 43. Chemglaze A276 white polyurethane paint, control specimen infrared spectra.

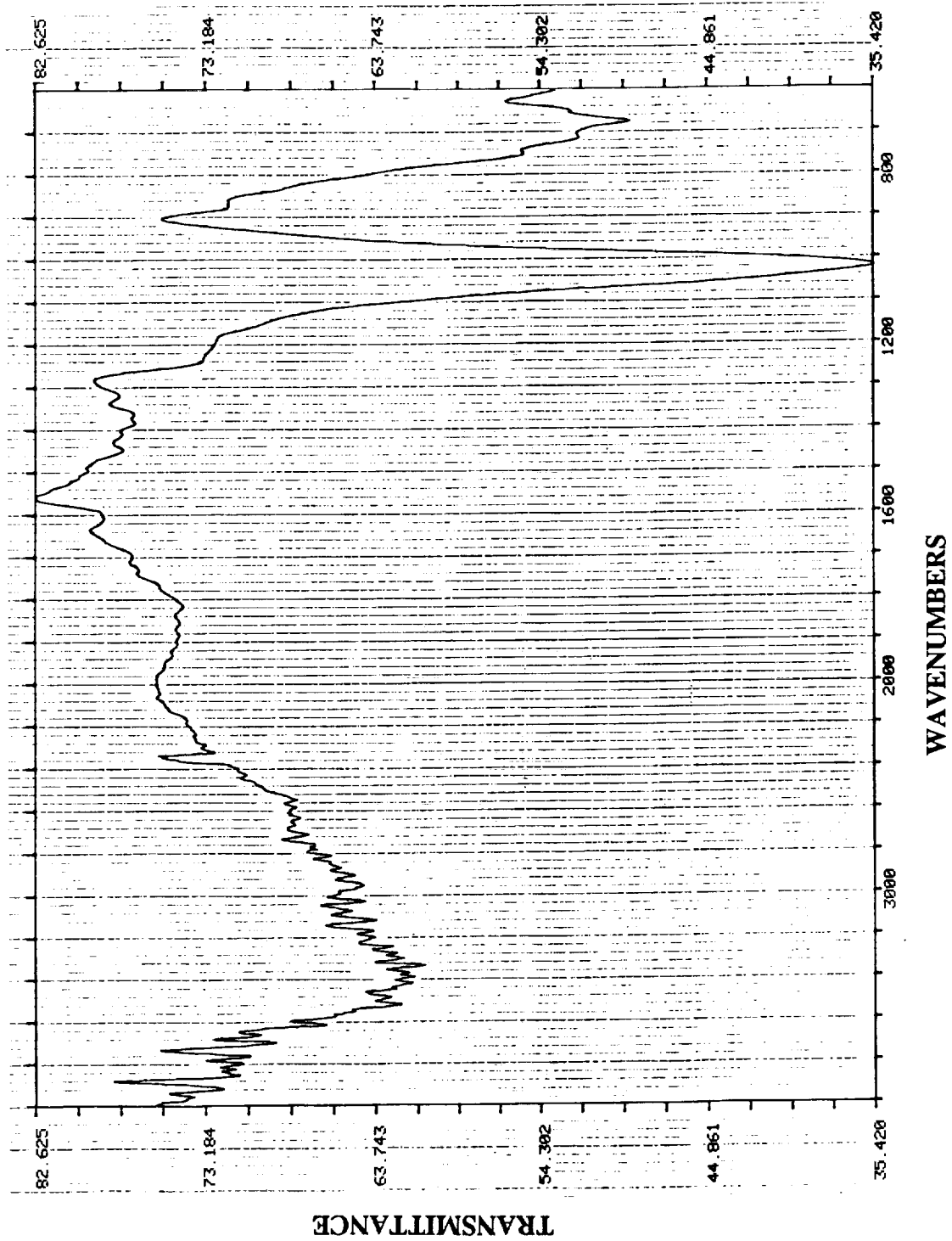


Figure 44. Chemglaze A276 white polyurethane paint , B9-7 specimen (leading edge) infrared spectra.

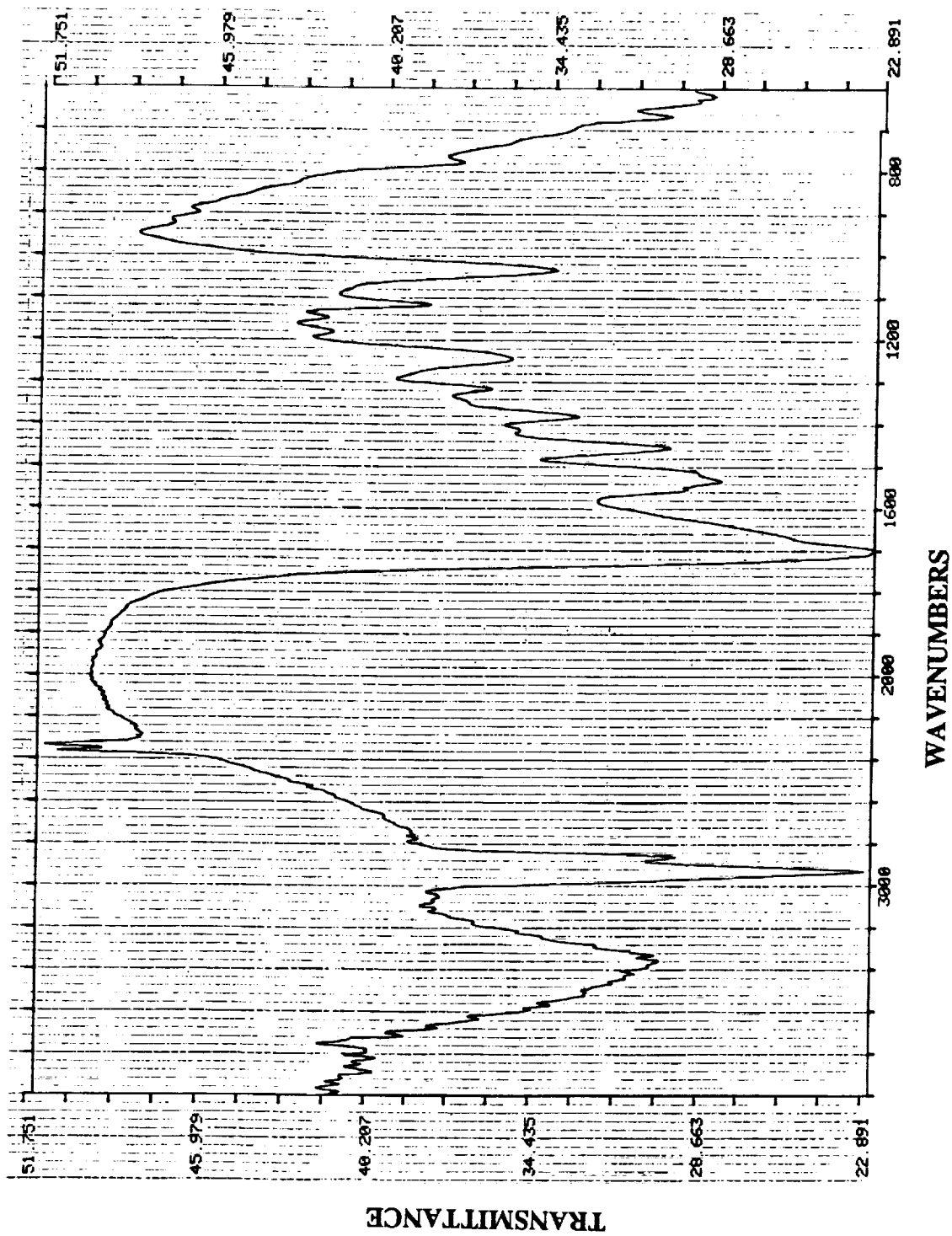


Figure 45. Chemglaze A276 white polyurethane paint , A3-7 specimen (trailing edge) infrared spectra.

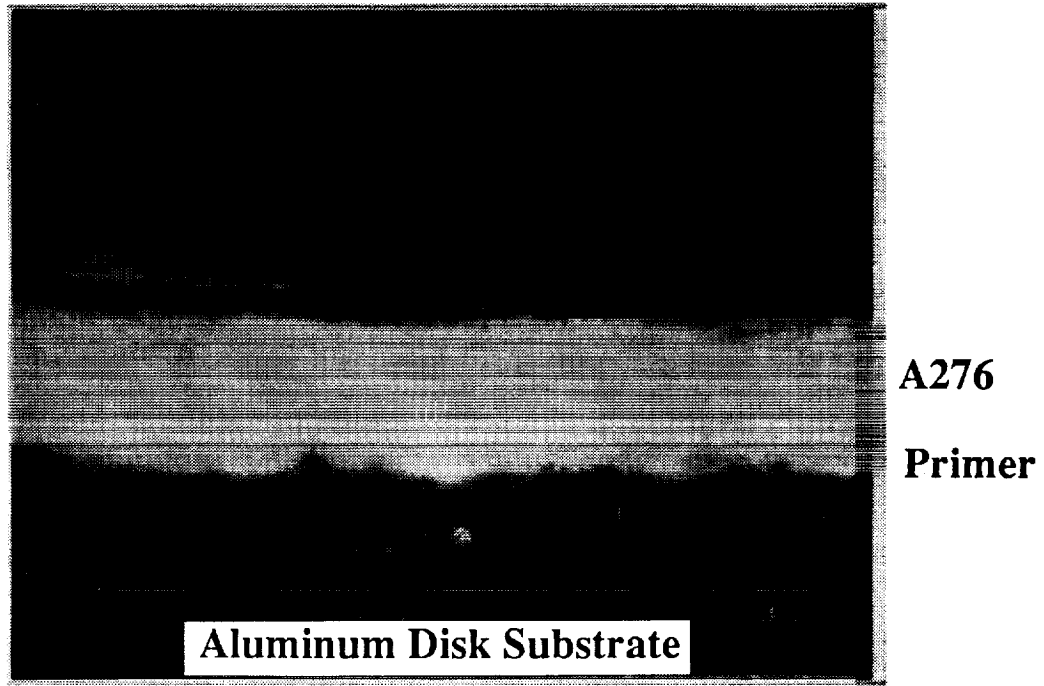


Figure 46. Cross-section of Chemglaze A276 white paint on tray clamp C8-5 (500X magnification), showing lifting of loose pigment into the encapsulant.

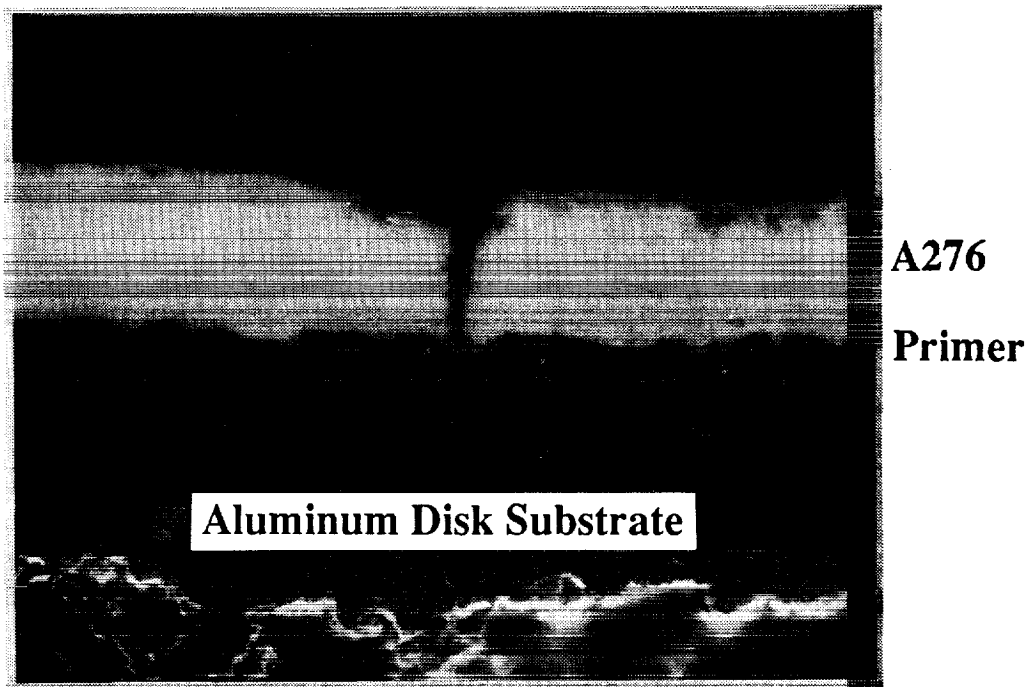


Figure 47. Cross-section of Chemglaze A276 white paint on tray clamp C8-5 (500X magnification), showing a typical crack passing down to aluminum substrate. See Appendix C for color figure.

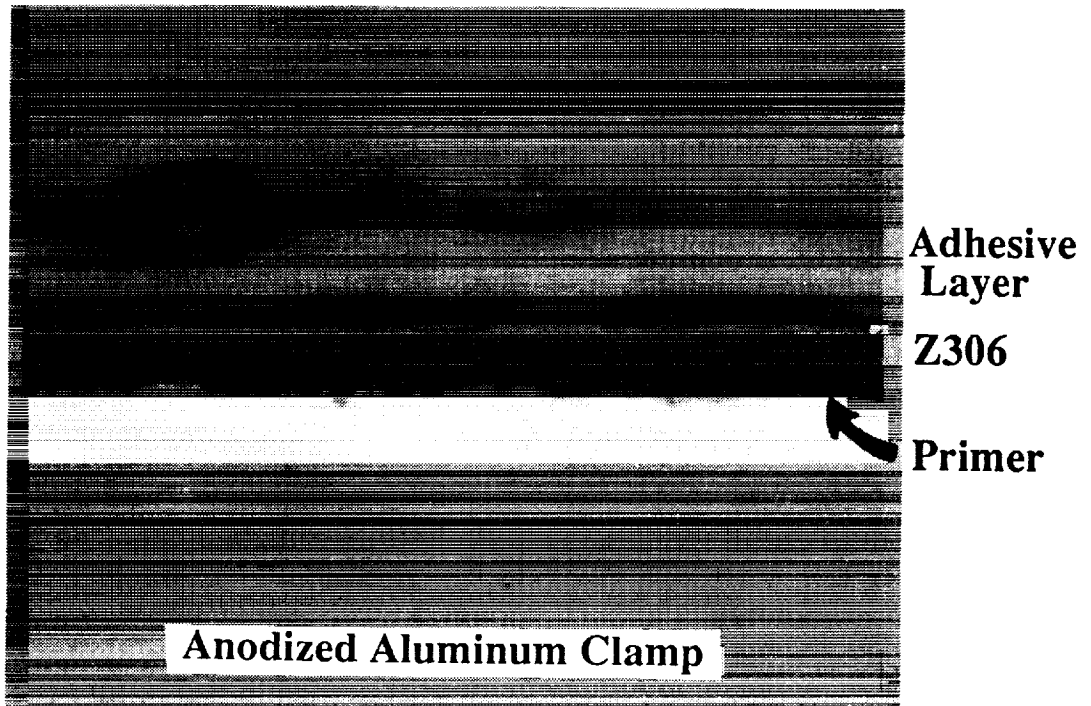


Figure 48. Cross-section of Chemglaze Z306 black polyurethane paint on tray clamp A6-2 at 500X magnification, protected from environmental exposure.

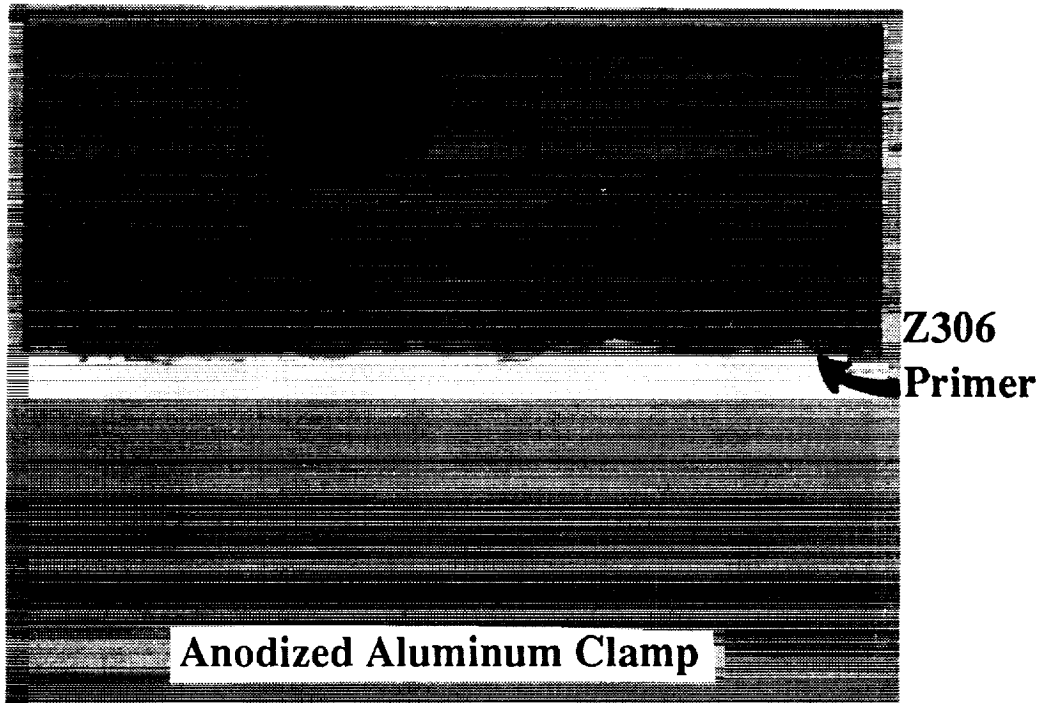


Figure 49. Cross-section of Chemglaze Z306 black polyurethane paint on tray clamp A6-2 at 500X magnification, full environmental exposure.

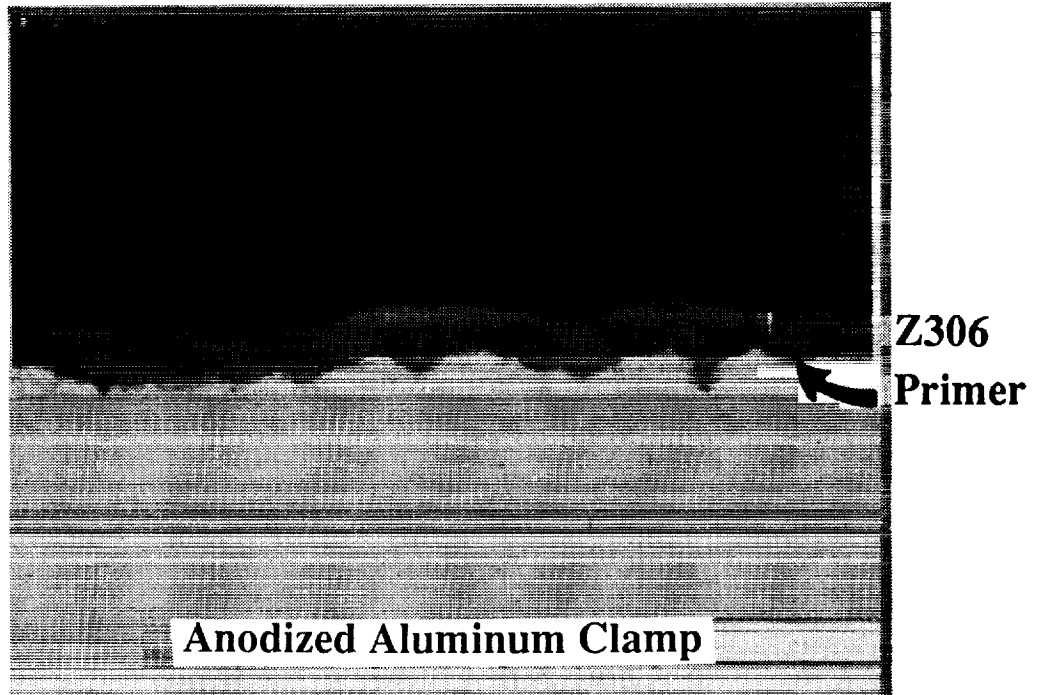


Figure 50. Cross-section of Chemglaze Z306 black polyurethane paint on tray clamp B4-7 at 500X magnification, protected from environmental exposure.

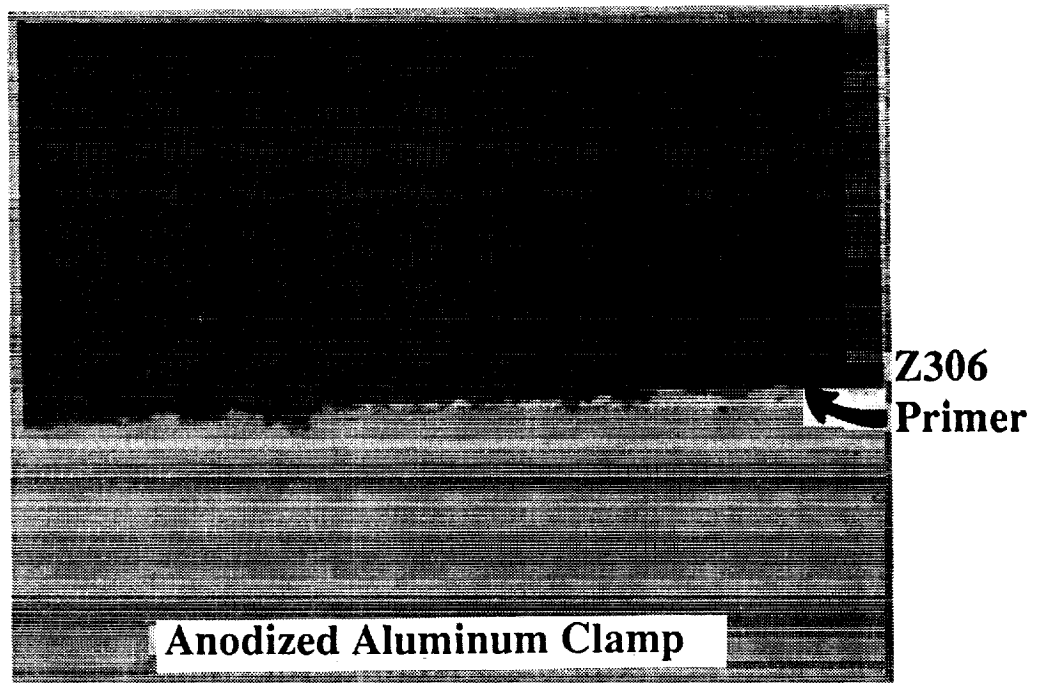


Figure 51. Cross-section of Chemglaze Z306 black polyurethane paint on tray clamp B4-7 at 500X magnification, full environmental exposure.

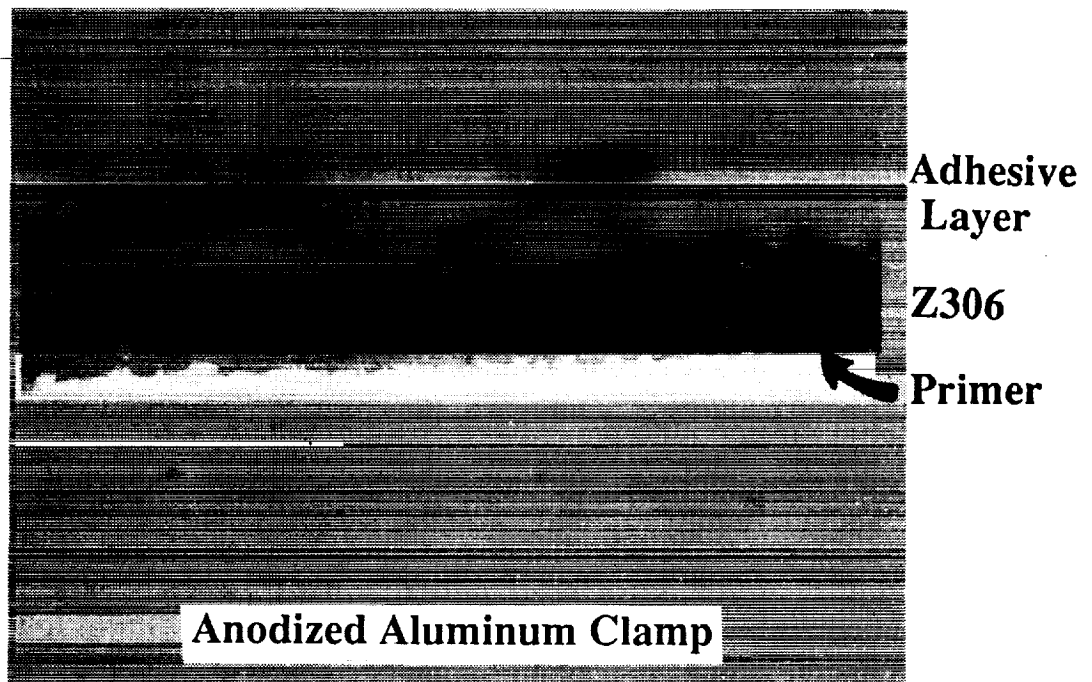


Figure 52. Cross-section of Chemglaze Z306 black polyurethane paint on tray clamp B7-2 at 500X magnification, protected from environmental exposure.

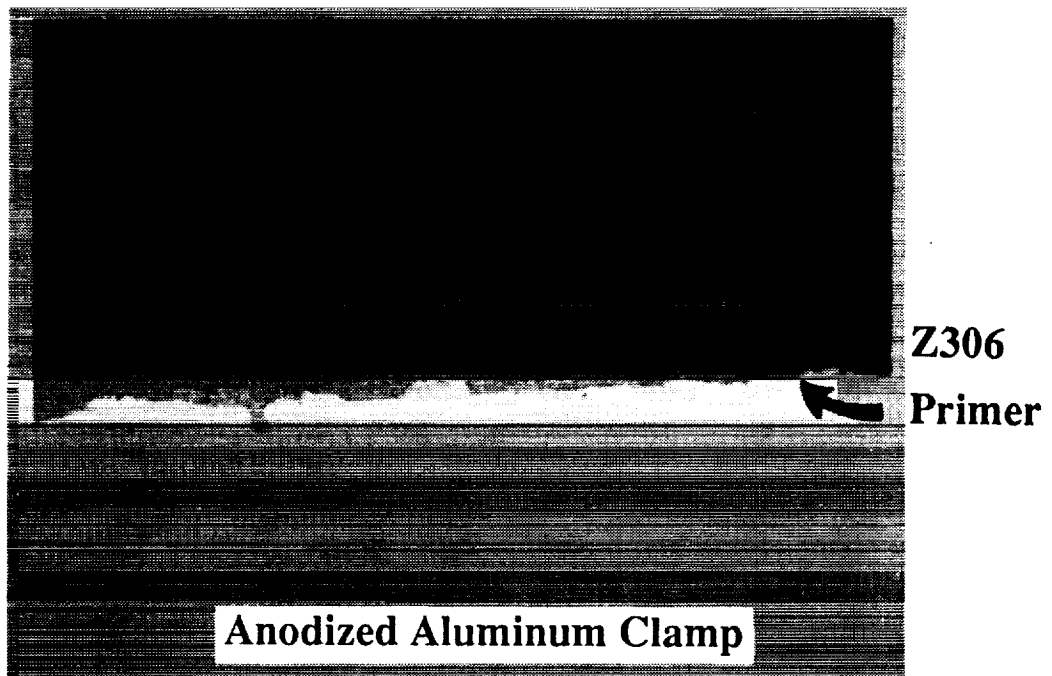


Figure 53. Cross-section of Chemglaze Z306 black polyurethane paint on tray clamp B7-2 at 500X magnification, full environmental exposure.

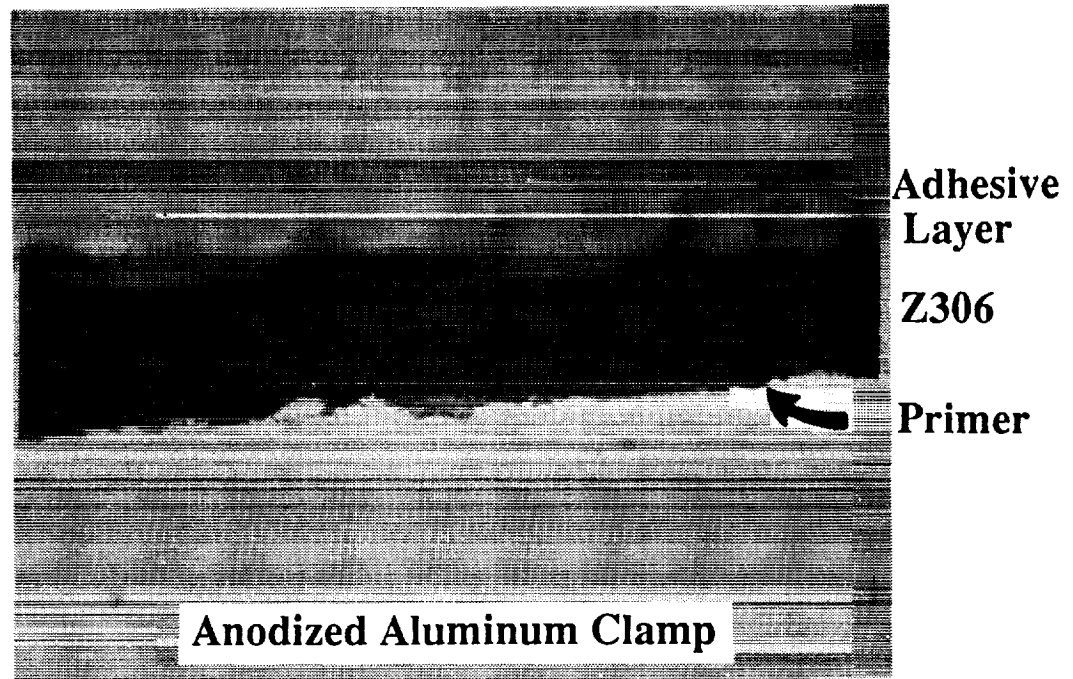


Figure 54. Cross-section of Chemglaze Z306 black polyurethane paint on tray clamp C8-5 at 500X magnification, protected from environmental exposure.

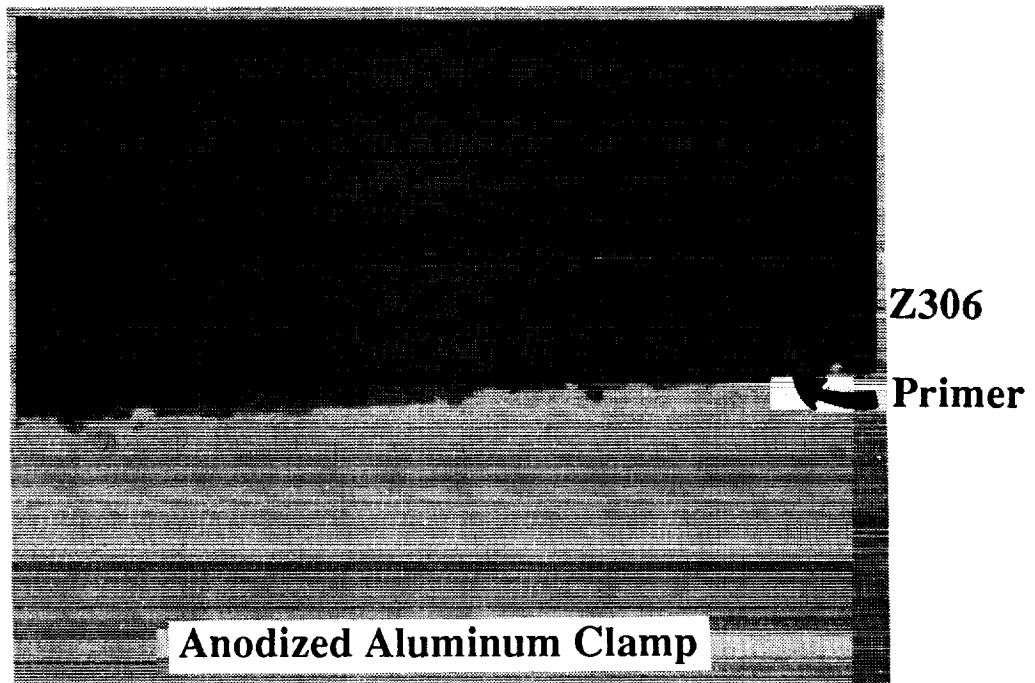


Figure 55. Cross-section of Chemglaze Z306 black polyurethane paint on tray clamp C8-5 at 500X magnification, full environmental exposure.

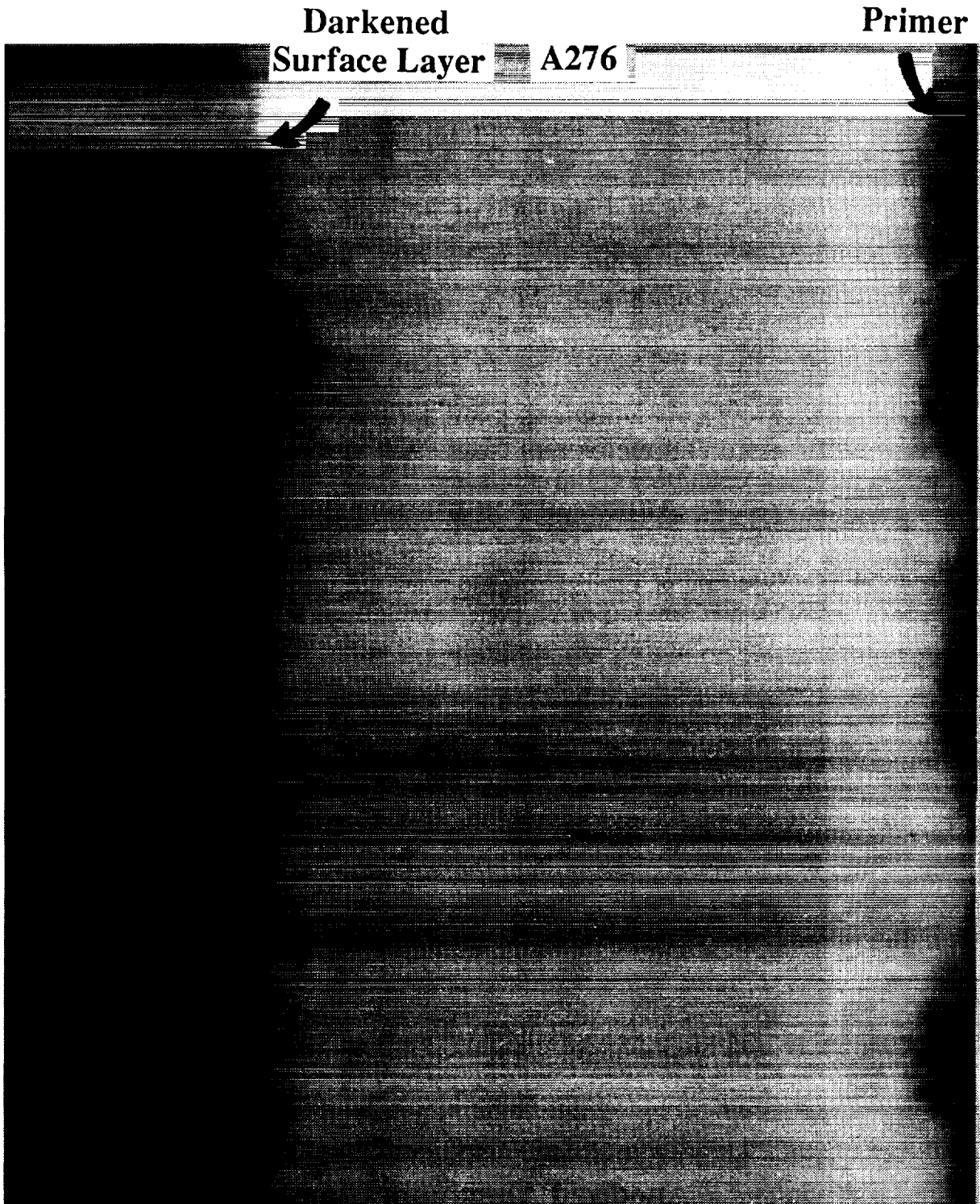


Figure 56. Cross-section of Chemglaze A276 white polyurethane paint on tray clamp B4-7 at 2500X magnification. Titania particles are visible to the very surface of the paint. The discolored layer is very thin,  $\sim 0.2 \mu\text{m}$ . See Appendix C for color figure.

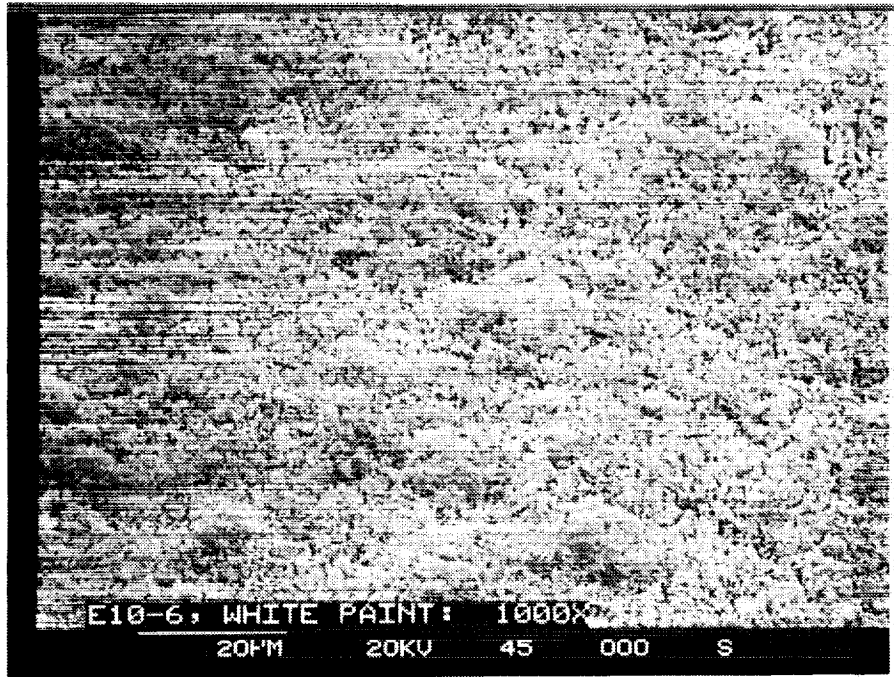


Figure 57. SEM of Chemglaze A276 white paint on tray clamp E10-6, 1000X magnification.

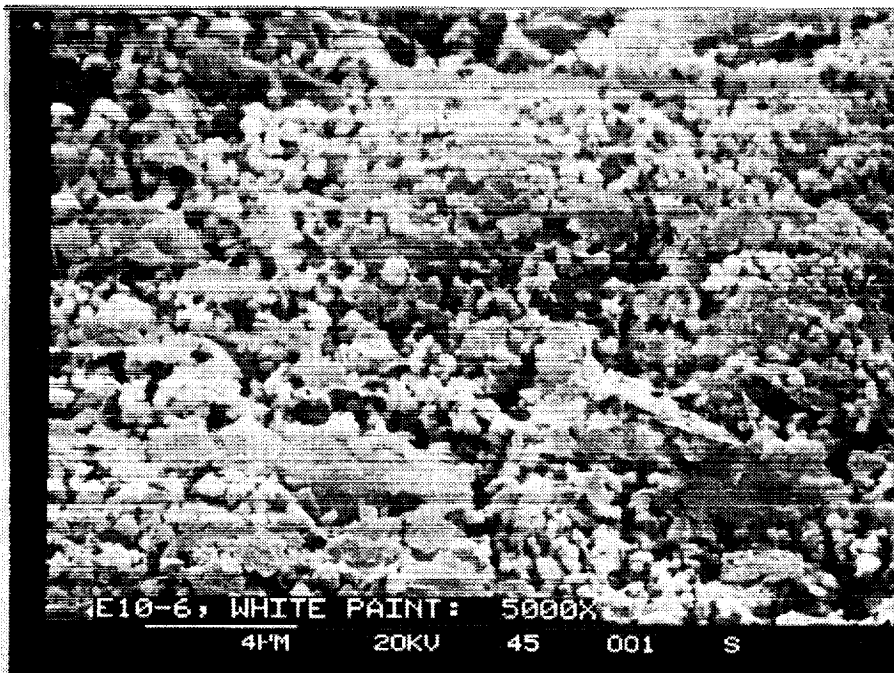


Figure 58. SEM of Chemglaze A276 white paint on tray clamp E10-6, 5000X magnification.

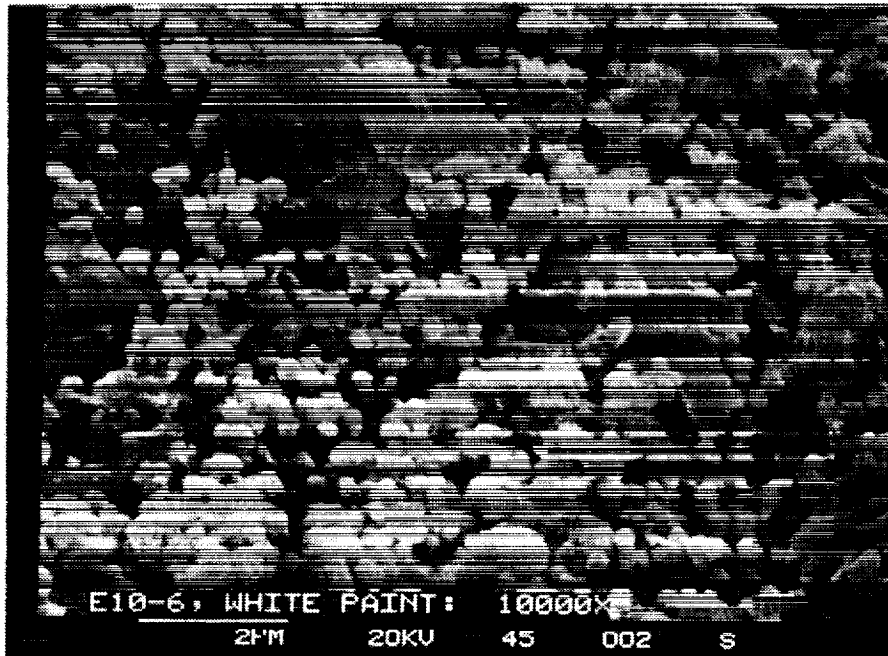


Figure 59. SEM of Chemglaze A276 white paint on tray clamp E10-6, 10,000X magnification.



Figure 60. SEM of Chemglaze A276 white paint on tray clamp E10-6, 25,000X magnification.

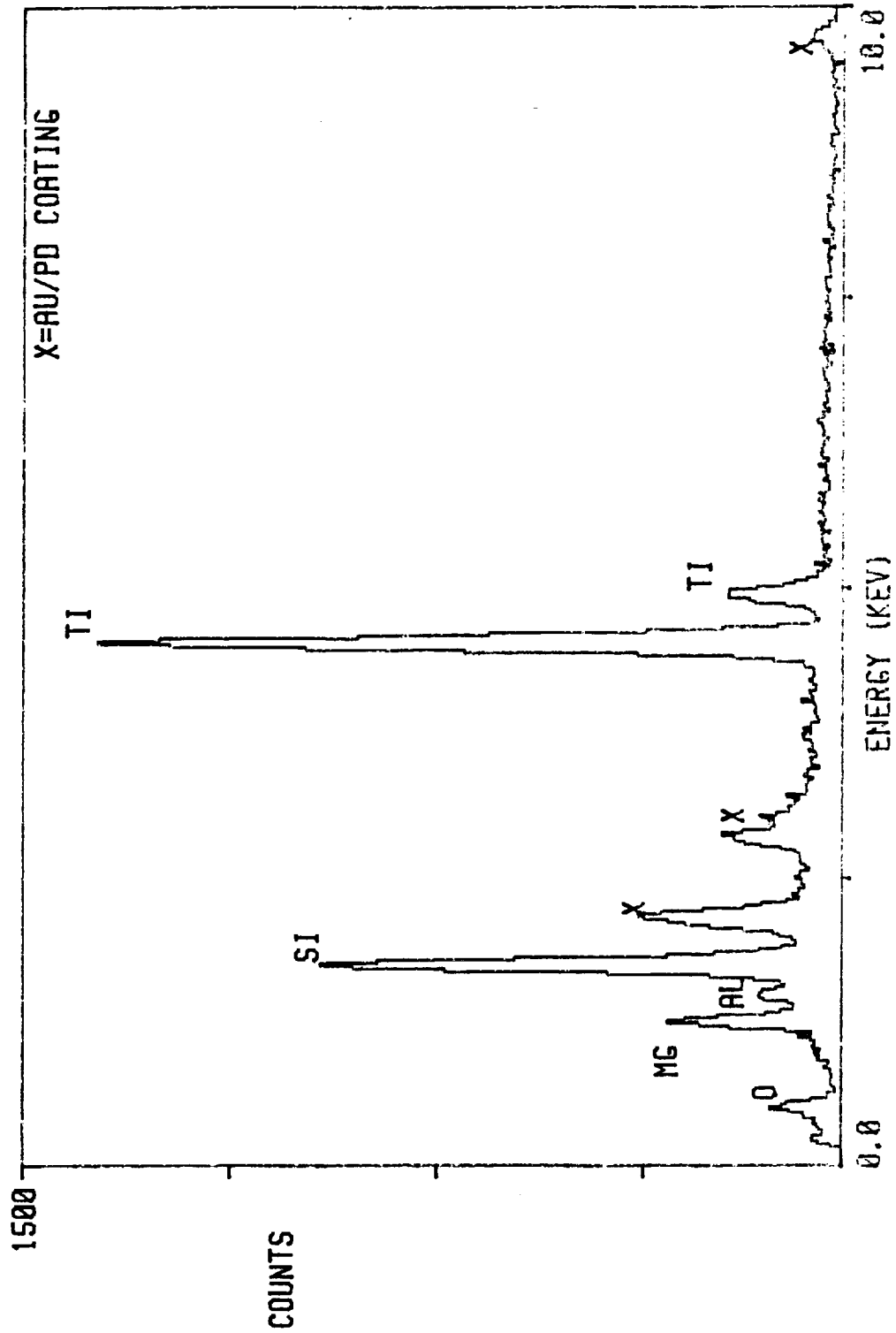


Figure 61. Electron microprobe chemical analysis of Chemglaze A276 white paint taken from tray clamp E10-6, during the scan for figure 58.

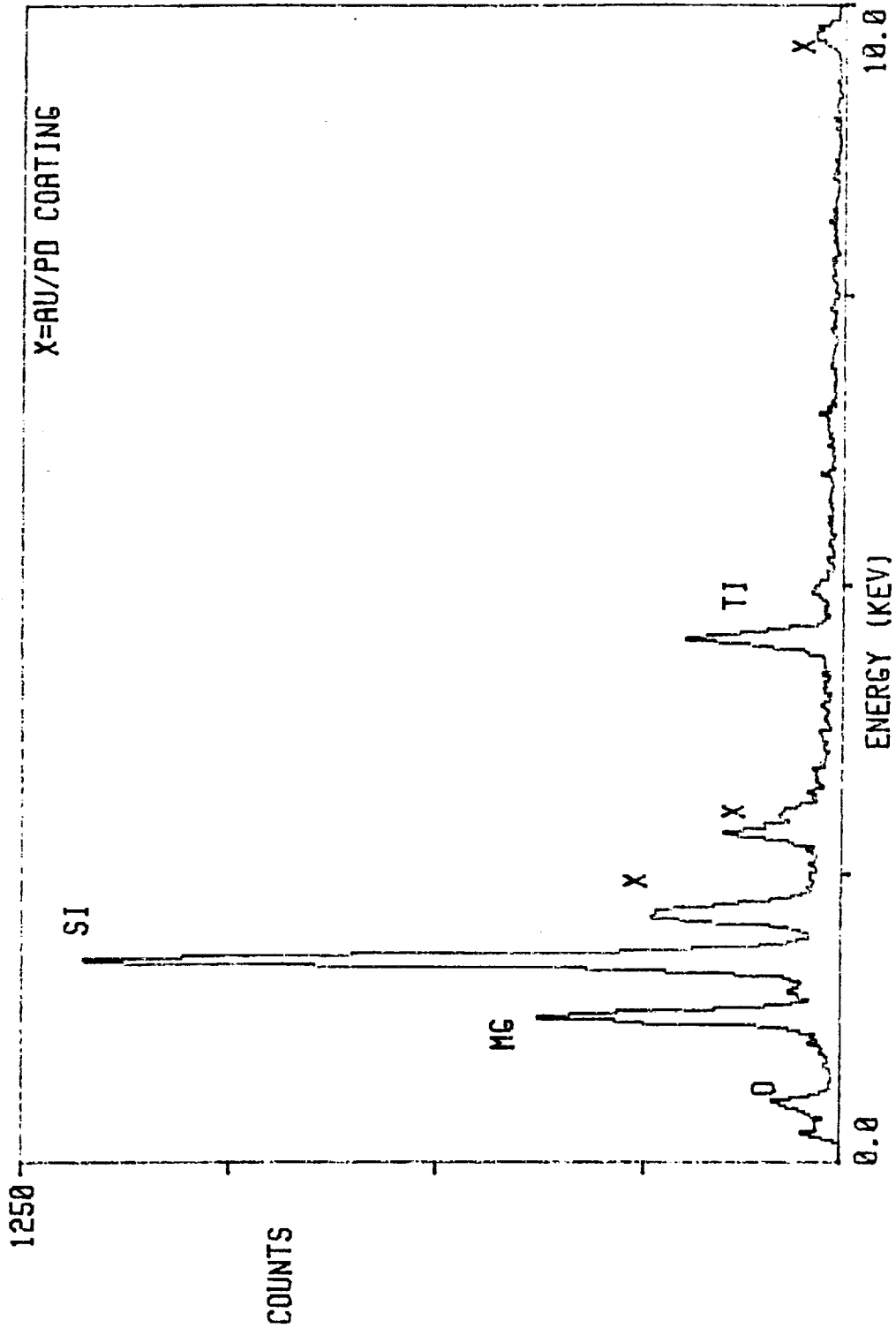


Figure 62. Electron microprobe chemical analysis of Chemglaze A276 white paint taken from tray clamp E10-6 during the scan for figure 60, focusing on the darker flake material.

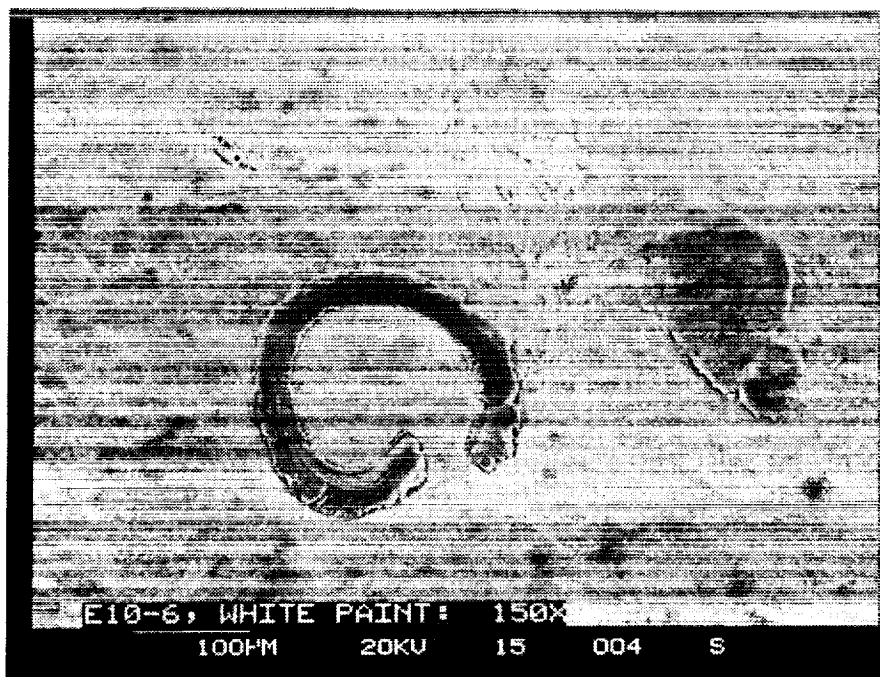


Figure 63. SEM of Chemglaze A276 white paint on tray clamp E10-6, showing two unusual and adjacent surface features at 150X magnification.

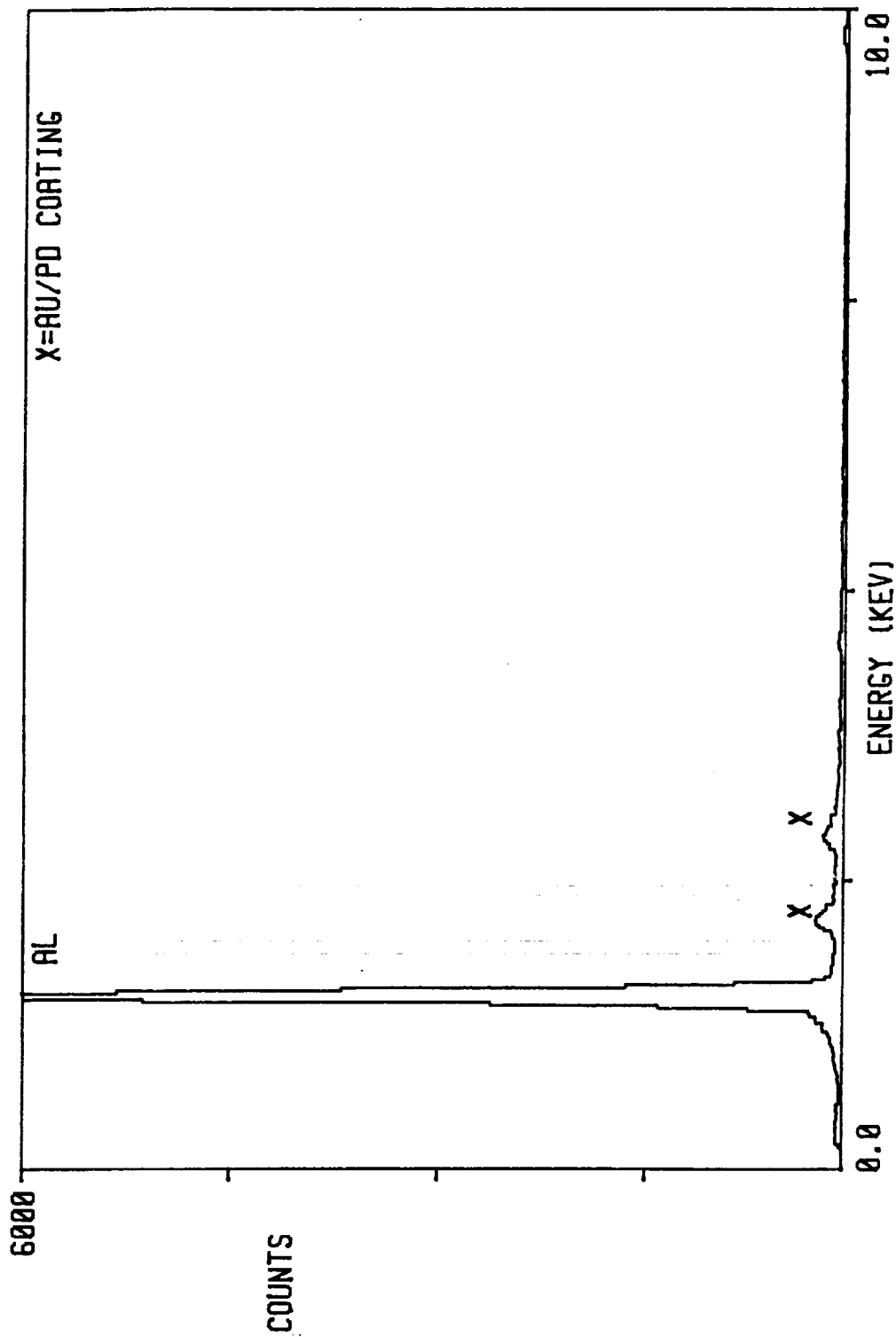


Figure 64. Electron microprobe chemical analysis of the spiral particle in figure 63.

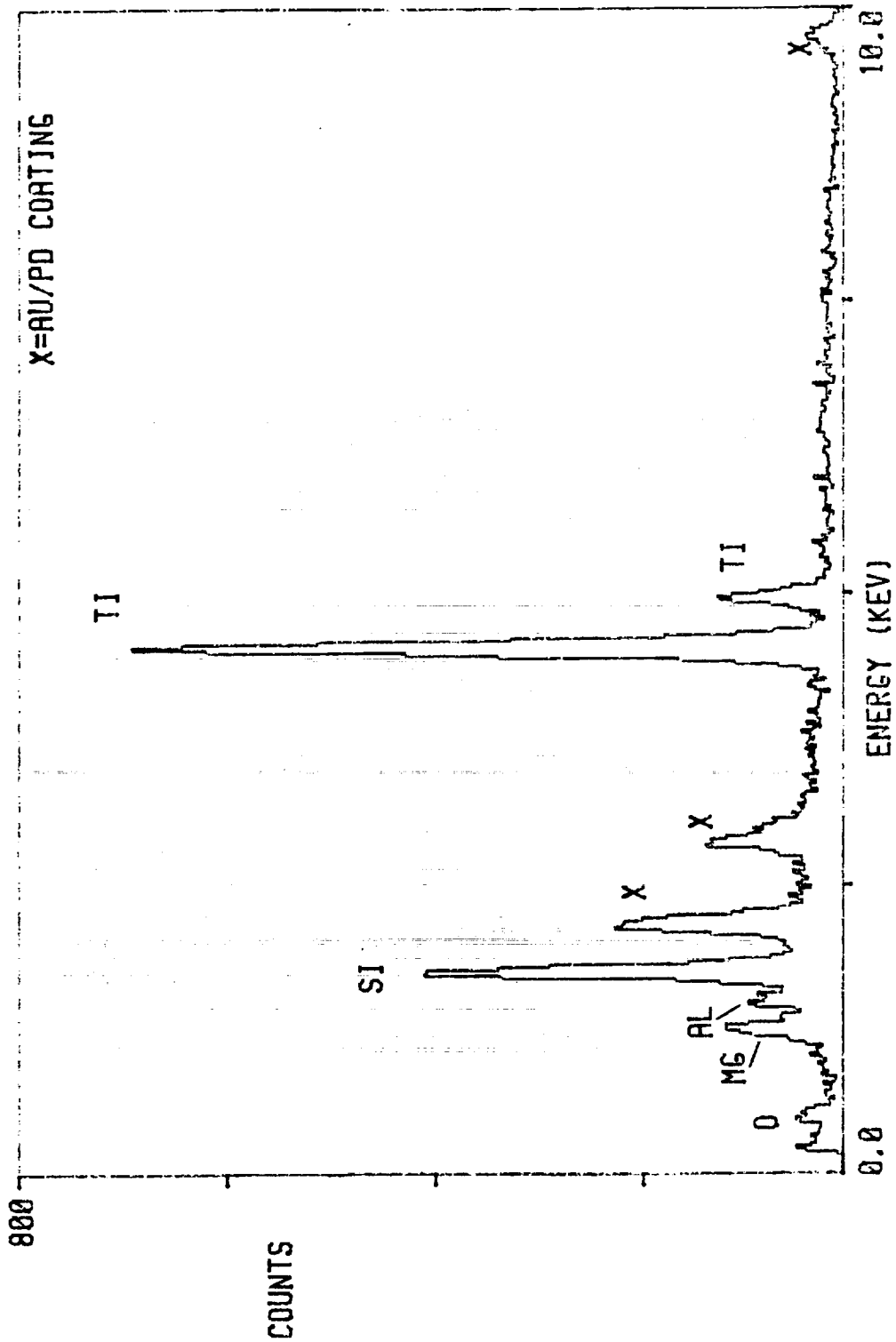


Figure 65. Electron microprobe chemical analysis of the dark clump adjacent to the spiral particle in figure 63.

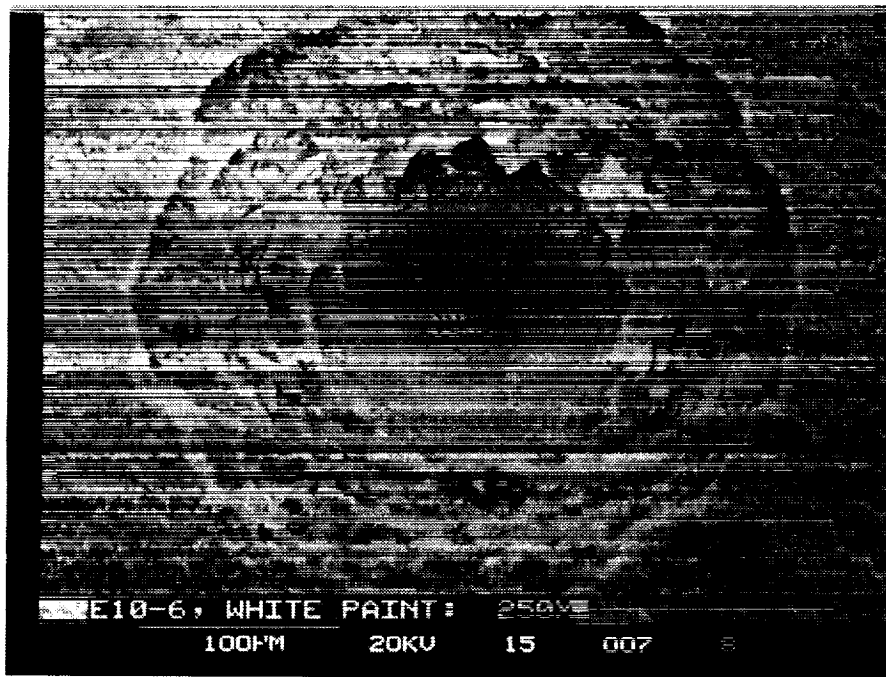


Figure 66. SEM of Chemglaze A276 white paint on tray clamp E10-6, focusing on a micrometeoroid or debris impact in the surface (250X magnification).

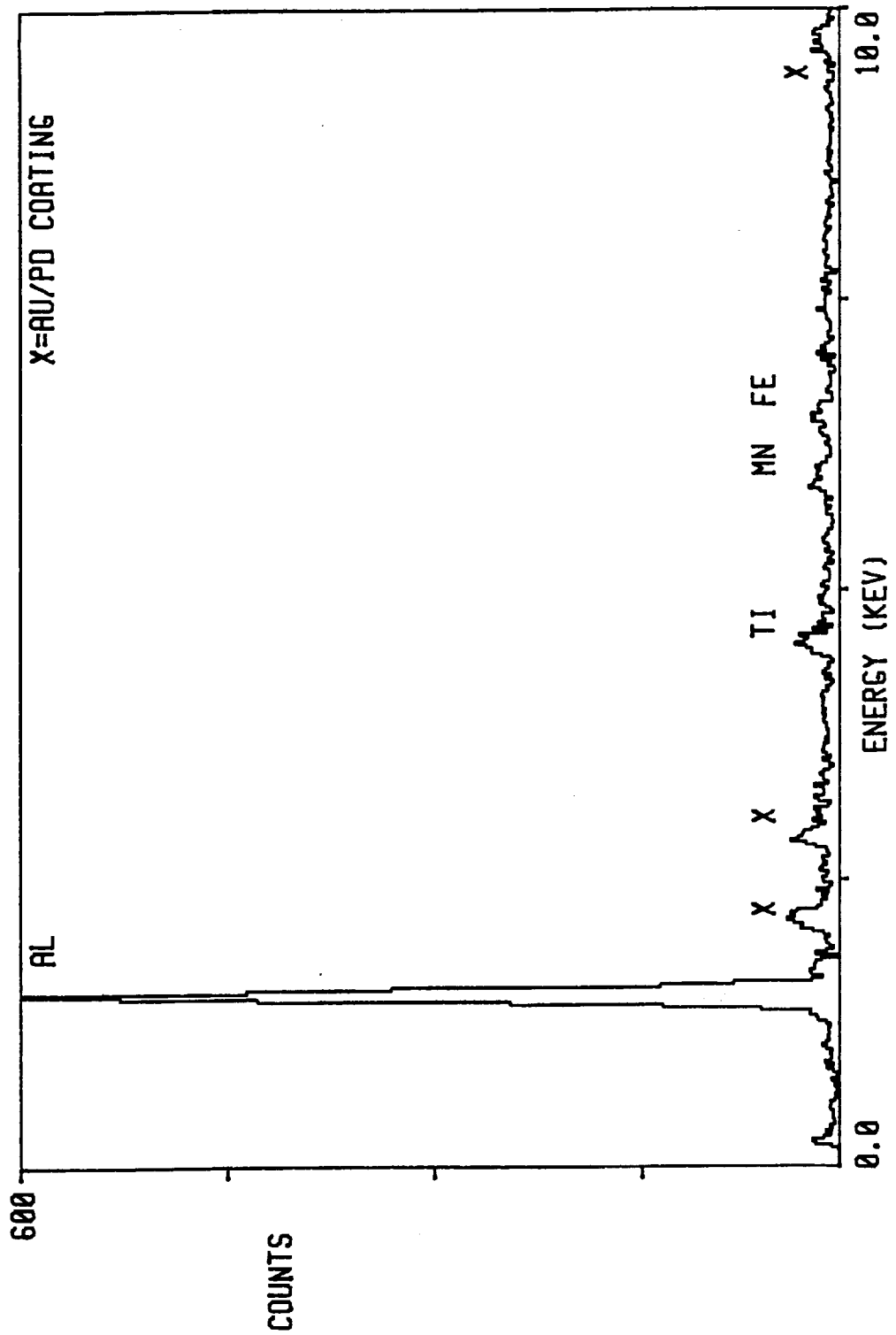


Figure 67. Electron microprobe chemical analysis of the crater bottom in figure 66.

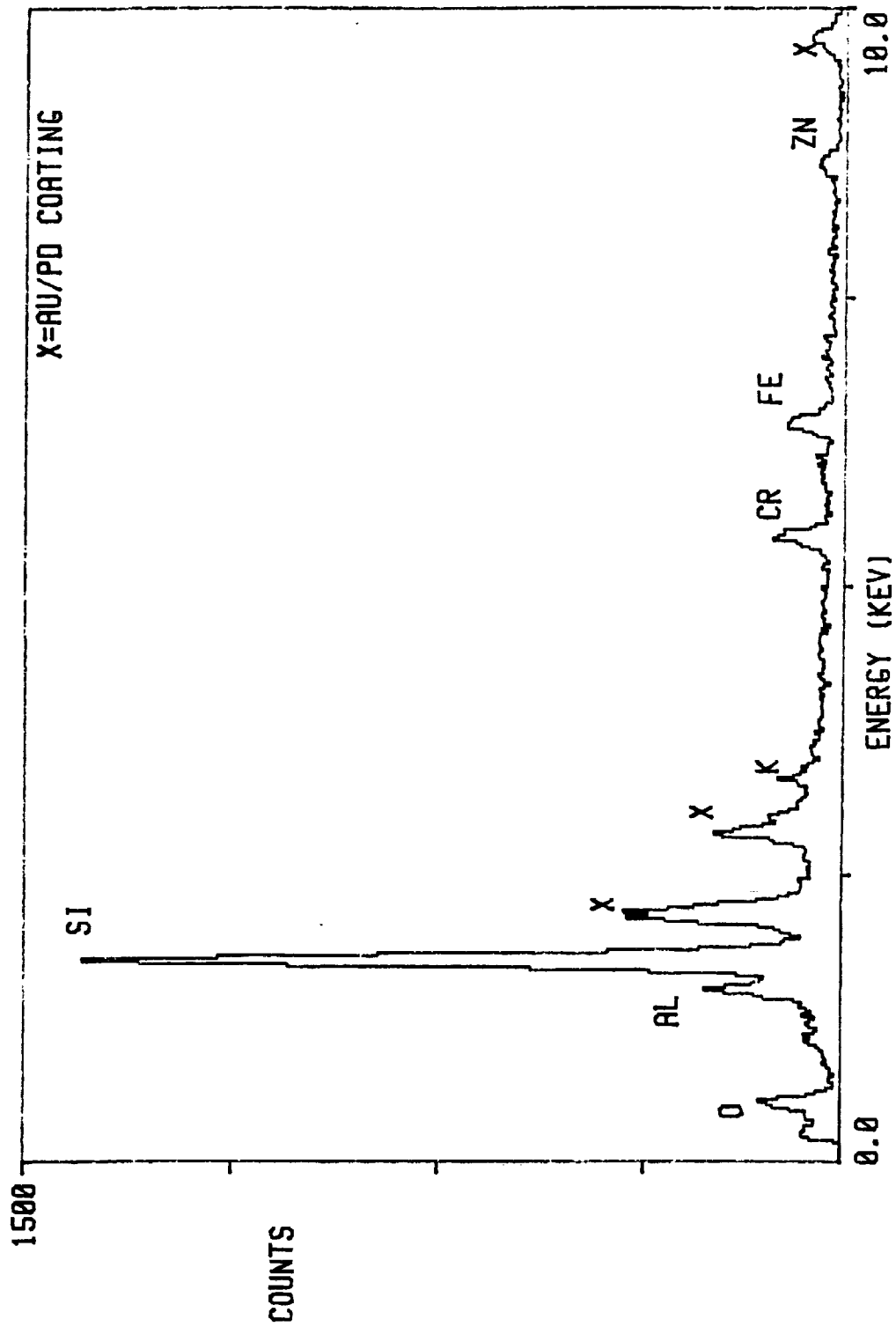


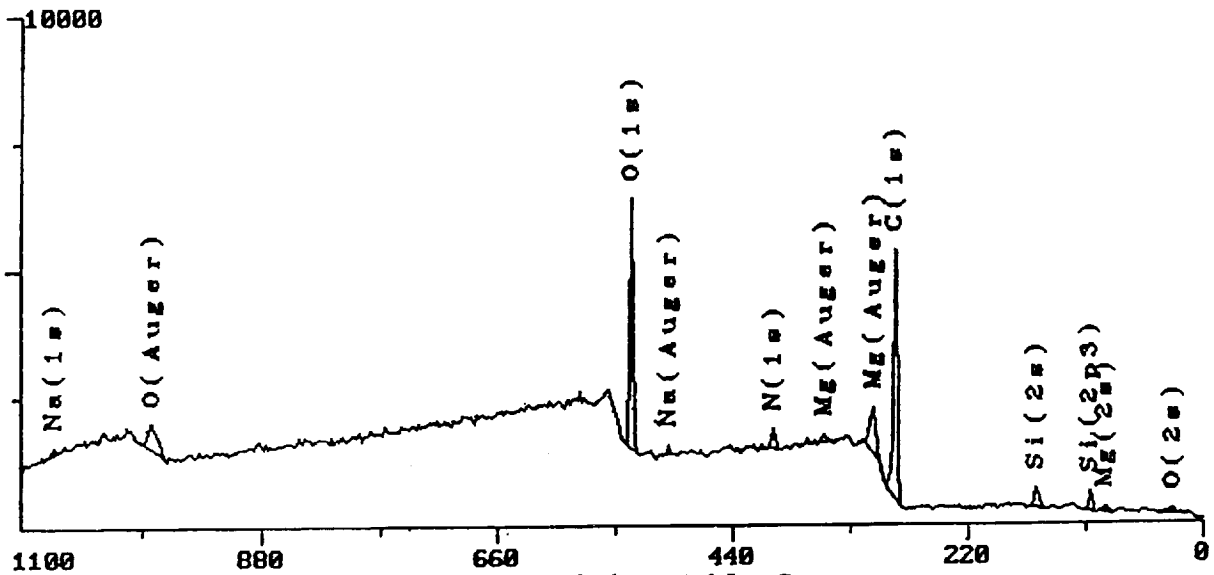
Figure 68. Electron microprobe chemical analysis of Chemglaze Z306 black paint on tray clamp E10-6.

CONTROL WHITE PAINT SURFACE

Spot: 400x1000µ  
 Scans: 8 of 8  
 Region: 1/ 1

Resolution: 4  
 Neutralizer: 0.0eU  
 Aperture: None

Energy:  
 Counts:



Surface Composition Table Summary

Element	Binding Energy	atom %
O (1s)	533.83	21.32 %
Na (Auger)	497.88	0.00 %
N (1s)	401.12	2.91 %
C (1s)	286.06	67.77 %
Si (2s)	154.63	5.22 %
Na (1s)	1069.94	0.40 %
Mg (2s)	92.17	2.39 %
Total Percent		100.00 %

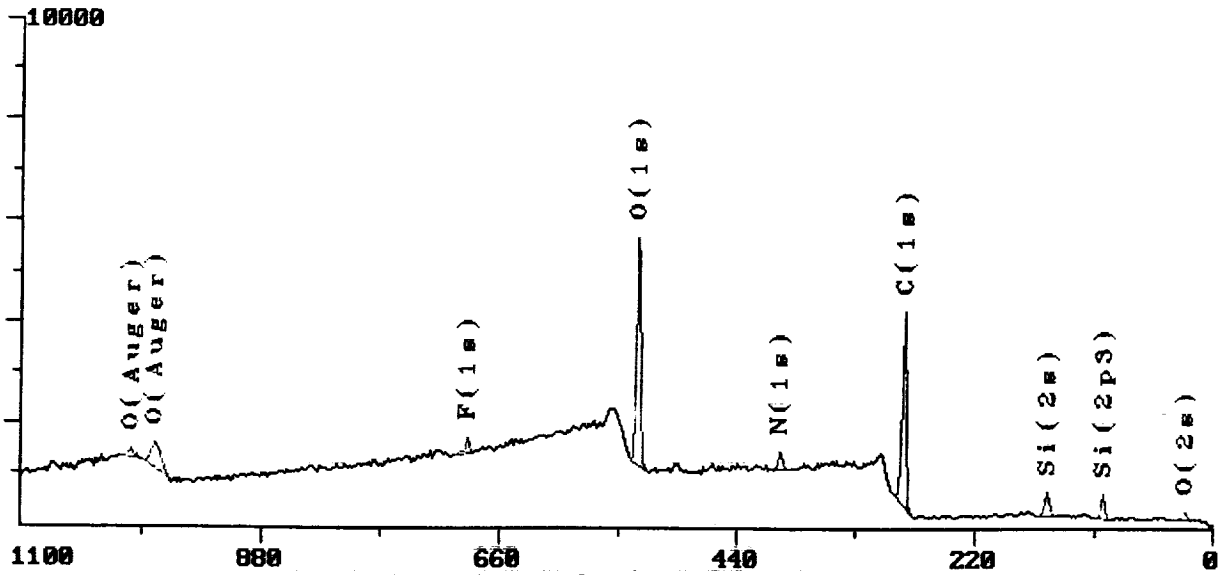
Figure 69. ESCA data for Chemglaze A276 white paint control specimen.

**E2-3 CLIP WHITE URETHANE SURFACE (SHINY)**

Spot: 400x1000µ  
 Scans: 4 of 4  
 Region: 1/ 1

Resolution: 4  
 Neutralizer: 2.0eV  
 Aperture: None

Energy:  
 Counts:



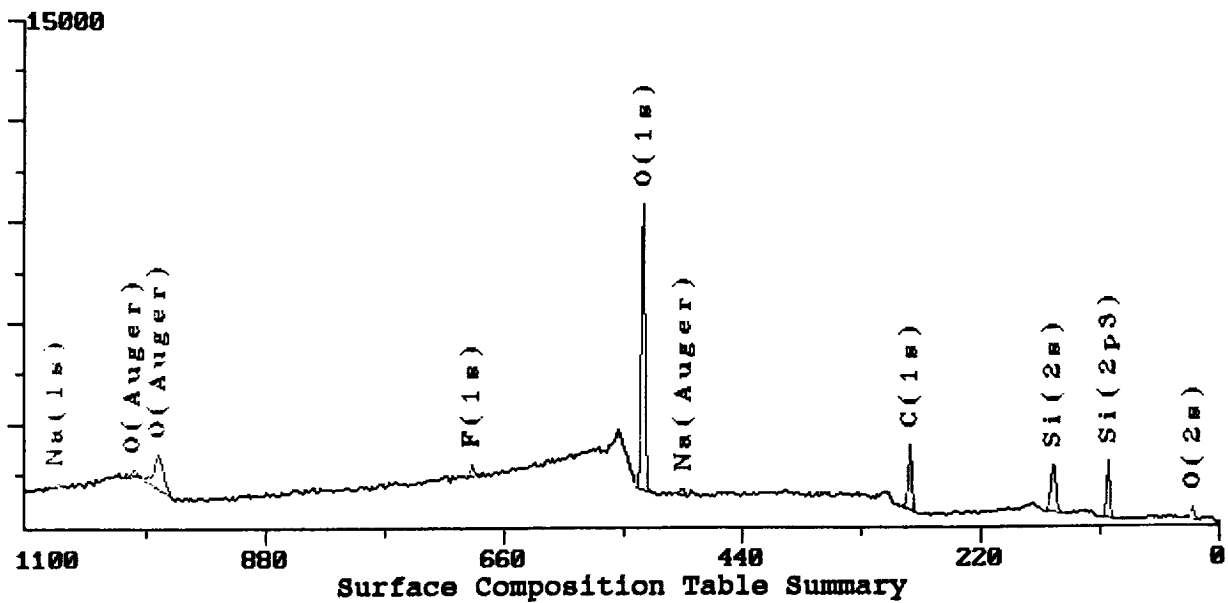
Surface Composition Table Summary

Element	Binding Energy	atom %
F (1s)	688.18	1.24 %
O (1s)	531.17	28.94 %
N (1s)	398.70	3.81 %
C (1s)	283.32	59.27 %
Si (2s)	152.20	6.74 %
Total Percent		100.00 %

Figure 70. ESCA data for Chemglaze A276 white paint on E2-3 specimen.

**C03-2 CLIP WHITE URETHANE SURFACE**

Spot: 400x1000µ Resolution: 4 Energy:  
 Scans: 4 of 4 Neutralizer: 0.5eV Counts:  
 Region: 1/ 1 Aperture: None



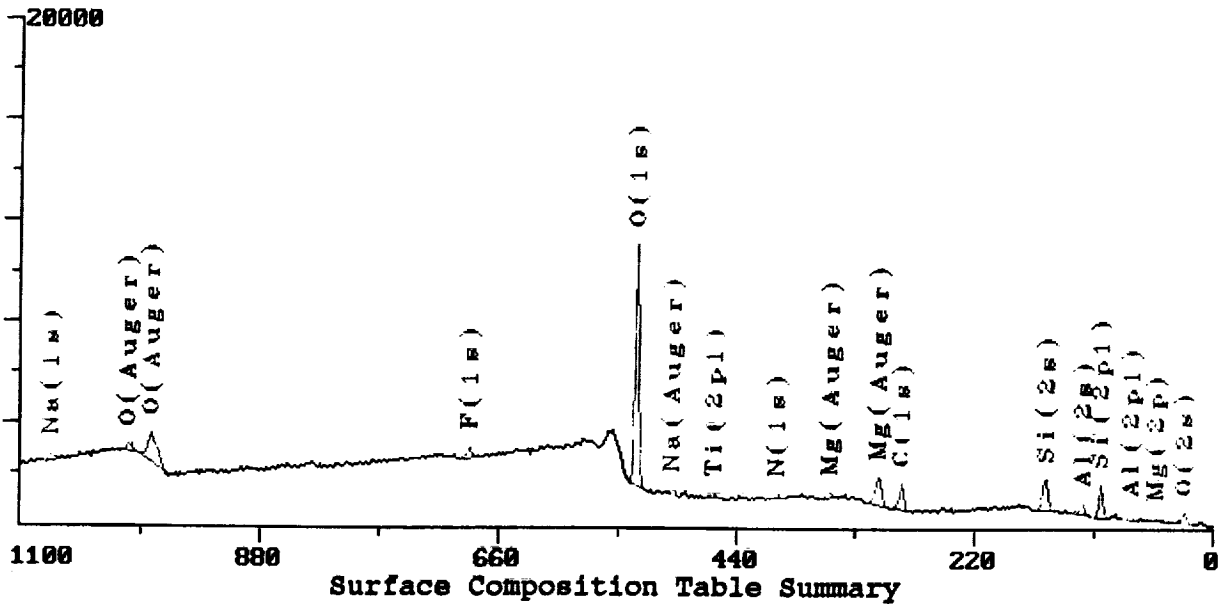
Surface Composition Table Summary

Element	Binding Energy	atom %
F (1s)	688.01	1.58 %
O (1s)	530.60	48.17 %
C (1s)	282.93	27.84 %
Si (2s)	151.67	22.29 %
Na (1s)	1071.95	0.11 %
Total Percent		100.00 %

Figure 71. ESCA data for Chemglaze A276 white paint on C3-2 specimen.

**B7-7 CLIP WHITE URETHANE SURFACE**

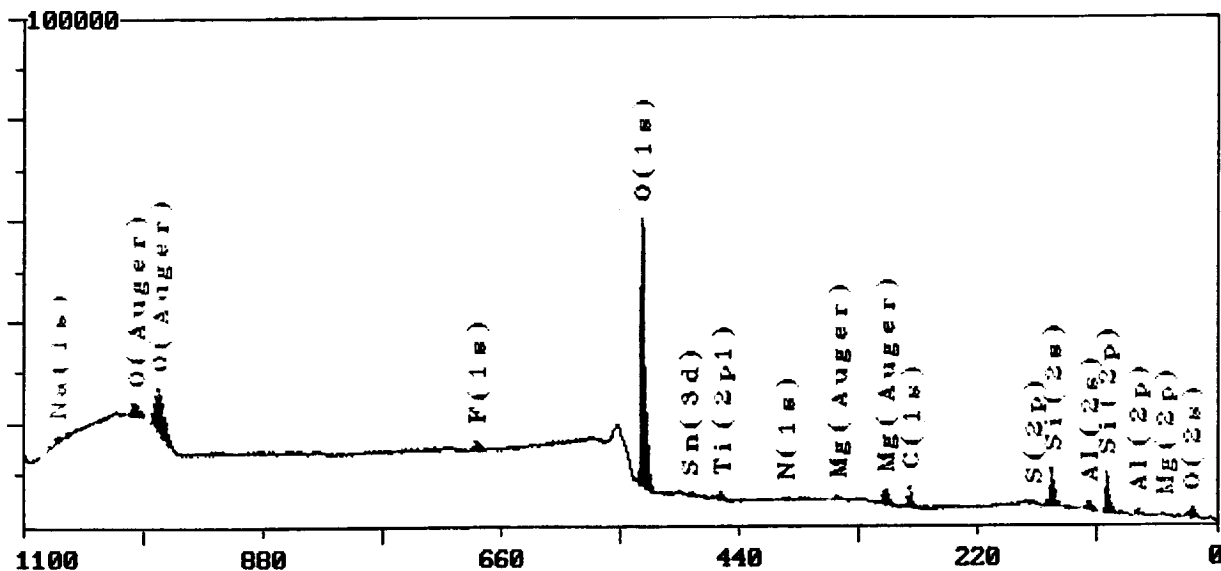
Spot: 400x1000µ Resolution: 4 Energy:  
 Scans: 4 of 4 Neutralizer: 2.0eV Counts:  
 Region: 1/ 1 Aperture: None



<u>Element</u>	<u>Binding Energy</u>	<u>atom %</u>
F (1s)	685.10	2.06 %
O (1s)	532.08	49.03 %
Ti (2p1)	459.43	1.11 %
Mg (Auger)	306.47	4.69 %
C (1s)	284.87	15.84 %
Si (2s)	153.11	18.04 %
Al (2s)	118.71	8.08 %
Na (1s)	1071.95	1.15 %
Total Percent		100.00 %

Figure 72. ESCA data for Chemglaze A276 white paint on B7-7 specimen.

LDEF - E09 Tray, Circlip 3 - White Paint  
 Spot: 400x1000µ Resolution: 4 Energy:  
 Scans: 20 of 20 Neutralizer: 2.0eV Counts:  
 Region: 1/ 1 Aperture: None



Surface Composition Table Summary

Element	Binding Energy	atom %
Na (1s)	1072.2	1.81
F (1s)	685.4	1.84
O (1s)	532.0	57.08
Sn (3d)	486.9	0.06
Ti (2p1)	458.6	2.08
N (1s)	399.7	1.00
C (1s)	284.6	11.33
S (2p)	170.2	1.22
Si (2p)	102.6	18.33
Al (2p)	74.0	3.07
Mg (2p)	50.0	2.17

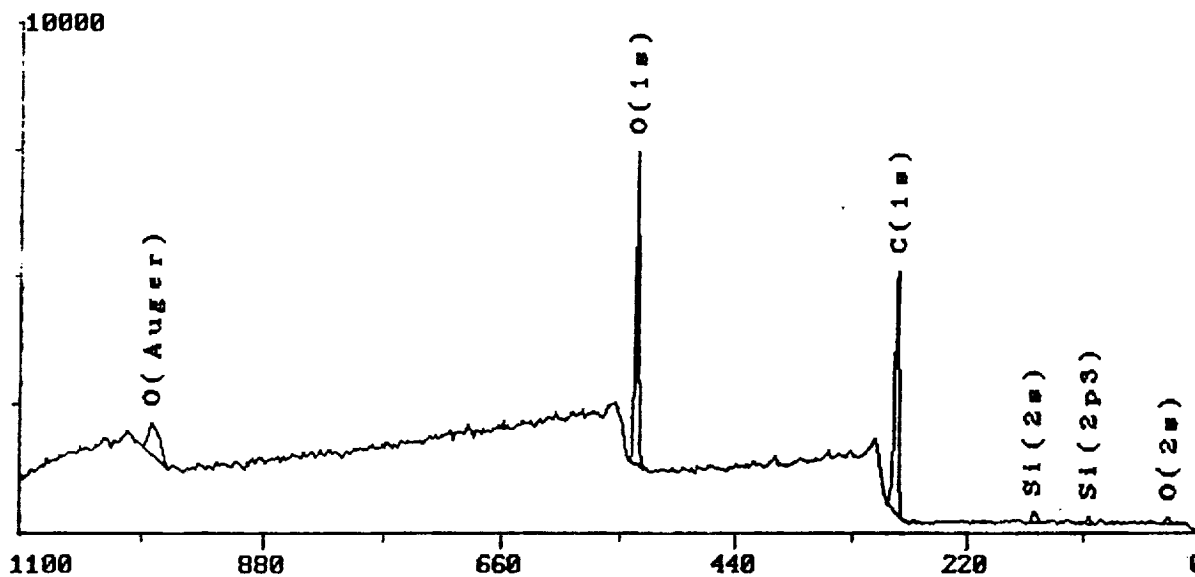
Figure 73. ESCA data for Chemglaze A276 white paint on E9-3 specimen.

CONTROL BLACK PAINT SURFACE

Spot: 400x1000µ  
 Scans: 8 of 8  
 Region: 1/ 1

Resolution: 4  
 Neutralizer: 0.0eV  
 Aperture: None

Energy:  
 Counts:



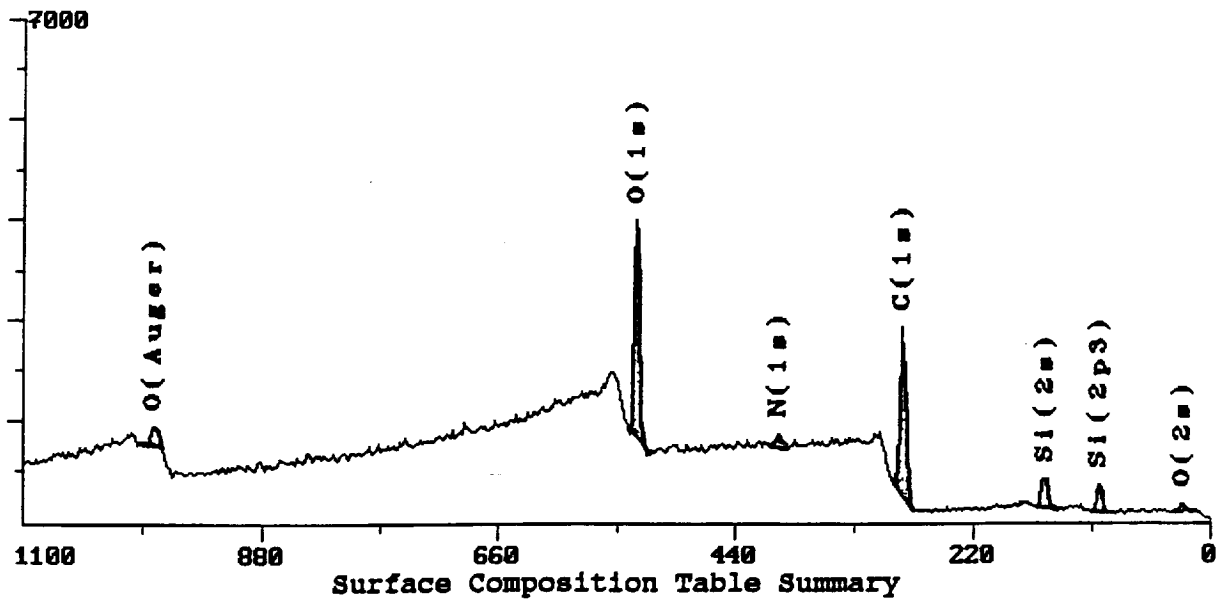
Surface Composition Table Summary

Element	Binding Energy	atom %
O (1s)	533.87	26.75 %
C (1s)	285.92	70.40 %
Si (2s)	154.27	2.85 %
Total Percent		100.00 %

Figure 74. ESCA data for Chemglaze Z306 black paint on control specimen.

**E2-3 CLIP BLACK URETHANE SURFACE**

Spot: 400x1000µ Resolution: 4 Energy:  
 Scans: 4 of 4 Neutralizer: 2.0eV Counts:  
 Region: 1/ 1 Aperture: None



Surface Composition Table Summary

Element	Binding Energy	atom %
O (1s)	531.42	30.44 %
C (1s)	284.58	56.00 %
Si (2s)	151.89	10.31 %
N (1s)	400.73	3.25 %
Total Percent		100.00 %

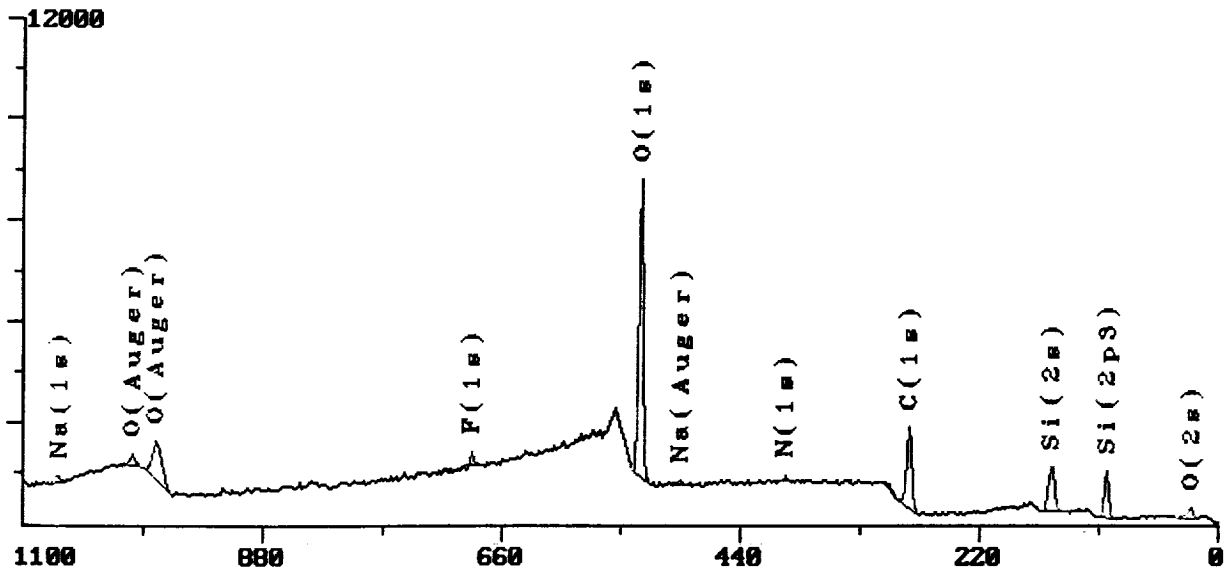
Figure 75. ESCA data for Chemglaze Z306 black paint on E2-3 specimen.

**CO3-2 CLIP BLACK URETHANE SURFACE**

Spot: 400x1000µ  
 Scans: 4 of 4  
 Region: 1/ 1

Resolution: 4  
 Neutralizer: 0.5eV  
 Aperture: None

Energy:  
 Counts:



**Surface Composition Table Summary**

Element	Binding Energy	atom %
F (1s)	686.55	1.84 %
O (1s)	530.41	42.40 %
N (1s)	397.82	1.40 %
C (1s)	282.79	33.59 %
Si (2s)	151.63	19.91 %
Na (1s)	1067.94	0.86 %
Total Percent		100.00 %

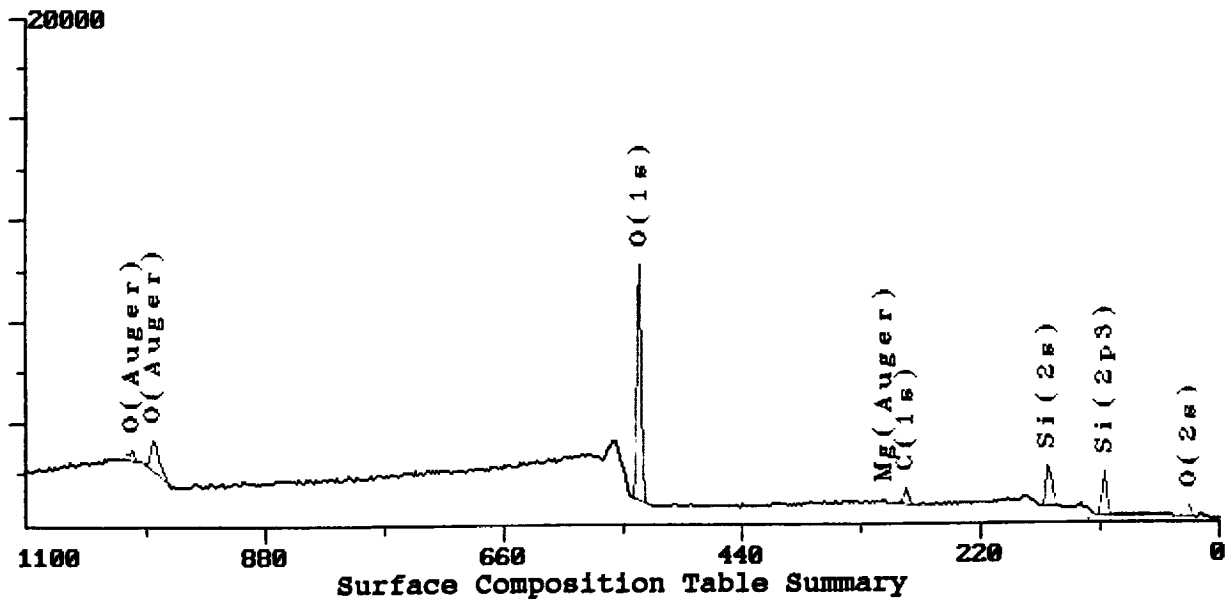
Figure 76. ESCA data for Chemglaze Z306 black paint on C3-2 specimen.

**B7-7 CLIP BLACK URETHANE SURFACE**

Spot: 400x1000µ  
 Scans: 4 of 4  
 Region: 1/ 1

Resolution: 4  
 Neutralizer: 2.0eV  
 Aperture: None

Energy:  
 Counts:

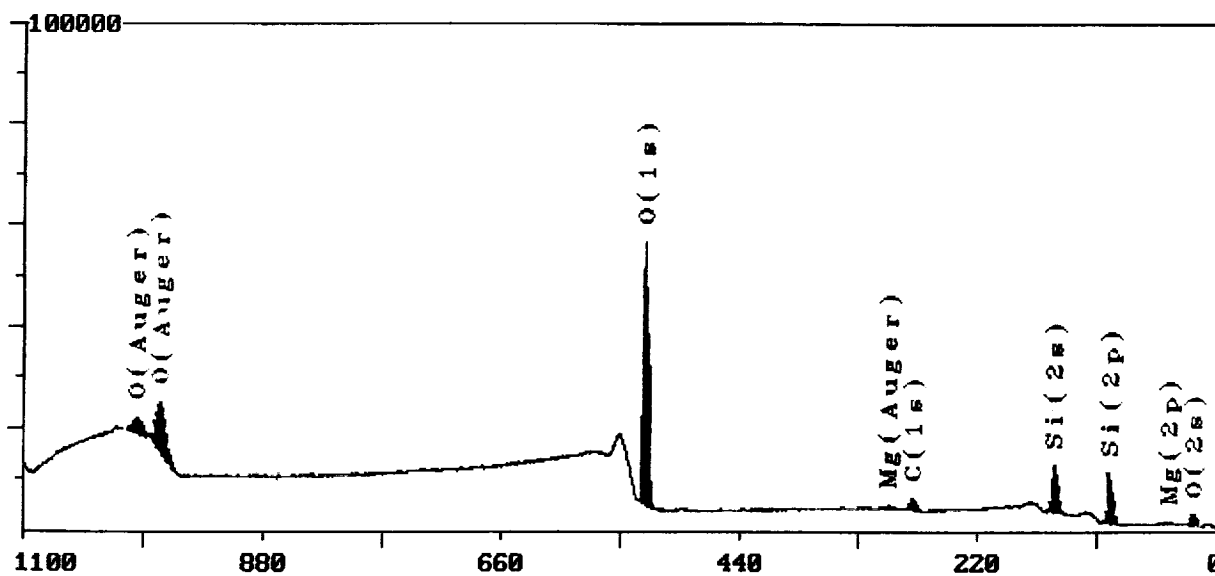


Surface Composition Table Summary

Element	Binding Energy	atom %
O (1s)	534.48	59.28 %
C (1s)	286.89	12.11 %
Si (2s)	155.62	28.38 %
Mg (Auger)	308.56	0.23 %
Total Percent		100.00 %

Figure 77. ESCA data for Chemglaze Z306 black paint on B7-7 specimen.

LDEF - E09 Tray, Circlip 3, Paint - Black Ring  
 Spot: 400x1000µ Resolution: 4 Energy:  
 Scans: 20 of 20 Neutralizer: 2.0eV Counts:  
 Region: 1/ 1 Aperture: None



Surface Composition Table Summary

Element	Binding Energy	atom %
O (1s)	532.7	63.30
C (1s)	284.6	8.06
Si (2p)	103.1	26.30
Mg (2p)	47.7	2.34

Figure 78. ESCA data for Chemglaze Z306 black paint on E9-3 specimen.

NUMBERS LOCATED NEAREST PAINT DISK SYMBOL IS THE MEASURED ABSORPTANCE TO EMITTANCE RATIO FOR WHITE PAINT DISK

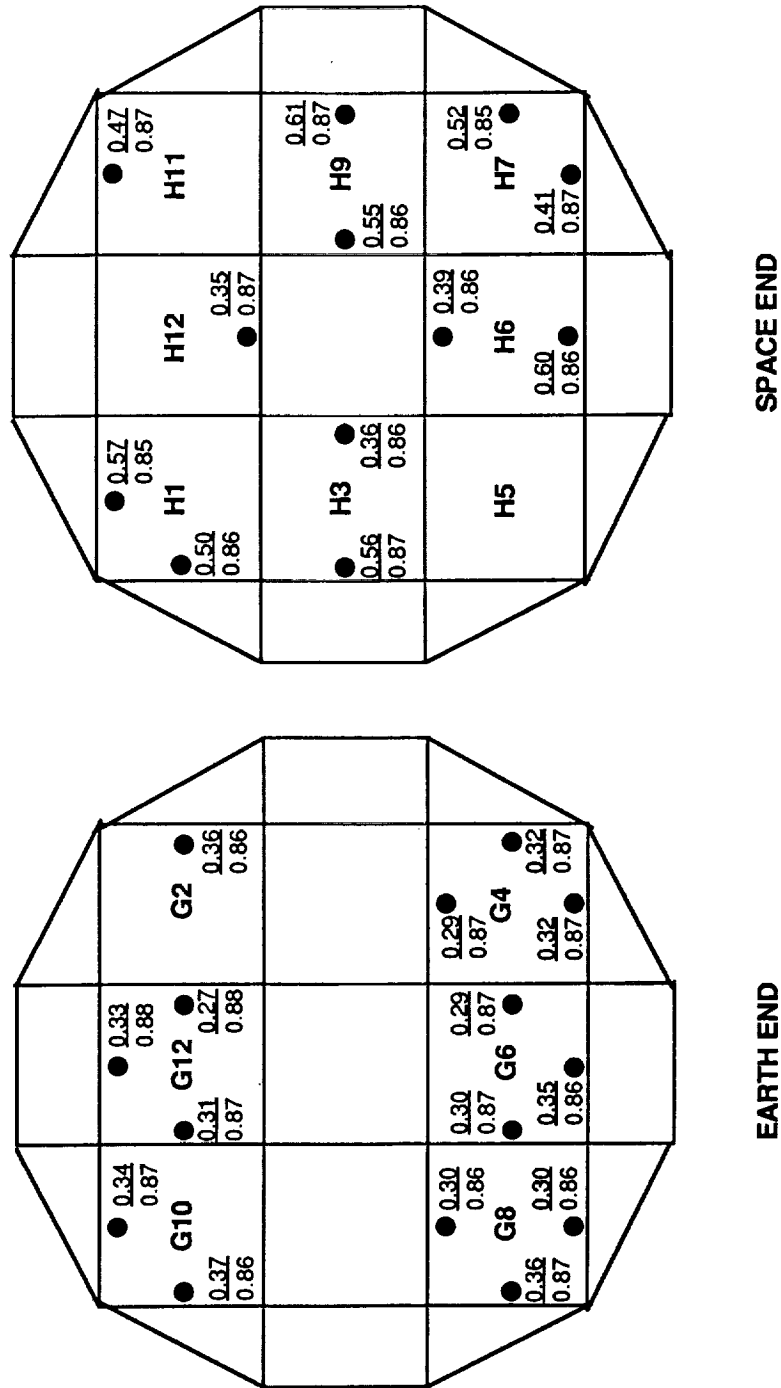
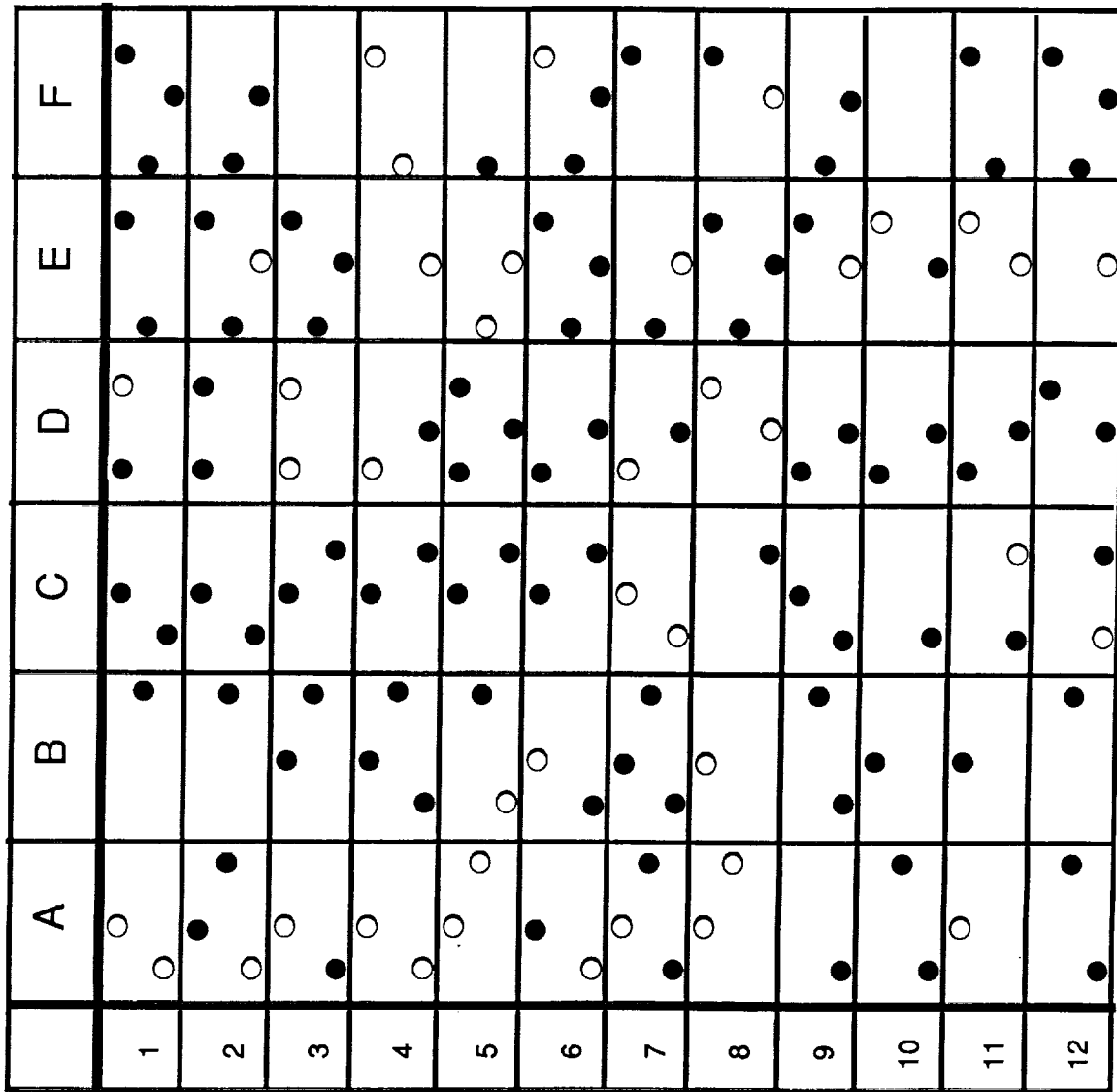


Figure 79. Solar absorptance / thermal emittance ratio for Chemglaze A276 white polyurethane paint on LDEF Earth and space end tray clamps.



○ NO OPTICAL PROPERTIES MEASURED  
 ● OPTICAL PROPERTIES MEASURED

Figure 80. Map of LDEF side tray clamps with thermal control paint disks available to the MSIG.

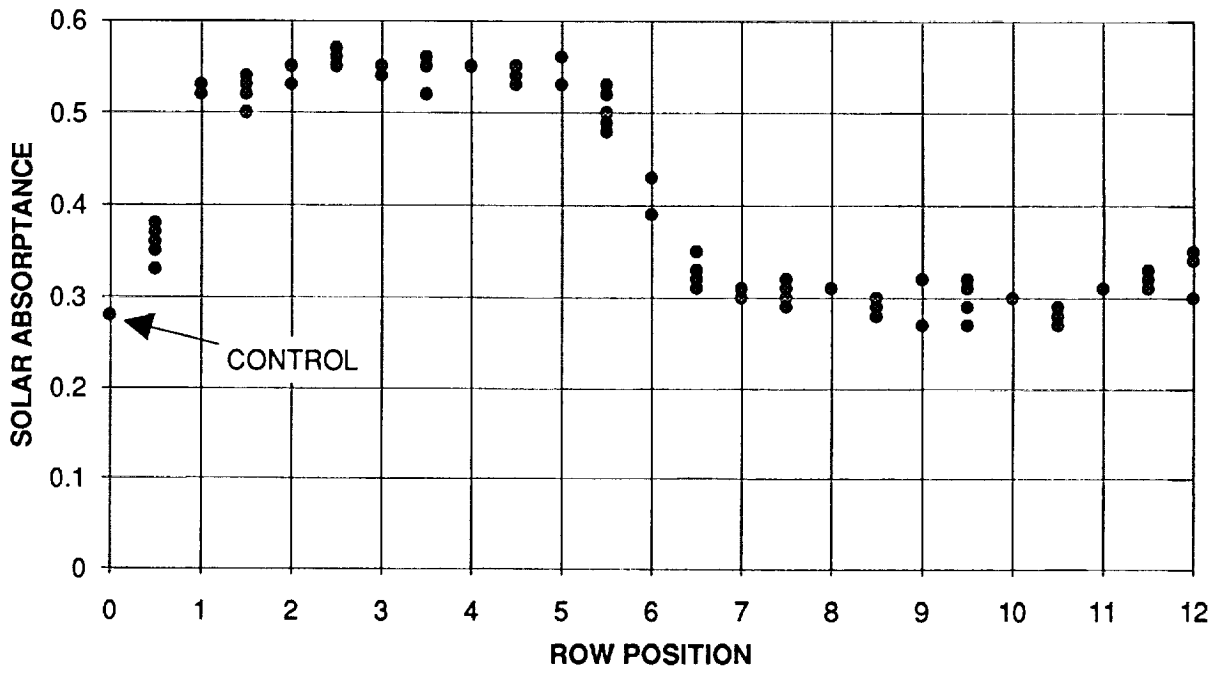


Figure 81. Solar absorbance for Chemglaze A276 white paint versus row position.

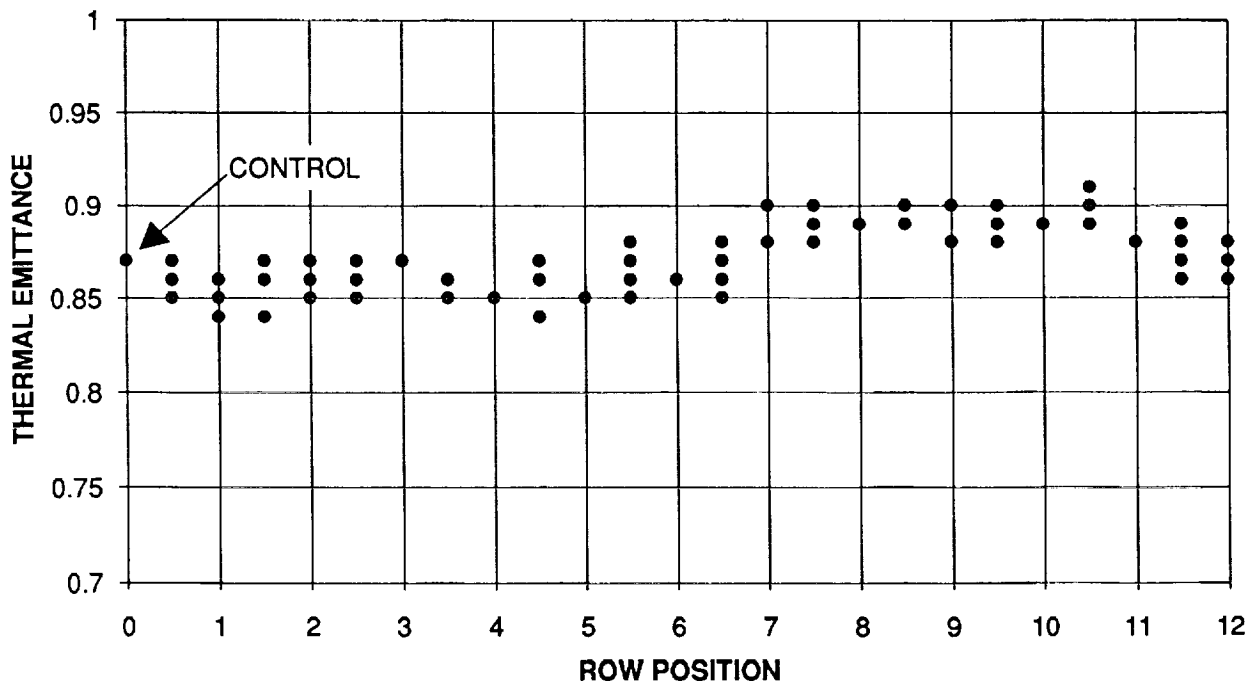


Figure 82. Thermal emittance for Chemglaze A276 white paint versus row position.

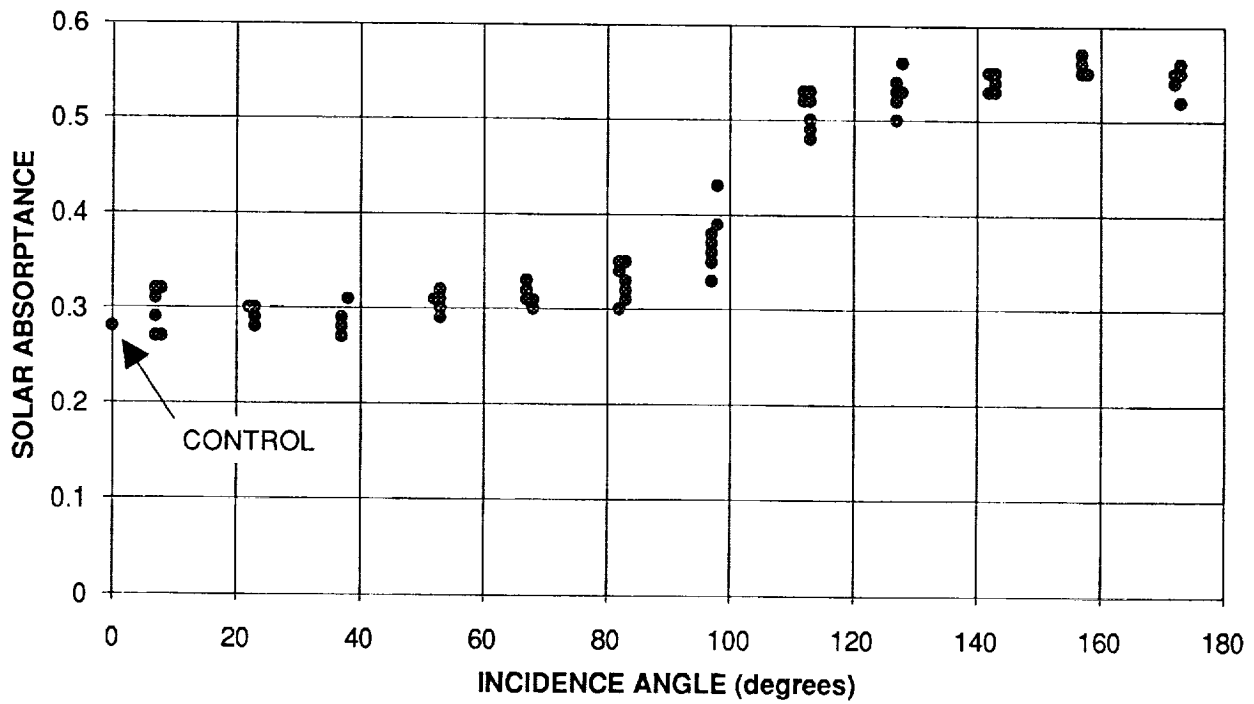


Figure 83. Solar absorbance for Chemglaze A276 white paint versus atomic oxygen incidence angle.

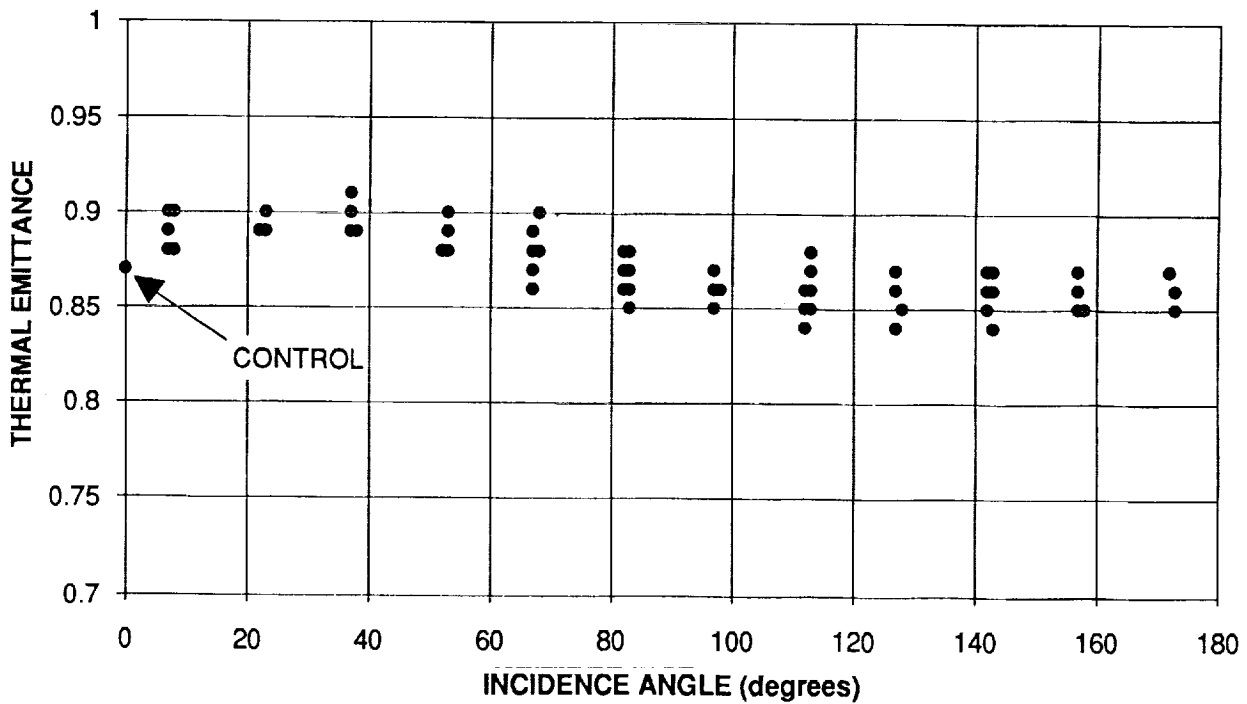


Figure 84. Thermal emittance for Chemglaze A276 white paint versus atomic oxygen incidence angle.

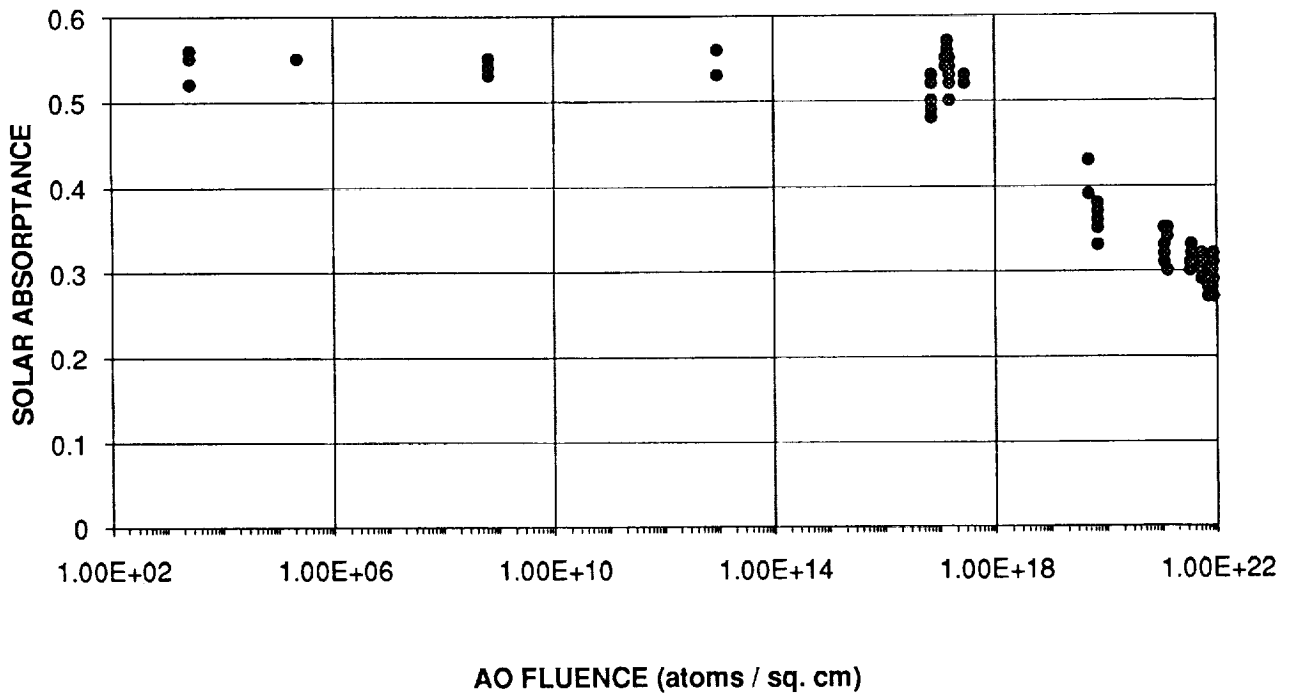


Figure 85. Solar absorbance for Chemglaze A276 white polyurethane paint versus atomic oxygen fluence.

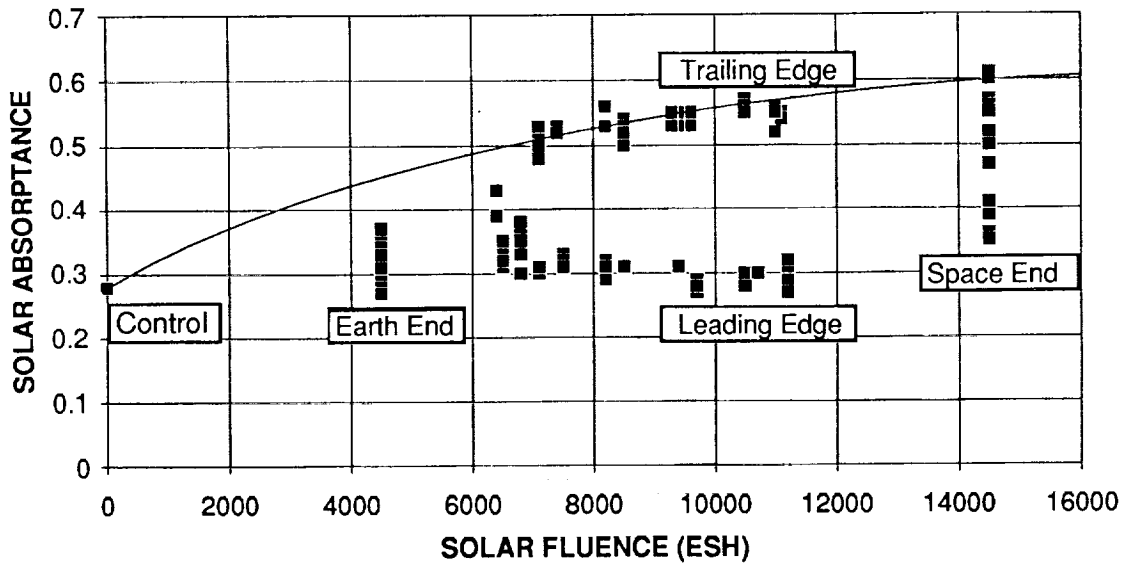


Figure 86. Solar absorbance for Chemglaze A276 white polyurethane paint versus ultraviolet radiation exposure.

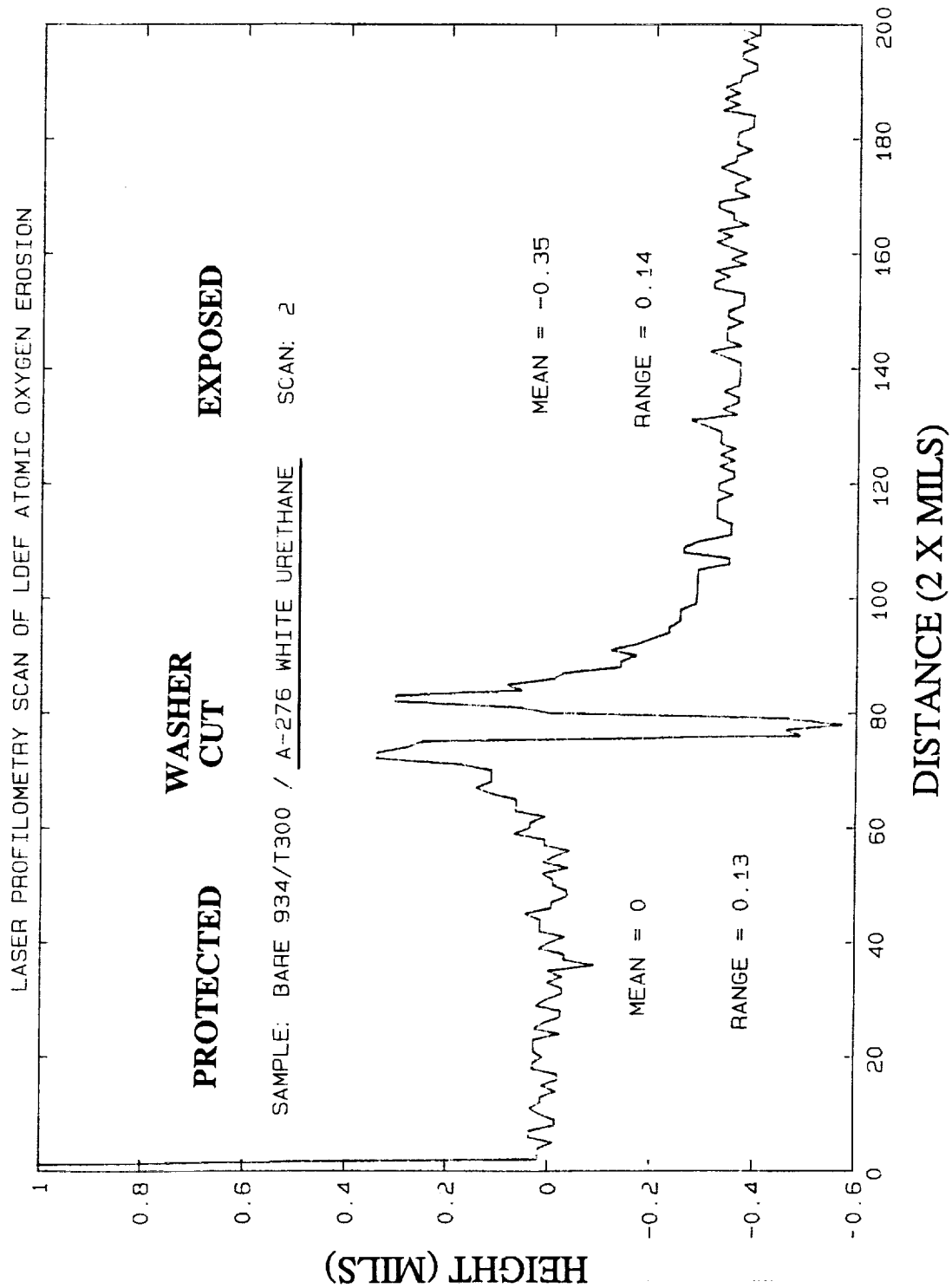


Figure 87. Laser profilometry scan of Chemglaze A276 white polyurethane paint, moving from a protected area to an AO exposed surface, from which all loose paint pigment had been removed. Specimen was taken from the bare-to-A276 paint interface on the Experiment M0003 composite panel (see figure 10).

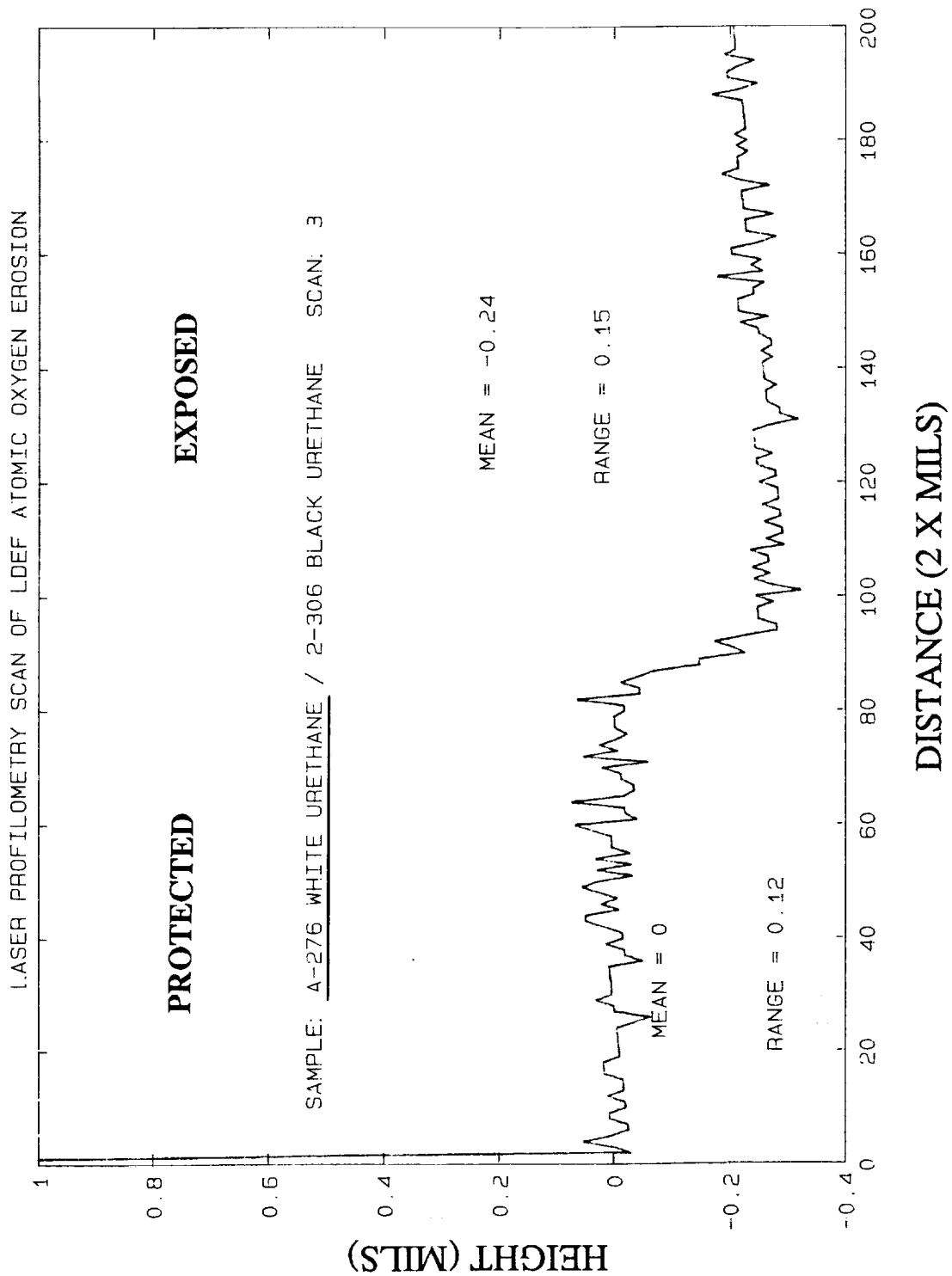


Figure 88. Laser profilometry scan of Chemglaze A276 white polyurethane paint, moving from a protected area to an AO exposed surface, from which all loose paint pigment had been removed. Specimen was taken from the Z306-to-A276 paint interface on the Experiment M0003 composite panel (see figure 10).

C-2.

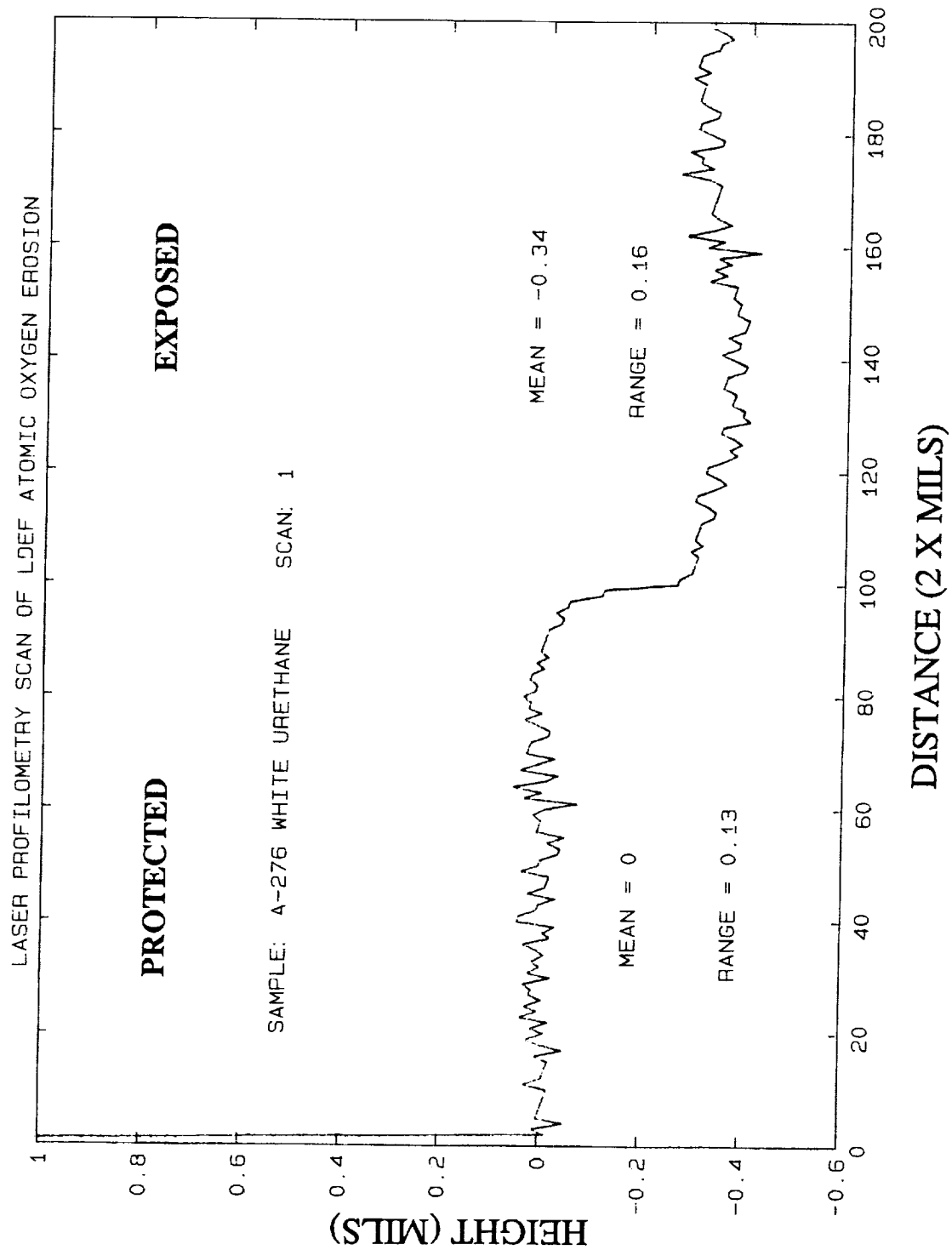


Figure 89. Laser profilometry scan of Chemglaze A276 white polyurethane paint, moving from a protected area to an AO exposed surface, from which all loose paint pigment had been removed. Specimen was taken from the A276 paint corner of the Experiment M0003 composite panel (see figure 10).

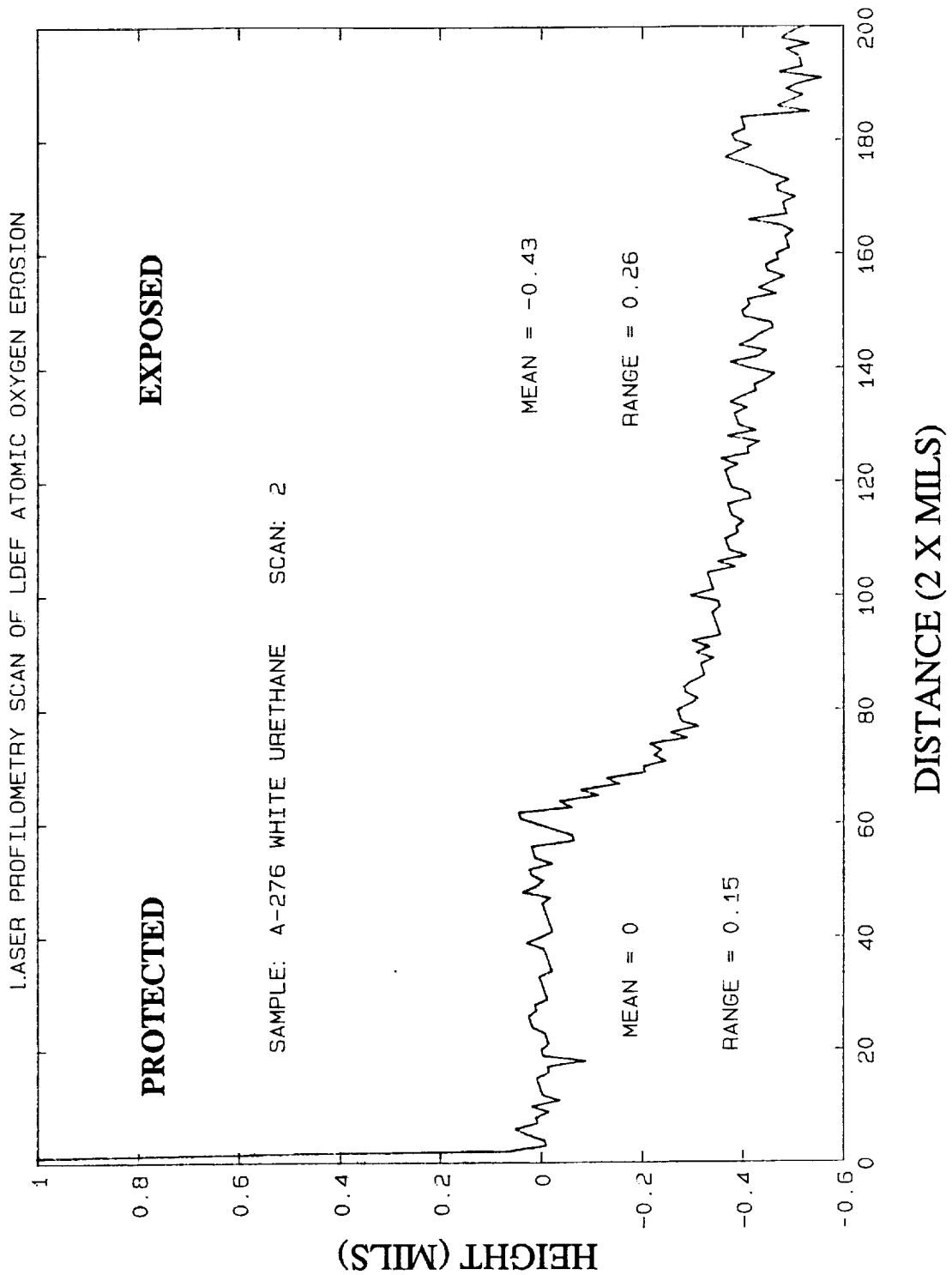


Figure 90. Laser profilometry scan of Chemglaze A276 white polyurethane paint, moving from a protected area to an AO exposed surface, from which all loose paint pigment had been removed. Specimen was taken from the A276 paint corner of the Experiment M0003 composite panel (see figure 10). Scan taken 90° from figure 89 scan.



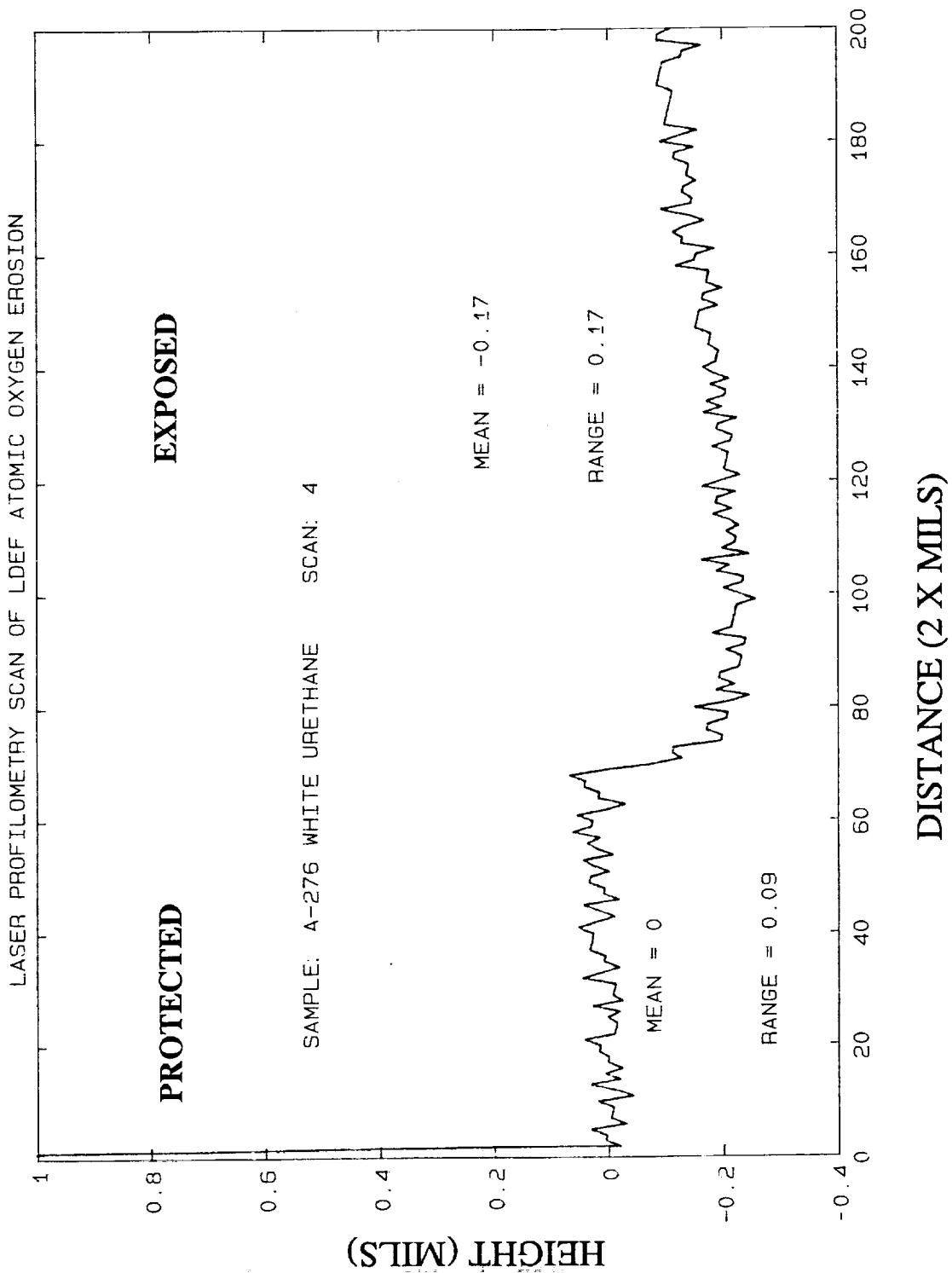


Figure 92. Laser profilometry scan of Chemglaze A276 white polyurethane paint, moving from a protected area to an AO exposed surface, from which all loose paint pigment had been removed. Specimen was taken from the A276 paint corner of the Experiment M0003 composite panel (see figure 10). Scan taken 90° from Figure 91 scan.

**APPENDIX A. Chemglaze A276 Optical Property and  
Environmental Exposure Data for the LDEF Mission**

Specimen	Row	Absorptance	Emittance	Angle (degrees)	AO Fluence (atoms/cm <sup>2</sup> )	Solar ESH (ESH)	Abs./Emit. Ratio
C1-2	0.5	0.36	0.86	97	7.22E+19	6800	0.42
D1-1	0.5	0.35	0.87	97	7.22E+19	6800	0.40
E1-3	0.5	0.37	0.85	97	7.22E+19	6800	0.44
F1-3	0.5	0.35	0.87	97	7.22E+19	6800	0.40
B1-4	1	0.53	0.86	112	2.92E+17	7400	0.62
E1-8	1	0.52	0.85	112	2.92E+17	7400	0.61
F1-8	1	0.52	0.84	112	2.92E+17	7400	0.62
A2-2	1.5	0.5	0.86	127	1.54E+17	8500	0.58
C1-7	1.5	0.52	0.86	127	1.54E+17	8500	0.60
C2-2	1.5	0.53	0.86	127	1.54E+17	8500	0.62
D2-1	1.5	0.5	0.87	127	1.54E+17	8500	0.57
D2-3	1.5	0.54	0.84	127	1.54E+17	8500	0.64
E2-3	1.5	0.53	0.86	127	1.54E+17	8500	0.62
F1-6	1.5	0.52	0.86	127	1.54E+17	8500	0.60
A2-4	2	0.53	0.85	142	1.54E+17	9600	0.62
B2-4	2	0.55	0.86	142	1.54E+17	9600	0.64
E2-8	2	0.53	0.87	142	1.54E+17	9600	0.61
F2-8	2	0.55	0.87	142	1.54E+17	9600	0.63
B3-2	2.5	0.55	0.86	157	1.43E+17	10500	0.64
C2-7	2.5	0.55	0.85	157	1.43E+17	10500	0.65
C3-2	2.5	0.57	0.87	157	1.43E+17	10500	0.66
E3-3	2.5	0.55	0.87	157	1.43E+17	10500	0.63
F2-6	2.5	0.56	0.86	157	1.43E+17	10500	0.65
B3-4	3	0.55	0.87	172	1.32E+17	11100	0.63
E3-8	3	0.54	0.87	172	1.32E+17	11100	0.62
A3-7	3.5	0.56	0.86	173	2.66E+03	11000	0.65
B4-2	3.5	0.55	0.85	173	2.66E+03	11000	0.65
C4-2	3.5	0.56	0.86	173	2.66E+03	11000	0.65
C3-5	3.5	0.52	0.86	173	2.66E+03	11000	0.60
E3-6	3.5	0.55	0.86	173	2.66E+03	11000	0.64
B4-4	4	0.55	0.85	158	2.31E+05	10500	0.65
B4-7	4.5	0.54	0.86	143	6.84E+08	9400	0.63
C4-5	4.5	0.53	0.87	143	6.84E+08	9400	0.61
C5-2	4.5	0.55	0.86	143	6.84E+08	9400	0.64
D4-6	4.5	0.55	0.86	143	6.84E+08	9400	0.64
D5-1	4.5	0.53	0.86	143	6.84E+08	9297	0.62
D5-3	4.5	0.55	0.84	143	6.84E+08	9297	0.65
B5-4	5	0.53	0.85	128	9.60E+12	8200	0.62
F5-8	5	0.56	0.85	128	9.60E+12	8200	0.66

**APPENDIX A. Chemglaze A276 Optical Property and  
Environmental Exposure Data for the LDEF Mission**

Specimen	Row	Absorptance	Emittance	Angle (degrees)	AO Fluence (atoms/cm <sup>2</sup> )	Solar ESH (ESH)	Abs./Emit. Ratio
A6-2	5.5	0.52	0.87	113	7.33E+16	7100	0.60
C5-5	5.5	0.49	0.88	113	7.33E+16	7100	0.56
C6-2	5.5	0.53	0.86	113	7.33E+16	7100	0.62
D5-6	5.5	0.5	0.85	113	7.33E+16	7100	0.59
D6-1	5.5	0.48	0.88	113	7.33E+16	7100	0.55
E6-3	5.5	0.53	0.86	113	7.33E+16	7100	0.62
E6-8	6	0.43	0.86	98	4.94E+19	6400	0.50
F6-8	6	0.39	0.86	98	4.94E+19	6400	0.45
B6-7	6.5	0.31	0.88	83	1.16E+21	6500	0.35
B7-2	6.5	0.32	0.88	83	1.16E+21	6500	0.36
C6-5	6.5	0.33	0.88	83	1.16E+21	6500	0.38
D6-6	6.5	0.35	0.85	83	1.16E+21	6500	0.41
E6-6	6.5	0.32	0.88	83	1.16E+21	6500	0.36
F6-6	6.5	0.35	0.86	83	1.16E+21	6500	0.41
F7-3	6.5	0.35	0.87	83	1.16E+21	6500	0.40
A7-4	7	0.3	0.9	68	3.39E+21	7100	0.33
B7-4	7	0.3	0.88	68	3.39E+21	7100	0.34
E7-8	7	0.31	0.88	68	3.39E+21	7100	0.35
A7-7	7.5	0.32	0.88	53	5.45E+21	8200	0.36
B7-7	7.5	0.3	0.9	53	5.45E+21	8200	0.33
D7-6	7.5	0.29	0.89	53	5.45E+21	8200	0.33
E8-3	7.5	0.31	0.88	53	5.45E+21	8200	0.35
F8-3	7.5	0.31	0.89	53	5.45E+21	8200	0.35
E8-8	8	0.31	0.89	38	7.15E+21	9400	0.35
C8-5	8.5	0.29	0.89	23	8.36E+21	10500	0.33
C9-2	8.5	0.3	0.89	23	8.36E+21	10500	0.34
D9-1	8.5	0.28	0.9	23	8.36E+21	10500	0.31
E8-6	8.5	0.28	0.9	23	8.36E+21	10500	0.31
E9-3	8.5	0.28	0.9	23	8.36E+21	10500	0.31
B9-4	9	0.27	0.9	8	8.99E+21	11200	0.30
F9-8	9	0.32	0.88	8	8.99E+21	11200	0.36
A9-7	9.5	0.31	0.89	7	9.02E+21	11200	0.35
B9-7	9.5	0.29	0.9	7	9.02E+21	11200	0.32
B10-2	9.5	0.32	0.88	7	9.02E+21	11200	0.36
C9-7	9.5	0.31	0.9	7	9.02E+21	11200	0.34
D9-6	9.5	0.32	0.89	7	9.02E+21	11200	0.36
D10-1	9.5	0.27	0.9	7	9.02E+21	11200	0.30
F9-6	9.5	0.32	0.88	7	9.02E+21	11200	0.36
A10-4	10	0.3	0.89	22	8.43E+21	10700	0.34

**APPENDIX A. Chemglaze A276 Optical Property and  
Environmental Exposure Data for the LDEF Mission**

Specimen	Row	Absorptance	Emittance	Angle (degrees)	AO Fluence (atoms/cm <sup>2</sup> )	Solar ESH (ESH)	Abs./Emit. Ratio
A10-7	10.5	0.29	0.89	37	7.27E+21	9700	0.33
B11-2	10.5	0.29	0.9	37	7.27E+21	9700	0.32
C10-7	10.5	0.28	0.89	37	7.27E+21	9700	0.31
D10-6	10.5	0.28	0.91	37	7.27E+21	9700	0.31
D11-1	10.5	0.27	0.9	37	7.27E+21	9700	0.30
E10-6	10.5	0.29	0.9	37	7.27E+21	9700	0.32
F11-3	10.5	0.28	0.91	37	7.27E+21	9700	0.31
F11-8	11	0.31	0.88	52	5.61E+21	8500	0.35
C11-7	11.5	0.31	0.89	67	3.56E+21	7500	0.35
D11-6	11.5	0.33	0.86	67	3.56E+21	7500	0.38
D12-3	11.5	0.32	0.88	67	3.56E+21	7500	0.36
F12-3	11.5	0.31	0.87	67	3.56E+21	7500	0.36
A12-4	12	0.34	0.86	82	1.33E+21	6800	0.40
B12-4	12	0.35	0.87	82	1.33E+21	6800	0.40
F12-8	12	0.3	0.88	82	1.33E+21	6800	0.34
A12-7	0.5	0.38	0.85	97	7.22E+19	6800	0.45
C12-5	0.5	0.33	0.87	97	7.22E+19	6800	0.38
D12-6	0.5	0.35	0.87	97	7.22E+19	6800	0.40
F12-6	0.5	0.35	0.87	97	7.22E+19	6800	0.40
control	0	0.28	0.87	0	0	0	0.32
H1-2	space	0.57	0.85	90	4.59E+20	14500	0.67
H1-11	space	0.5	0.86	90	4.59E+20	14500	0.58
H3-5	space	0.36	0.86	90	4.59E+20	14500	0.42
H3-11	space	0.56	0.87	90	4.59E+20	14500	0.64
H6-5	space	0.39	0.86	90	4.59E+20	14500	0.45
H6-11	space	0.6	0.86	90	4.59E+20	14500	0.70
H7-2	space	0.41	0.87	90	4.59E+20	14500	0.47
H7-11	space	0.52	0.85	90	4.59E+20	14500	0.61
H9-5	space	0.55	0.86	90	4.59E+20	14500	0.64
H9-11	space	0.61	0.87	90	4.59E+20	14500	0.70
H11-11	space	0.47	0.87	90	4.59E+20	14500	0.54
H12-5	space	0.35	0.87	90	4.59E+20	14500	0.40
G2-5	Earth	0.36	0.86	90	3.33E+20	4500	0.42
G4-2	Earth	0.32	0.87	90	3.33E+20	4500	0.37
G4-5	Earth	0.32	0.87	90	3.33E+20	4500	0.37
G4-11	Earth	0.29	0.87	90	3.33E+20	4500	0.33
G6-2	Earth	0.29	0.87	90	3.33E+20	4500	0.33
G6-5	Earth	0.35	0.86	90	3.33E+20	4500	0.41
G6-8	Earth	0.3	0.87	90	3.33E+20	4500	0.34

**APPENDIX A. Chemglaze A276 Optical Property and  
Environmental Exposure Data for the LDEF Mission**

Specimen	Row	Absorptance	Emittance	Angle (degrees)	AO Fluence (atoms/cm <sup>2</sup> )	Solar ESH (ESH)	Abs./Emit. Ratio
G8-2	Earth	0.32	0.86	90	3.33E+20	4500	0.37
G8-5	Earth	0.36	0.87	90	3.33E+20	4500	0.41
G8-8	Earth	0.3	0.86	90	3.33E+20	4500	0.35
G10-2	Earth	0.37	0.86	90	3.33E+20	4500	0.43
G10-5	Earth	0.34	0.87	90	3.33E+20	4500	0.39
G12-2	Earth	0.31	0.87	90	3.33E+20	4500	0.36
G12-5	Earth	0.33	0.88	90	3.33E+20	4500	0.38
G12-8	Earth	0.27	0.88	90	3.33E+20	4500	0.31

**APPENDIX B. Infrared Reflectance Measurements for Chemglaze A276**

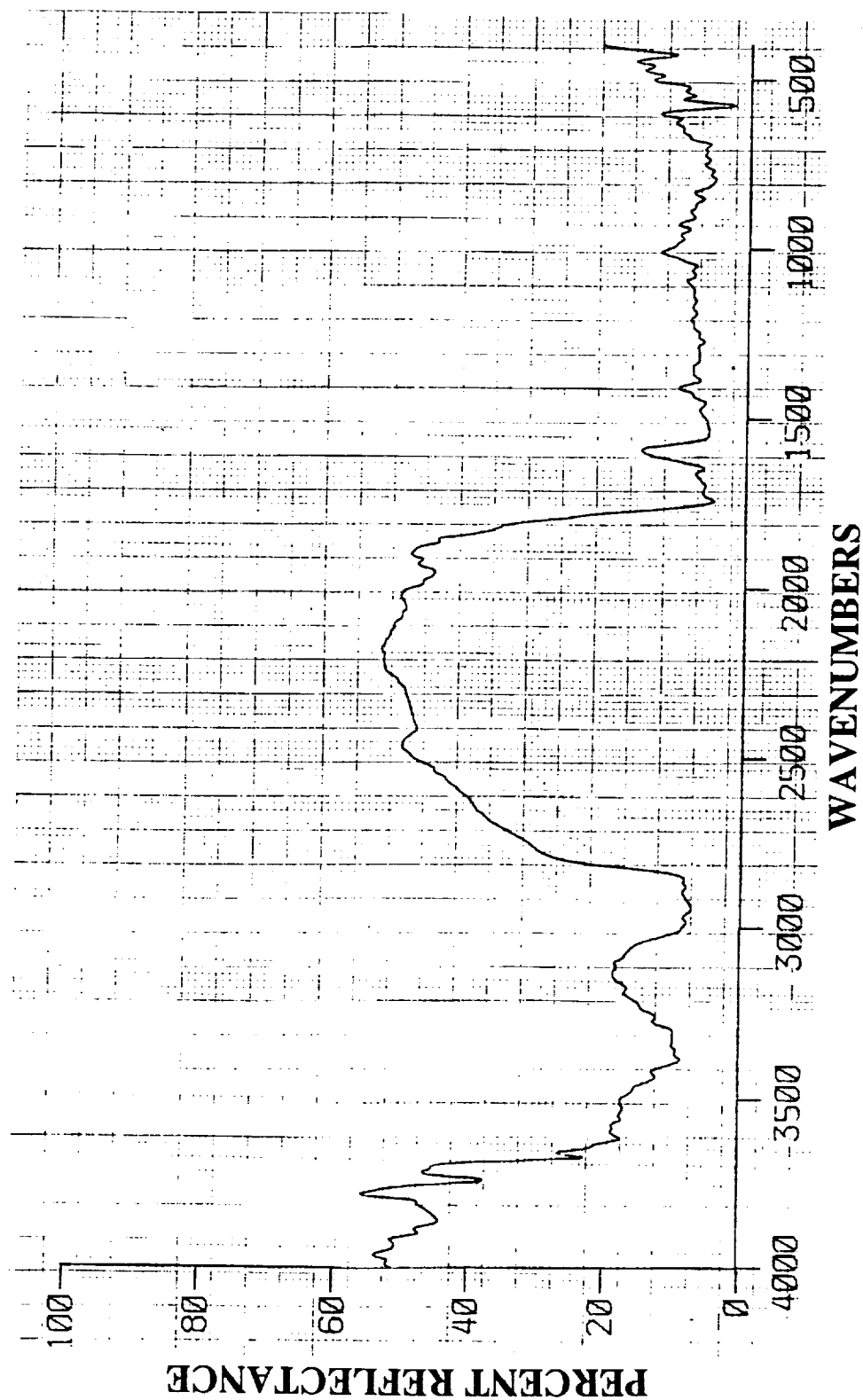


Figure B1. Chemglaze A276 Control Specimen - Total Hemispherical Infrared Reflectance

APPENDIX B. Infrared Reflectance Measurements for Chemglaze A276

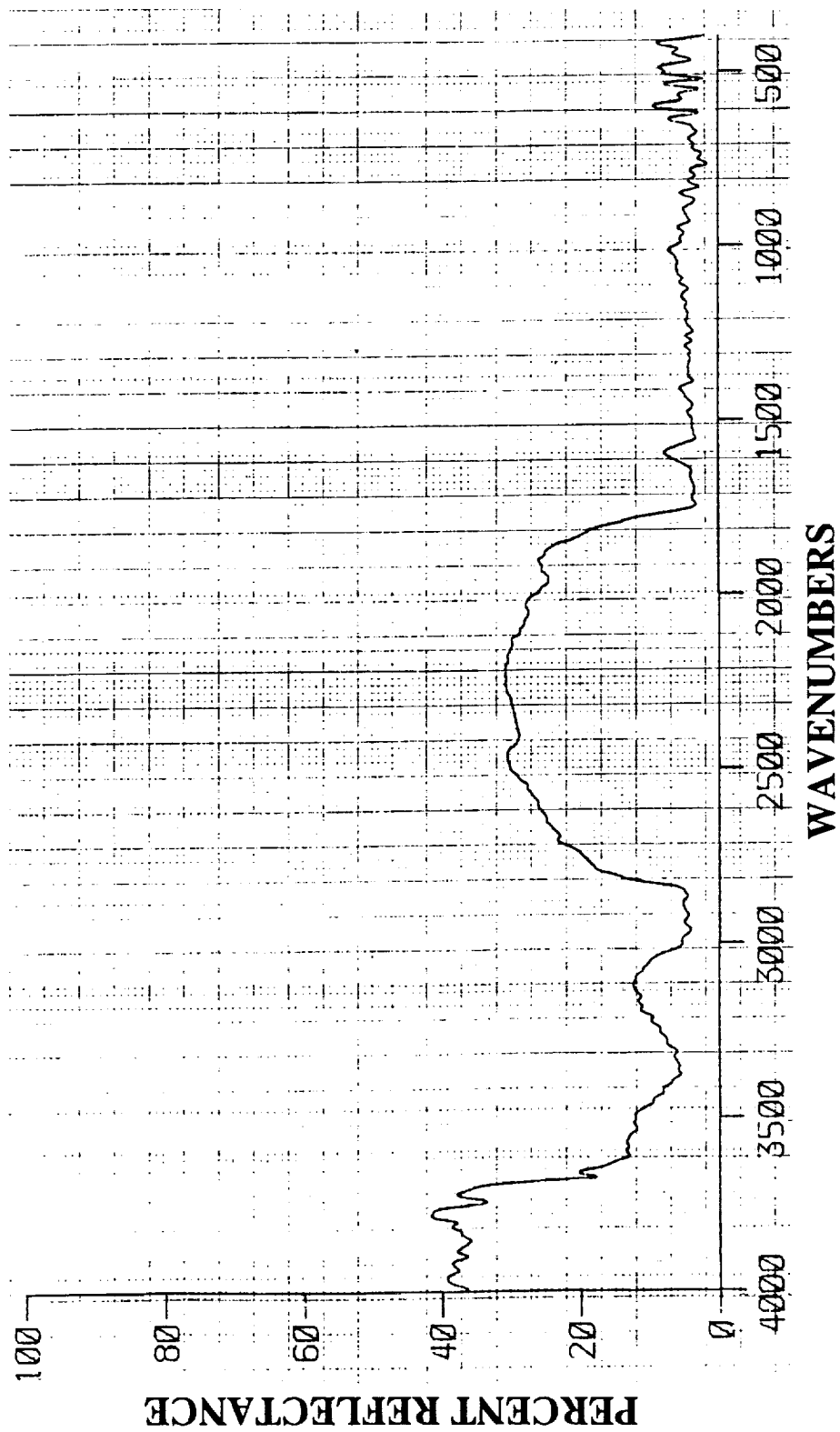


Figure B2. Chemglaze A276 Control Specimen - Diffuse Infrared Reflectance

APPENDIX B. Infrared Reflectance Measurements for Chemglaze A276

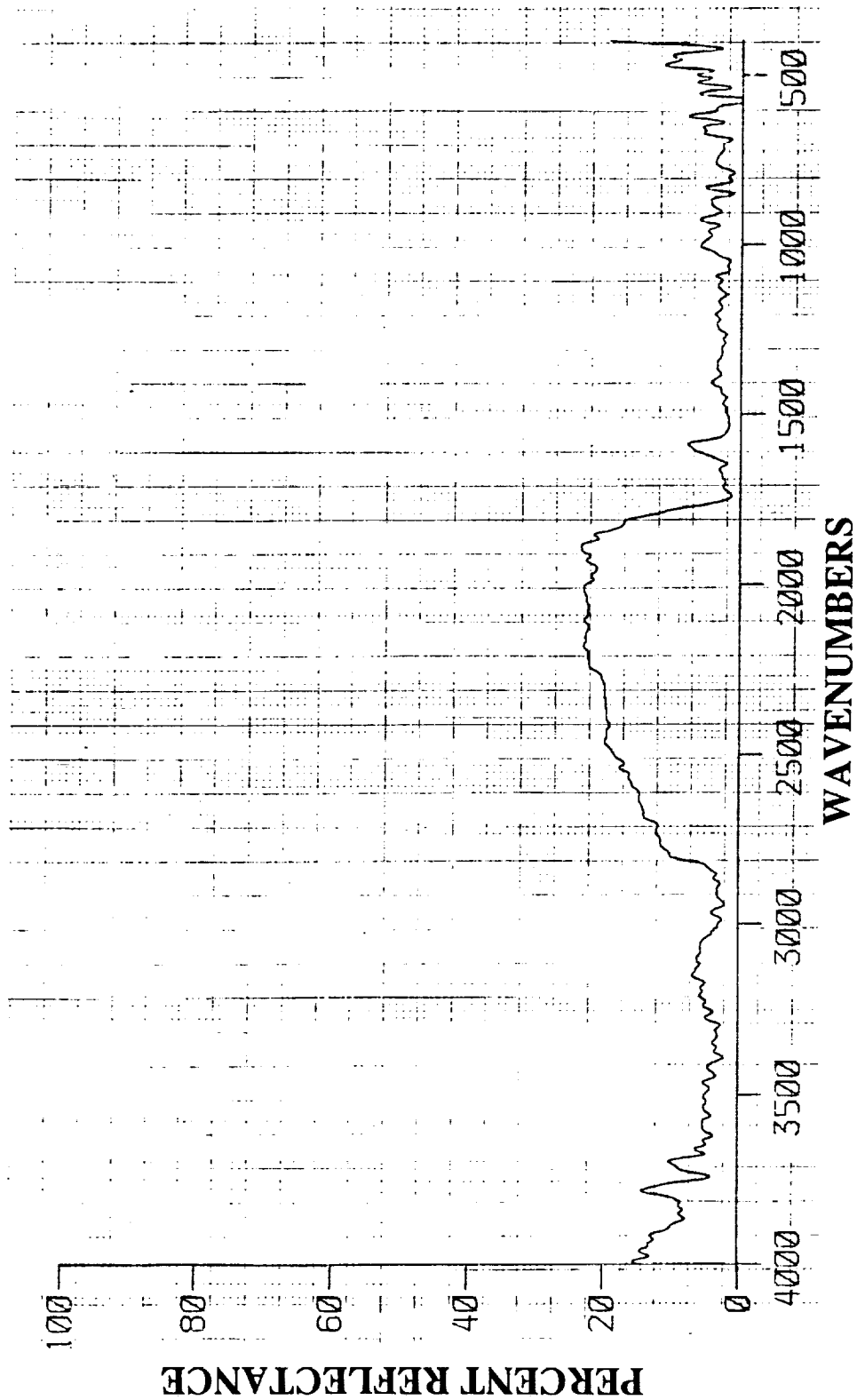


Figure B3. Chemglaze A276 Control Specimen - Specular Infrared Reflectance

APPENDIX B. Infrared Reflectance Measurements for Chemglaze A276

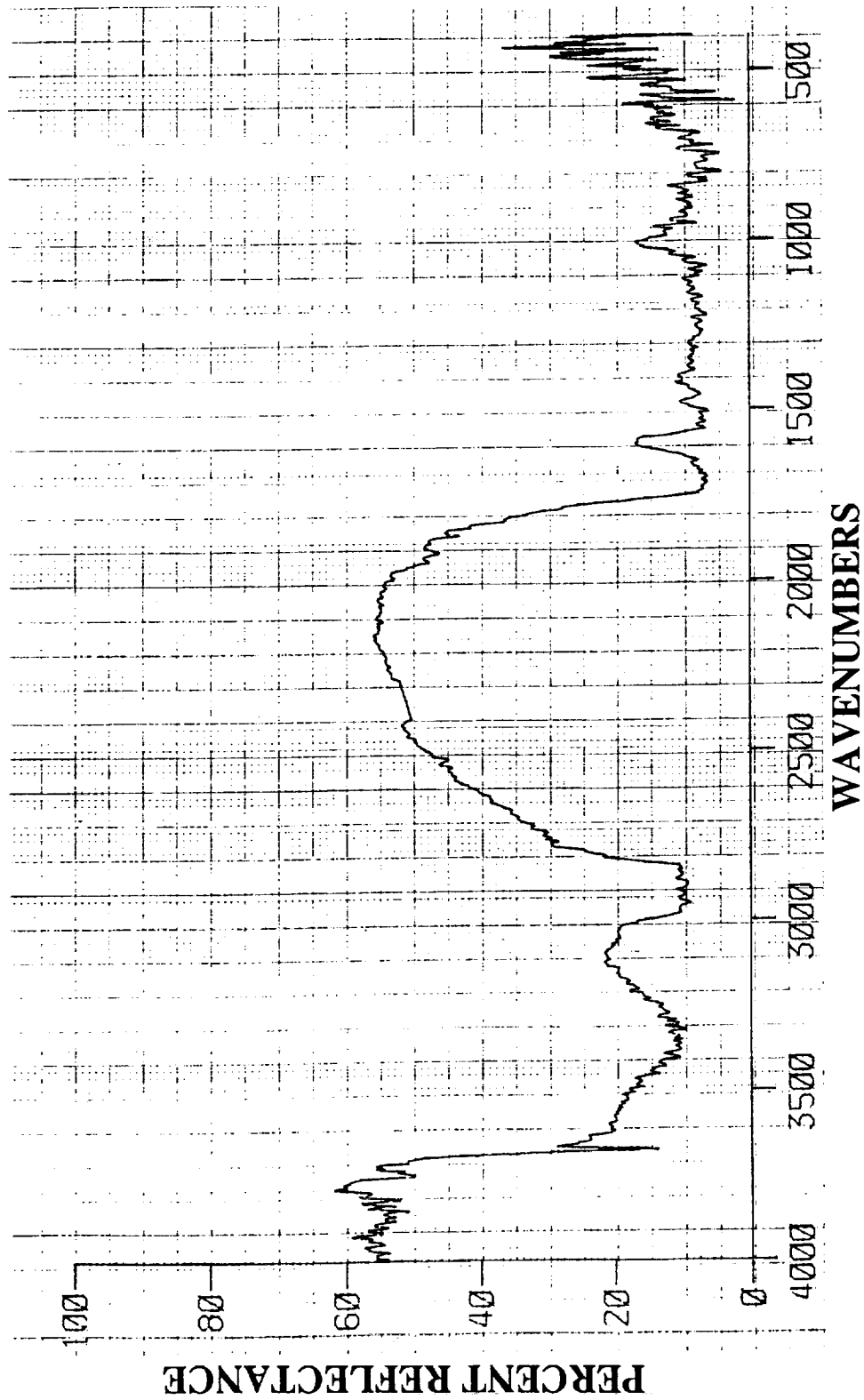


Figure B4. Chemglaze A276 B1-4 Specimen - Total Hemispherical Infrared Reflectance

APPENDIX B. Infrared Reflectance Measurements for Chemglaze A276

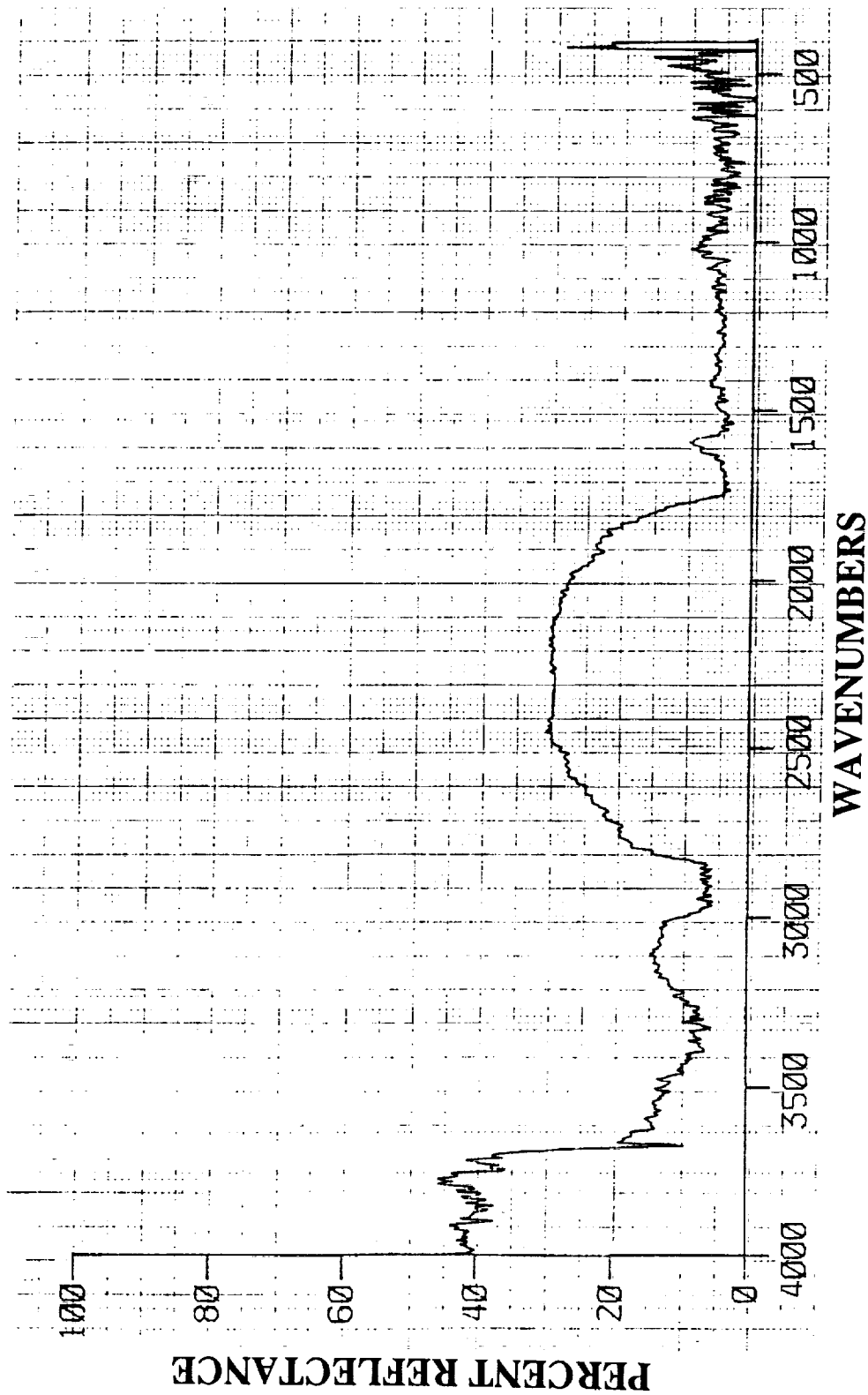


Figure B5. Chemglaze A276 B1-4 Specimen - Diffuse Infrared Reflectance

**APPENDIX B. Infrared Reflectance Measurements for Chemglaze A276**

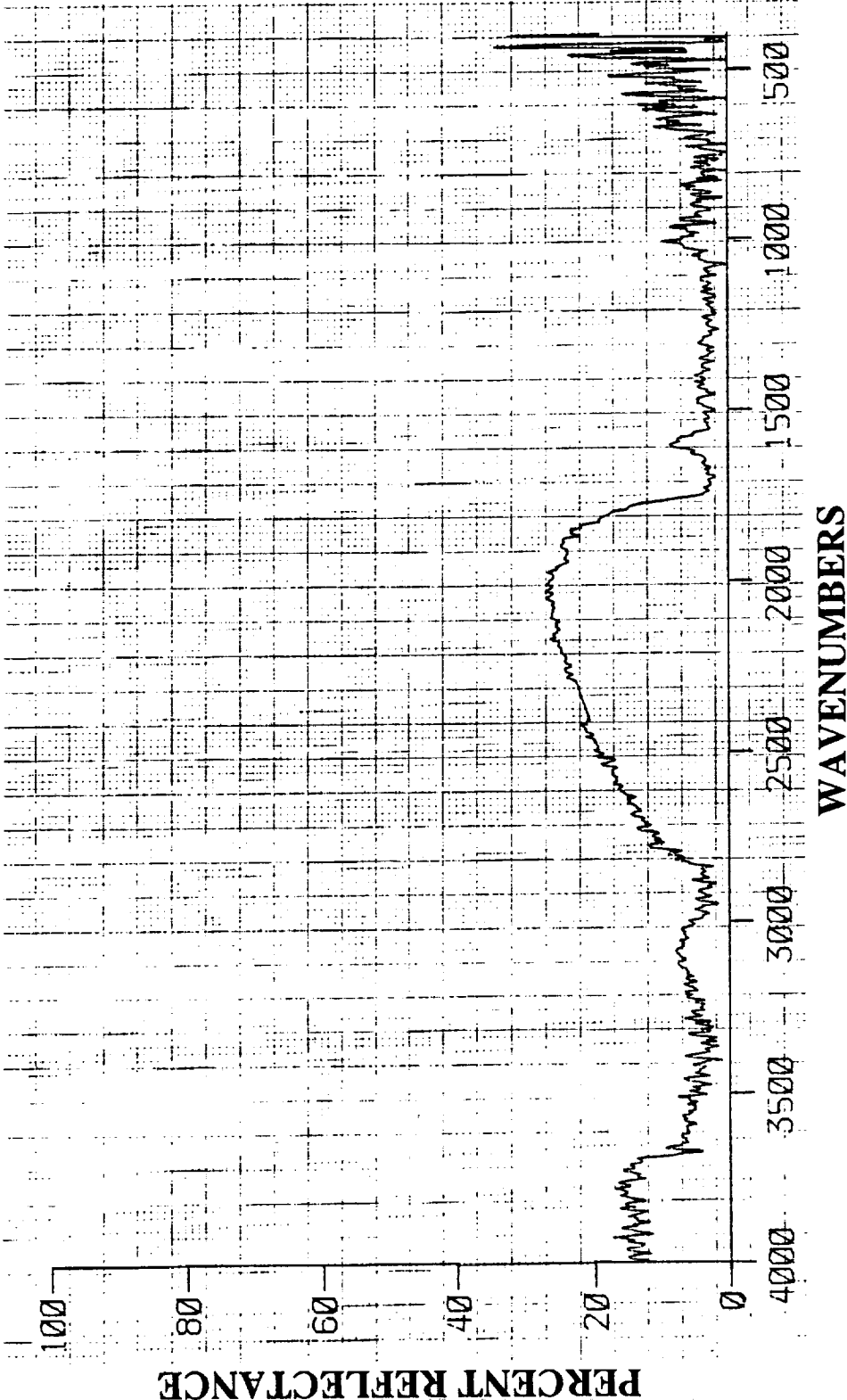


Figure B6. Chemglaze A276 B1-4 Specimen - Specular Infrared Reflectance

**APPENDIX B. Infrared Reflectance Measurements for Chemglaze A276**

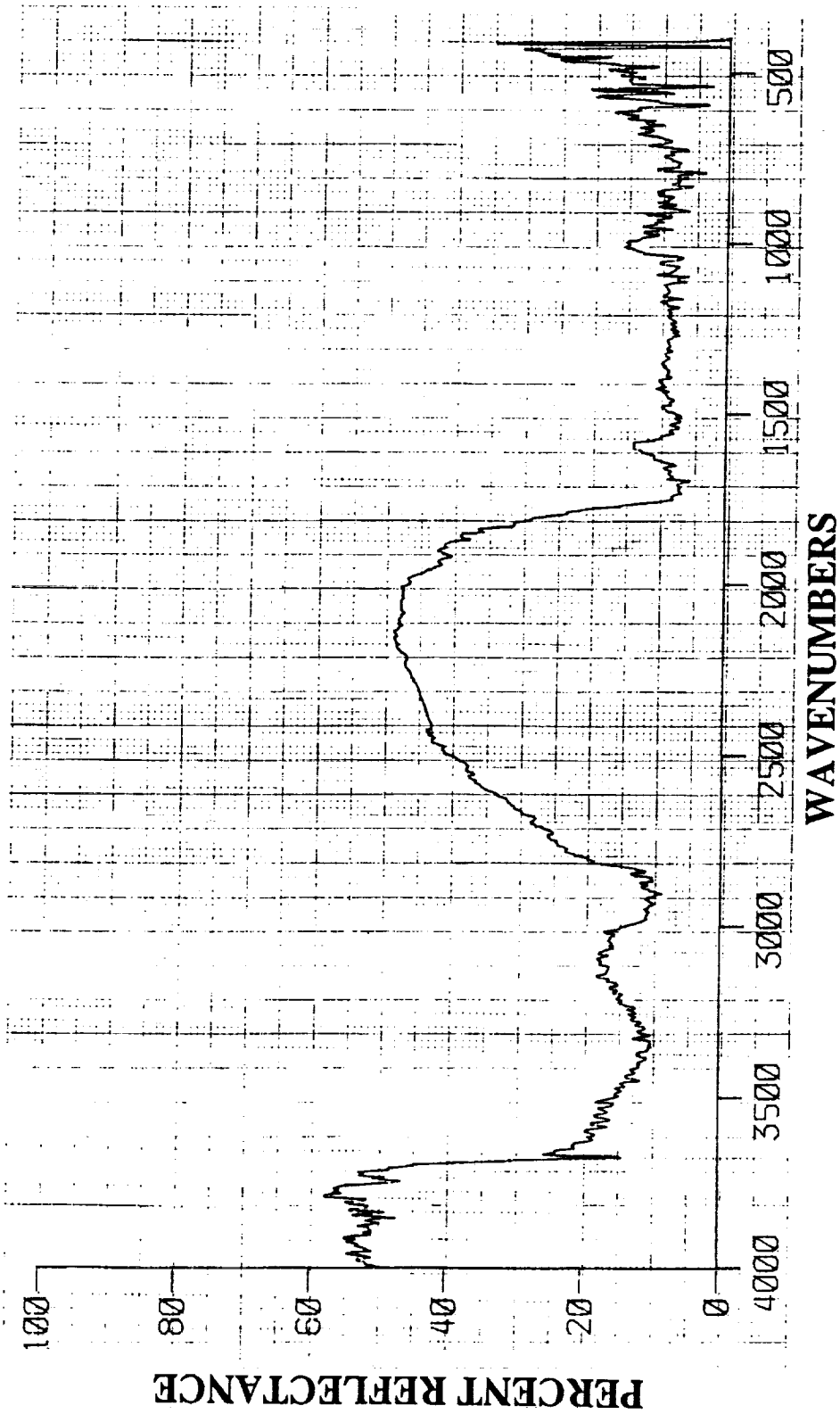


Figure B7. Chemglaze A276 E2-3 Specimen - Total Hemispherical Infrared Reflectance

APPENDIX B. Infrared Reflectance Measurements for Chemglaze A276

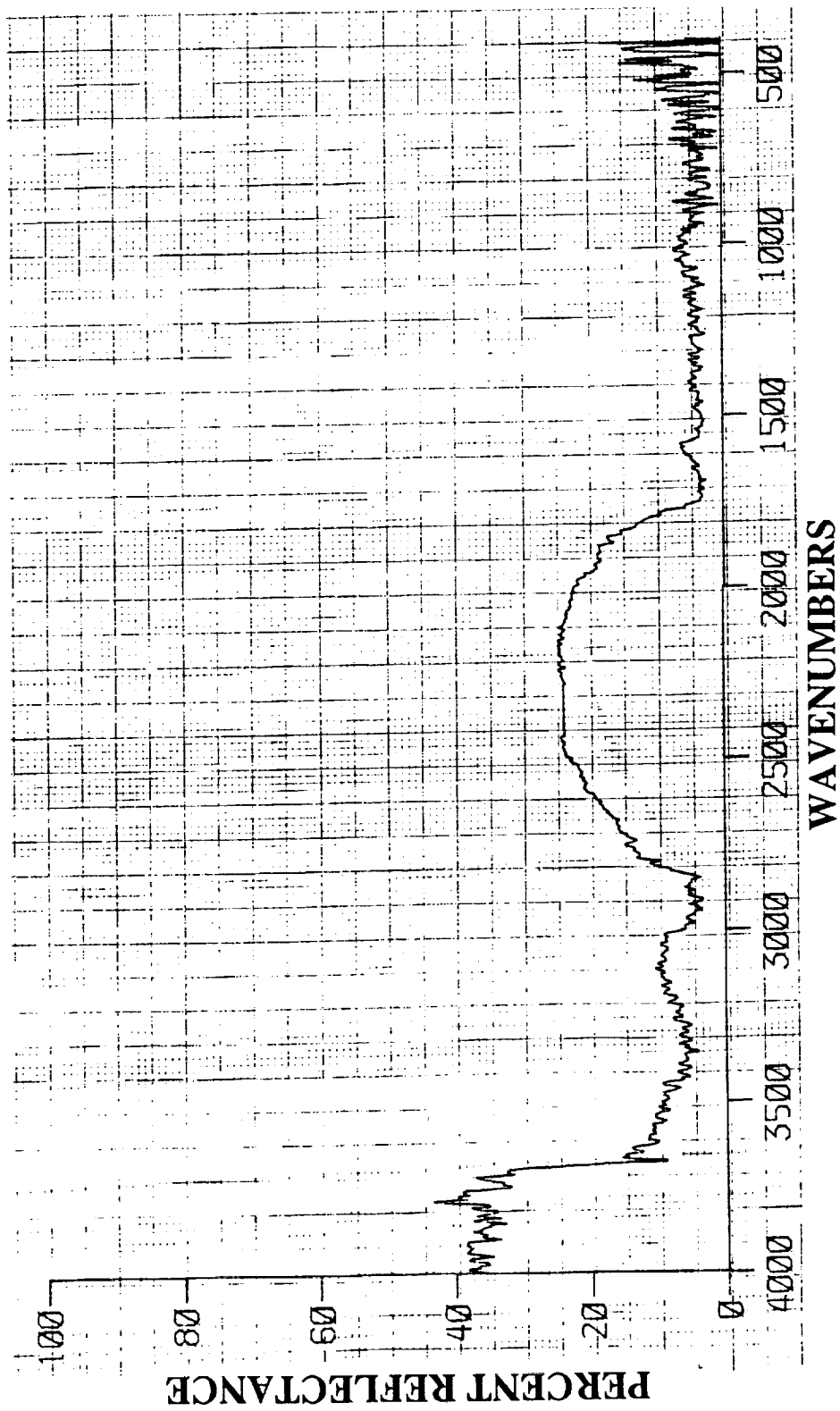


Figure B8. Chemglaze A276 E2-3 Specimen - Diffuse Infrared Reflectance

APPENDIX B. Infrared Reflectance Measurements for Chemglaze A276

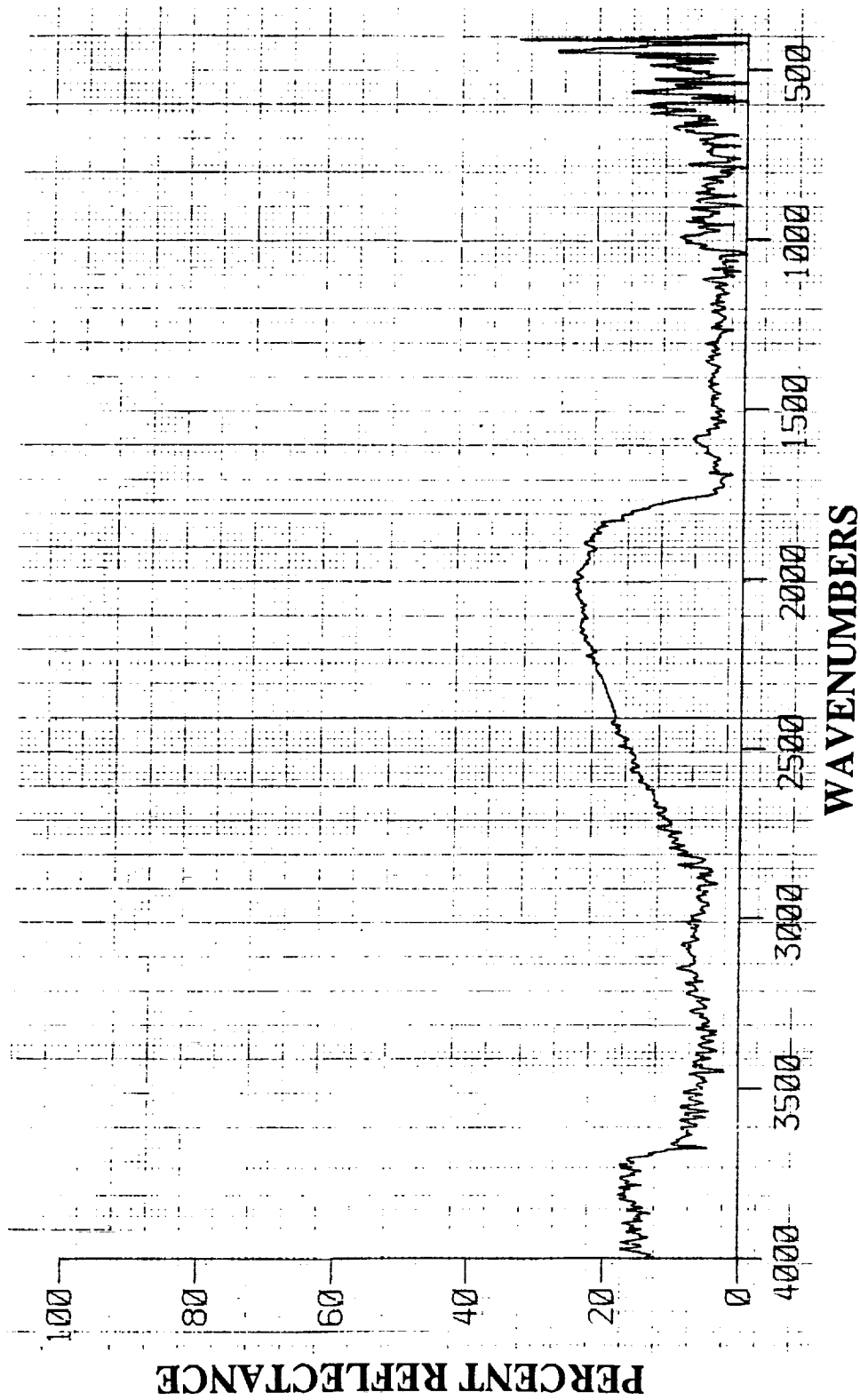


Figure B9. Chemglaze A276 E2-3 Specimen - Specular Infrared Reflectance

APPENDIX B. Infrared Reflectance Measurements for Chemglaze A276

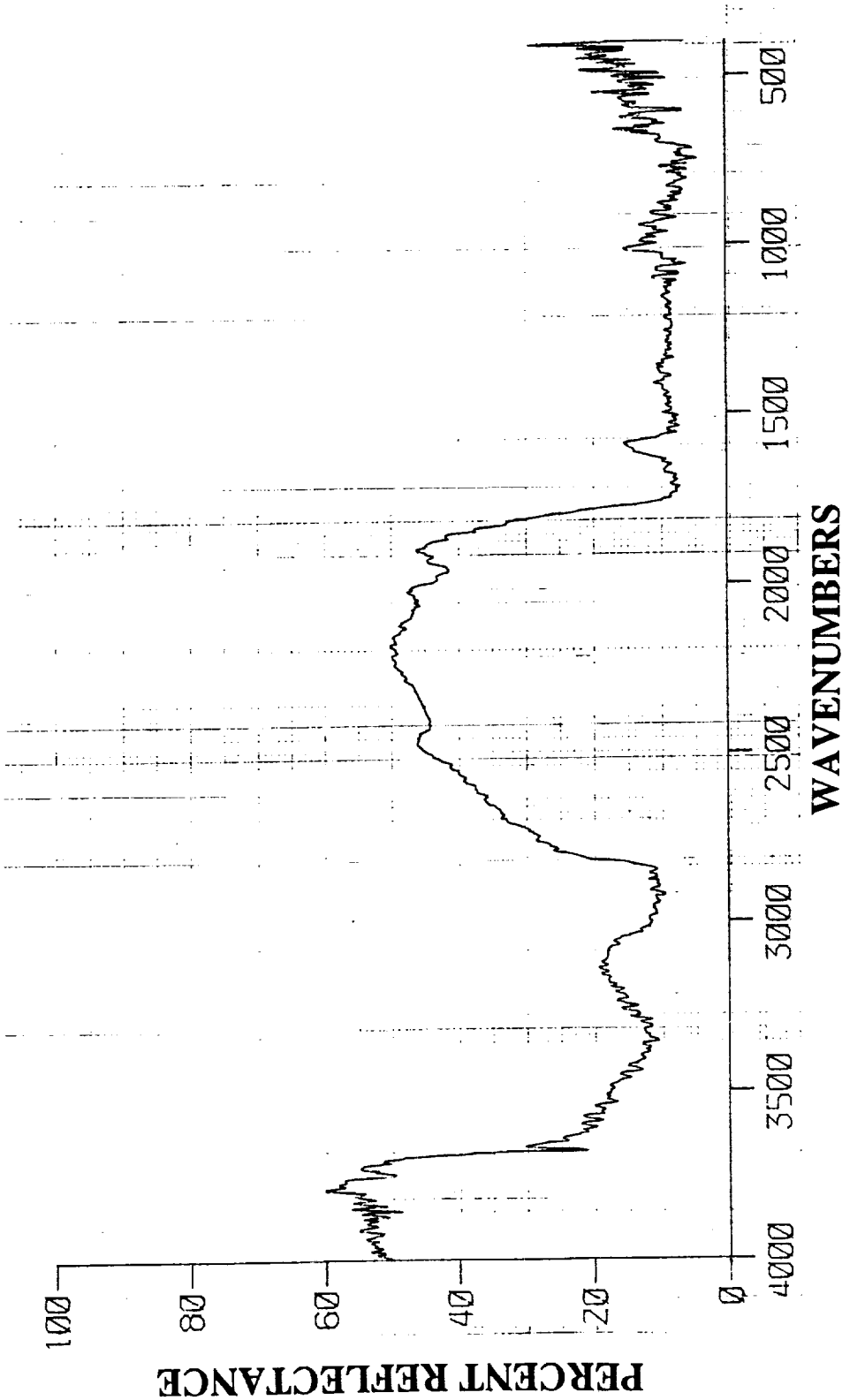


Figure B10. Chemglaze A276 E2-8 Specimen - Total Hemispherical Infrared Reflectance

APPENDIX B. Infrared Reflectance Measurements for Chemglaze A276

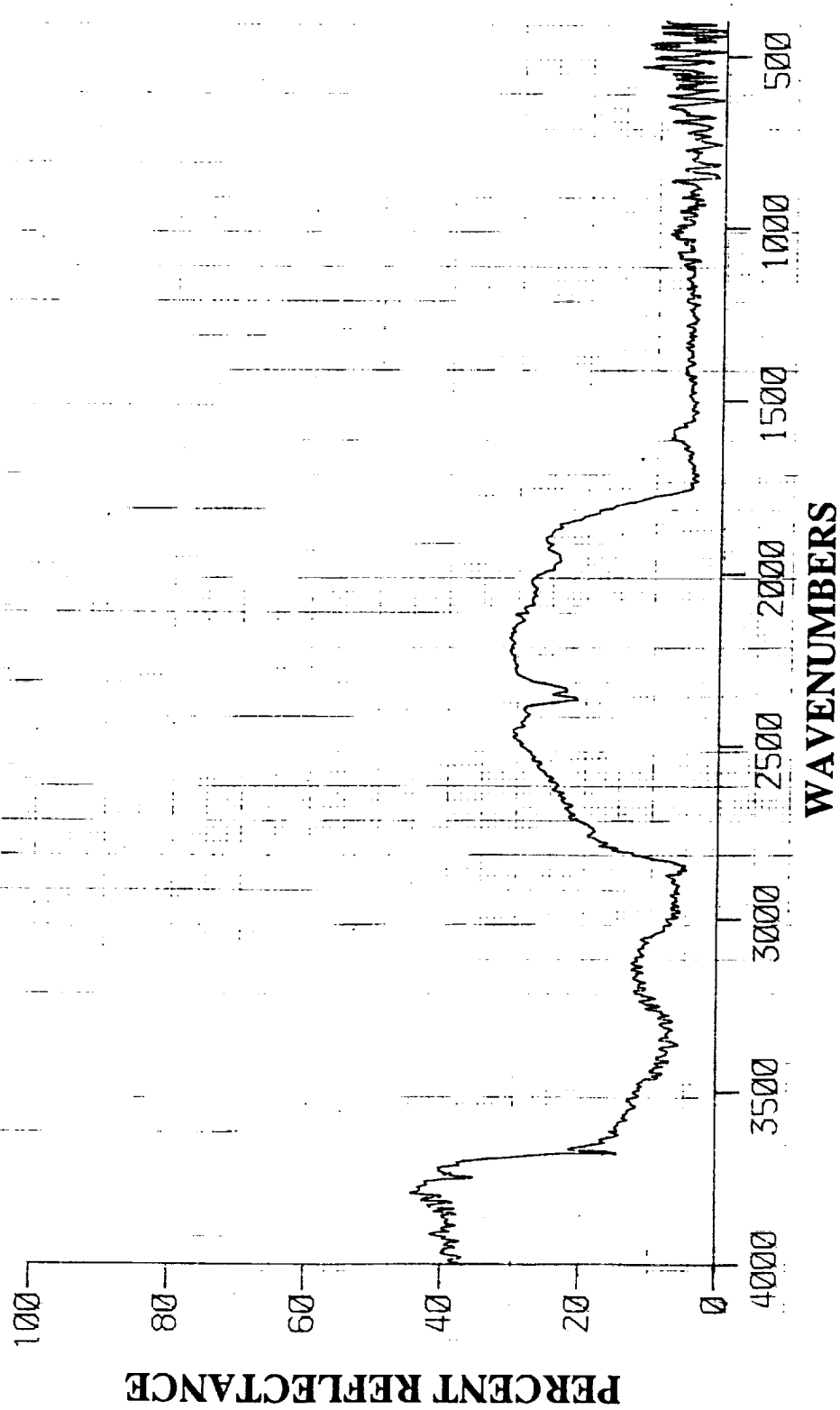


Figure B11. Chemglaze A276 E2-8 Specimen - Diffuse Infrared Reflectance

APPENDIX B. Infrared Reflectance Measurements for Chemglaze A276

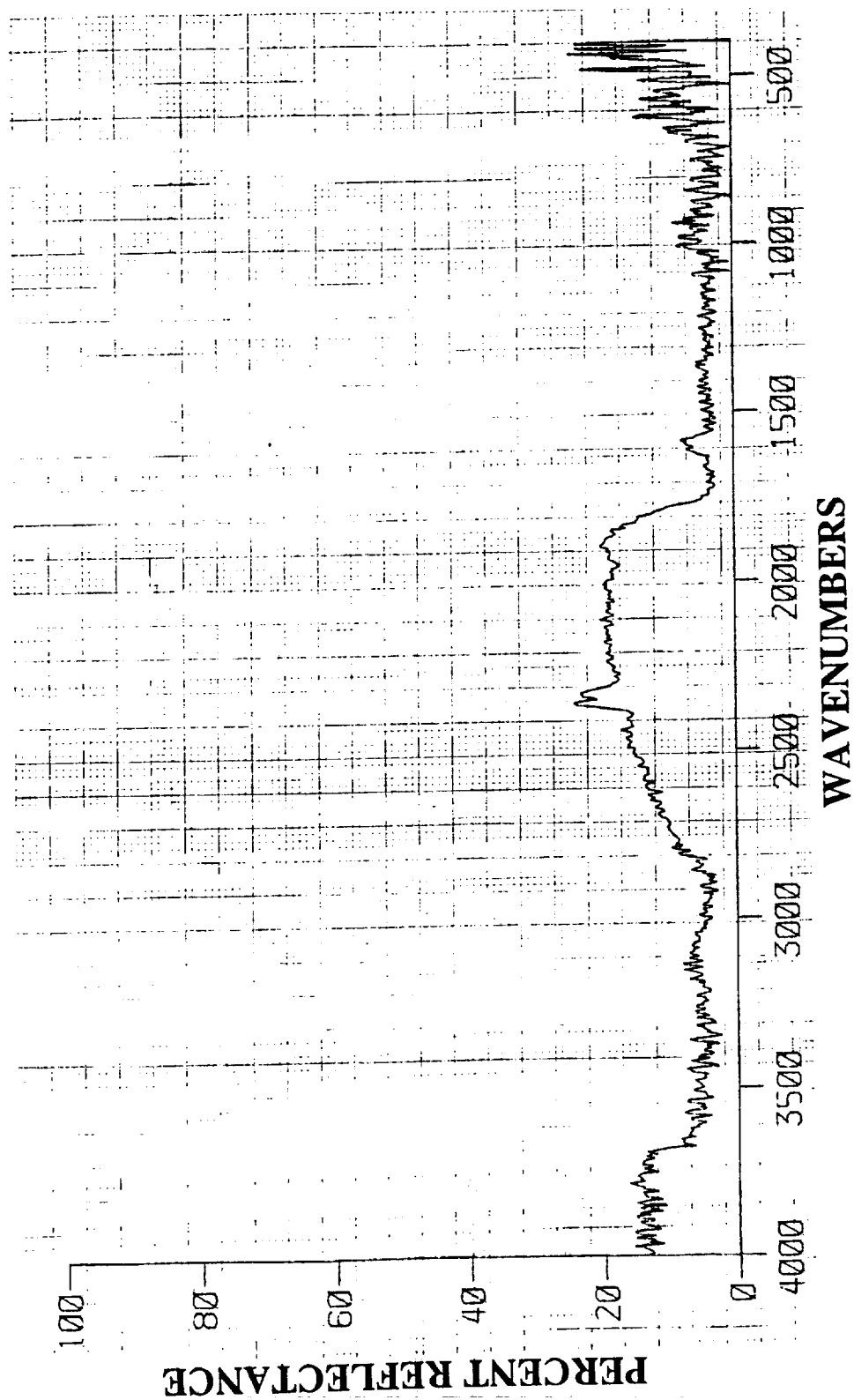


Figure B12. Chemglaze A276 E2-8 Specimen - Specular Infrared Reflectance

APPENDIX B. Infrared Reflectance Measurements for Chemglaze A276

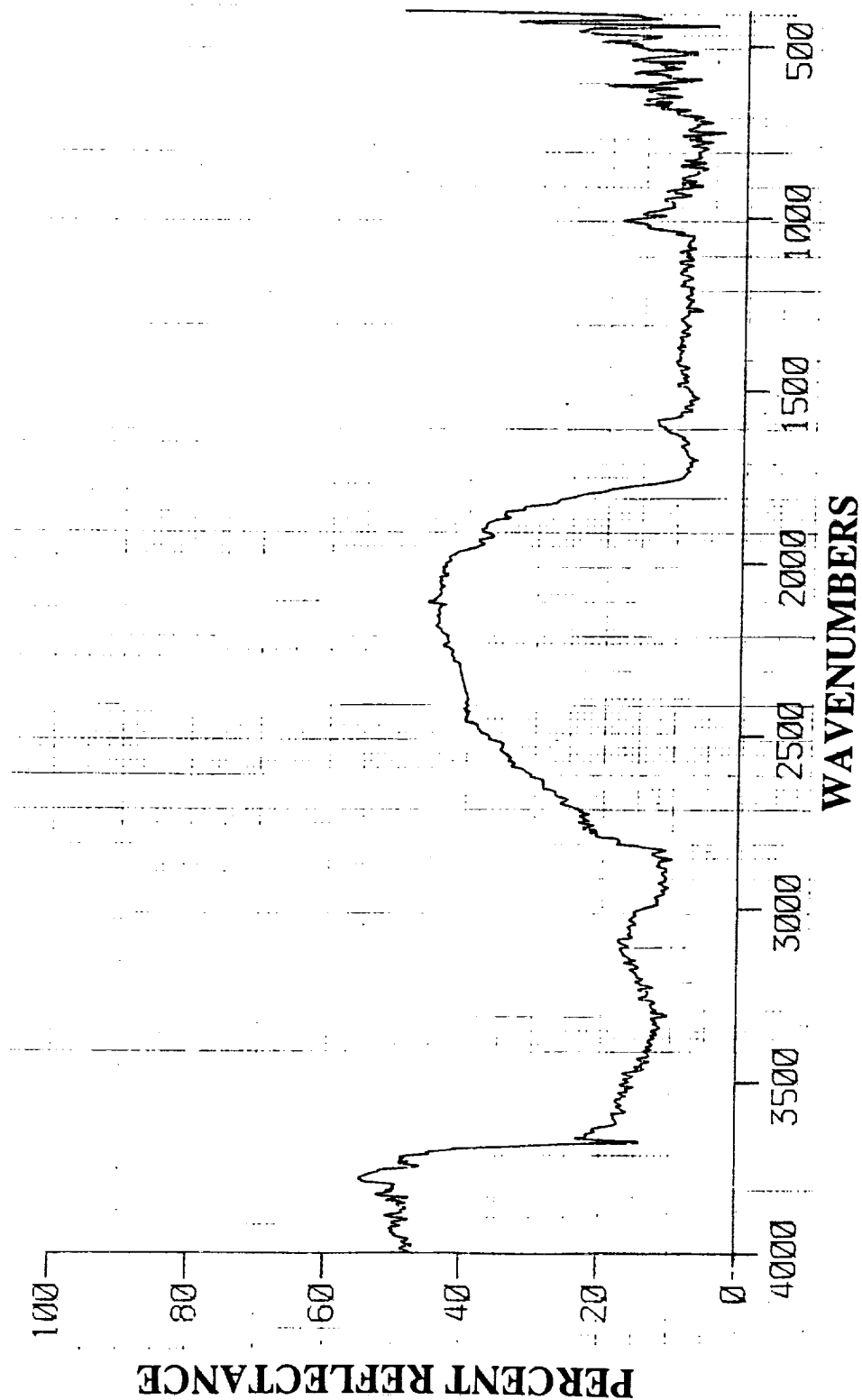


Figure B13. Chemglaze A276 C3-2 Specimen - Total Hemispherical Infrared Reflectance

APPENDIX B. Infrared Reflectance Measurements for Chemglaze A276

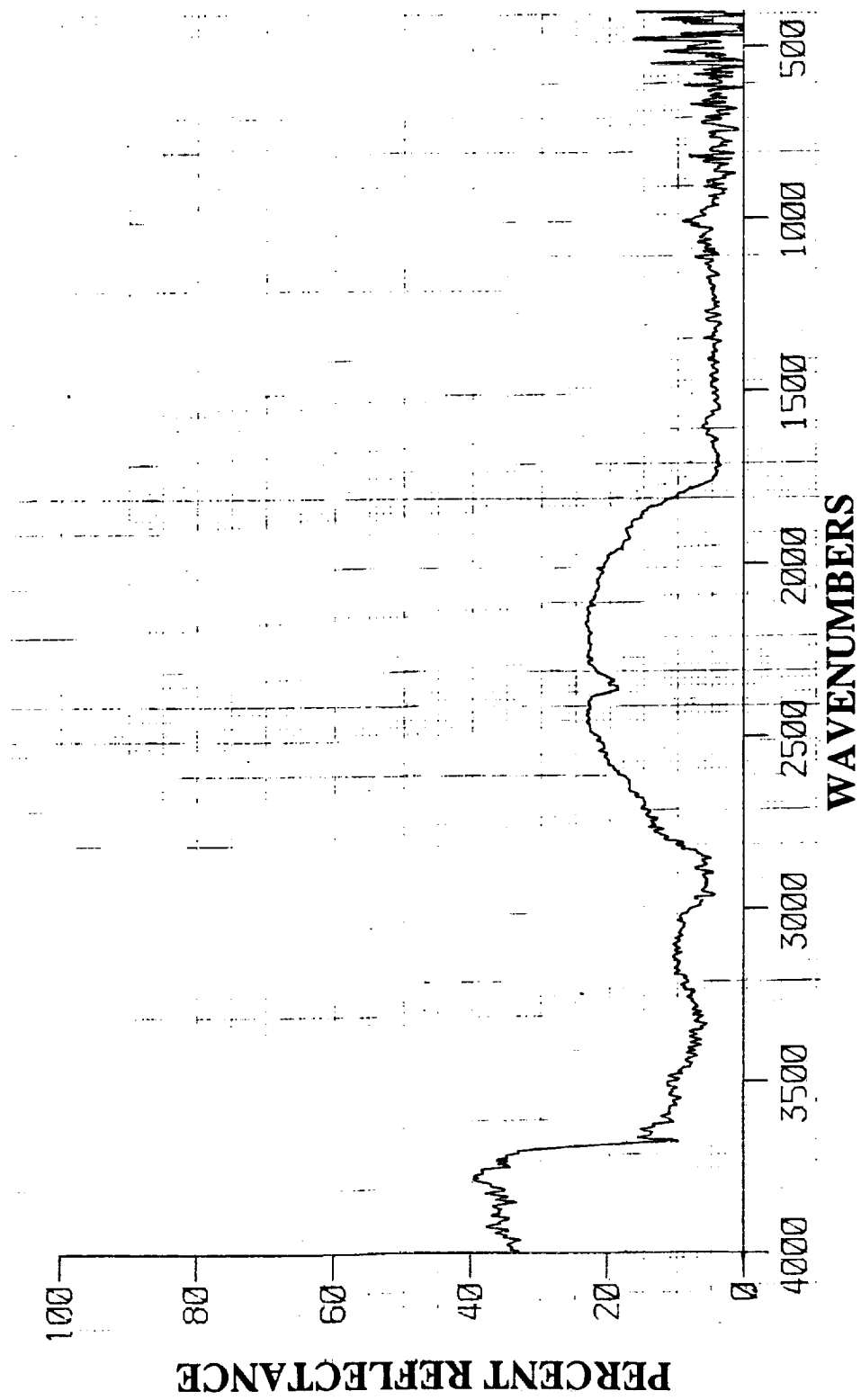


Figure B14. Chemglaze A276 C3-2 Specimen - Diffuse Infrared Reflectance

APPENDIX B. Infrared Reflectance Measurements for Chemglaze A276

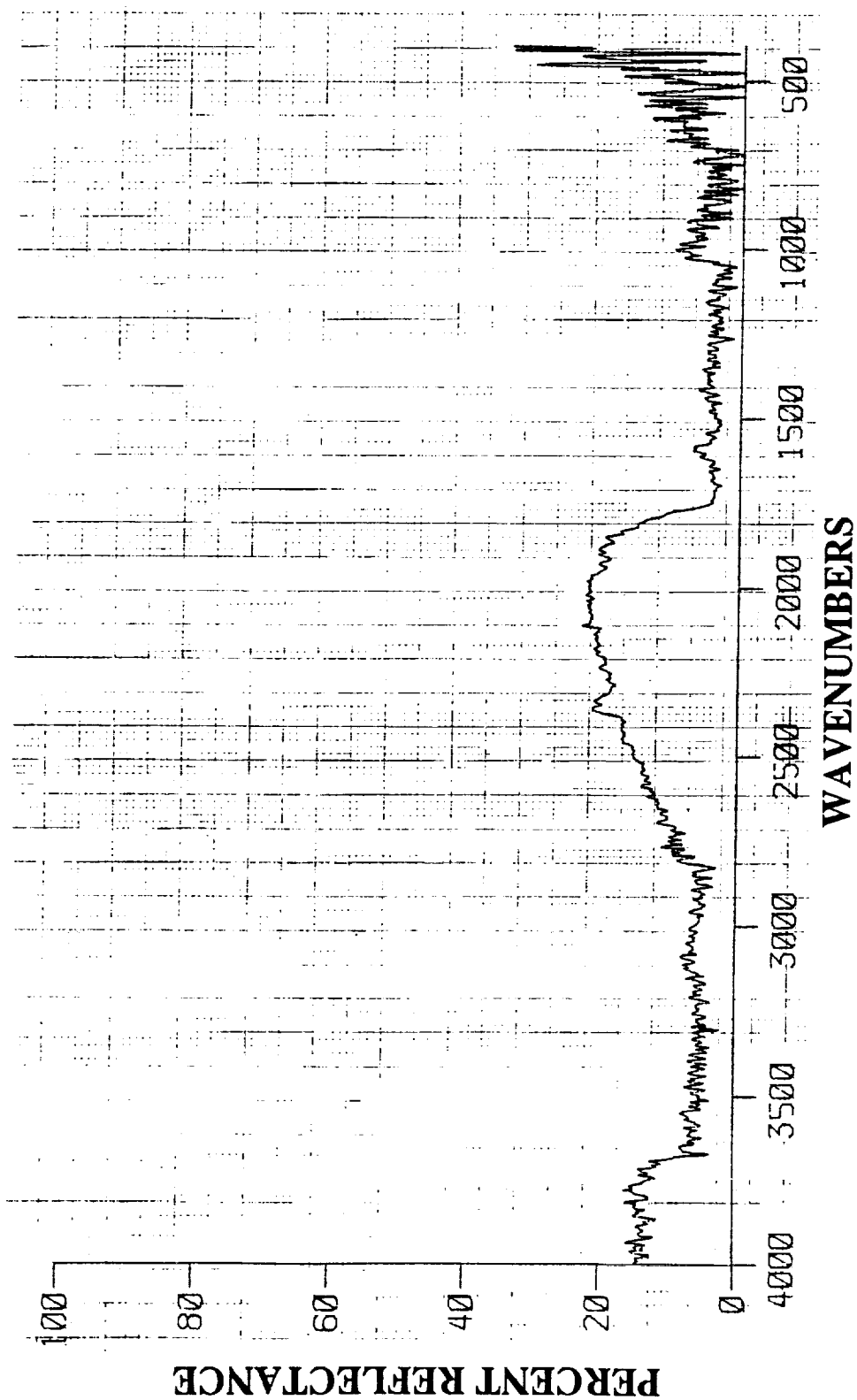


Figure B15. Chemglaze A276 C3-2 Specimen - Specular Infrared Reflectance

APPENDIX B. Infrared Reflectance Measurements for Chemglaze A276

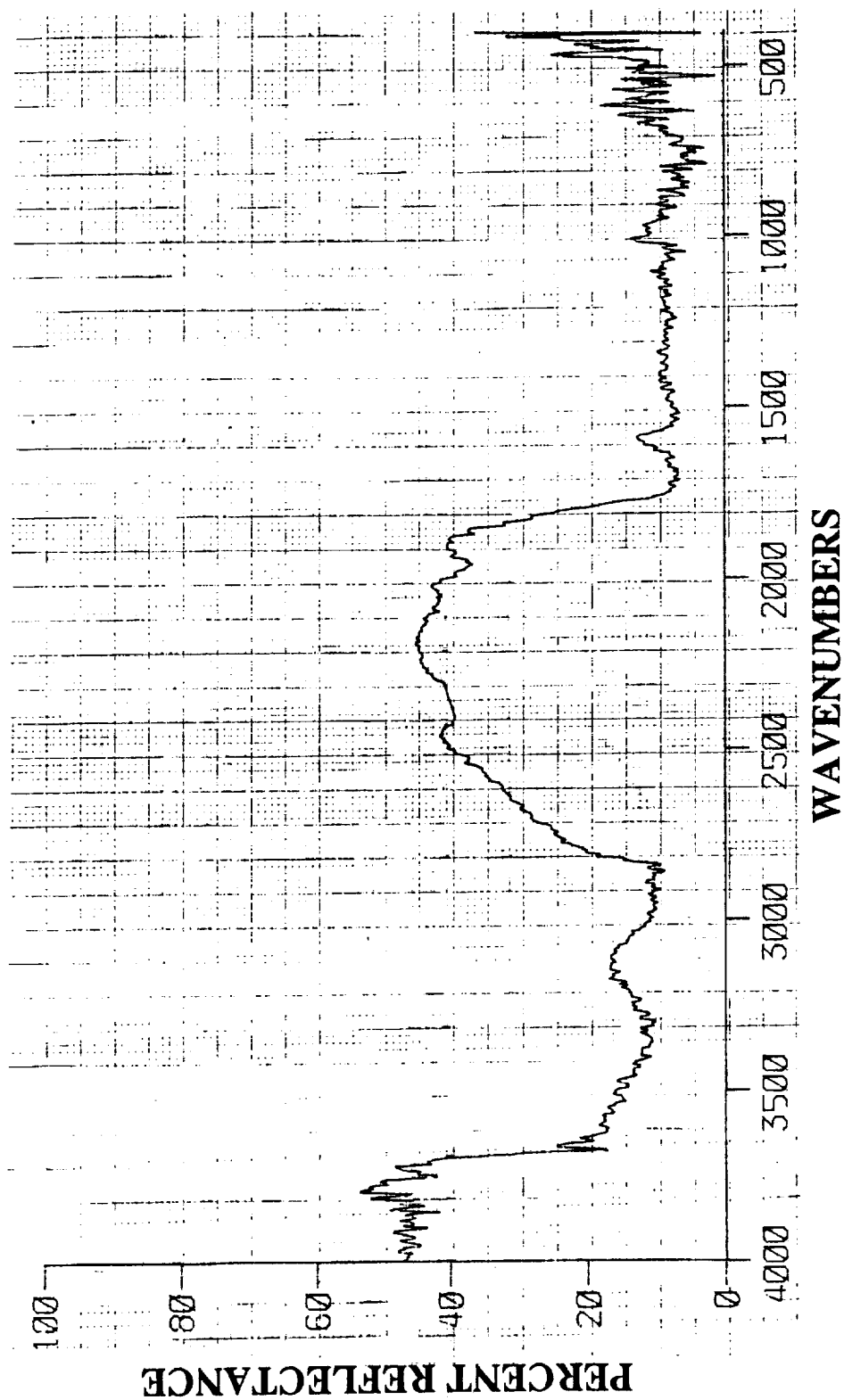


Figure B16. Chemglaze A276 E3-8 Specimen - Total Hemispherical Infrared Reflectance

APPENDIX B. Infrared Reflectance Measurements for Chemglaze A276

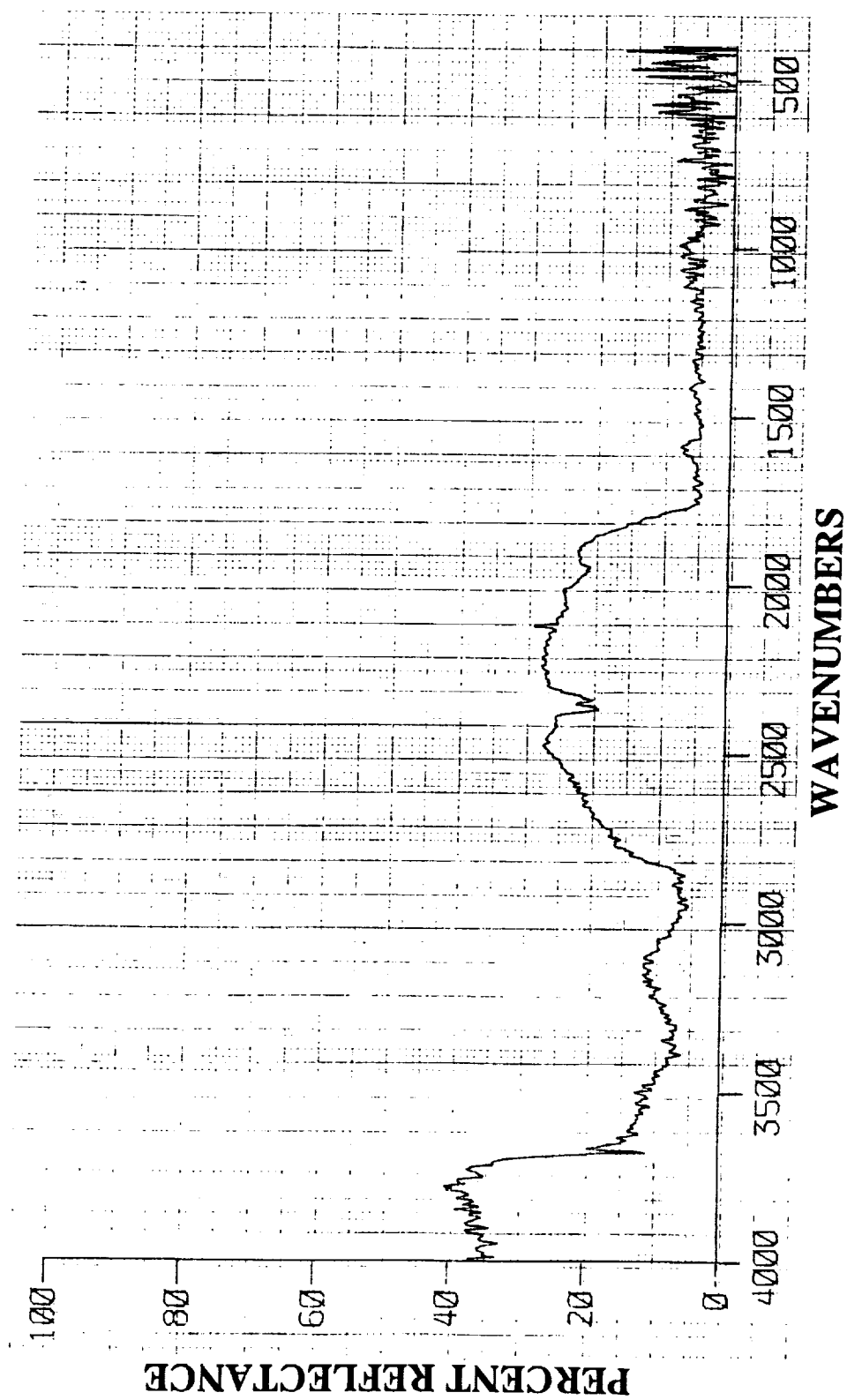


Figure B17. Chemglaze A276 E3-8 Specimen - Diffuse Infrared Reflectance

APPENDIX B. Infrared Reflectance Measurements for Chemglaze A276

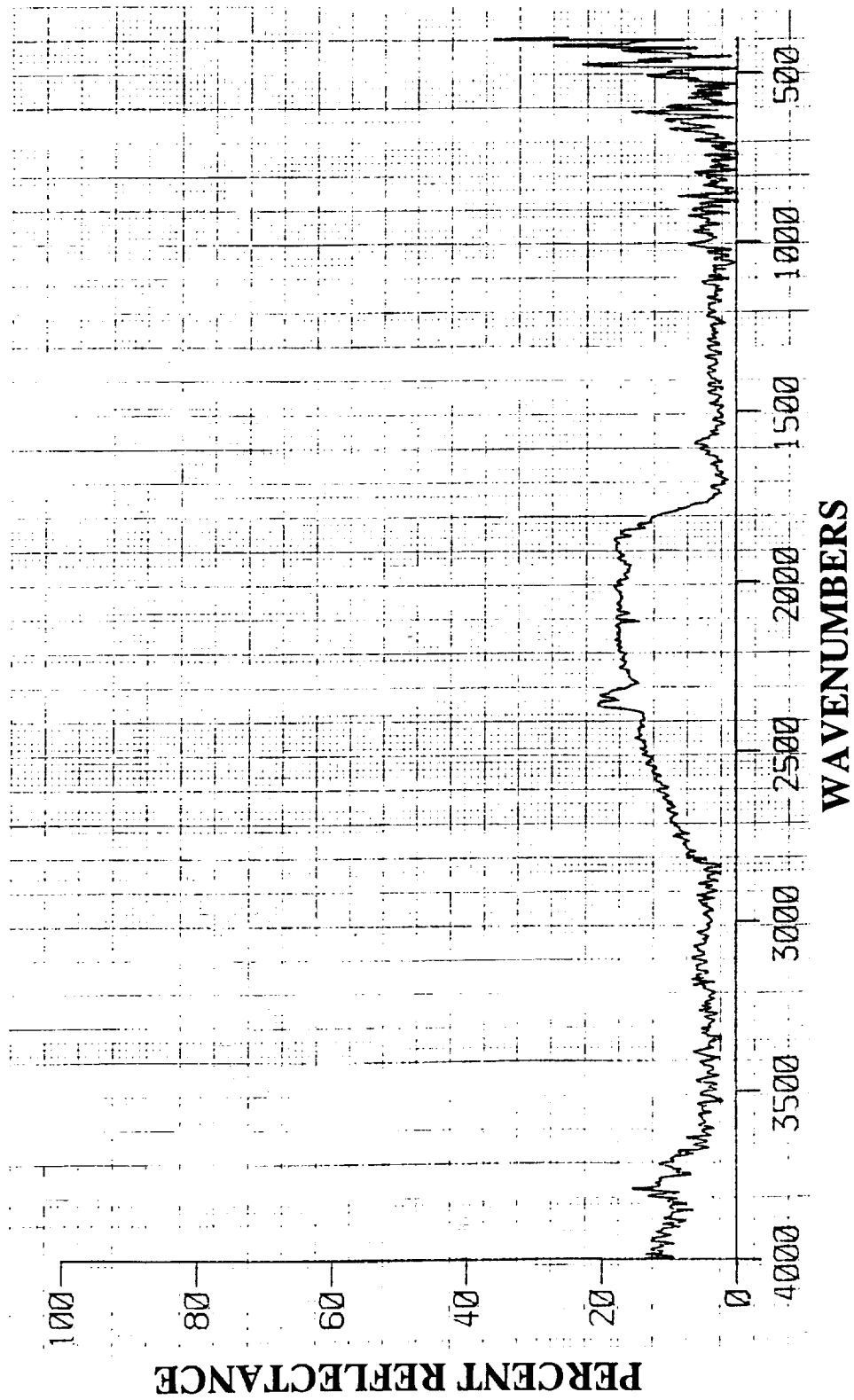


Figure B18. Chemglaze A276 E3-8 Specimen - Specular Infrared Reflectance

APPENDIX B. Infrared Reflectance Measurements for Chemglaze A276

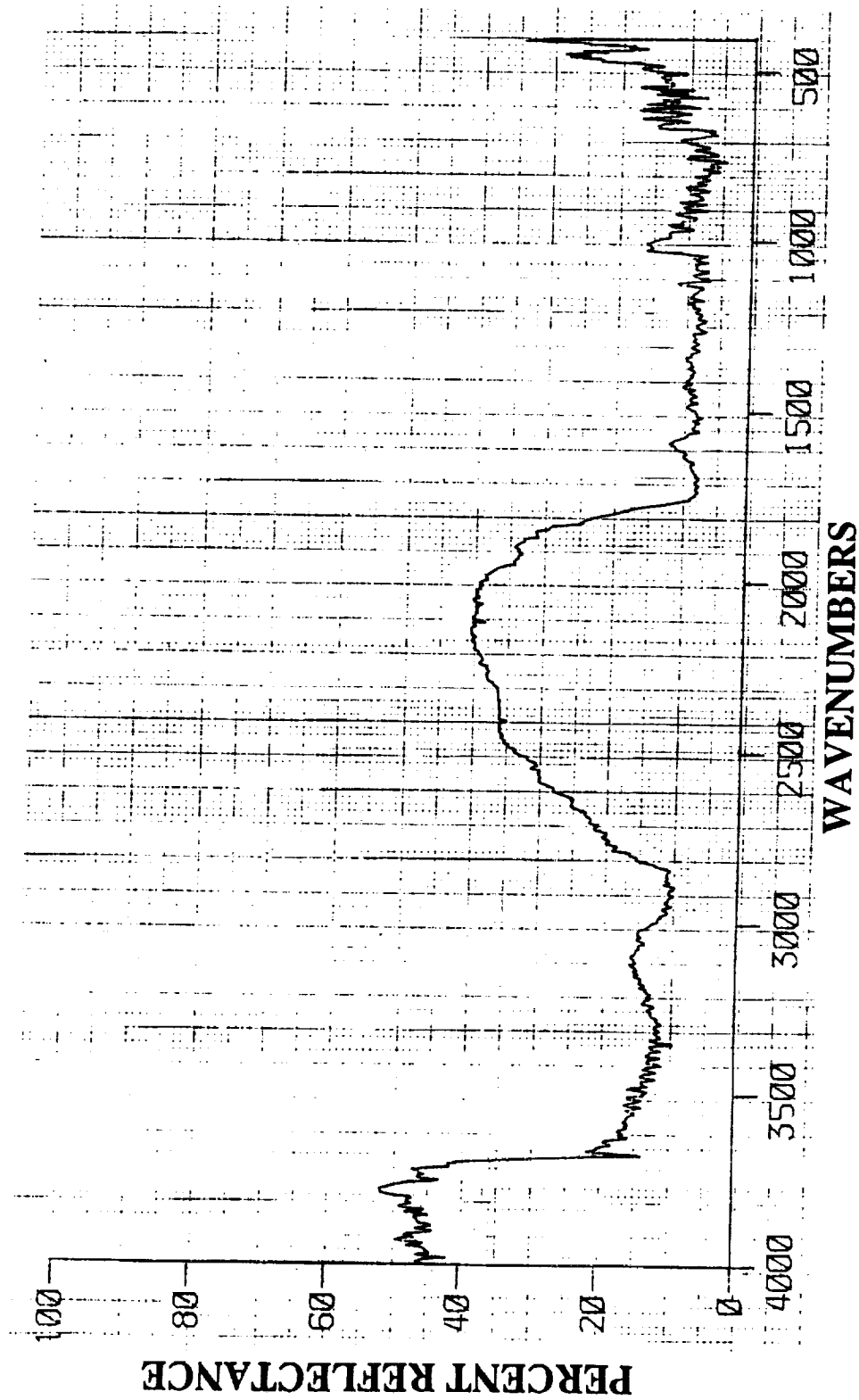


Figure B19. Chemglaze A276 B4-7 Specimen - Total Hemispherical Infrared Reflectance

APPENDIX B. Infrared Reflectance Measurements for Chemglaze A276

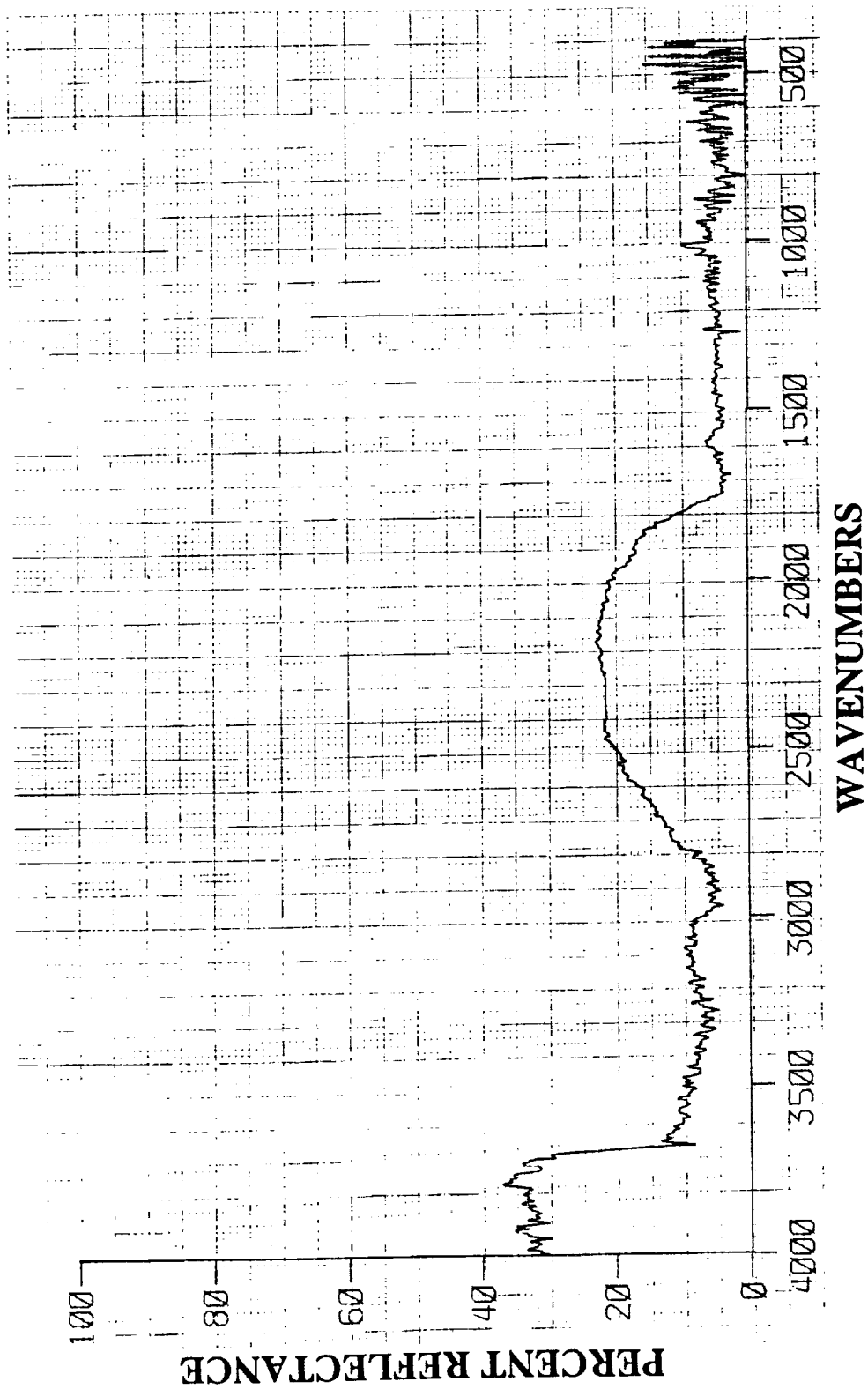


Figure B20. Chemglaze A276 B4-7 Specimen - Diffuse Infrared Reflectance

APPENDIX B. Infrared Reflectance Measurements for Chemglaze A276

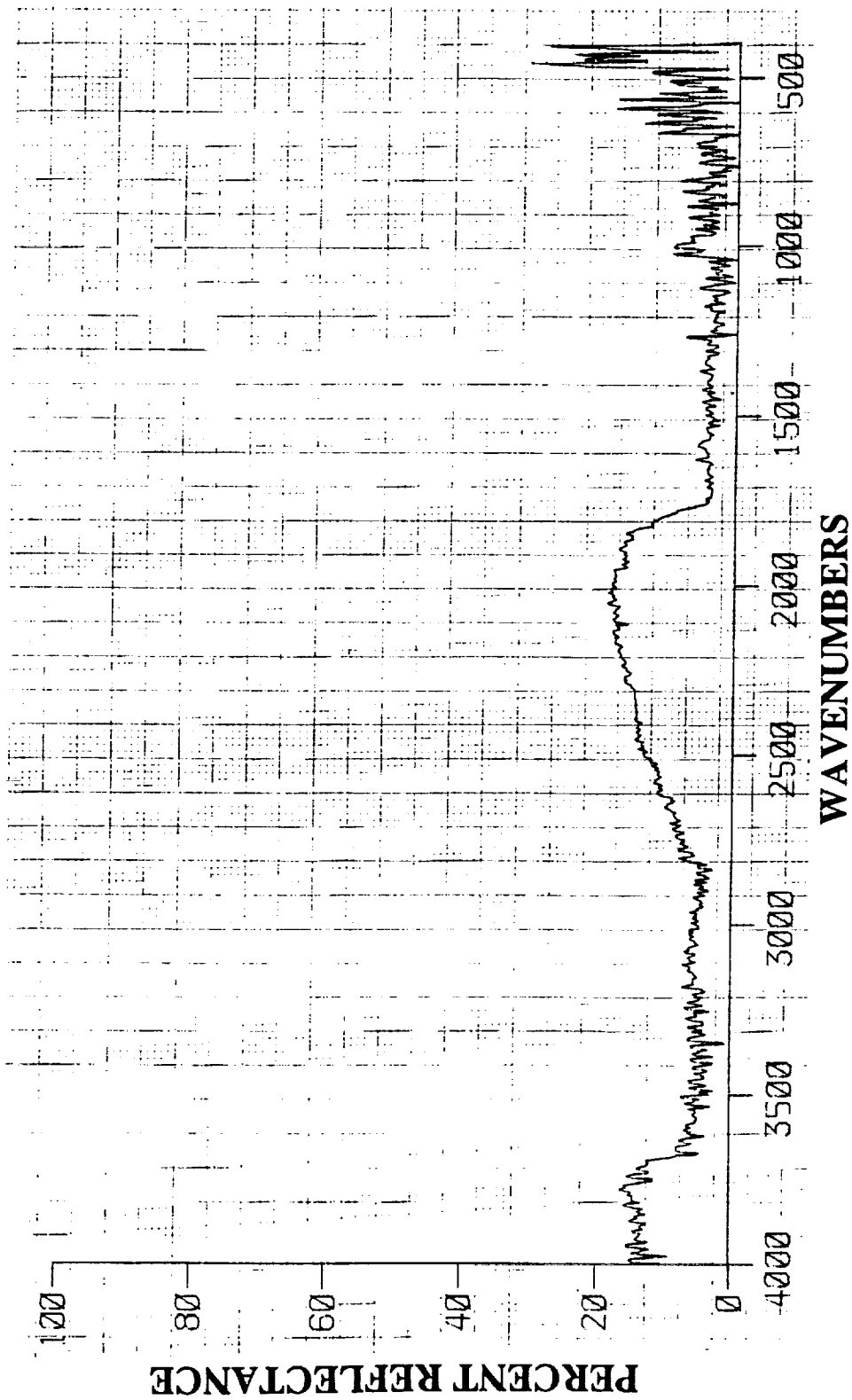


Figure B21. Chemglaze A276 B4-7 Specimen - Specular Infrared Reflectance

**APPENDIX B. Infrared Reflectance Measurements for Chemglaze A276**

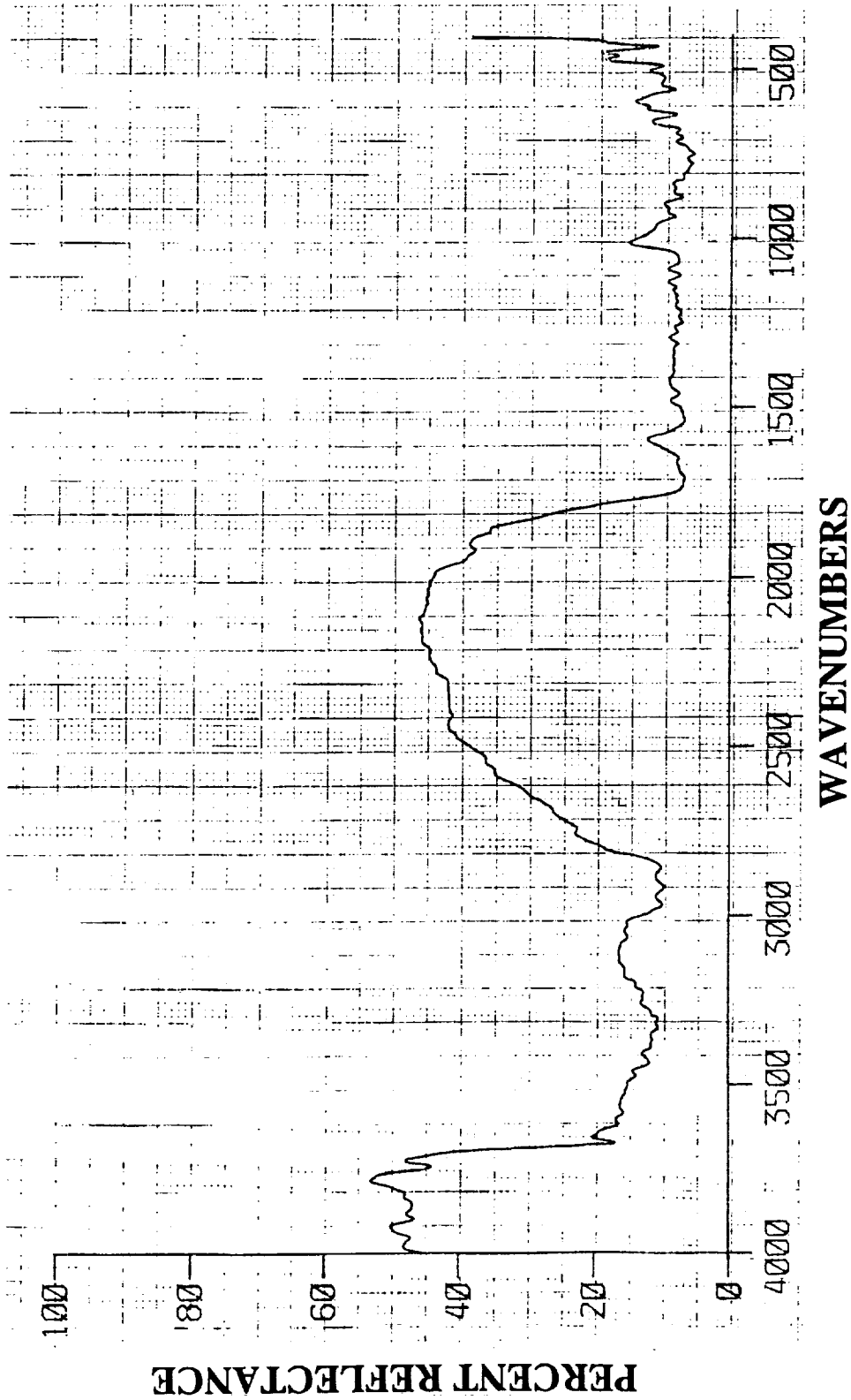


Figure B22. Chemglaze A276 A6-2 Specimen - Total Hemispherical Infrared Reflectance

**APPENDIX B. Infrared Reflectance Measurements for Chemglaze A276**

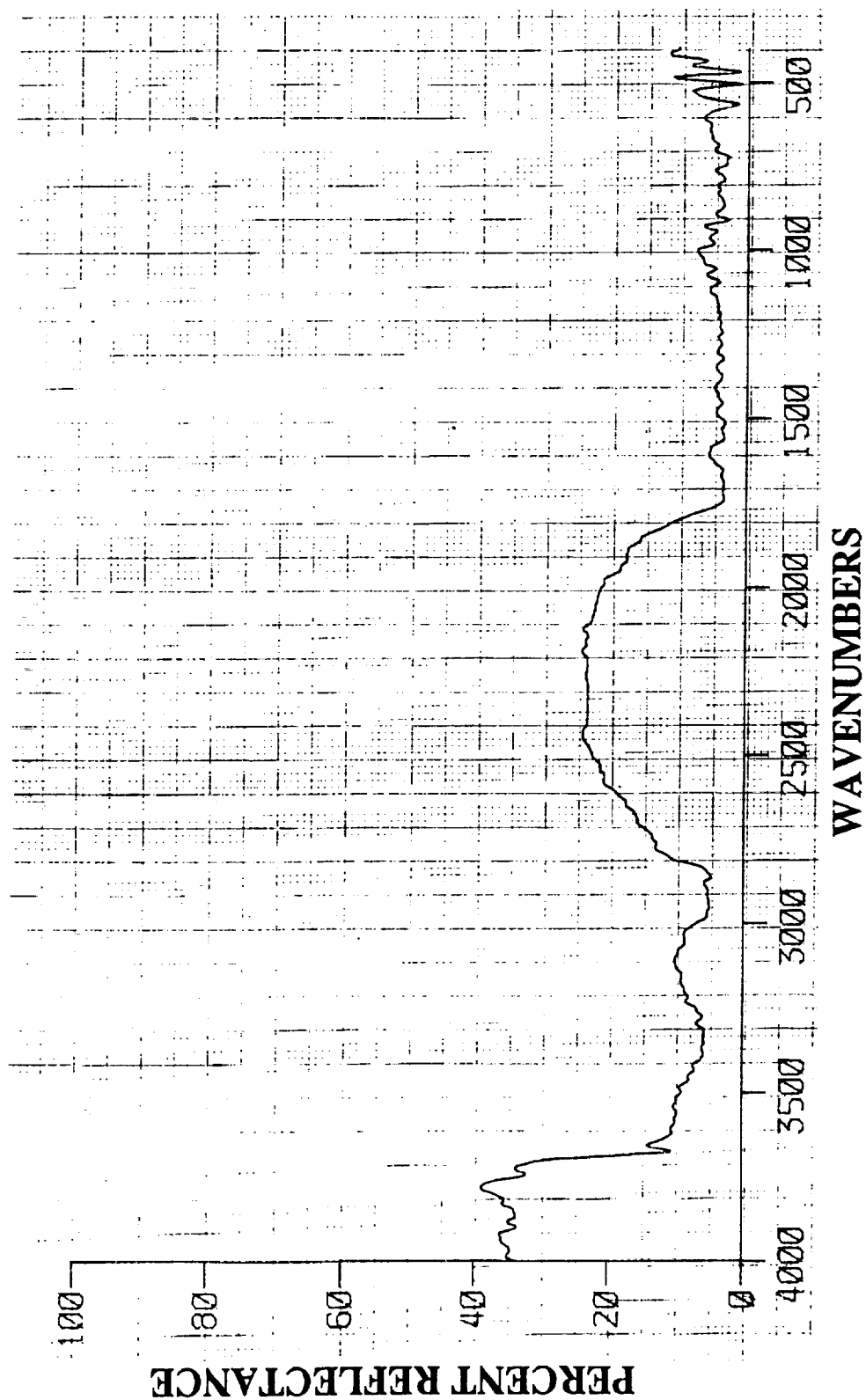


Figure B23. Chemglaze A276 A6-2 Specimen - Diffuse Infrared Reflectance

APPENDIX B. Infrared Reflectance Measurements for Chemglaze A276

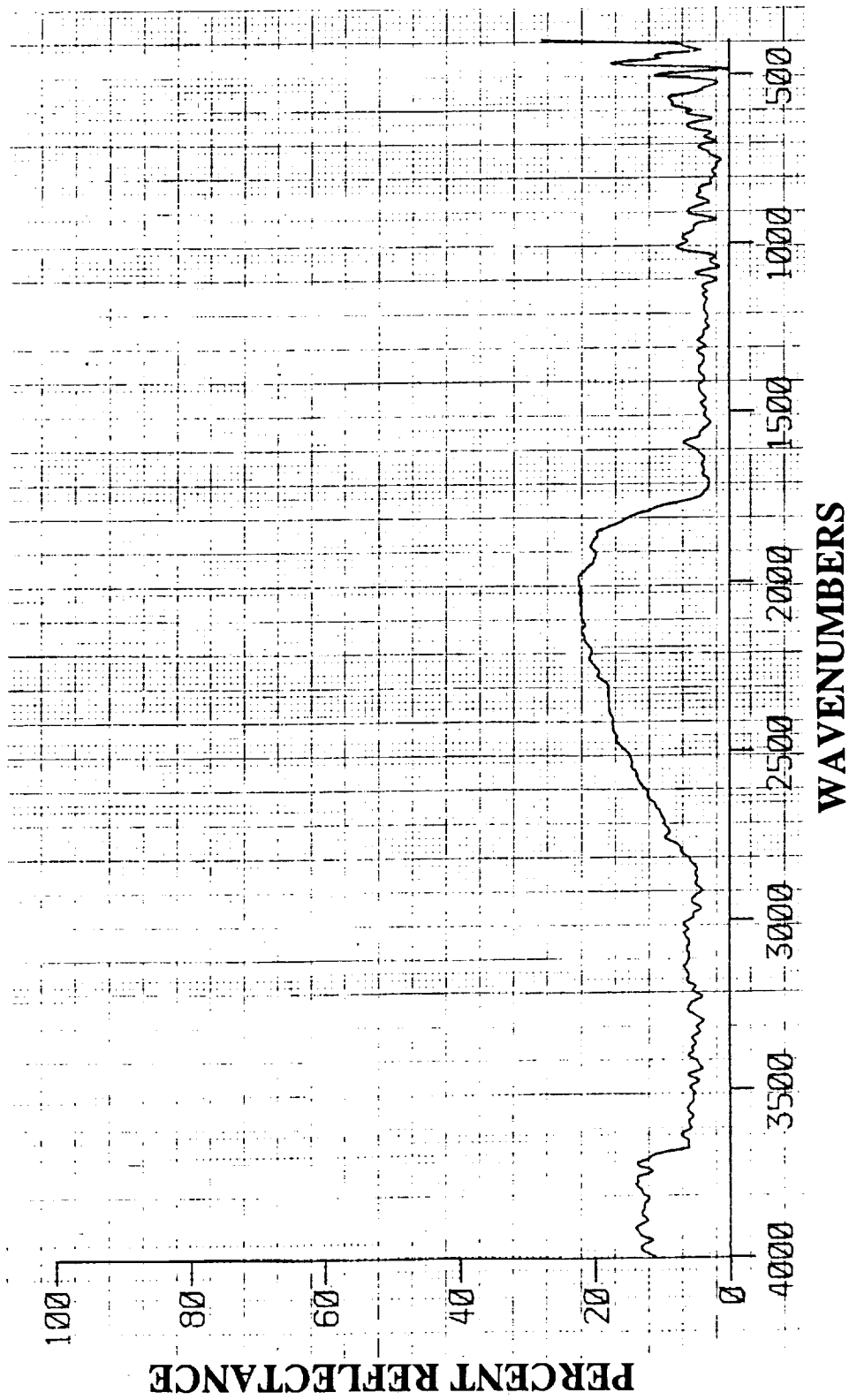


Figure B24. Chemglaze A276 A6-2 Specimen - Specular Infrared Reflectance

APPENDIX B. Infrared Reflectance Measurements for Chemglaze A276

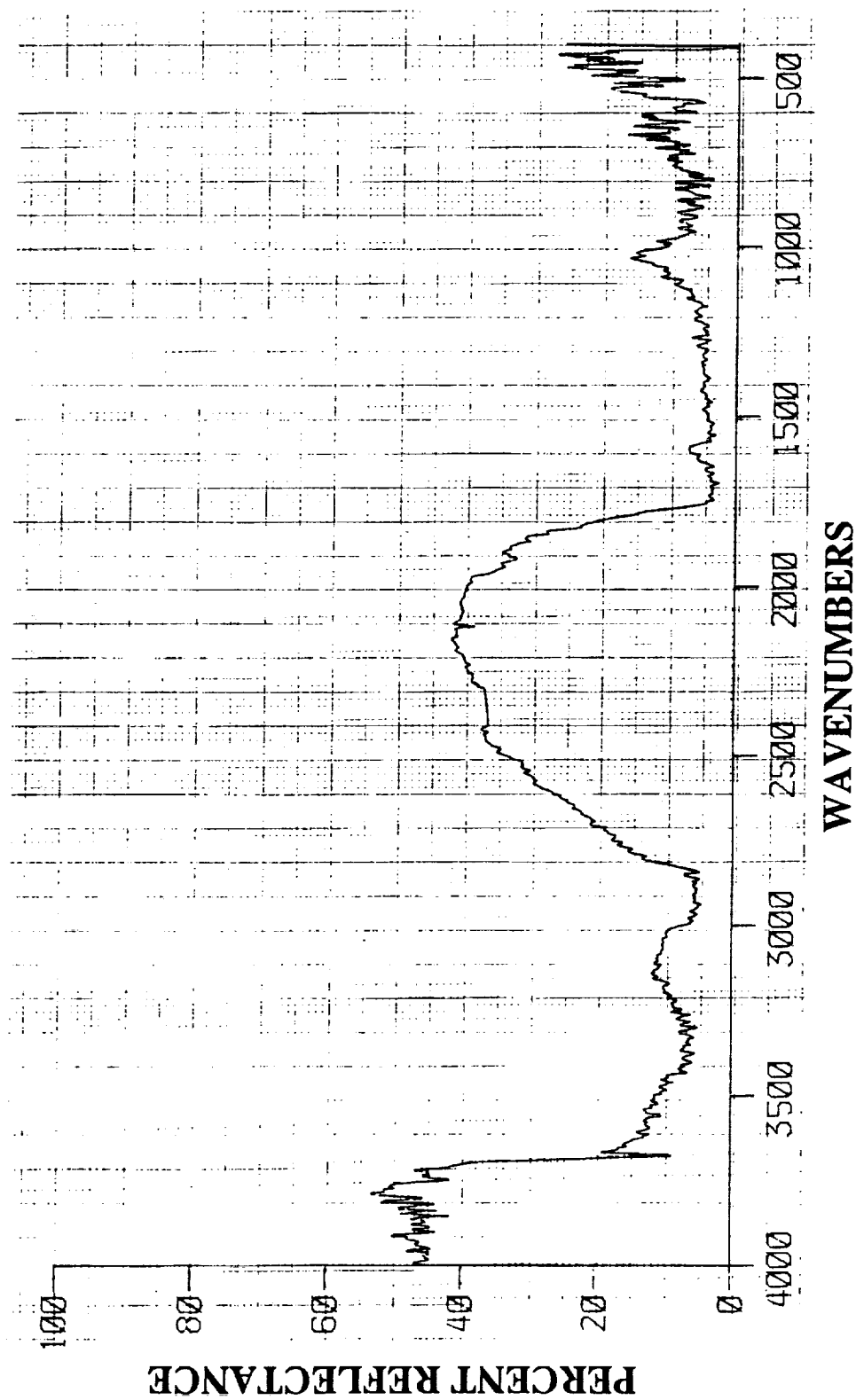


Figure B25. Chemglaze A276 B7-2 Specimen - Total Hemispherical Infrared Reflectance

APPENDIX B. Infrared Reflectance Measurements for Chemglaze A276

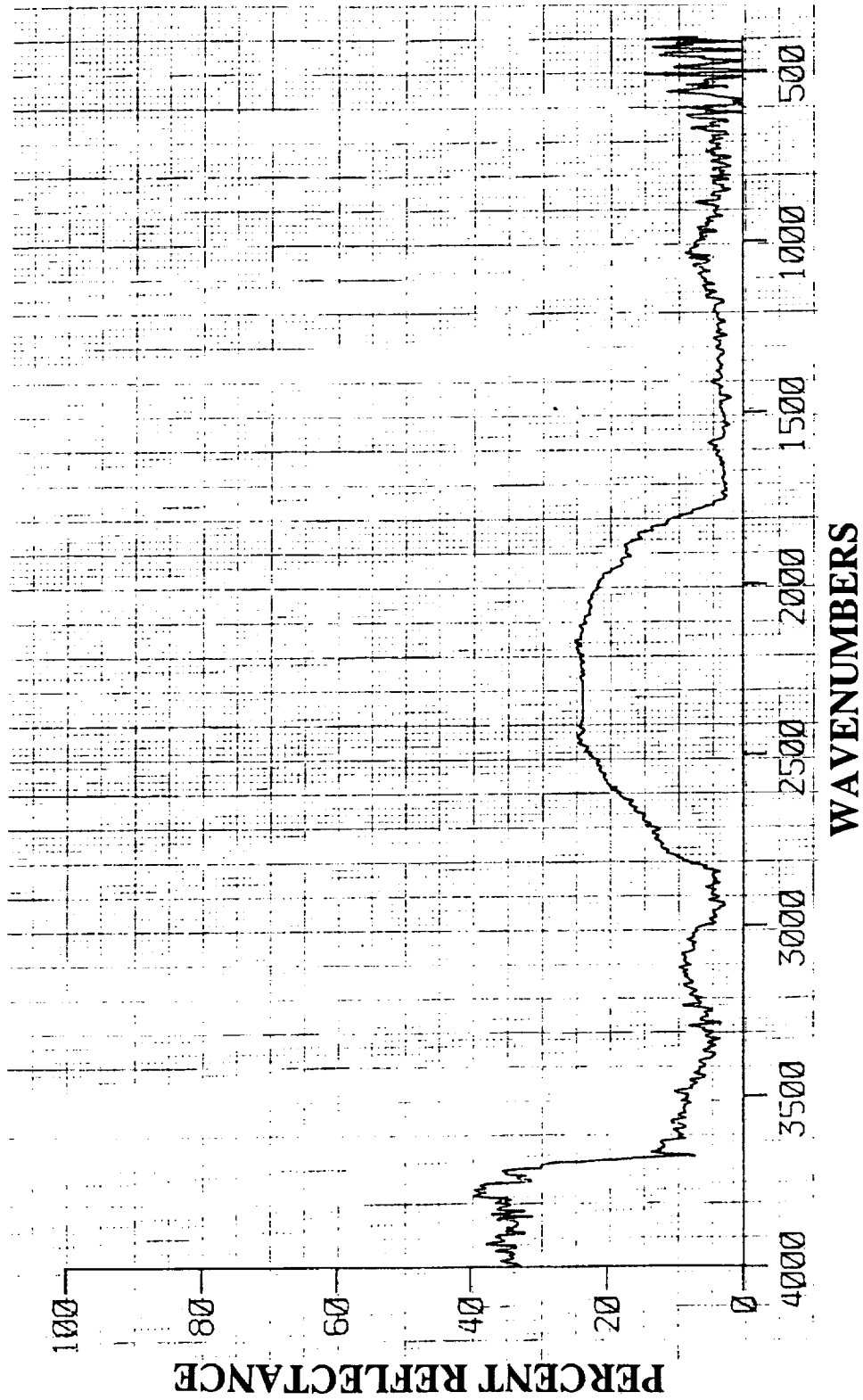


Figure B26. Chemglaze A276 B7-2 Specimen - Diffuse Infrared Reflectance

APPENDIX B. Infrared Reflectance Measurements for Chemglaze A276

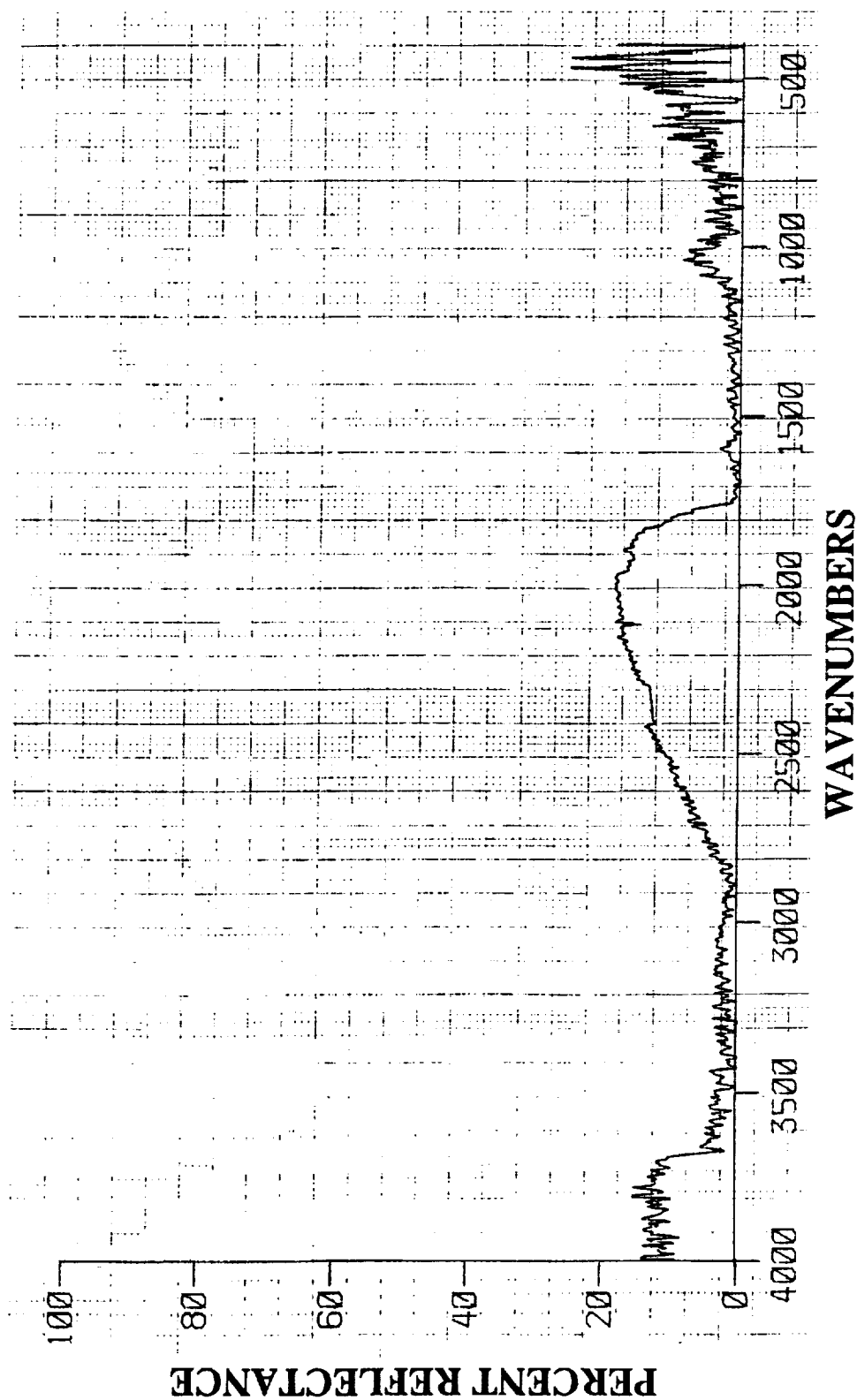


Figure B27. Chemglaze A276 B7-2 Specimen - Specular Infrared Reflectance

APPENDIX B. Infrared Reflectance Measurements for Chemglaze A276

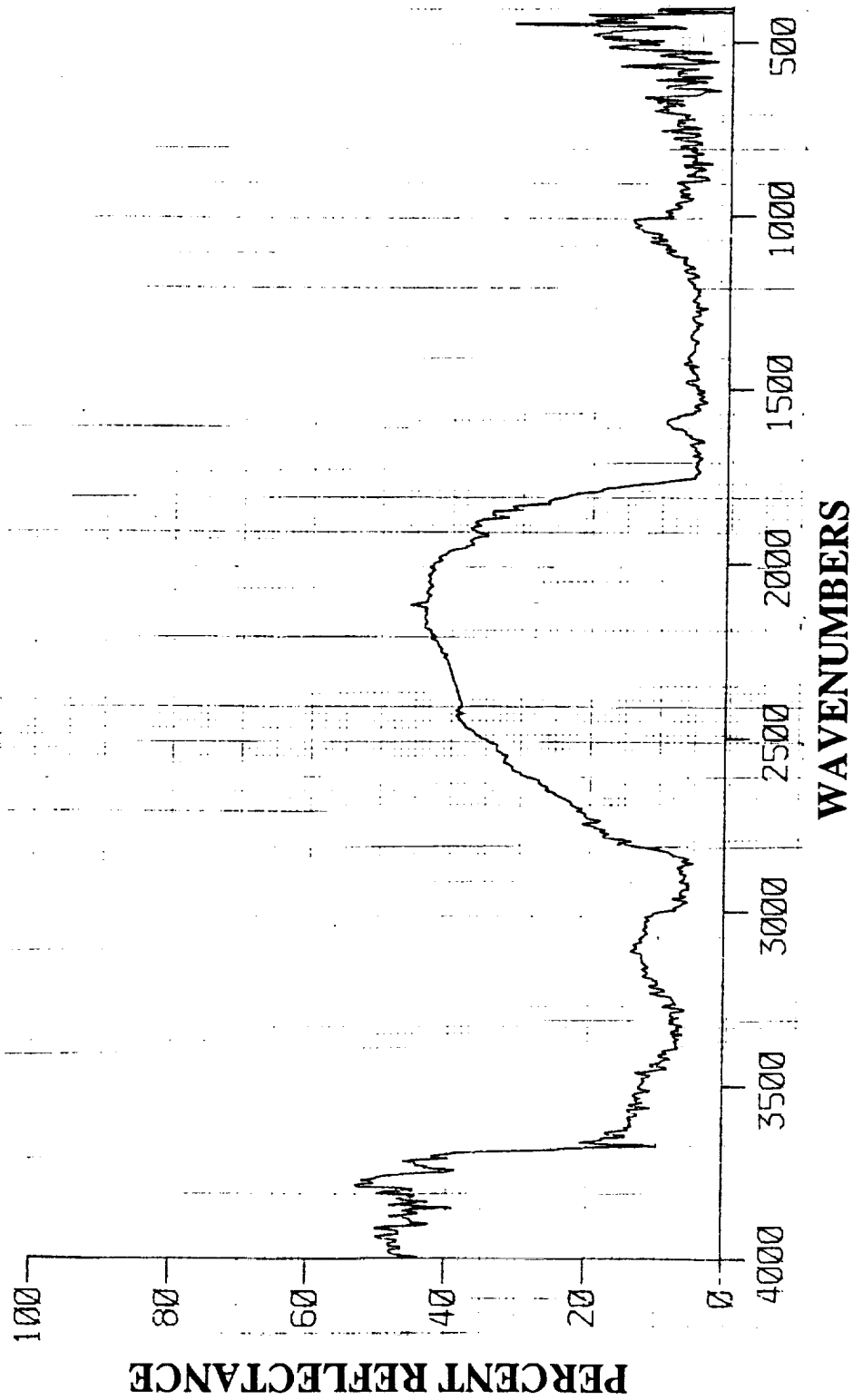


Figure B28. Chemglaze A276 B7-7 Specimen - Total Hemispherical Infrared Reflectance

APPENDIX B. Infrared Reflectance Measurements for Chemglaze A276

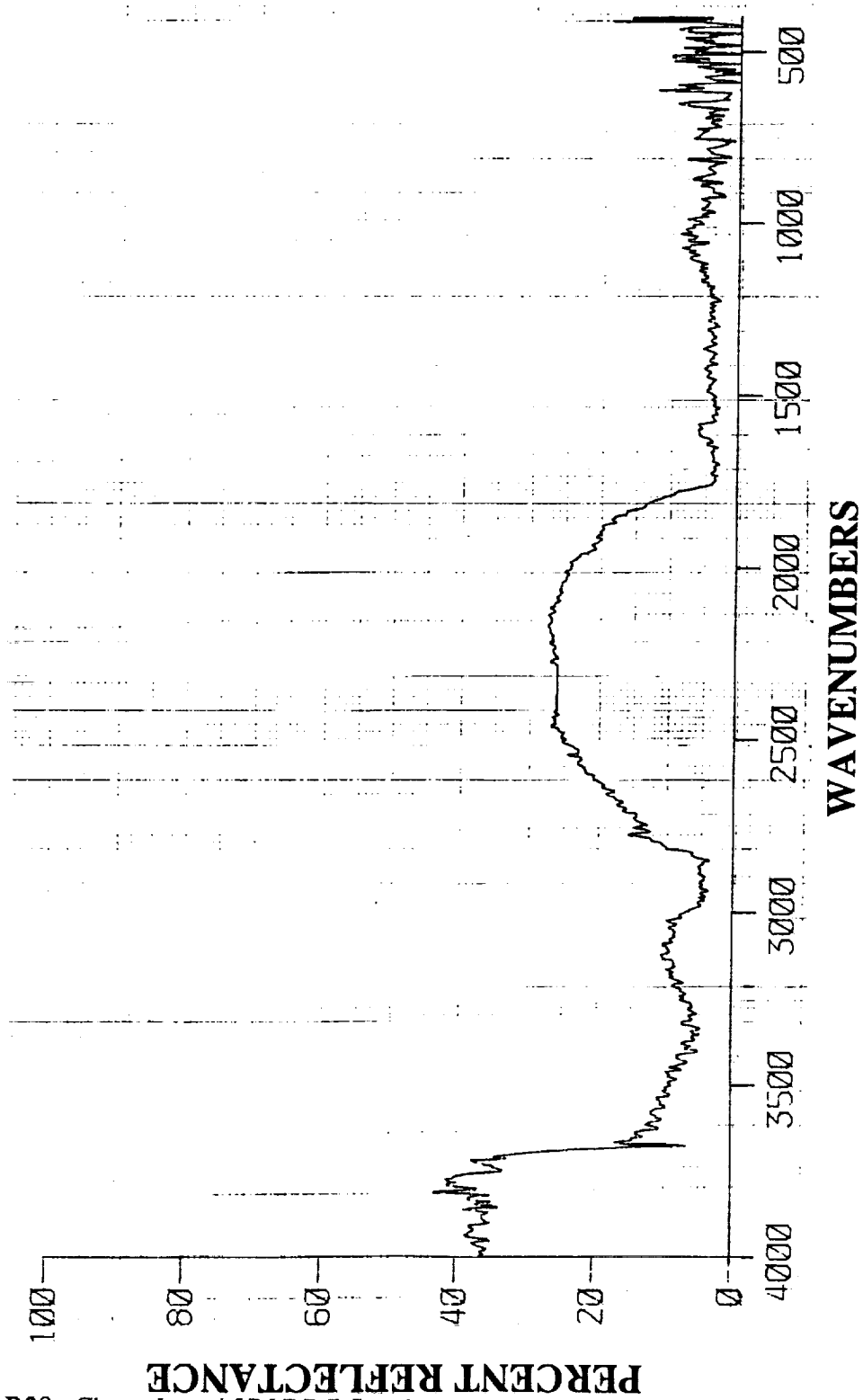


Figure B29. Chemglaze A276 B7-7 Specimen - Diffuse Infrared Reflectance

APPENDIX B. Infrared Reflectance Measurements for Chemglaze A276

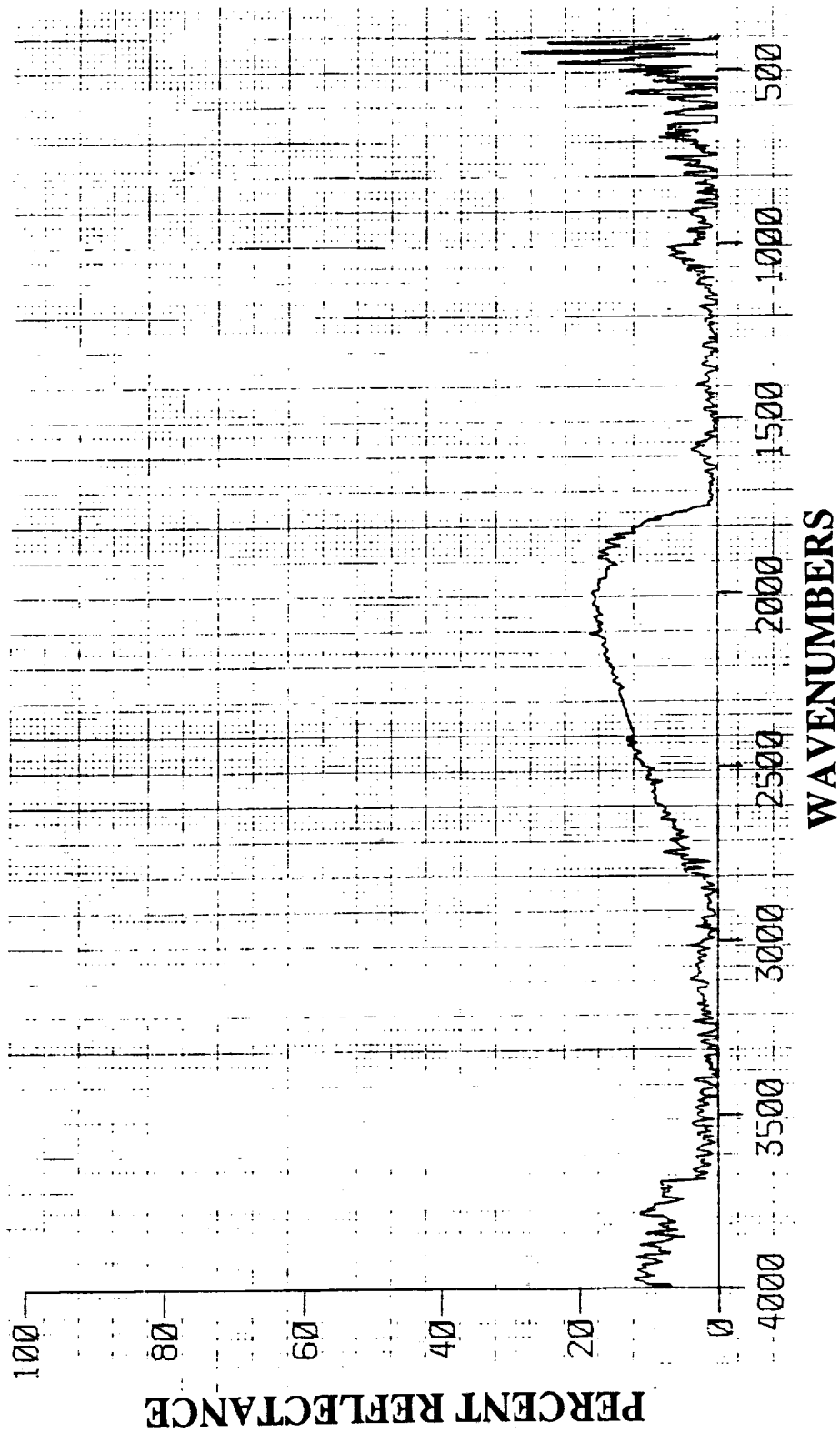


Figure B30. Chemglaze A276 B7-7 Specimen - Specular Infrared Reflectance

APPENDIX B. Infrared Reflectance Measurements for Chemglaze A276

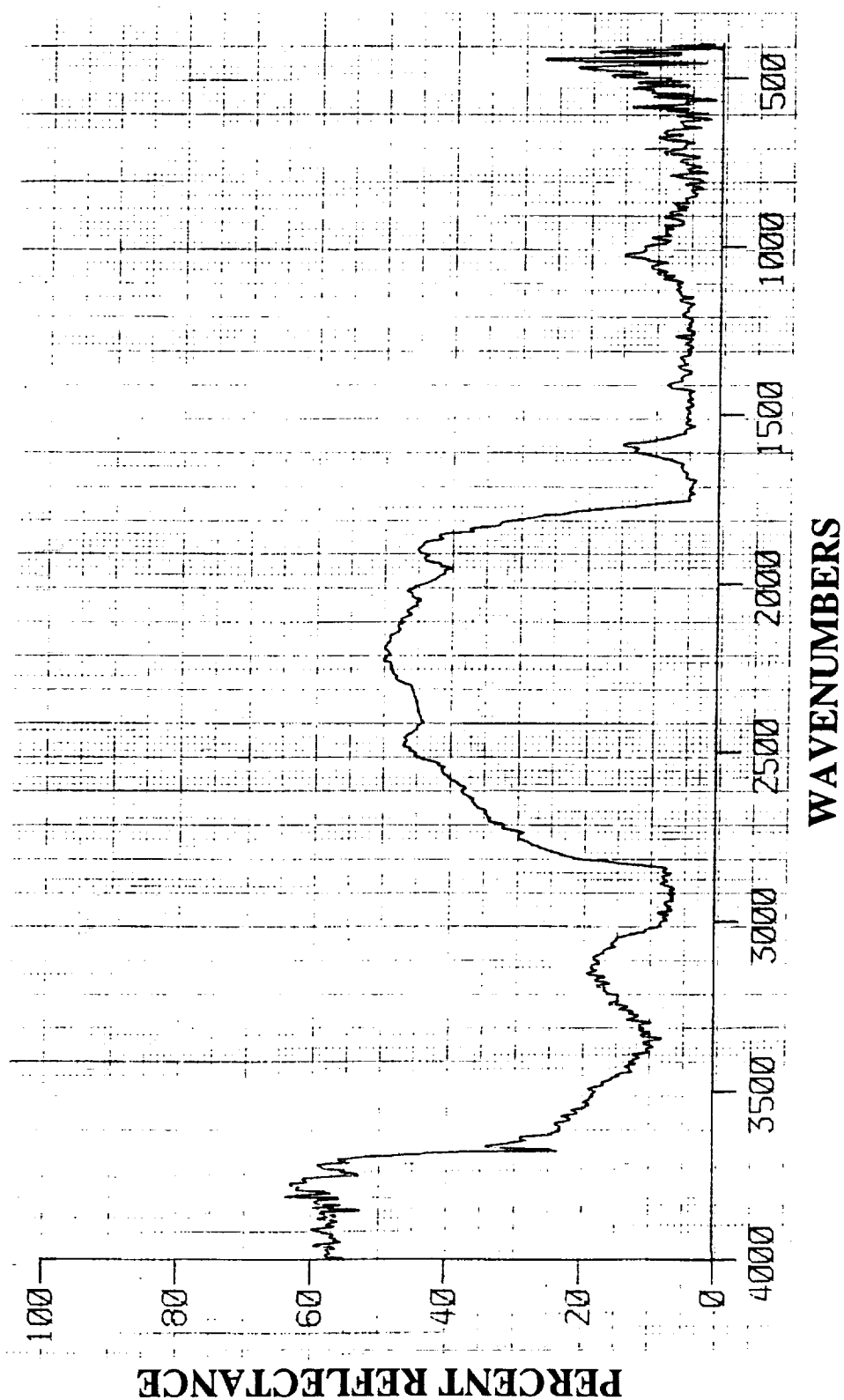


Figure B31. Chemglaze A276 C8-5 Specimen - Total Hemispherical Infrared Reflectance

APPENDIX B. Infrared Reflectance Measurements for Chemglaze A276

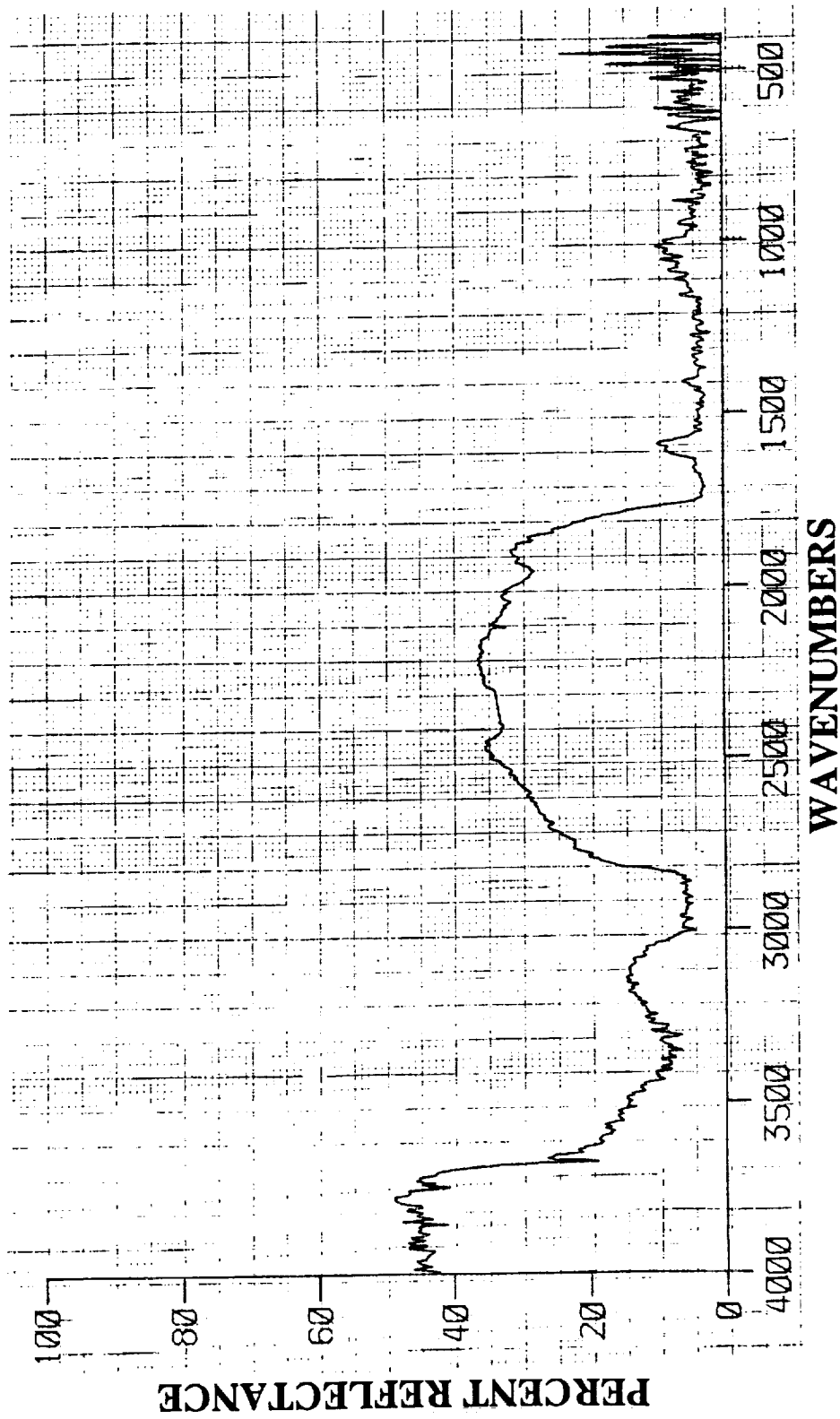


Figure B32. Chemglaze A276 C8-5 Specimen - Diffuse Infrared Reflectance

APPENDIX B. Infrared Reflectance Measurements for Chemglaze A276

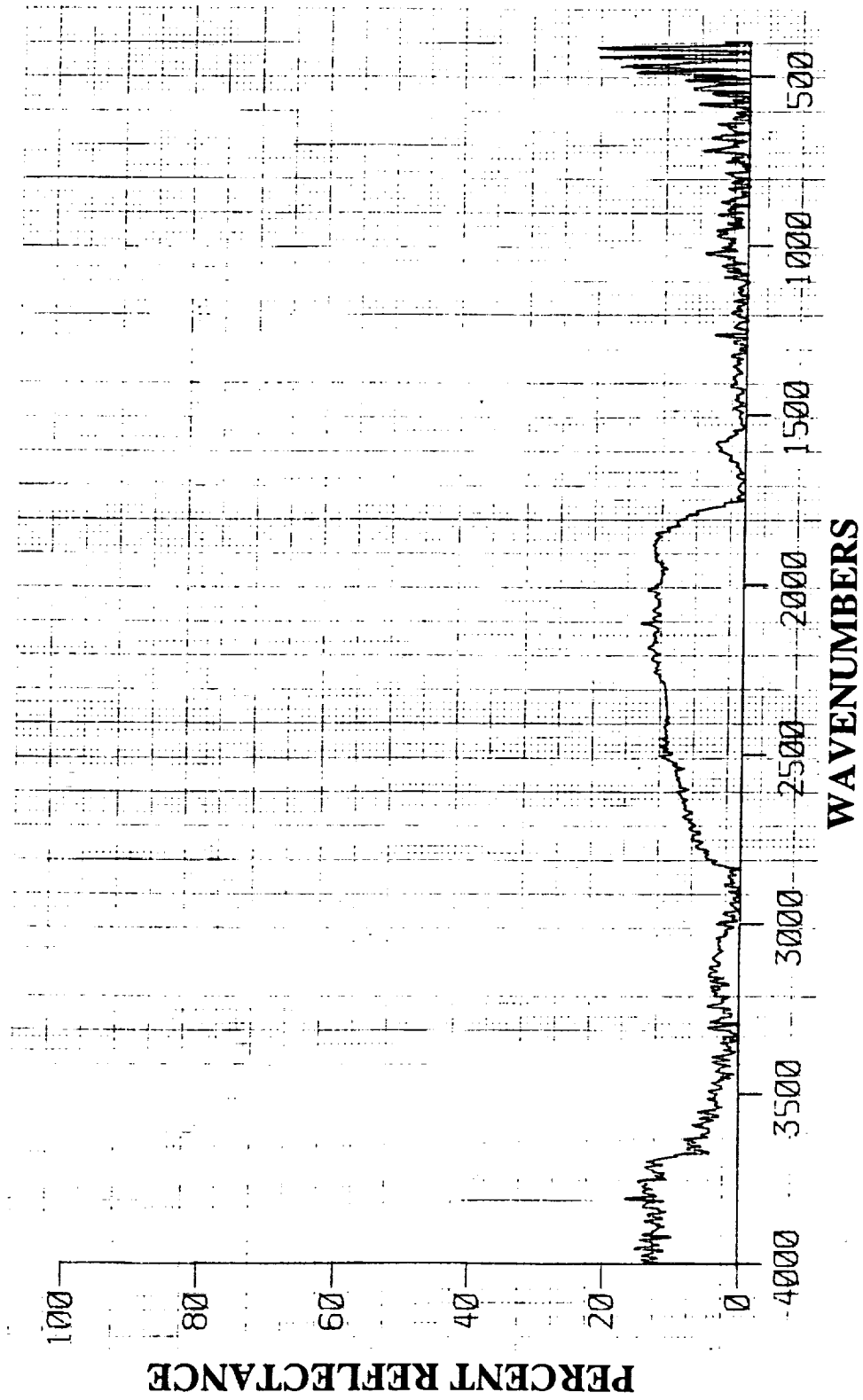


Figure B33. Chemglaze A276 C8-5 Specimen - Specular Infrared Reflectance

APPENDIX B. Infrared Reflectance Measurements for Chemglaze A276

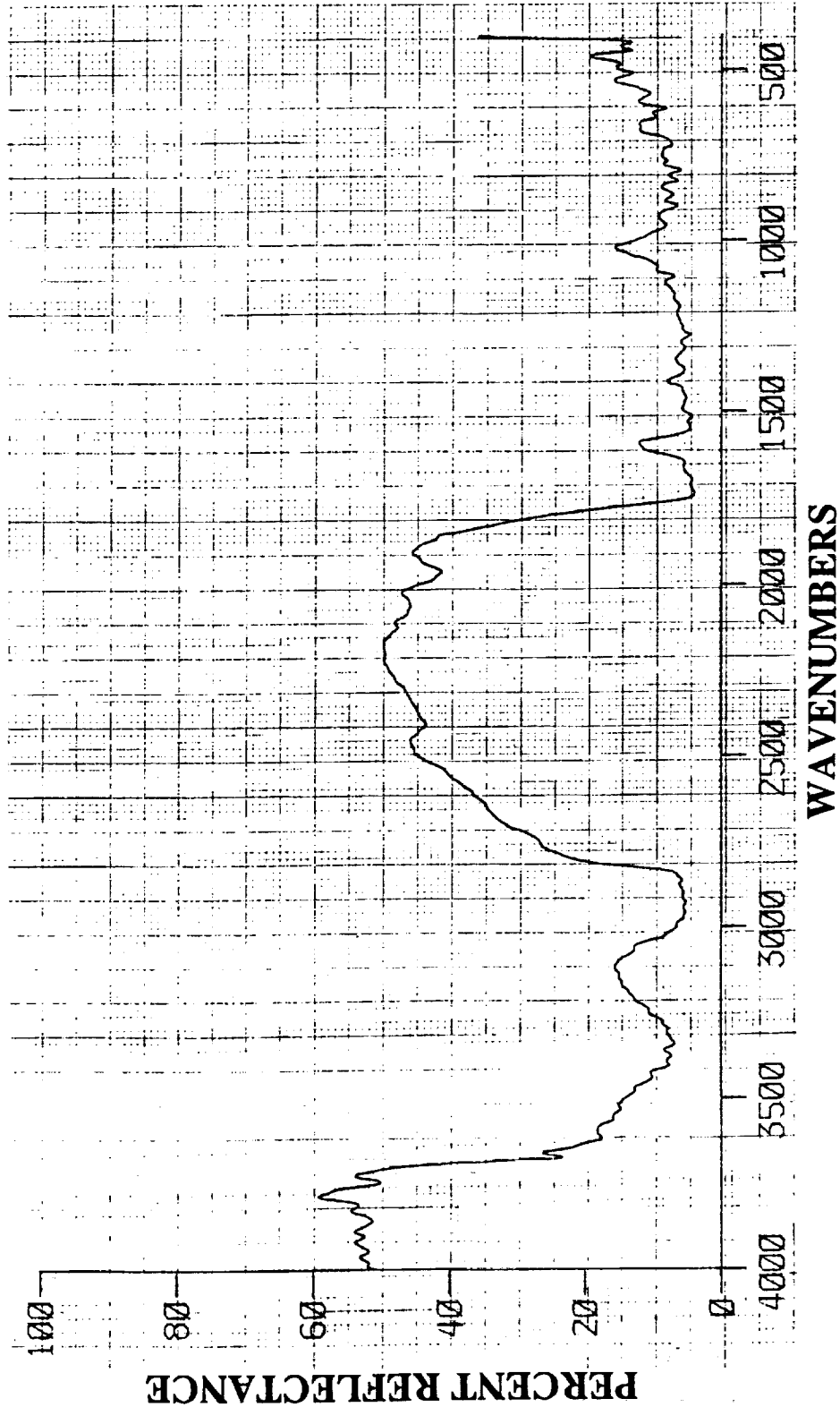


Figure B34. Chemglaze A276 G6-2 Specimen - Total Hemispherical Infrared Reflectance

APPENDIX B. Infrared Reflectance Measurements for Chemglaze A276

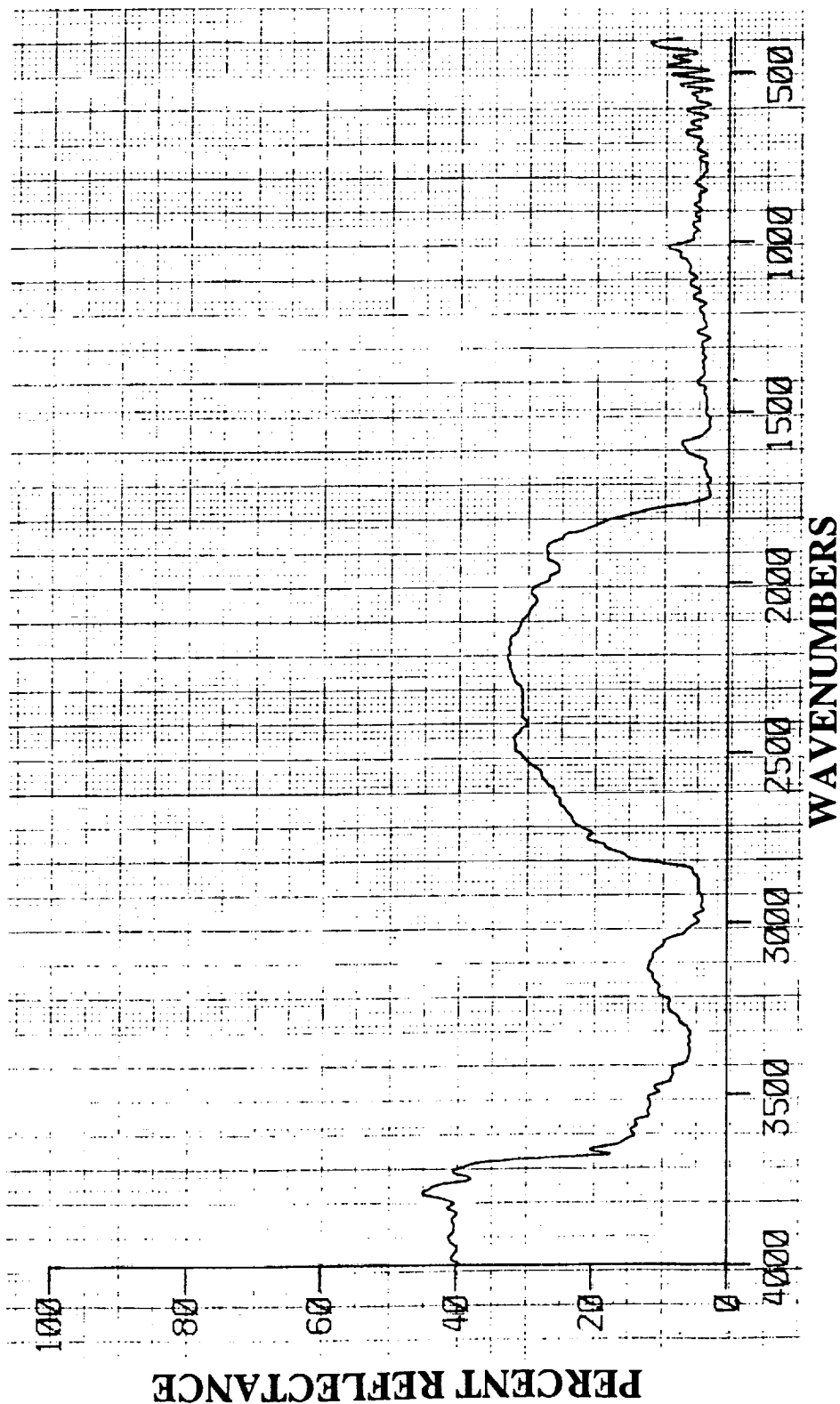


Figure B35. Chemglaze A276 G6-2 Specimen - Diffuse Infrared Reflectance

APPENDIX B. Infrared Reflectance Measurements for Chemglaze A276

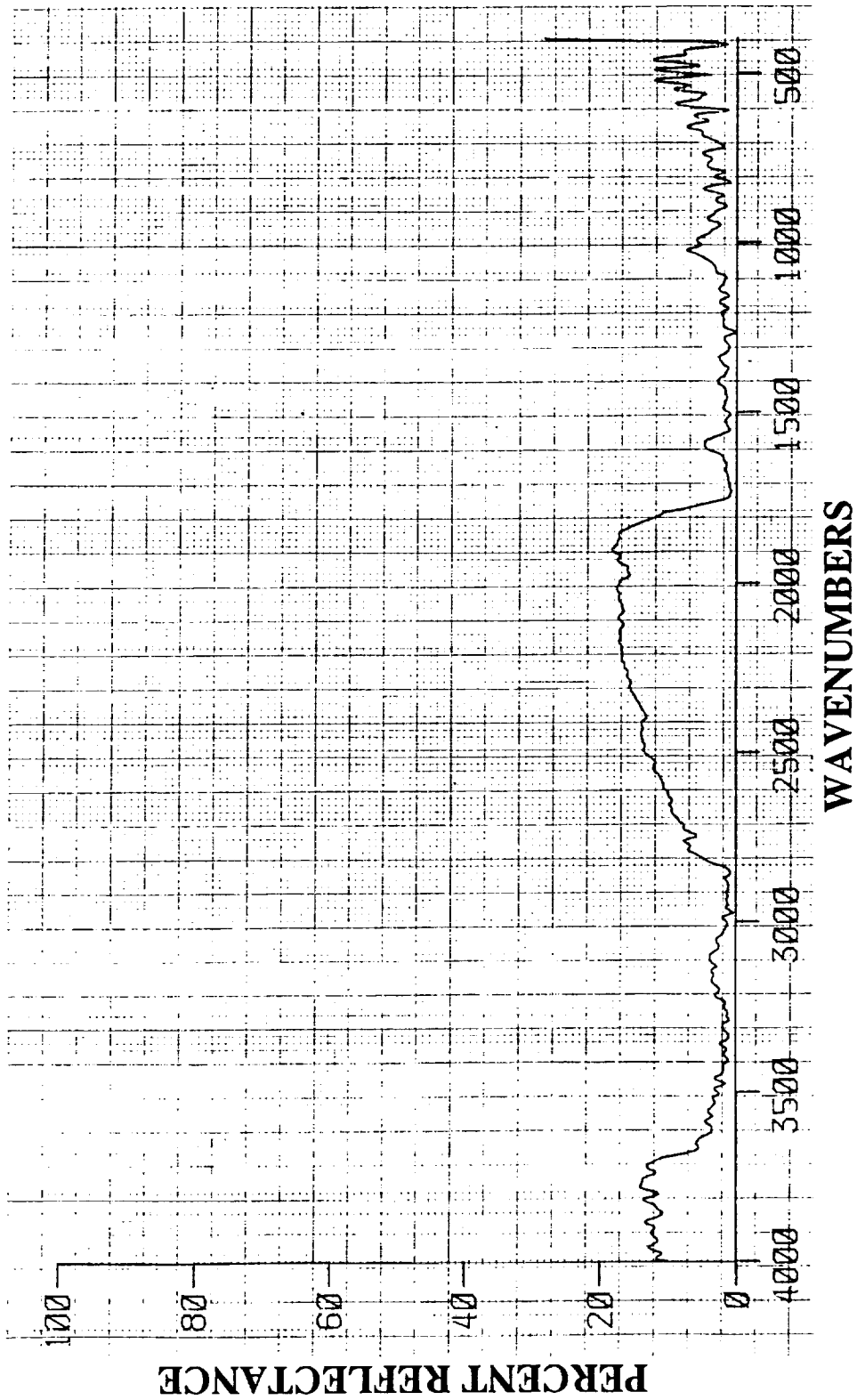


Figure B36. Chemglaze A276 G6-2 Specimen - Specular Infrared Reflectance

APPENDIX C. Color Photographs From Section 7.0 Figures

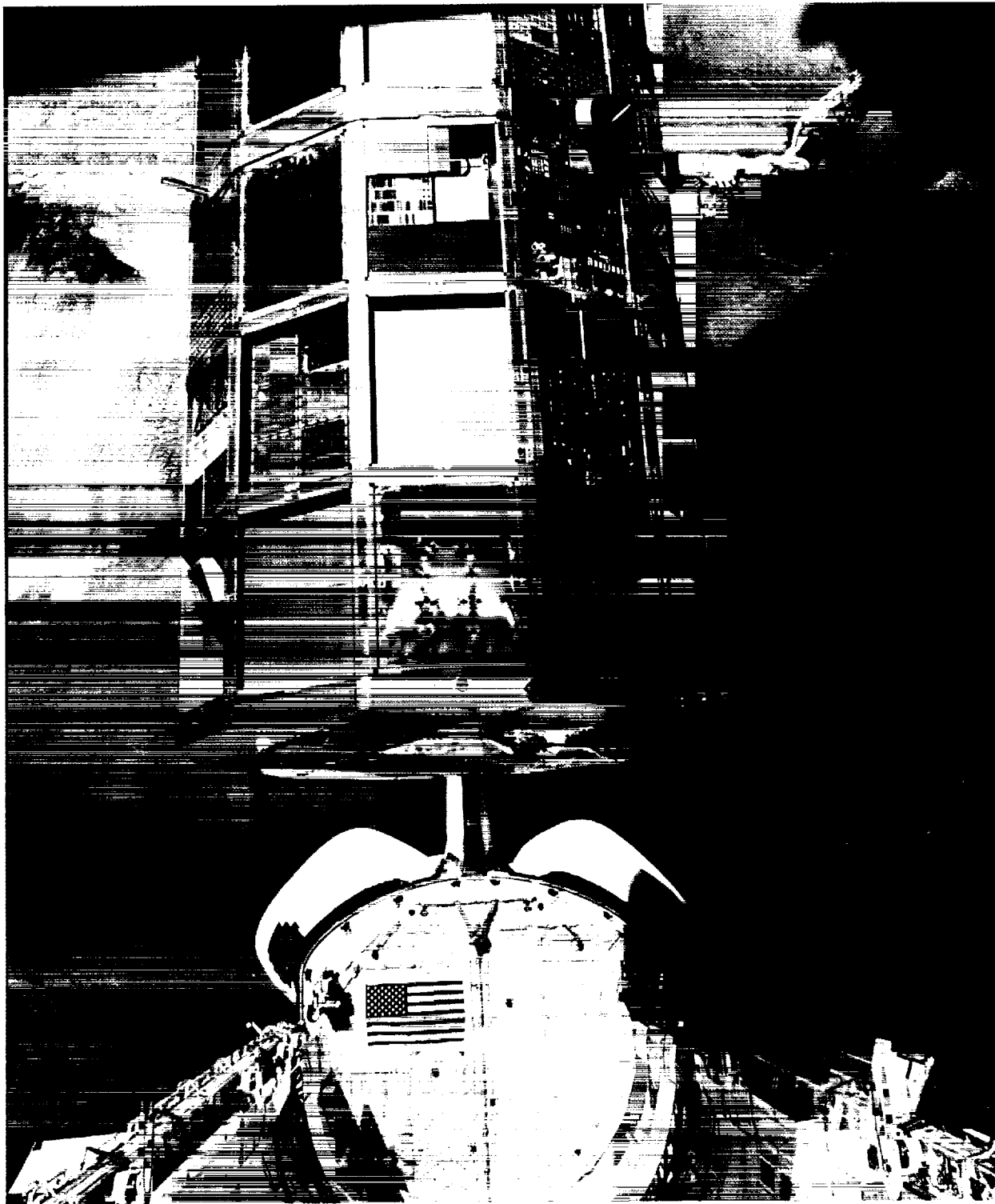


Figure C1. LDEF retrieved as viewed from the Shuttle Columbia on January 12, 1990. NASA Langley Research Center Photo No. 90-10472. Color version of figure 1, page 13.

## APPENDIX C. Color Photographs From Section 7.0 Figures

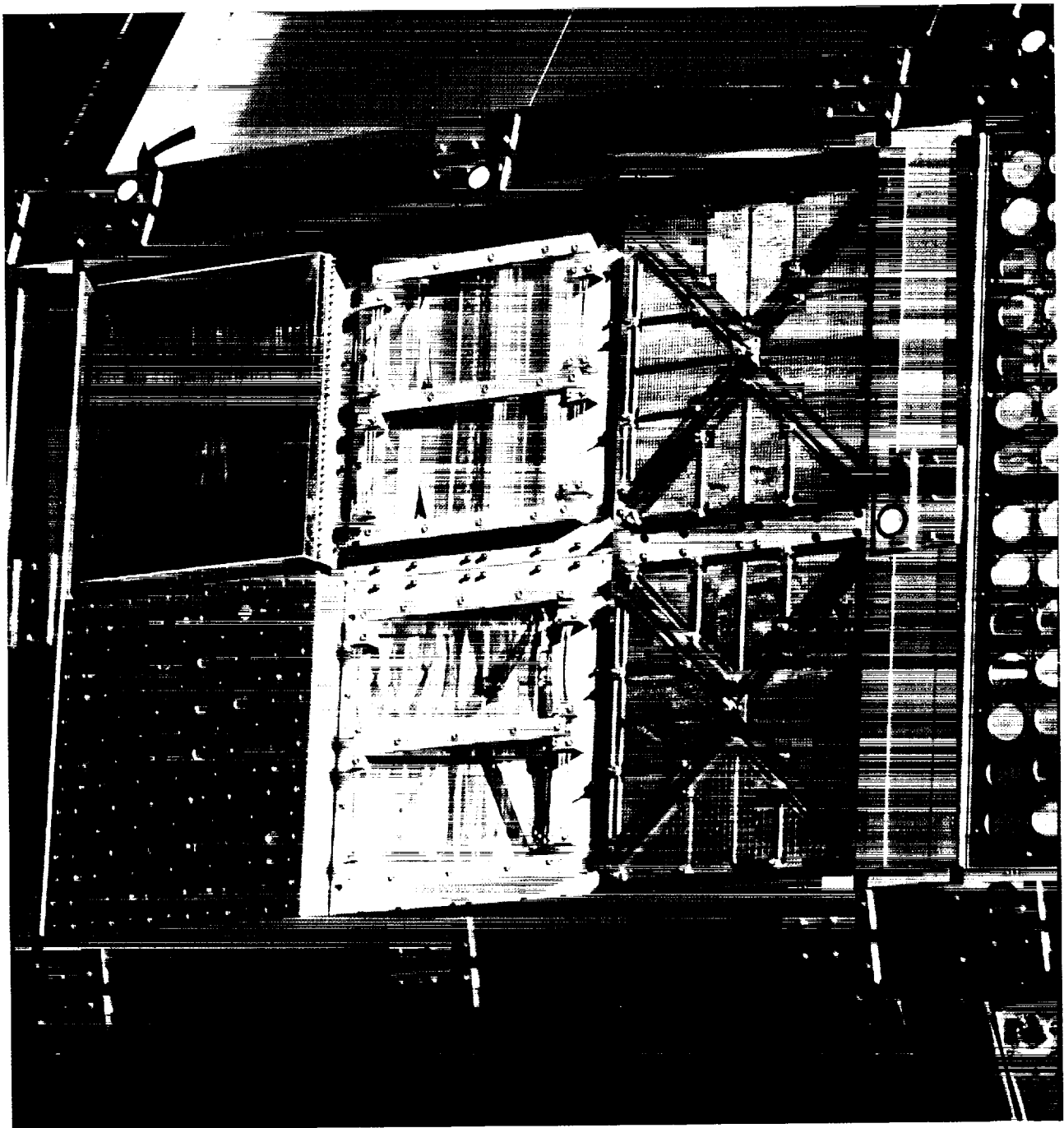


Figure C4. On-Orbit view of paint disks on LDEF tray clamps in the atomic oxygen fluence transition area, tray E6. NASA Johnson Space Center Photo No. S32-82-040. Disks on upper longeron were in high AO fluence and are white, disks on lower longeron were in low AO fluence and are brown. Color version of figure 4, page 15.

APPENDIX C. Color Photographs From Section 7.0 Figures

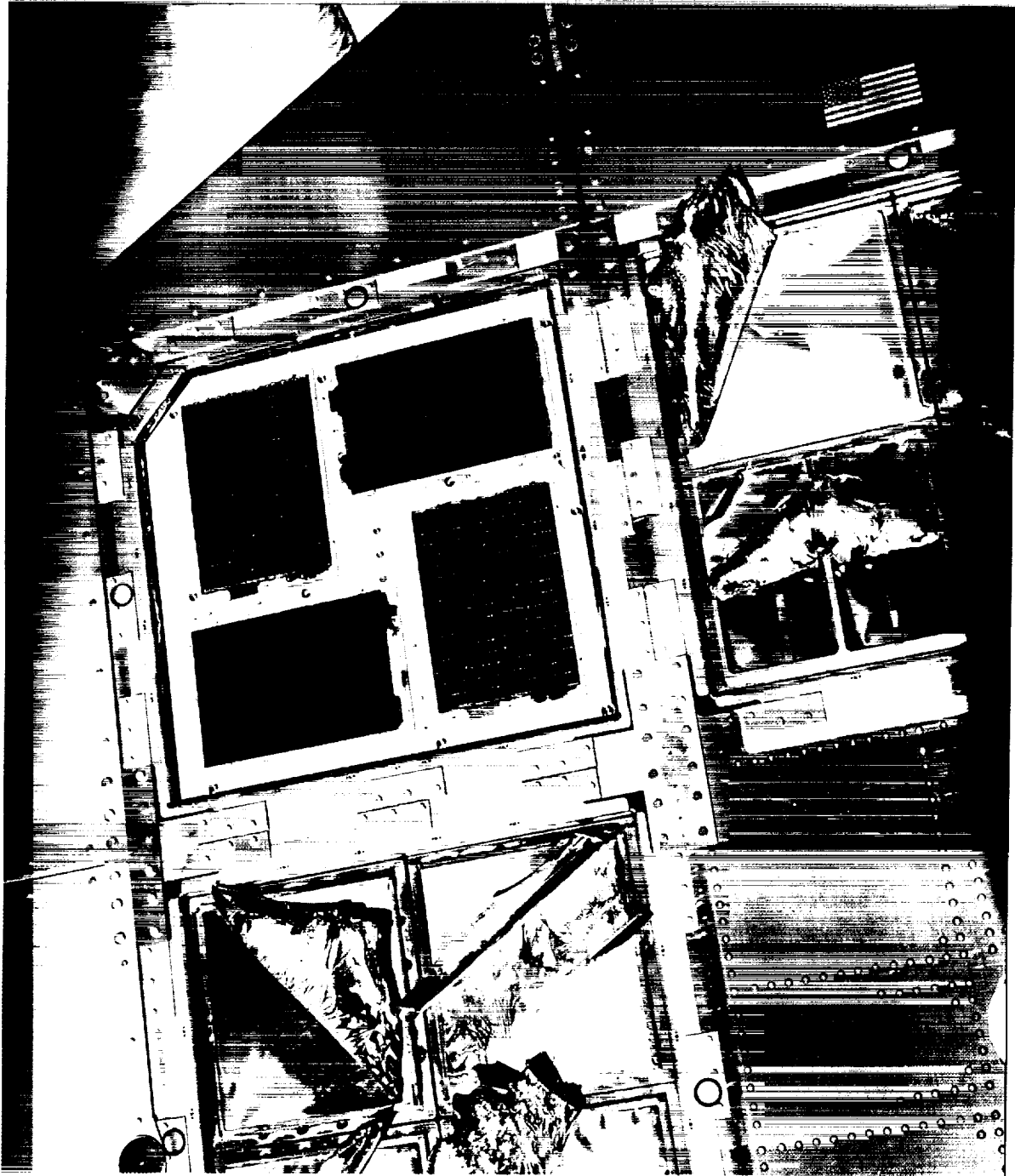


Figure C6. On-Orbit view of paint disks on the space end of LDEF. NASA Johnson Space Center Photo No. S32-75-036. U. S. flag is above tray H12. Color version of figure 6, page 17.

**APPENDIX C. Color Photographs From Section 7.0 Figures**

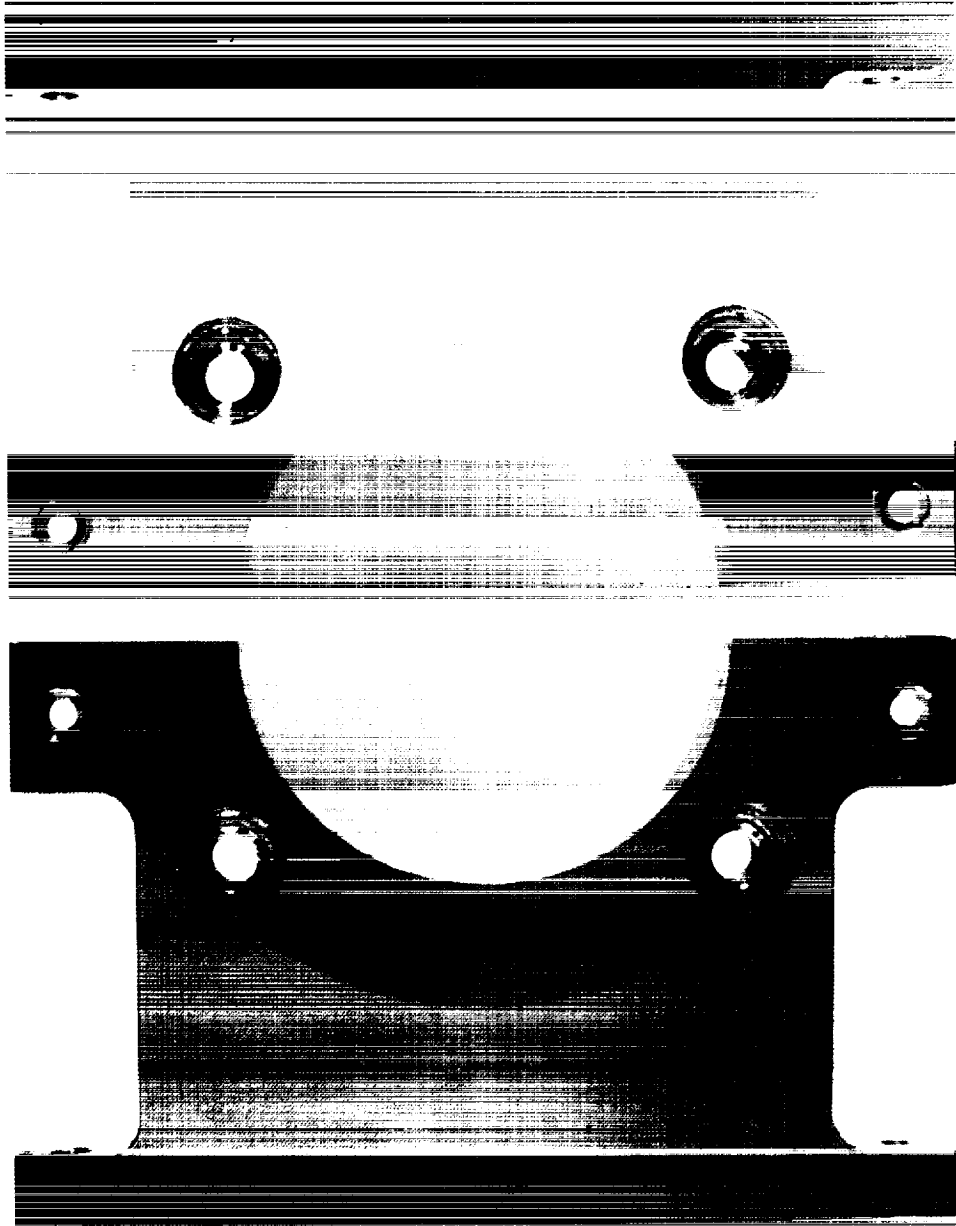


Figure C11. Chemglaze A971 yellow paint on components of the leading (above) and trailing edge scuff plates. Color version of figure 11, page 22.

APPENDIX C. Color Photographs From Section 7.0 Figures

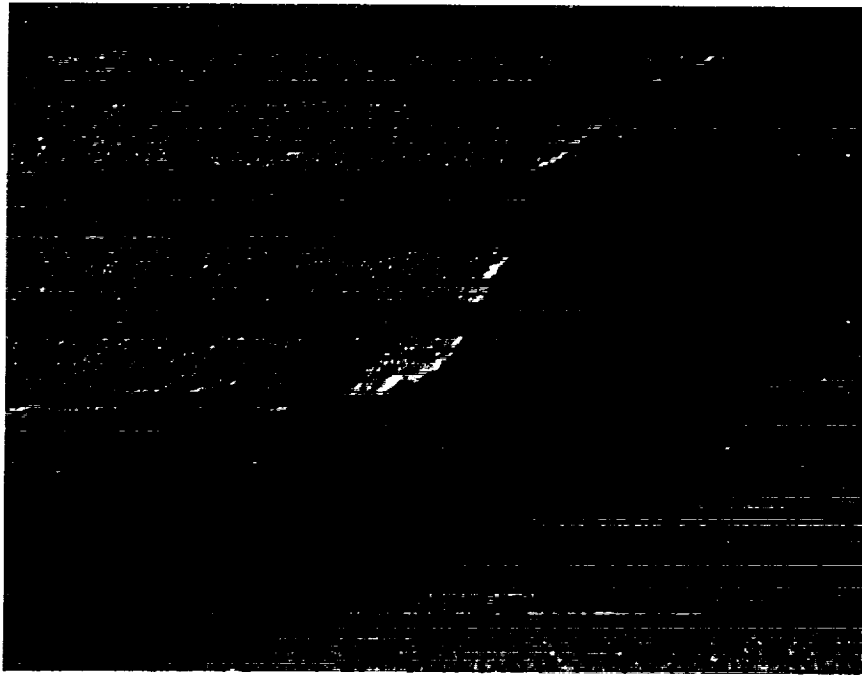


Figure C12. Chemglaze Z306 black polyurethane paint on tray clamp position A6-2, viewed at 16X magnification. Contaminant fiber imbedded in the paint film. Color version of figure 12, page 23.

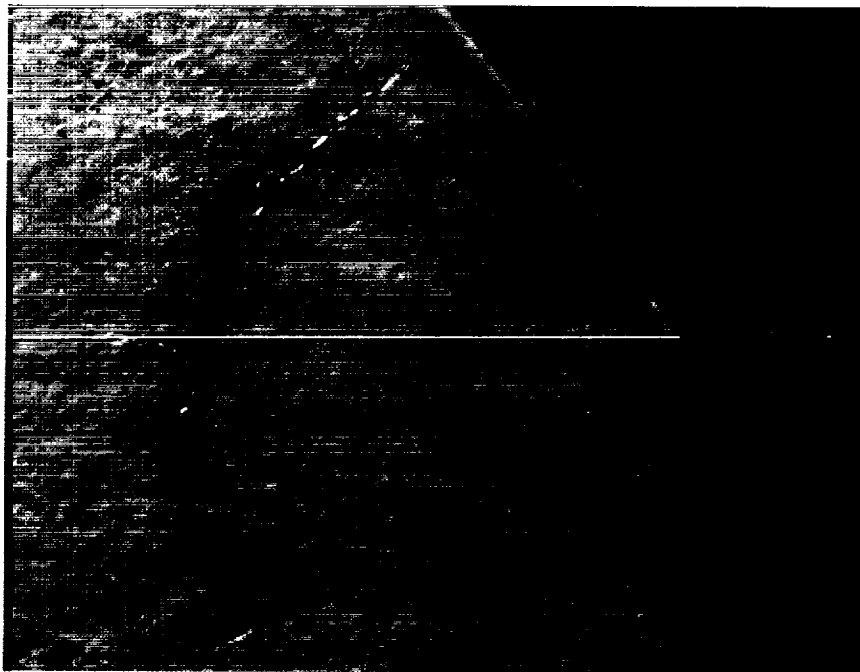


Figure C13. Chemglaze A276 white polyurethane paint on tray clamp A6-2, viewed at 16X magnification. A contaminant fiber is imbedded in the coating and solvent marks are visible. Color version of figure 13, page 23.

APPENDIX C. Color Photographs From Section 7.0 Figures

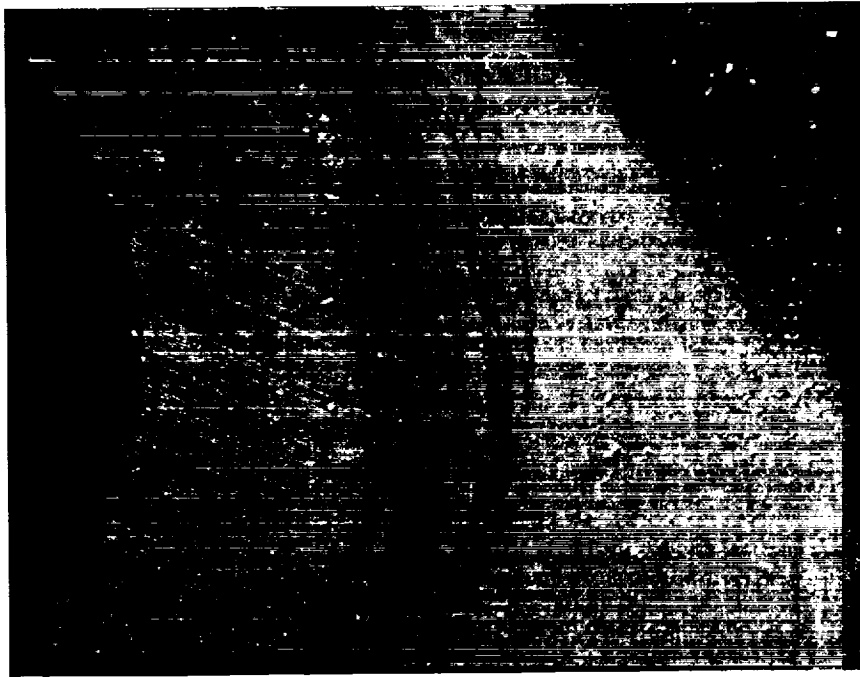


Figure C14. Chemglaze Z306 black polyurethane paint on tray clamp B7-2, viewed at 16X magnification. Visible are a fastener hole and particles of yellow paint, intact on most of the surface but smeared under the washer during assembly. Color version of figure 14, page 24.

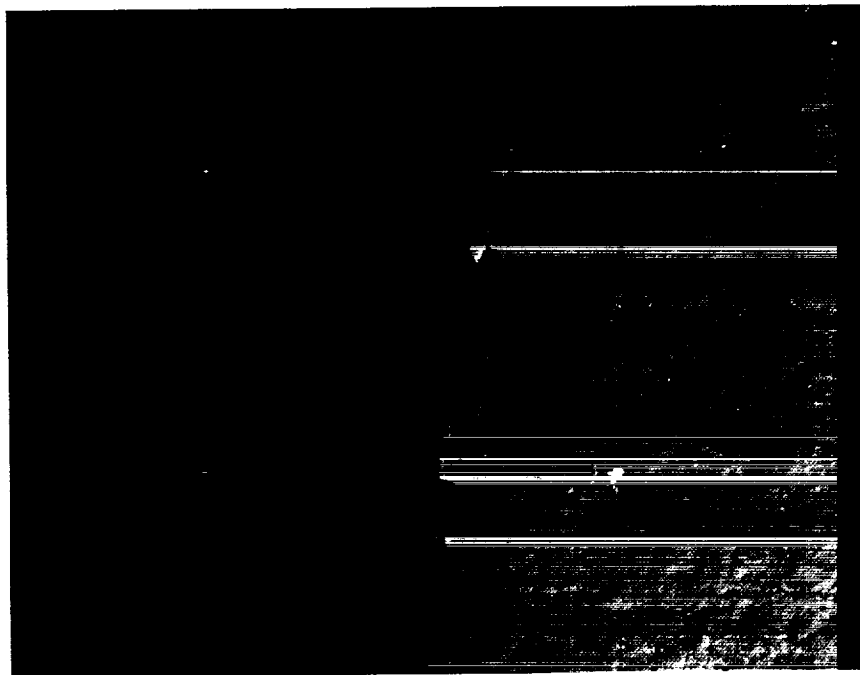


Figure C15. Chemglaze A276 white polyurethane paint on tray clamp B4-7, viewed at 16X magnification. Solvent mark discoloration. Color version of figure 15, page 24.

APPENDIX C. Color Photographs From Section 7.0 Figures

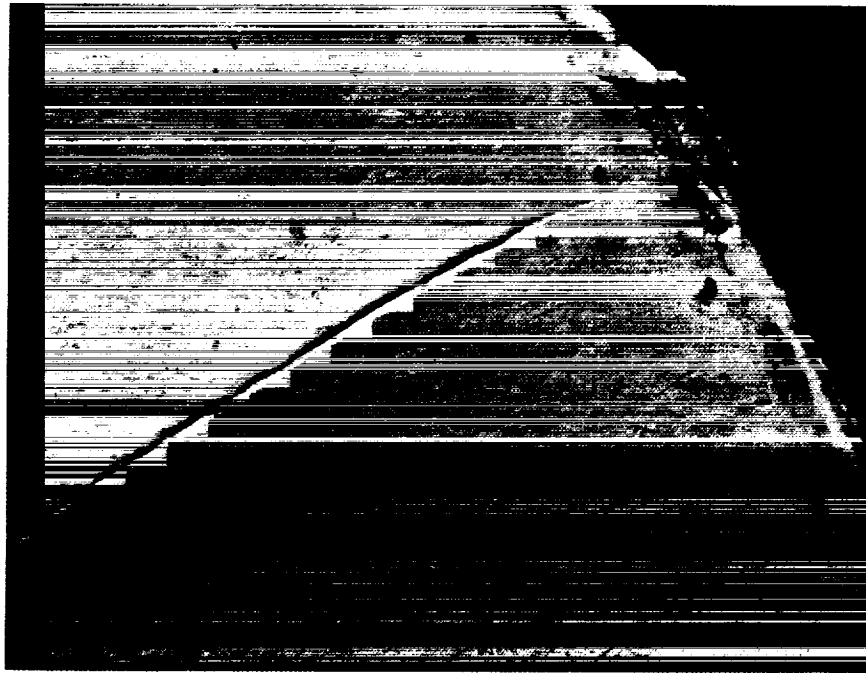


Figure C16. Chemglaze A276 white polyurethane paint on tray clamp B7-2, viewed at 16X magnification. Example of cracking with atomic oxygen erosion. Color version of figure 16, page 25.

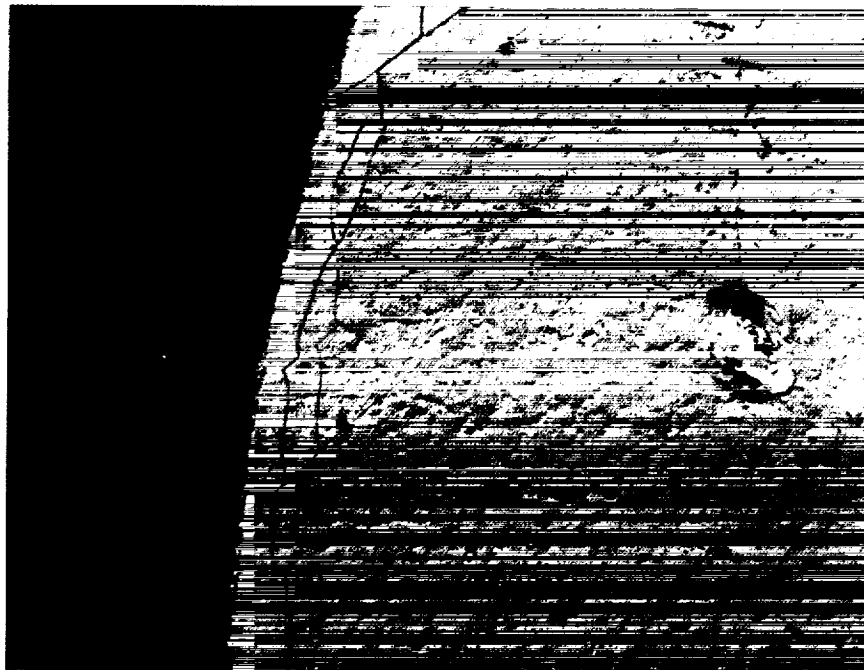


Figure C17. Chemglaze A276 white polyurethane paint on tray clamp C8-5, viewed at 16X magnification. Edge cracking and fragility of the surface are shown. Color version of figure 17, page 25.

**APPENDIX C. Color Photographs From Section 7.0 Figures**

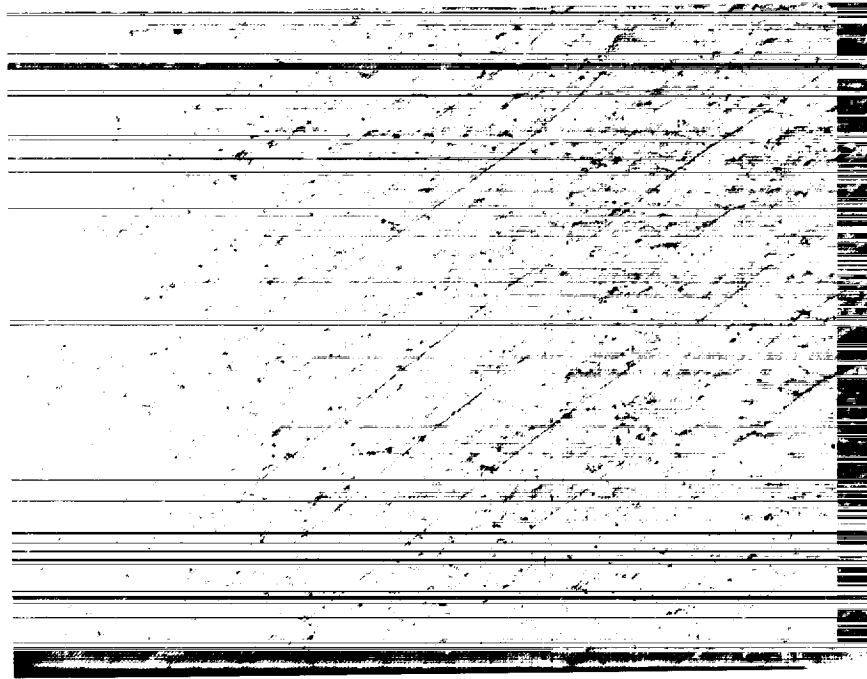


Figure C18. Chemglaze A276 white polyurethane paint on tray clamp C8-5, viewed at 16X magnification, showing parallel surface cracks. Color version of figure 18, page 26.

APPENDIX C. Color Photographs From Section 7.0 Figures

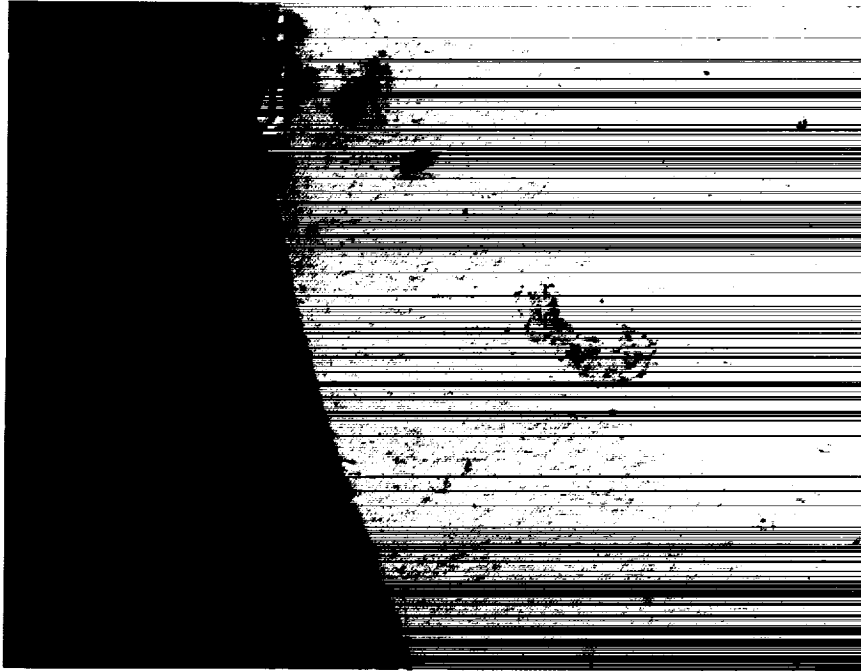


Figure C19. Chemglaze A276 white polyurethane paint on tray clamp B7-2, viewed at 16X magnification. Occlusions in paint were exposed with AO erosion. Color version of figure 19, page 27.

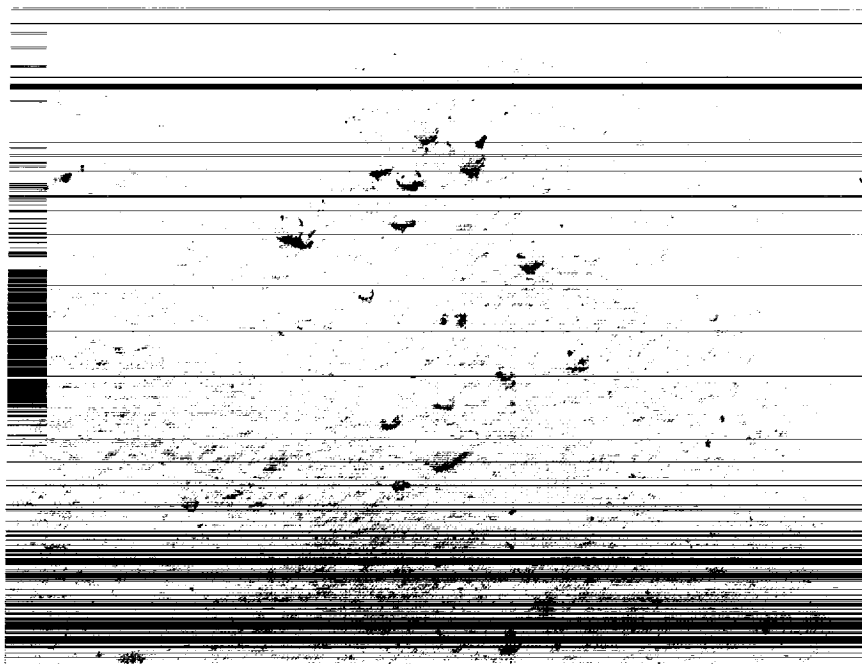


Figure C20. Chemglaze A276 white polyurethane paint on tray clamp B7-2, viewed at 16X magnification, showing more AO erosion exposed paint contaminants. Color version of figure 20, page 27.

APPENDIX C. Color Photographs From Section 7.0 Figures

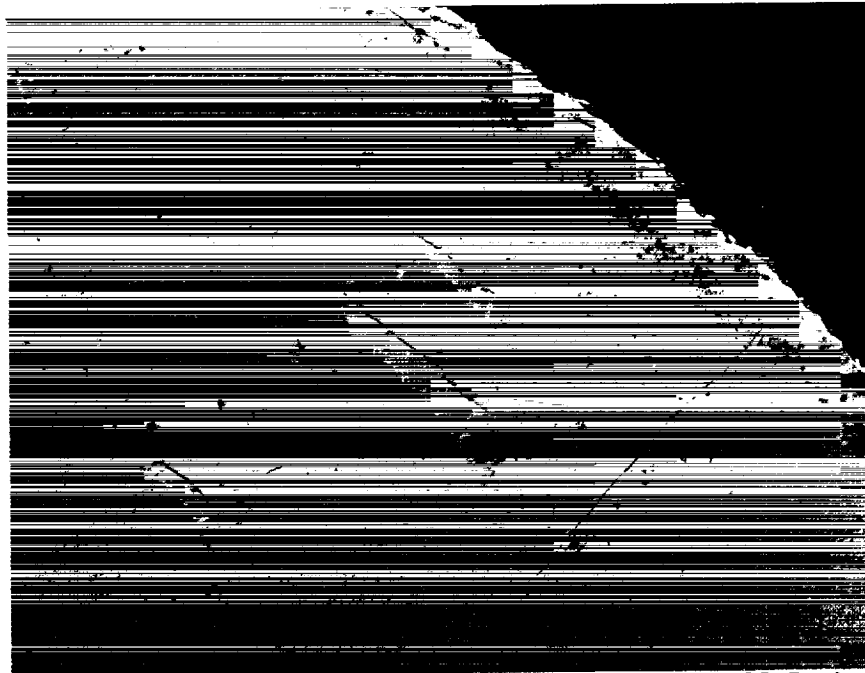


Figure C21. Chemglaze A276 white polyurethane paint on tray clamp C8-5, viewed at 16X magnification, showing the fragile nature of the eroded surface layer. Color version of figure 21, page 28.

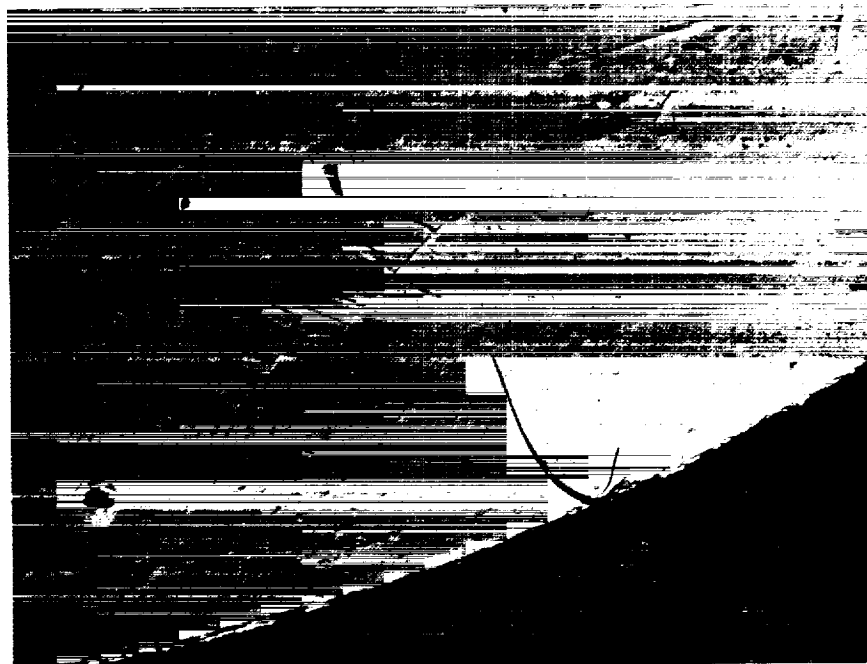


Figure C22. Chemglaze A276 white polyurethane paint on tray clamp C8-5, viewed at 16X magnification, showing a small debris impact and handling damage. Color version of figure 22, page 28.

APPENDIX C. Color Photographs From Section 7.0 Figures

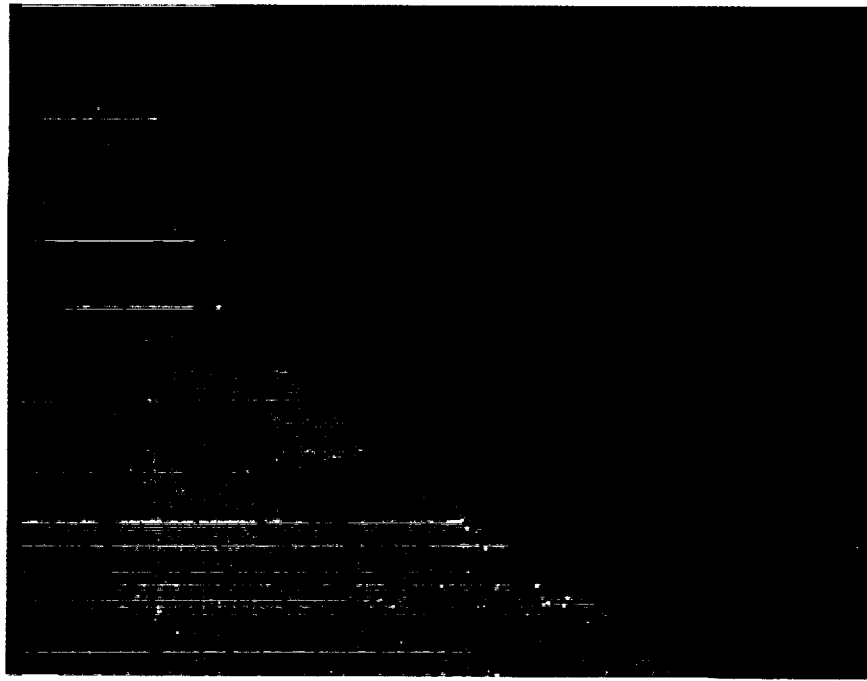


Figure C23. Chemglaze Z306 black polyurethane paint on tray clamp C8-5, viewed at 16X magnification, near a fastener location. Erosion through to the red primer occurred in a band just inside of the paint edge. Color version of figure 23, page 29.

## APPENDIX C. Color Photographs From Section 7.0 Figures

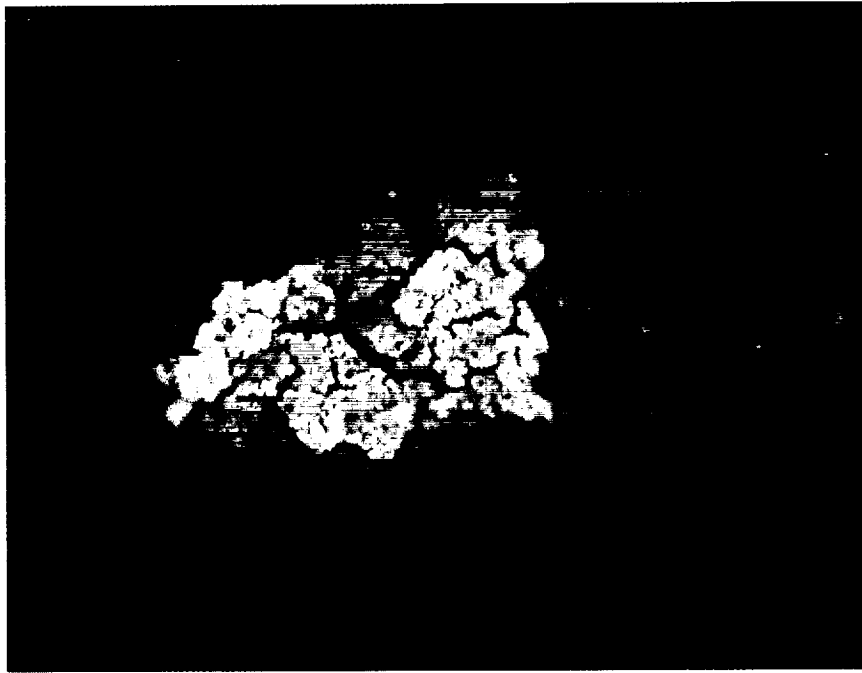


Figure C32. Chemglaze Z306 black polyurethane paint on Experiment M0003 composite panel, viewed at 200X magnification. The focus is on a silicate inclusion but atomic oxygen erosion to the red primer layer is visible. Color version of figure 32, page 34.

APPENDIX C. Color Photographs From Section 7.0 Figures



Figure C33. Chemglaze Z306 black polyurethane paint on Experiment M0003 composite panel, viewed at 200X magnification. The focus is on another silicate inclusion but atomic oxygen erosion to the red primer layer is visible. Color version of figure 33, page 35.



Figure C34. Chemglaze Z306 black polyurethane paint on Experiment M0003 composite panel, viewed at 200X magnification, showing a dispersed silicate layer. Color version of figure 34, page 35.

## APPENDIX C. Color Photographs From Section 7.0 Figures

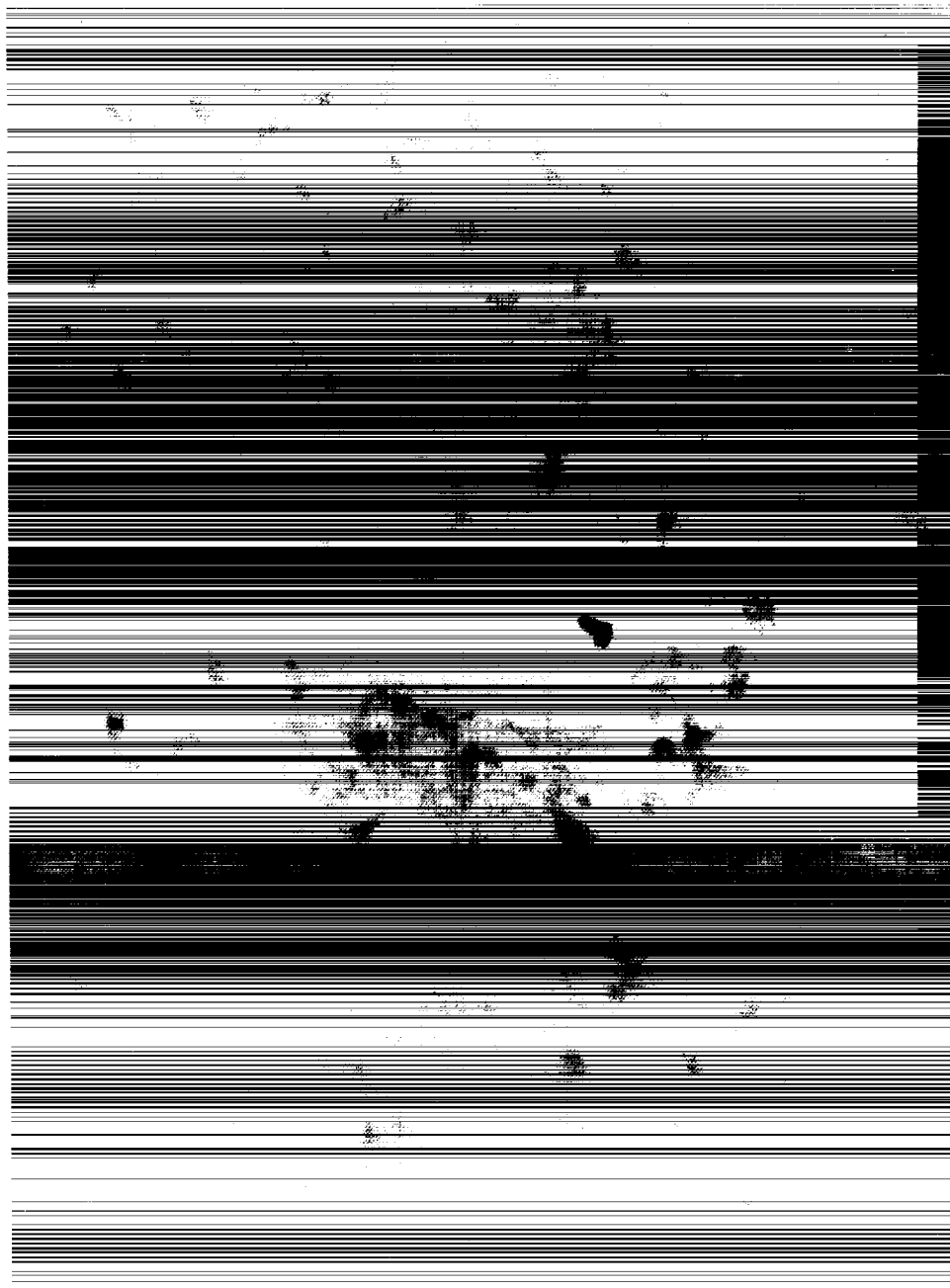


Figure C35. Chemglaze A971 yellow polyurethane paint from the leading edge (row 9) scuff plate, shown at 200X magnification. At center is loose clump of pigment, dark freckles are areas of darkened organic resin. Color version of figure 35, page 36.

APPENDIX C. Color Photographs From Section 7.0 Figures

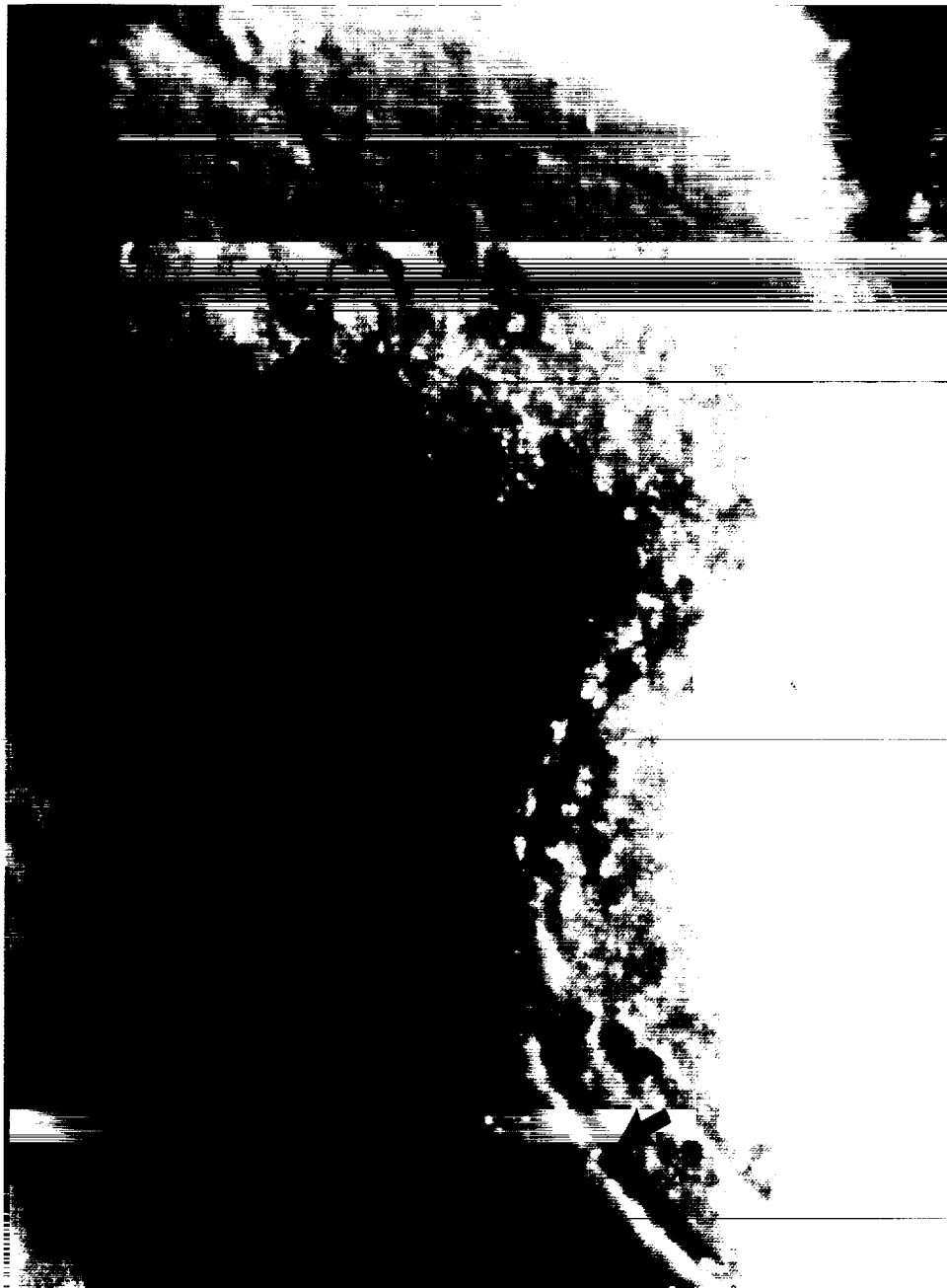


Figure C36. Chemglaze A971 yellow polyurethane paint from the leading edge (row 9) scuff plate, shown at 200X magnification. The focus is on the track of a organic fiber which was a contaminant in the paint and subsequently eroded by AO where it emerged through the surface. Color version of figure 36, page 37.

**APPENDIX C. Color Photographs From Section 7.0 Figures**

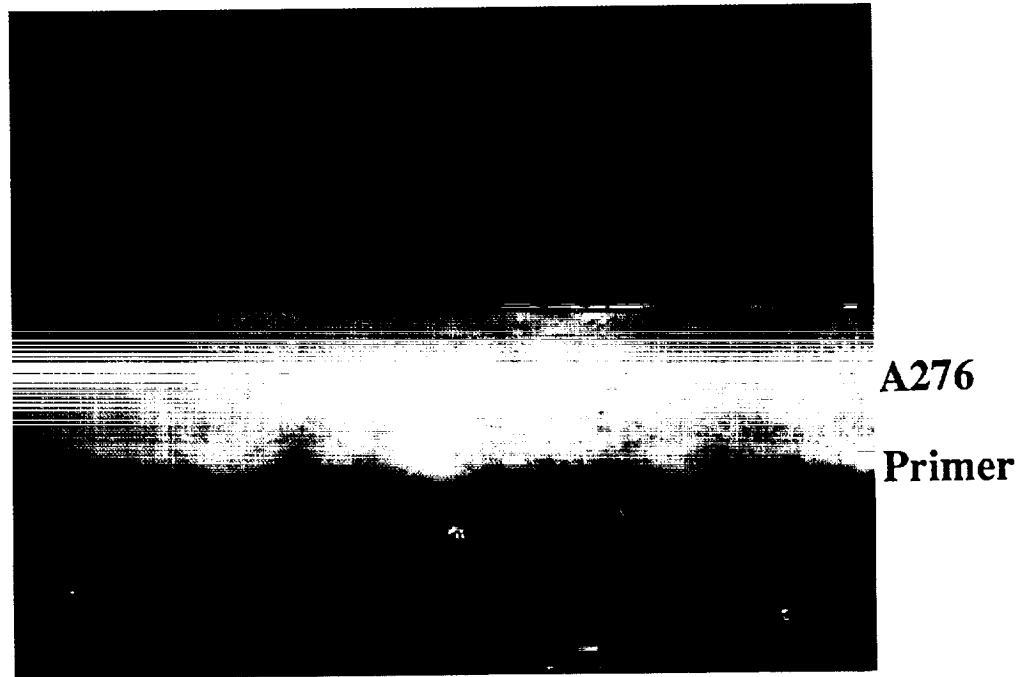


Figure C46. Cross-section of Chemglaze A276 white paint on tray clamp C8-5 (500X magnification), showing lifting of loose pigment into the encapsulant. Color version of figure 46, page 47.

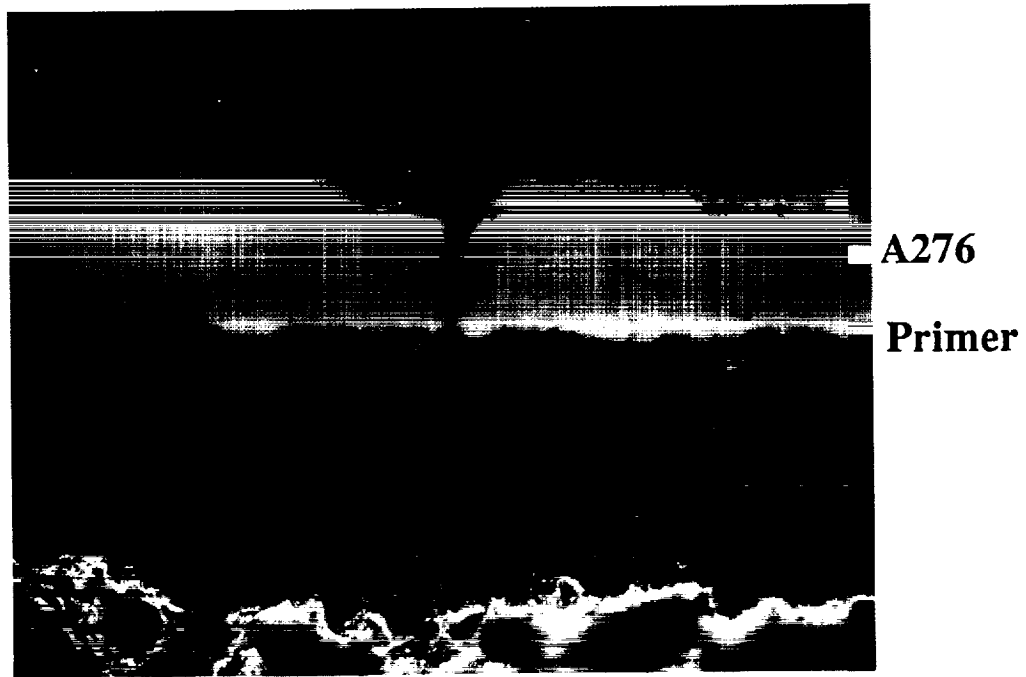


Figure C47. Cross-section of Chemglaze A276 white paint on tray clamp C8-5 (500X magnification), showing a typical crack passing down to aluminum substrate. Color version of figure 47, page 47.

APPENDIX C. Color Photographs From Section 7.0 Figures

Darkened  
Surface Layer

A276

Primer

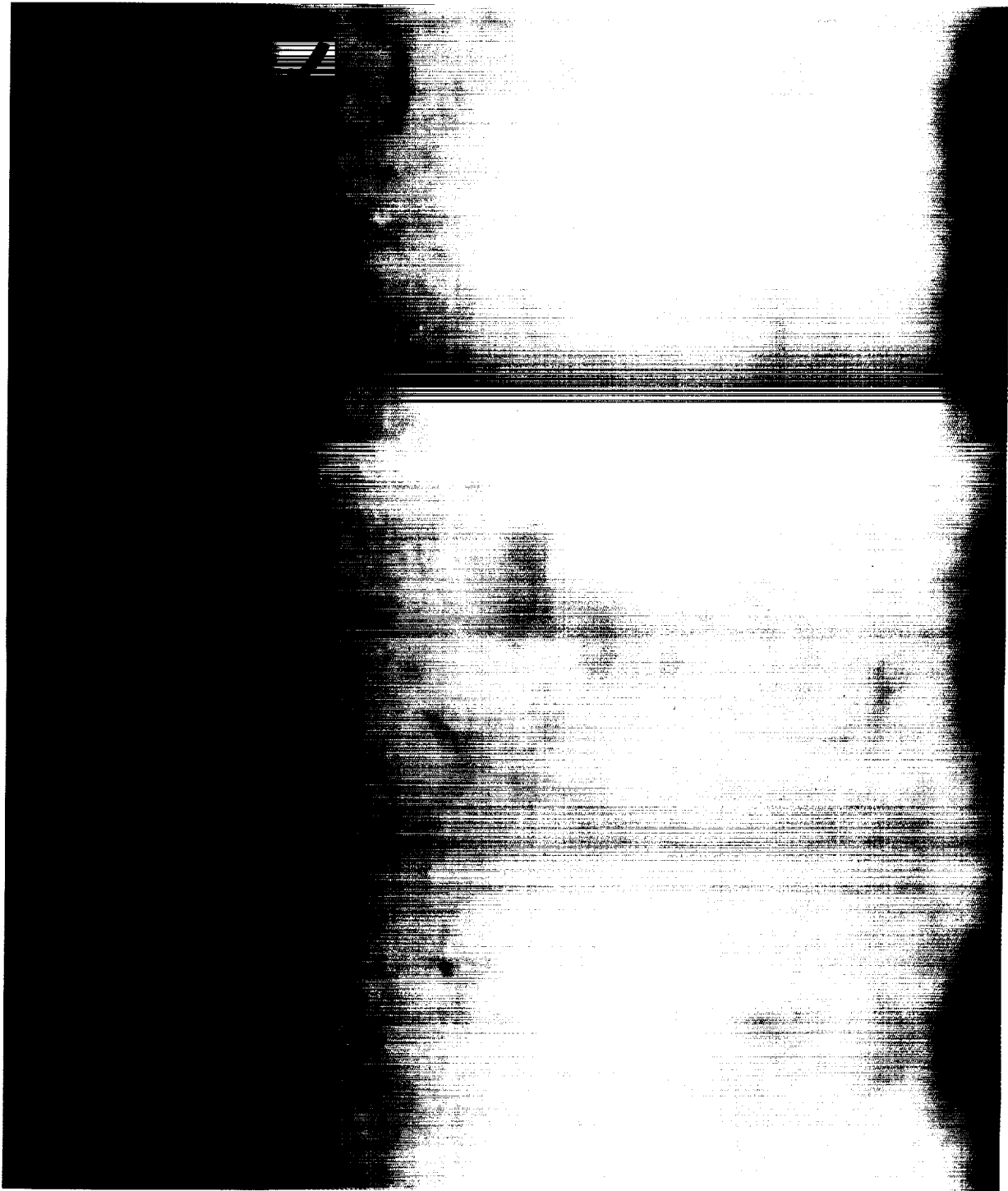


Figure C56. Cross-section of Chemglaze A276 white polyurethane paint on tray clamp B4-7 at 2500X magnification. Titania particles are visible to the very surface of the paint. The discolored layer is very thin,  $\sim 0.2 \mu\text{m}$ . Color version of figure 56, page 52.

REPORT DOCUMENTATION PAGE			Form Approved OMB No. 0704-0188	
Public reporting burden for this collection of information is estimated to average 1 hour per response, including the time for reviewing instructions, searching existing data sources, gathering and maintaining the data needed, and completing and reviewing the collection of information. Send comments regarding this burden estimate or any other aspect of this collection of information, including suggestions for reducing this burden, to Washington Headquarters Services, Directorate for Information Operations and Reports, 1215 Jefferson Davis Highway, Suite 1204, Arlington, VA 22202-4302, and to the Office of Management and Budget, Paperwork Reduction Project (0704-0188), Washington, DC 20503.				
1. AGENCY USE ONLY (Leave blank)	2. REPORT DATE July 1994	3. REPORT TYPE AND DATES COVERED Contractor Report (Oct. 1989 - Aug. 1993)		
4. TITLE AND SUBTITLE Results of the Examination of LDEF Polyurethane Thermal Control Coatings		5. FUNDING NUMBERS NAS1-18224, NAS1-19247 506-43-61-02, 233-03-02-04		
6. AUTHOR(S) Johnny L. Golden				
7. PERFORMING ORGANIZATION NAME(S) AND ADDRESS(ES) Boeing Defense & Space Group P.O. Box 3999 Seattle, WA 98124-2499		8. PERFORMING ORGANIZATION REPORT NUMBER		
9. SPONSORING/MONITORING AGENCY NAME(S) AND ADDRESS(ES) National Aeronautics and Space Administration Langley Research Center Hampton, VA 23681-0001		10. SPONSORING/MONITORING AGENCY REPORT NUMBER NASA CR-4617		
11. SUPPLEMENTARY NOTES Langley Technical Monitor: Joan G. Funk				
12a. DISTRIBUTION/AVAILABILITY STATEMENT Unclassified--Unlimited Subject Category 23		12b. DISTRIBUTION CODE		
13. ABSTRACT (Maximum 200 words) This report summarizes the condition of polyurethane thermal control coatings subjected to 69 months of low Earth orbit (LEO) exposure on the Long Duration Exposure Facility (LDEF) mission. Specimens representing all environmental aspects obtainable by LDEF were analyzed. Widely varying changes in the thermo-optical and mechanical properties of these materials were observed, depending on atomic oxygen and ultraviolet radiation fluences. High atomic oxygen fluences, regardless of ultraviolet radiation exposure levels, resulted in near original optical properties for these coatings but with a degradation in their mechanical condition. A trend in solar absorptance increase with ultraviolet radiation fluence was observed. Contamination, though observed, exhibited minimal effects.				
14. SUBJECT TERMS Low Earth Orbit, Polyurethane Thermal Control Coatings, LDEF		15. NUMBER OF PAGES 162		
		16. PRICE CODE A08		
17. SECURITY CLASSIFICATION OF REPORT Unclassified	18. SECURITY CLASSIFICATION OF THIS PAGE Unclassified	19. SECURITY CLASSIFICATION OF ABSTRACT Unclassified	20. LIMITATION OF ABSTRACT Unlimited	

